Quaternary Stratigraphy and Glacial Dynamics from a Core Region of the Laurentide Ice Sheet, Aberdeen Lake, Kivalliq, Nunavut

by Tyler James Hodder

A thesis
presented to the University of Waterloo
in fulfilment of the
thesis requirement for the degree of
Master of Science
in
Earth Sciences

Waterloo, Ontario, Canada, 2014

Author's Declaration

I hereby declare that I am the sole author of this thesis. This is a true copy of the thesis, including any required final revisions, as accepted by my examiners.

I understand that my thesis may be made electronically available to the public.

Abstract

Central Kivalliq, mainland Nunavut west of Hudson Bay and north of Manitoba, was a long-standing core region of the Laurentide Ice Sheet (LIS). The location of the Keewatin Ice Divide (KID), a major ice spreading region of the LIS, has been shown to have shifted position throughout the Wisconsinan glacial cycle. The surficial record is characterized by near continuous till blanket and cross-cutting streamlined landforms. The occurrence of multi-till stratigraphy across the region raises a number of questions regarding deposition and preservation under a migrating ice divide. This study provides further mapping on the surficial record and investigates the linkages with the subsurface stratigraphy to assess the glacial dynamics evolution throughout the Aberdeen Lake region. This study was motivated by unique access to over 100 drillcores and helicopter based fieldwork, allowing a unique three-dimensional study of the glacial geology record of the Aberdeen Lake region.

Field-based mapping of erosional paleo-ice flow indicators, accompanied by remote sensing mapping based on SPOT imagery of subglacial streamlined lineations exhibited a complex surficial history, recording the migration of the KID across the study area. In particular, five paleo-ice flow events are recognized: old WSW (255°) and S (180°) followed by NNW (340°), NW (300°) and finally W (270°) ice flow phases. Landforms corresponding with the NNW, NW and W ice flow phases are recognized. Landforms corresponding to the NNW ice flow phase are part of a larger northward converging landform tract that extends into northern Kivalliq. Southeast of Aberdeen Lake, a paleo-ice stream onset region was interpreted based on the erosional and depositional record observed.

Quaternary stratigraphy southeast of Aberdeen Lake can reach up to 71 m in thickness, with till stratigraphy reaching 36 m in thickness. The regional till stratigraphy is grouped into five till lithofacies (Dmm 1-5 – oldest to youngest) based on their texture, geochemistry, lithological signature and colour. Dmm 1 represents an early advance into the region, possibly as a result of the WSW (255°) ice flow phase or could be a preserved depositional imprint of a previous glaciation. Evidence for deposition by an early southerly ice flow phase is recognized within Dmm 2. Dmm 3 and 4 are preceded by a southern migration of the KID and are interpreted to have been deposited by northerly ice flow phases. Dmm 5 is interpreted to be late-glacial in age, corresponding to deposition by NW – W ice flow phases.

The northern ice flow phase is responsible for the majority of till production across the study area, reaching a known maximum of approximately 12 m in thickness and representing 45-70% of the stratigraphy thickness logged at across the Tatiggaq target. The recovery of Pitz Fm volcanics within the pebble fraction (4-8 mm) of this till unit south of Qamanaarjuk Lake points to transport distances of at least 55 km from the Baker Lake basin. The extent of large streamlined lineations and associated till production suggests a strong ice flow phase affected the region at a time when the Aberdeen Lake region was not in an ice-marginal setting, but instead a core region of the LIS. Based on the convergent landform imprint and extent, it is suggested this ice flow phase could represent propagation of an ice stream catchment region into central Kivalliq, which could be contemporaneous with southern migration of the KID. Furthermore, it is suggested that the documented late glacial migration of the KID could be a result of competing ice stream catchment areas, with the Hudson Strait Ice Stream catchment becoming more dominant at a later period in time. The propagation of ice stream catchment regions deep into the LIS would suggest that theoretical constructs may be underestimating the proportion of warm-based conditions and erosion/till production that existed during periods of thick ice in central Kivalliq as well as the role of migrating ice divides.

This study has provided insight on the glacial dynamics of a former core region of the LIS. The Quaternary stratigraphy was delineated through river bluff and drillcores, emphasizing the dynamics of paleo-ice flow phases which is a necessary first step for successful drift prospecting in this remote region that has known uranium and gold prospects.

Acknowledgements

This project was funded primarily by Cameco Corporation and a National Science and Engineering Research (NSERC) research grant to Dr. Martin Ross (UW). Funding through the Northern Scientific Training Program (NSTP) also helped with field travel expenses. I would first like to thank my supervisor Dr. Martin Ross for his guidance and mentorship throughout both my B.Sc. and M.Sc. thesis and assisting me over the past 3+ years. Officemates throughout my time at UW in the Quaternary research group have made this a great experience: Cassia, Aaron, Uly, Shawn, Jessey, Ying. In particular, Aaron for his constant thoughtful conversation regarding the project we have both been diligently working on. Thanks to my committee members Dr. Isabelle McMartin and Dr. Shoufa Lin for insightful reviews and comments throughout the project. Cameco personnel made this project a success. I appreciate, and thank in particular Joel Lesperance and Rebecca Hunter for their field insight and logistical support throughout the project, as well as Gerard Zaluski for countless thoughtful reviews of conference abstracts. Lastly, I would thank the field and lab assistants (Ros, Caroline, Fidele) for collecting and processing the many kilograms of till involved with this project.

Table of Contents

List of Figures

List of Tables

Chapter 1 : Introduction

1.1 Research Problem

Subglacial erosion underneath ice divides is considered negligible due to the near zero horizontal velocity experienced in these regions (e.g. Benn and Evans 2010), and thus the resultant landscape can be a region of widespread subglacial preservation. Boulton (1996) investigated the nature of erosion and deposition across a hypothetical ice sheet based on numerical ice sheet flow parameters. Boulton's (1996) findings suggested that in core regions of ice sheets (zone 1) net deposition occurred during advance of an ice sheet ('advance phase' till), net erosion during the majority of the glacial cycle followed by deposition during ice sheet retreat (Fig. 1-1; 'retreat phase' till). Boulton's (1996) zone 2 is characterized by strong erosion with till derived from the retreat phase only. Vast expanses of the Canadian Shield are characterized by these zone 2 attributes of Boulton (1996), which has led to a generalization that the Canadian shield is a hard bed consisting of thin drift. As noted by Boulton (1996), this simple model is more complicated for core regions since ice divides are not stationary and the movement of an ice divide throughout a glacial cycle can lead to a complex depositional/erosional relationship in ice sheet core regions. Ice divide migration can result in the preservation of previously deposited till sheets during the glacial cycle from subsequent erosion as well as allow for these early till sheets to be incorporated into retreat phase till sheets. This simplified model also does not take ice stream dynamics into account. Catchments of large ice streams, including networks of tributaries have been shown to propagate far inside an ice sheet (e.g. Bamber et al. 2000a; Bamber et al. 2000b). This would suggest till production may not all be ice marginal (retreat phase) tills. The degree of till production from successive ice flow phases, as well as the inheritance signature from previously preserved till sheets has important implications to understanding the glacial dynamics of ice sheet core regions throughout an entire glacial cycle.

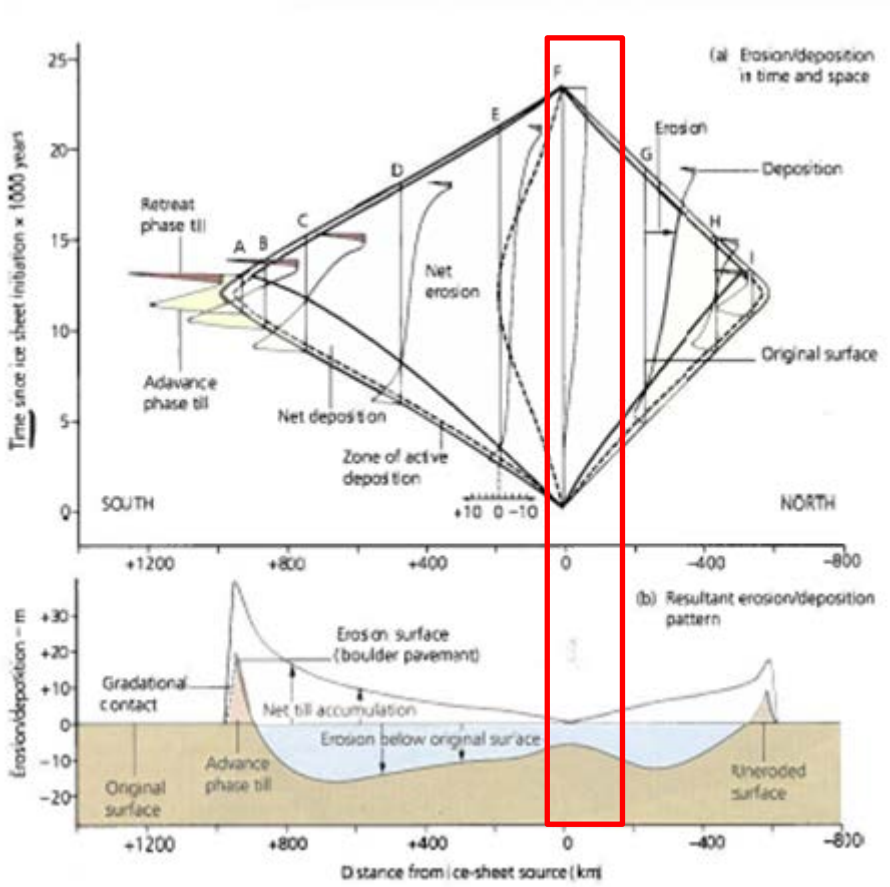

Figure 1-1: Model of erosion and deposition through time, with increasing distance from an ice divide for a hypothesized ice sheet over a glacial cycle. The red polygon depicts the approximate distance from the Keewatin ice divide for this study. Modified from Benn and Evans (2010) after Boulton (1996).

Central mainland Nunavut was a core region of the Laurentide ice sheet (LIS) during the last glacial cycle (Wisconsinan) that experienced a complex ice flow history with the Keewatin Ice Divide (KID) migrating up to 500 km between ice flow phases (McMartin and Henderson 2004a). Thick drift has been documented in central mainland Nunavut through surficial geology mapping (e.g. Aylsworth 1990; McMartin et al. 2008) as well as field observations of thick multi-till stratigraphy river bluffs (Tyrrell 1897; Klassen 1995; McMartin and Henderson 2004b; McMartin et al. 2006). Central mainland Nunavut has a complex landform record consisting of cross-cutting lineations (e.g. Boulton and Clark 1990; De Angelis 2007) and a relative abundance of mega-scale glacial landforms (Stokes and Clark 2003; Greenwood and Kleman 2010; Stokes et al. 2013). Therefore, this region provides an interesting glacial geology setting to investigate till production of successive ice flow phases from a core region of the LIS. Limited work has been conducted on documenting the stratigraphy of the thick till successions and

relating this depositional record to the known complex surficial record of the region. Where investigations have been conducted they have been spatially limited to natural river bluff sections or shallow drillcores, with no previous stratigraphic work conducted within the Aberdeen Lake map area (NTS 66B; Fig. 1-2). The Quaternary stratigraphy record is also an integral constraint on numerical models of the LIS (Kleman et al. 2002; Stokes et al. 2012), which could benefit greatly from an increased knowledge of till stratigraphy from a core region of the LIS.

For the LIS, modeling experiments show low basal ice flow velocities and extensive cold-based conditions across its core regions for most of the last glacial cycle (Tarasov and Peltier 2007; Stokes et al. 2012), as well as low erosion rates and sediment production (Melanson et al. 2013). Even during the last glacial maximum when this region was under a thick ice sheet, prevailing cold-based conditions with sluggish ice flow are thought to have existed (Kleman and Glasser 2007; Tarasov and Peltier 2007; Stokes et al. 2012). This raises questions regarding the relative timing of till production in this region. Early advance phases are suspected to be primarily through ice creep of a thin ice sheet (e.g. Stokes et al. 2012), which would account for minimal till production. Late glacial retreat phase tills would also have been produced under a much smaller glacier. It is unlikely that such a reduced ice mass would be capable of producing 100 ft (~30 m) of till in the Aberdeen Lake (Tyrrell 1897) and Garry Lake regions (Taylor 1956).

The relationship between the subsurface till stratigraphy and the surficial glacial landform record can provide insight into the till production of ice flow phases, which has direct implications for paleo-ice sheet reconstructions and drift prospecting. Understanding the till stratigraphy and provenance of a prospective region is an integral necessity for successful drift prospecting. For example, a multi-till stratigraphy created by separate ice flows over an exploration target can hinder the commodity signature in the surficial till unit relative the lower till units (e.g. Paulen 2009). Furthermore, complex interactions between the degree of inheritance and incorporation of previously deposited tills from successive ice flow phases (Stea and Finck 2001; Trommelen et al. 2013) can result in more cryptic surficial palimpsest dispersal trains (Parent et al. 1996). The region of interest is a prospective area for uranium exploration specifically unconformity-type uranium deposits (e.g. Hiatt et al. 2010). Exploration efforts are complicated by thick sequences of Quaternary sediments masking the buried ore and altered rock signature. Understanding the

provenance of subsurface till units in context with the surficial erosional and landform record is a necessary initial step for successful drift prospecting. For example, questions arise such as: is the surficial till sampled reflective of the local bedrock? Are drillcore samples necessary to link the subsurface and surficial record for identification of dispersal trains? Is there a multi-till stratigraphy and if so, what effect does this have on dispersal train analysis?

This study was motivated to understand the Quaternary history of this remote region through unique access to continuous drillcores of Quaternary sediments to bedrock and helicopter assisted field work provided by Cameco Corporation. This field work component was coupled with remote sensing observations of the surficial landform record of the Aberdeen Lake area.

1.1.1 Study Location

The region of interest is in mainland Kivalliq, Nunavut, which occupies the region west of Hudson Bay and was formerly referred to as the Keewatin region prior to the inception of Nunavut Territory. The focus of this study is central Kivalliq, with field work restricted to an area southeast of Aberdeen Lake and south of Qamanaarjuk Lake (black polygon Fig. 1-2), with remote work conducted on a broader region of Kivalliq encompassing national topographic system (NTS) zones 66 B and parts of 66 G, H, A, P and O (yellow polygon in Fig. 1-2). This region was part of a core region of the LIS, referred to as the 'Keewatin Sector' during the Wisconsinan glaciation and was host to a major ice dome during the Late Wisconsinan (e.g. McMartin and Henderson 2004a). The region of interest has been mapped primarily as till blanket (Fig. 1-2) and is located in the heart of the Canadian Shield.

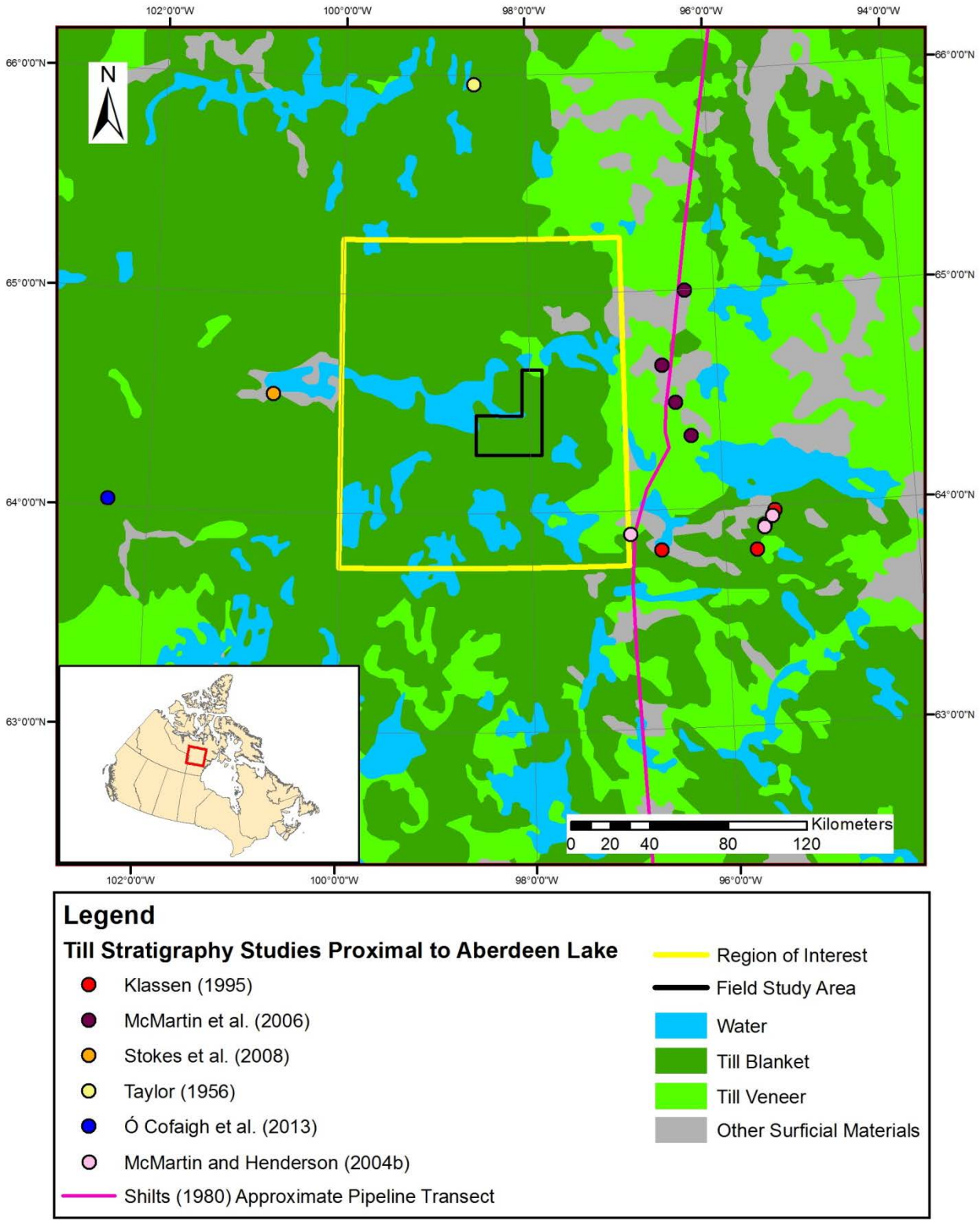

Figure 1-2: Simplified surficial materials map of central mainland Nunavut. Till stratigraphy studies conducted proximal to the Aberdeen Lake area are shown. The region of interest for the study is outlined by the yellow polygon and field study area by black polygon (Modified from Fulton 1995).

1.2 State of Knowledge

1.2.1 Bedrock Geology

The study area lies within the Archean Rae domain of the Western Churchill Province. This Province is primarily composed of variably reworked meso- to neo-Archean rocks with Proterozoic outliers of gently folded sediments, basins and intrusive suites (Hoffman 1988). The field study area was last mapped by Patterson and LeCheminant (1985) and incorporated into a larger compilation of the Western Churchill Province by Paul et al. (2002) and is reproduced in Fig. 1-3.

The Neoarchean rocks of the Woodburn Lake Group (Gp) are composed of metasedimentary and metavolcanics rocks (Zaleski et al. 2000). The Amer Gp consists of clastic-dominated supracrustal rocks of early-mid Paleoproterozoic age (Rainbird et al. 2010) and outcrop in the northern and western part of the study area. Intrusive suites within the study area consist of the Nueltin granite and Hudson intrusive suite. The Nueltin granites are strongly porphyritic with phenocrysts of quartz, alkali feldspar and plagioclase (Peterson et al. 2002) and outcrop near Mallery Lake, but are more extensive south of the study area near Dubawnt and Tulemalu Lake.

The Dubawnt Supergroup consists of three unconformity-bound sequences referred to as the Baker Lake, Wharton and Barrensland Groups (Gall et al. 1992). The Barrensland Gp are the most spatially extensive rocks within the study area and outcrop in the Thelon Basin to the NW and Baker Lake Basin to the SE. The Barrensland Gp is primarily composed of the Thelon Fm that is overlain by a thin Kuungmi Fm and Lookout Point Fm; however, only the Thelon Fm is present within the study area. The Thelon Fm consists of unmetamorphosed quartz-dominated sandstones and conglomerates (Rainbird et al. 2003). The Wharton Gp consists of clastic continental redbeds of the Amarook Fm overlain by felsic volcanics of the Pitz Fm, which is intercalated with coarse alluvial red beds (Rainbird et al. 2003). The Pitz volcanics are a purple-mauve rhyolite with distinctive chalky sanidine and quartz phenocrysts (Peterson et al. 2002) and are one of the most distinctive rocks within the region and also one of the most useful indicators of till provenance (e.g. McMartin et al. 2006; Trommelen et al. 2013). Exposures of the Pitz Fm occur on the north edge of the Baker Lake basin and western portions of the study area (Fig. 1-3). The Baker Lake group comprises the South Channel, Kazan, Christopher Island, Kunwak and Angikuni formations consisting of conglomerates, arkosic sandstones and alkaline volcanic

rocks, which also have a distinctive colour (Hadlari et al. 2006). Paleozoic rocks are scarce, but a small outlier of limestone is present within the Thelon basin north of Aberdeen Lake. Drillcores investigated within this study area are primarily related to two uranium prospects that have sub-cropping alteration present. Both prospects contain wide-spread illitization with intervals of strong hematization and bleaching (Hunter et al. 2011a, 2011b).

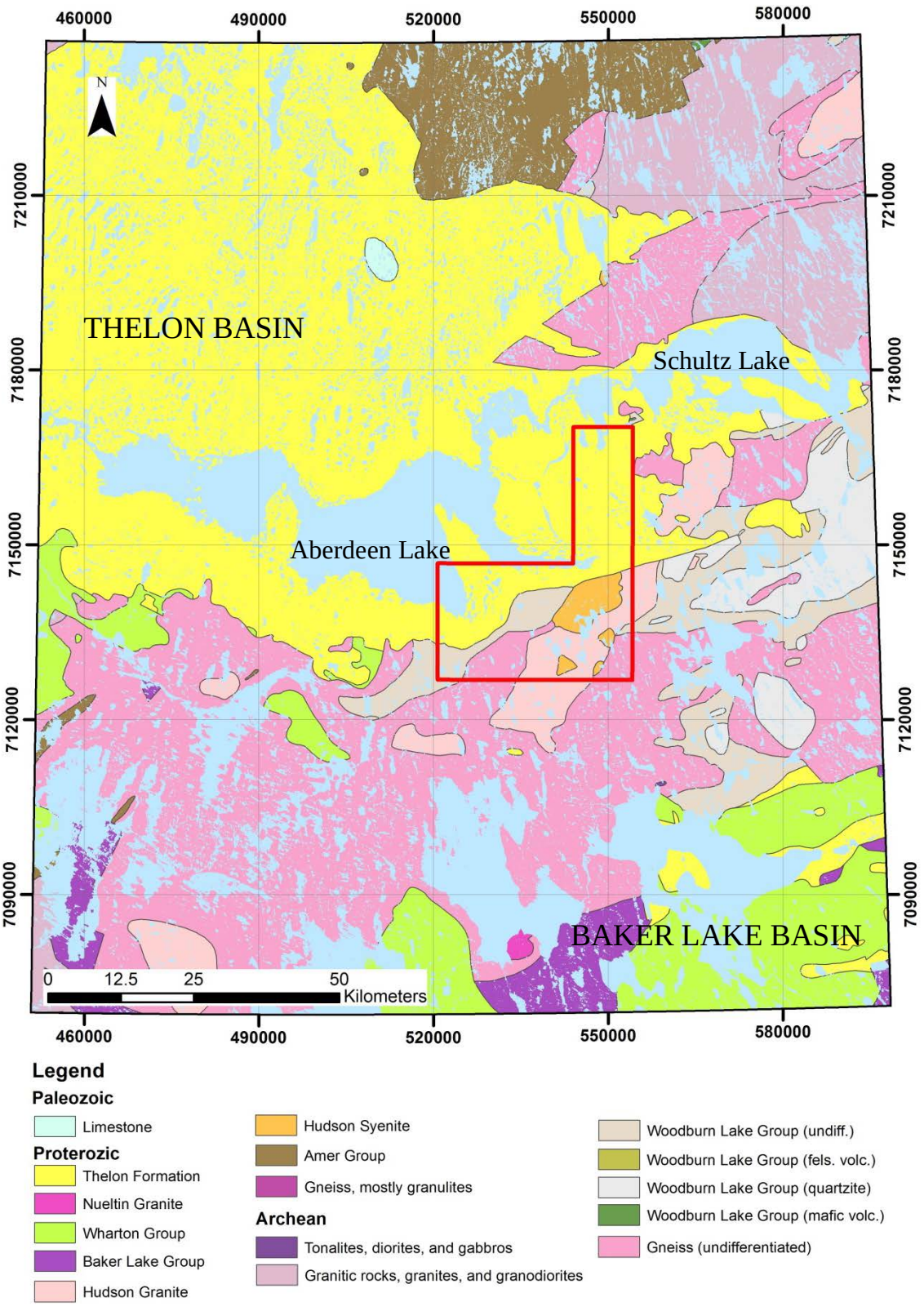

Figure 1-3: Bedrock geology of the remote sensing study area (modified from Paul et al. 2002). The field study area is highlighted by the red polygon.

1.2.2 Surficial Geology and Glacial Landscape

The surficial geology of the Aberdeen Lake area was last mapped by Aylsworth (1990) primarily through air photo interpretation at a scale of 1:125 000. Within the Aberdeen Lake area, drift is relatively thick (>5 m) and is the dominant surficial sediment throughout the Aberdeen and Schultz Lake region (Aylsworth 1990; Aylsworth et al. 1990; McMartin et al. 2008). Within the Aberdeen Lake map area, till is generally thicker south of Aberdeen lake, whereas till veneer is more common north of the lake (Aylsworth 1990). A similar situation is observed within the Schultz Lake map area where drift is generally thick (>5 m) and continuous south of the Thelon River and predominately thin north of the Thelon River (McMartin et al. 2006).

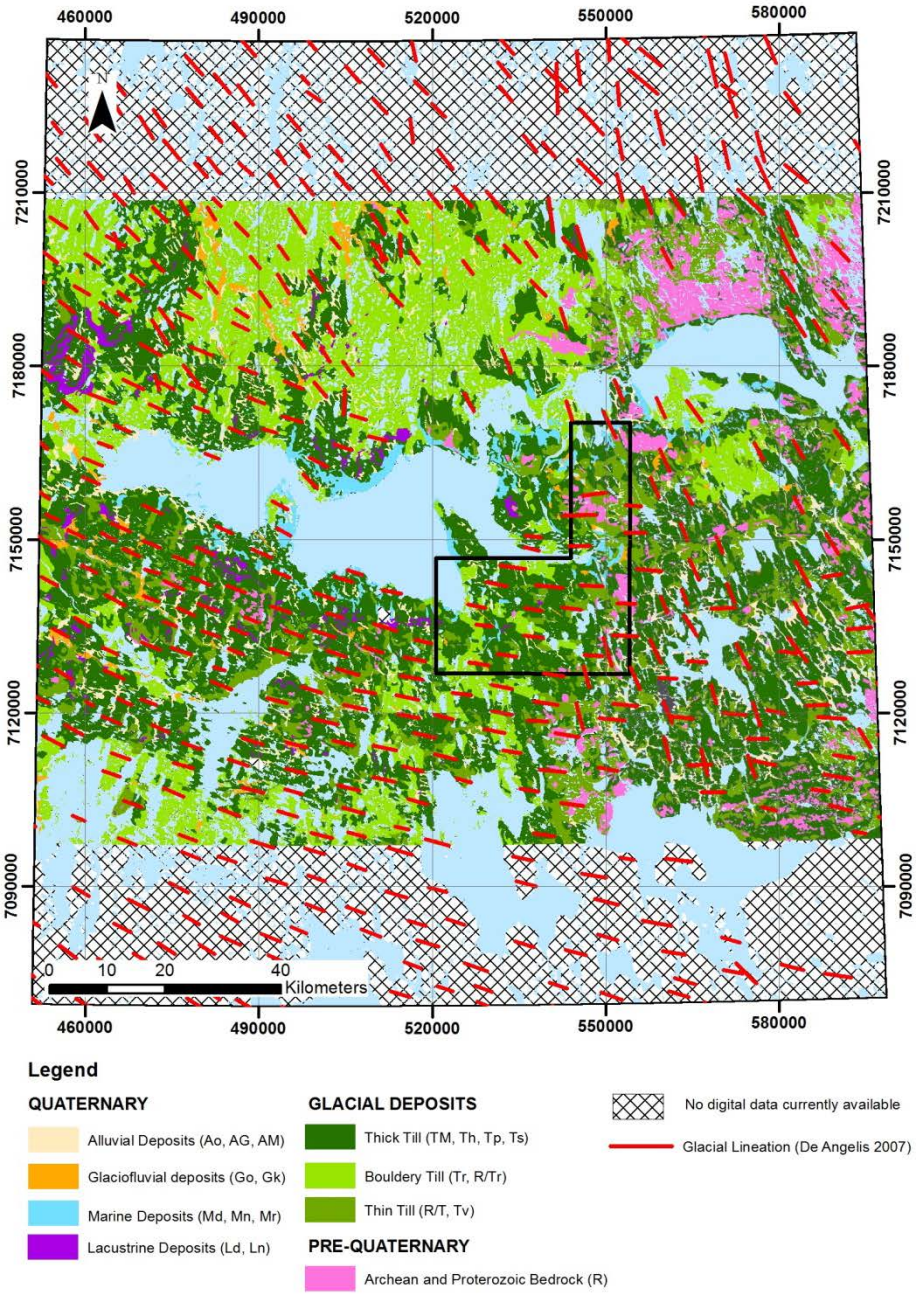

Figure 1-4: Simplified surficial geology in the vicinity of the remote sensing area, where digital data was available (modified from Aylsworth 1990 and Grunsky et al. 2006). The field study area is depicted by the black polygon in the center of the figure. The general trend of glacial lineations is also depicted (De Angelis 2007).

A significant paleo-glaciological concept for the Keewatin Sector of the LIS is the presence of a long-standing ice divide (Dyke et al. 2002), referred to as the KID as originally defined by Lee et al. (1957). The KID has been documented to have shifted position throughout the Wisconsinan glaciation (McMartin and Henderson 2004a) and the last known position is depicted in Fig. 1-5.

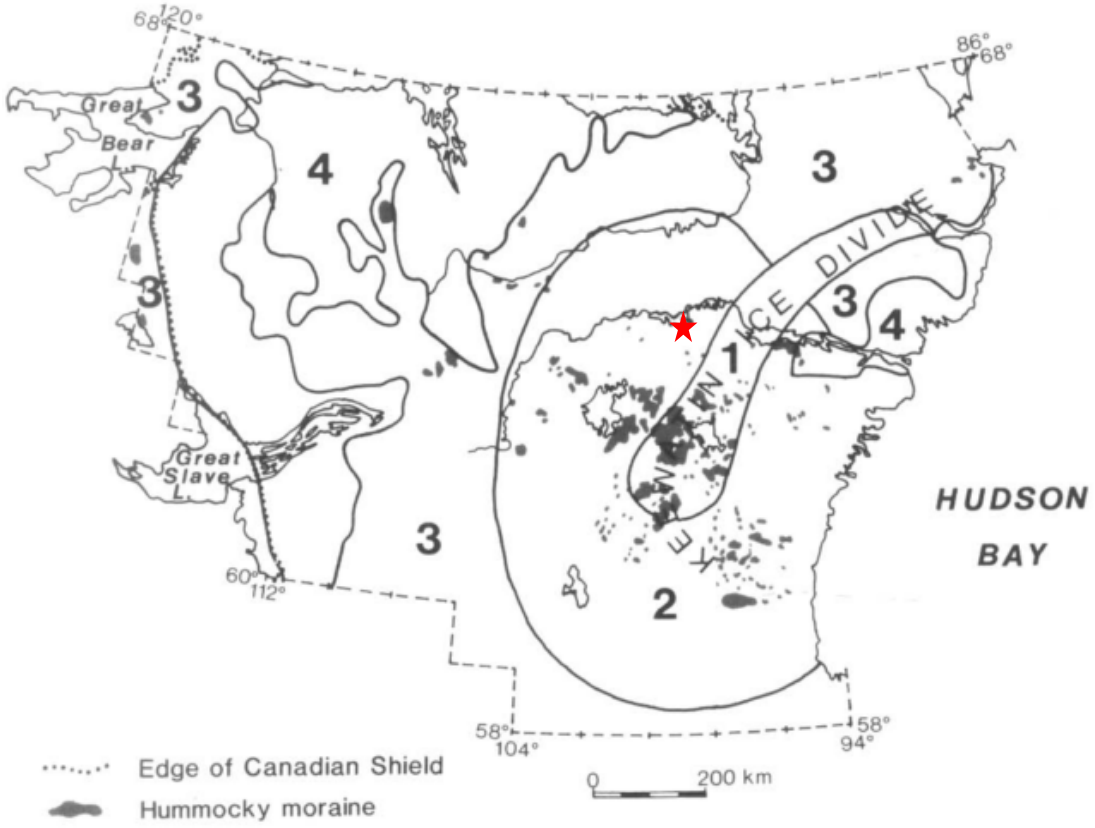

Figure 1-5: Location of the last-known position of the KID based upon glacial landform assemblages of the Keewatin Sector. Distinct landform-sediment zones have also been delineated radiating from the KID, zones 1-4. The field study location is denoted by the red star (Modified from Aylsworth and Shilts 1989).

The last known position of the KID is characterized by a landscape that lacks eskers or oriented landforms, with hummocky moraine being the most common landforms present (Aylsworth and Shilts 1989). Aylsworth and Shilts (1989) noticed distinct landform-sediment assemblages radiating from the KID. Zone 2 (Fig. 1-5) is defined by the distribution of ribbed moraines in the region and the occurrence of extensive drumlin fields (Aylsworth and Shilts 1989). Zone 3 (Fig. 1-5) is characterized by drumlinized drift cover while Zone 4 is mainly comprised of bedrock with minimal drift cover (Aylsworth and Shilts 1989). Glaciofluvial activity is primarily recorded by eskers and meltwater channels carved into drift or bedrock (Aylsworth and Shilts 1989). As discussed, eskers are not present within zone 1 and form a radiating pattern around the region defined by the last known position of the KID. This pattern suggests that during the final demise of the LIS when the ice sheet was limited to zone 1, it was likely thin and cold-based with melt water drainage primarily through surficial melt restricting the formation of eskers within the region formerly occupied by the last-known position of the KID (Storrar et al. 2014).

During retreat of the LIS, the western part of the Thelon Basin was blocked by ice to the east and a large pro-glacial lake formed referred to as Glacial Lake Thelon (Craig 1964). Within the Aberdeen Lake map area, maximum lacustrine submergence is observed at 210 m asl in the west and 180-170 m asl in the east (Aylsworth 1990). After the breach of the blocked outlet, post-glacial marine submergence occurred in the region. Marine limits vary across the region and within the Schultz Lake map area reported maximum elevations are at 151 m asl east of Aberdeen Lake and approximately 125 m asl north of Pitz Lake (McMartin et al. 2008). Radiocarbon dating of marine shells within the Schultz Lake map area provides a minimum deglaciation age of 6 ka BP for the region (McMartin et al. 2006). These episodes of post-glacial lacustrine and marine submergence reworked the surficial materials while creating paleo-shorelines and ice shoved ridges throughout the study area.

1.2.3 Regional Glacial History

1.2.3.1 Paleo-ice Flow Record

Central mainland Nunavut was covered by the LIS during the last glacial episode (Wisconsin) and was host to a major ice divide during the late Wisconsinan (Tyrrell 1897; Lee et al. 1957; Dyke and Prest 1987; Aylsworth & Shilts 1989; McMartin and Henderson 2004a). The early history of the LIS is still poorly constrained, but evidence for old ice flow phases in the Keewatin Sector of the LIS is recognized within the landform (Aylsworth and Shilts 1989; Boulton & Clark 1990; Kleman et al. 2002; Kleman et al. 2010), erosional (Tyrrell 1897; Lee et al 1957; McMartin et al. 2005) and stratigraphy record (Cunningham and Shilts 1977; Dredge & Thorleifson 1987; McMartin et al 2006). The two early ice flow phases identified by Kleman et al. (2010), the 'Garry' and 'Aberdeen' event swarms follow a similar ice flow trend emanating from ice domes located in northeastern Kivalliq, with the Garry swarm from a slightly more westerly position (Fig. 1-6). Based on landform cross-cutting relationships the authors suggest the Garry swarm to be older and indicative of early eastward migration of the KID in northern Kivalliq. This is similar to the erosional record which suggests early southerly ice flow phases emanating from the northeastern Kivalliq region (McMartin and Henderson 2004a). As noted by Kleman et al. (2010), the exact timing of these ice flow phases in the Keewatin Sector is poorly understood because "no chronological constraints seem to exist." Based on some LIS assumptions and correlations, Kleman et al. (2010) provide two chronological scenarios: 1. 'Garry' event to OIS 5B (~90 ka) and the 'Aberdeen' Swarm to OIS 4 (~65 ka) or 2. 'Garry' event to OIS 4 (~65 ka) and the 'Aberdeen' Swarm to OIS 3 (~ 45 ka), nonetheless, these ice flow phases are suspected to be early-mid Wisconsinan in age. Moraine clusters in southern Kivalliq indicating two ice-marginal zones that are overprinted and discordant to the later ice flow phases, the 'Ennadai Lake Moraine' (Kleman et al. 2002) and the 'Tadoule Lake' moraine cluster (Greenwood and Kleman 2010) are possible ice marginal positions for one of the early ice flow phases (Greenwood and Kleman 2010). The Wisconsinan record of the LIS is well preserved within the Hudson Bay lowlands (Dredge and Thorleifson 1987; Thorleifson et al. 1992) and suggests the presence of interstadial non-subglacial deposition during parts of the Wisconsinan and complex interactions between deposition from Keewatin and Quebec/Labrador sector derived ice flow phases. The presence of an older ('early to main') Keewatin derived till

in northern Manitoba (e.g. Dredge and McMartin 2011), suggests that early ice flows may have extended past the moraines in southern Keewatin.

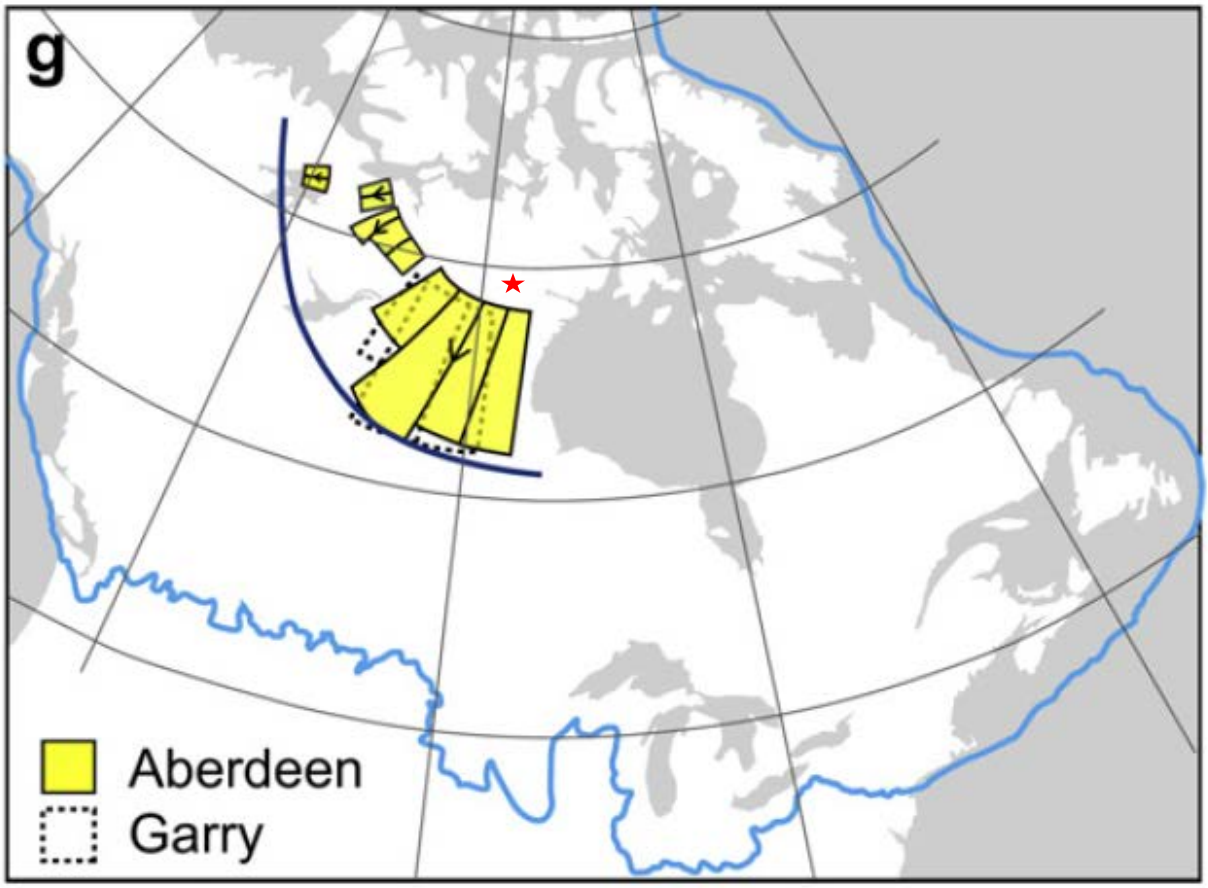

Figure 1-6: Aberdeen and Garry swarms recognized by Kleman et al. (2010). The red star denotes the location of this study. Modified from Kleman et al. (2010).

Recent modelling efforts suggest inception in Foxe Basin and the Arctic Archipelago highlands with advance into the Kivalliq region at approximately 110 ka (Stokes et al. 2012). These early ice sheets were largely thin and cold-based, likely advancing through ice creep. This initial advance of ice into the region would have been followed by ice retreat to a thin ice sheet at ~ 80 ka (OIS 5 minimum) with possible ice-free conditions in central Kivalliq and rapid growth to a large ice sheet at ~65 ka (OIS 4) which is proposed to have had a similar extent to the last glacial maximum (LGM) ice sheet (Stokes et al. 2012). In terms of the basal thermal regime of the modelled ice sheets, the ice sheets are largely cold-based during advance phases and within the study area prevailing cold-based conditions present throughout glaciation. This has implications

for till production/landform generation and would suggest that major retreat phases of the LIS in central Kivalliq were likely responsible for the majority of till production.

Following these early glacial phases a major ice flow reversal occurred with the ancestral KID migrating into central Kivalliq, resulting in northwesterly ice flow phases within the study area (McMartin and Henderson 2004a). Large north-northwesterly oriented drumlins within the Schultz Lake map area (McMartin et al. 2008) and across the Keewatin Sector (Greenwood & Kleman 2010) suggest a strong ice flow phase. Following this phase, the orientation of the KID rotated counter-clockwise resulting in a northwesterly ice flow phase and a final westerly ice flow as the KID migrated into the southeastern portion of the Schultz Lake map area (Fig. 1-7; McMartin & Henderson 2004a; McMartin et al. 2006). The configuration of the LIS from LGM to deglaciation has a much greater constraint due to the preserved landform record and significant dating efforts (Dyke & Prest 1987; Dyke et al. 2003). The deglaciation of the Keewatin Sector is characterized by the Dubawnt Lake paleo-ice stream whose landform assemblage terminus is in close agreement with the discontinuous MacAlpine moraine system (Stokes and Clark 2003).

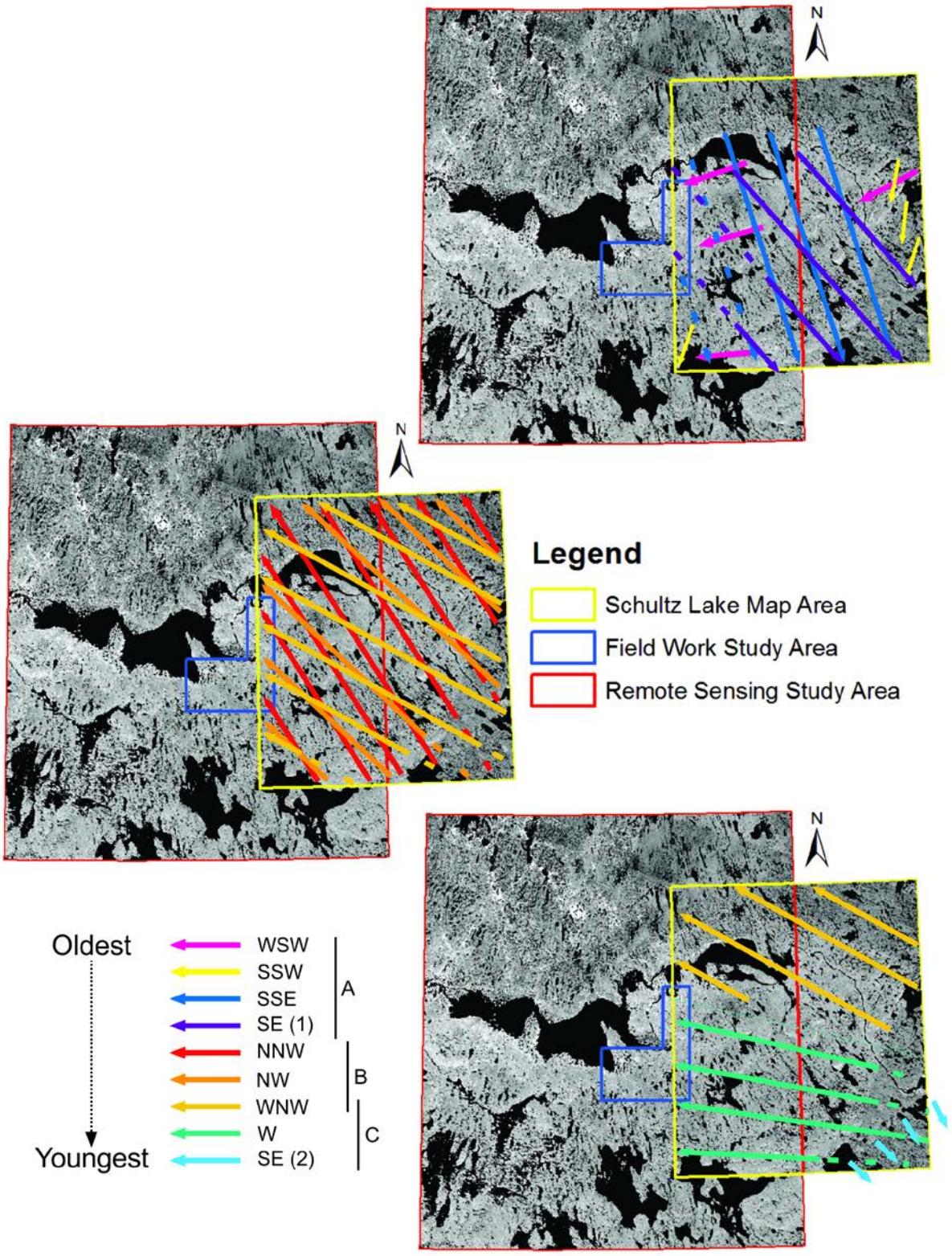

Figure 1-7: Ice flow record of the Schultz Lake map area (NTS 66A) based on the erosional and depositional glacial record in context with the regions of interest for this study. Modified from McMartin et al. (2006).

1.2.3.2 Paleo-ice Streams

Ice streams are corridors of fast-flowing ice within an ice-sheet that are responsible for the majority of ice and sediment discharge from most ice sheets (Bennett 2003). Geophysical surveys of contemporary glaciers have shown that they are capable of producing elongate subglacial landforms (King et al. 2009) and that the subglacial environment can erode and generate subglacial landforms over decadal time scales (e.g. Smith et al. 2007). Paleo-ice streams can be recognized within both the marine and terrestrial record of formerly glaciated terrains (Livingstone et al. 2012). In the geomorphic record, fast ice is thought to be recorded through the formation of subglacial landforms exceeding a length:width (elongation) ratio of 10:1, referred to as mega-scale glacial lineations (MSGL; Stokes & Clark 2002). Paleo-ice streams of the LIS are also recognized by converging flow sets with increasing landform elongation within the trunk of the paleo-ice stream (e.g. Stokes and Clark 2003) and by the presence of elongate landforms bound by hummocky moraines representing distinctive shear margins (e.g. Ross et al. 2009).

Due to the dynamic nature of these ice sheet features, recognizing and mapping of paleo-ice streams is imperative for improving paleo-ice sheet reconstruction and ice sheet models (Stokes et al. 2012). Identification of LIS paleo-ice streams is an ongoing process (Winsborrow et al. 2004; Margold et al. 2014) and many such features have been identified within the Kivalliq region. A significant landform flow set thought to be indicative of a paleo-ice stream has been documented within north-central Kivalliq (Fig. 1-8; McMartin & Henderson 2004; De Angelis & Kleman 2005). The age of the ice flow phase that created the landforms is unknown, but is proposed to indicate an onset region for the ice streams that flowed along the M'Clintock Channel and across Boothia Peninsula (De Angelis & Kleman 2005). The most notable and well documented paleo-ice stream of central Kivalliq is the terrestrially terminating Dubawnt Lake paleo-ice stream (Stokes and Clark 2003). The Dubawnt Lake paleo-ice stream operated during deglaciation of the Keewatin Sector at approximately 8000-9200 (uncalibrated) yr BP (Stokes & Clark 2003). The region of interest for this project lies within the confines of the Dubawnt paleo-ice stream and in close proximity to the north-central paleo-ice stream (ice stream #67 of De Angelis and Kleman 2005).

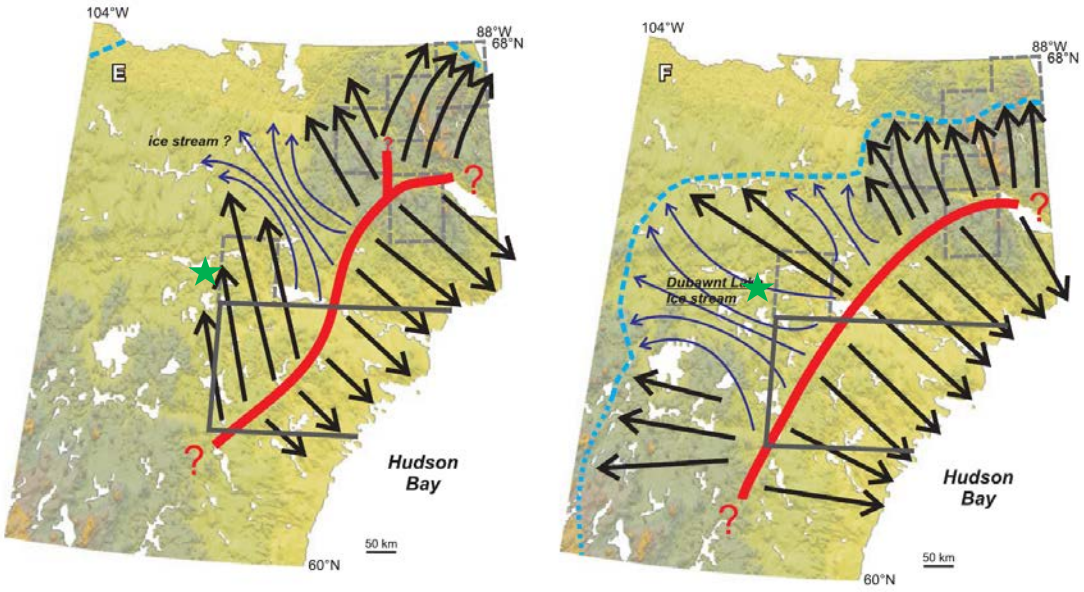

Figure 1-8: Ice streams identified within the Keewatin Sector of the LIS. The field study area of this study is denoted by the green star. Modified from McMartin and Henderson (2004a).

1.2.3.3 Quaternary Stratigraphy Record

The Quaternary stratigraphy record of central Nunavut is unknown or very poorly constrained for the majority of the region. Studies within the Kivalliq region have been limited to natural river bluff sections (Taylor 1956; Klassen 1995; McMartin and Henderson 2004b; McMartin et al. 2006; Stokes et al. 2008; Ó Cofaigh et al. 2013) or shallow drillholes (Shilts 1980; Klassen 1995) with limited coverage of central Nunavut (Fig. 1-2). Quaternary stratigraphy south of Nunavut suggests Keewatin derived till was emplaced during the Wisconsinan with evidence for shifts between Keewatin and Labradorean derived till (e.g. Dredge and McMartin 2011). The only known information regarding till stratigraphy within the Aberdeen Lake map area (NTS 66B) is that from Tyrrell (1897) who was the first scientist to explore the region and recorded detailed observations regarding the Quaternary sediments he observed along river sections during his expedition. Tyrrell (1897) explored vast regions of Kivalliq during the 1890's and within the study area provides observations regarding paleo-ice flow indicators and sediment composition around Wharton, Marjorie, Aberdeen and Schultz Lake reporting till thicknesses of up to 100 feet (~30 m).

Shilts (1980) reported results from a geotechnical pipeline transect extending from northern Ontario to Somerset Island which was later summarized by Klassen (1995) for central Kivalliq.

Near the Thelon River crossing of the pipeline transect, a multi-till stratigraphy including grey, grey-brown and pink till and waterlain sediments was present (Klassen 1995). Geochemical analysis suggests that within apparent monolithic red till, the lower parts of the drillcore appears geochemically distinct from the upper till sampled. Heavy mineral separates within a drillcore near Pitz Lake suggests that the lower portions of the drillcore has a provenance from crystalline bedrock north of the Baker Lake basin (Klassen 1995). Ni:Cu ratios support the notion of a northern provenance for the lower till as Ni:Cu ratios increase with depth suggesting a provenance derived from the Christopher Island Fm located to the north (Klassen 1995).

Klassen (1995) investigated three Quaternary sections along the Kazan River and two sections at Pitz Lake in close proximity to the last known position of the KID. Along the Kazan River three compositionally distinct till units were encountered. The upper till is a red to reddish-brown sandy diamicton characterized by its high proportion of Thelon Fm clasts relative to other Dubawnt clasts (Klassen 1995). The middle till unit is a reddish-brown sandy diamicton characterized by similar proportions of Thelon Fm and other Dubawnt Supergroup pebbles and was only observed at two out of the three sections logged. The lower till unit was observed at only one section and is a red sandy silt diamicton similar in colour, texture and geochemistry to the upper till in the other two sections. Klassen (1995) attributed the lower till to an easterly ice flow phase based on a high proportion of Dubawnt lithologies clasts relative to greenstone/plutonic lithologies and lower base metal concentrations. The middle till unit is attributed to a NW provenance (SE ice flow), north of Pitz Lake due to an absence of Pitz Fm clasts. The upper till is characterized by an abundance of Thelon Fm pebbles compared to Dubawnt, and is also attributed to a southeasterly ice flow phase. This section records the migration in orientation of the KID and thus ice flow direction from eastward to southeastward and suggests a dominant southeastward ice flow throughout the Wisconsinan (Klassen 1995). Klassen (1995) also noted compositional changes with depth occur in drillcores and stratigraphic sections even within till that appears monolithic, necessitating textural, geochemical and lithological characterization to identify till lithofacies.

McMartin et al (2006) investigated sediment exposures along the Thelon River between Schultz Lake and Baker Lake, as well as at a trench near the Meadowbank gold deposit. At four of the sections a dark greyish-brown to brown till was observed. Along the Thelon River near Baker

Lake a two till stratigraphy was observed, consisting of a reddish brown (upper unit) and pinkish grey unit. Clast lithological identification and fabric analysis from the 'brownish' till, suggests a northerly provenance, whereas the reddish till was likely derived from southerly sources (McMartin et al. 2006). McMartin et al. (2006) and Klassen (1995) found relating river section observations to drillcore observation from in the early 1980's to be puzzling, and very little correlation possible (Refer to Fig. 1-2 for locations).

Stokes et al. (2008) investigated Quaternary exposures along the Thelon River near the upstream inlet of Beverly Lake. Four to five meters of reddish, highly consolidated, matrix-supported diamicton was overlain by ~3 m of light grey normally consolidated sand and gravel (Stokes et al. 2008). The reddish diamict was interpreted to be a subglacial till with clast a-axis oriented NW-SE, likely related to last ice flow phase to the NW the region experienced.

Ó Cofaigh et al. (2013) investigated exposures of mega-scale lineations along the Finnie River, NWT. Four lithofacies were identified, with two of these interpreted as subglacial diamicts. The basal unit was a brown diamicton and was overlain by a discontinuous gravel and sand lithofacies. A red upper diamict was present and was overlain by a gravel, sand and mud lithofacies. Through till fabric analysis the authors interpreted the upper red diamict to be deposited by ice flow related to the late Dubawnt Lake paleo-ice stream and the lower brown diamict deposited by a northeasterly ice flow phase of LGM or pre-LGM age, which is opposite to what is recorded elsewhere.

1.2.3.4 Clast dispersal

The southeast Kivalliq region had extensive till sampling conducted during the 1970's by the Geological Survey of Canada (e.g. Shilts et al. 1979; Kaszycki and Shilts 1980). Sample analysis and clast lithology counts revealed a very large (>300 km) dispersal train within distinctive red surficial till containing Dubawnt Supergroup clasts extending to the coast of Hudson Bay (Fig. 1-9; Kaszycki and Shilts 1980). The Dubawnt dispersal train is thought to be indicative of a long-standing south-easterly ice flow phase (Kaszycki and Shilts 1980), or propagation into the core of the LIS of the Hudson Strait Ice Stream catchments as Dubawnt clasts can be traced to the head of the Hudson Strait (Laymon 1992; Ross et al. 2011).

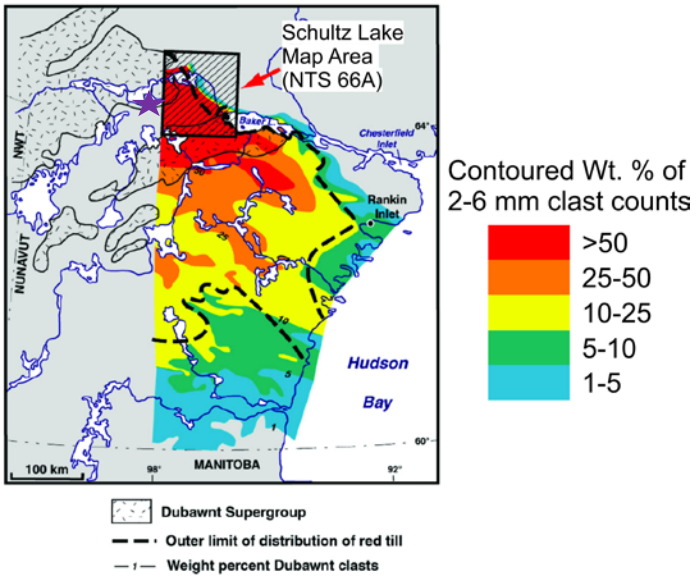

Figure 1-9: Dubawnt dispersal train extending from the Baker Lake and Thelon basins to Hudson Bay in the east and the Manitoba border in the south (Modified From McMartin et al. 2006 after Kaszycki and Shilts 1980). The location of the field study area is denoted by the purple star.

Clasts from this dispersal train are also identified in till from northern Manitoba (e.g. Trommelen et al. 2013). McMartin et al. (2006) delineated a north-westward dispersal train of Thelon Fm clasts in the Long Lake area northwest of Pitz Lake emanating from the edge of the Baker Lake basin which agrees with the local landform and striation record. The distribution of Dubawnt volcanic clasts is in agreement with the Thelon Fm dispersal within the Schultz Lake map area and attests to a north-westward dispersal signature within the surficial till (McMartin et al. 2006). McMartin et al. (2006) suggest that within the Schultz Lake map area north-westward glacial transport may be the more prominent transport direction opposed to earlier work suggesting limited north-westward dispersal (Shilts and Cunningham 1977; Klassen 1995). McMartin et al. (2006) observed differences between samples 2 km apart from a northwest and west oriented drumlin, with the westward drumlin having more locally derived Dubawnt sediments. This is the only evidence for late deglacial westward glacial transport reported in the Schultz Lake map area (McMartin et al. 2006). There is a sharp Dubawnt dispersal train boundary in the north-eastern portion of the study area, with Dubawnt derived clasts minimal recovered (< 5wt. %) outside of this boundary (Fig. 14 of McMartin et al. 2006). This boundary is observed to have a change in surficial till colour from red (Dubawnt- rich) to grey (Basement-rich) (Cunningham and Shilts 1977).

1.2.4 Knowledge gaps, important research questions, and opportunities

Knowledge gaps regarding the Quaternary geology of the region include:

- This region is documented to have a complex ice flow history through remote and ground surficial observations but we have limited knowledge regarding the depositional imprint and till production resulting from these paleo-ice flow phases. A long-standing core region of the LIS, suggests a potentially complex record from ice divide migration and the stratigraphy needs to be further characterized. Past stratigraphic studies have been largely limited to river bluffs and shallow drillholes over large distances (Fig. 1-2). Vast areas of Kivalliq with potentially thick till and multi-unit stratigraphy lies beneath the flat till plain and have remained unexplored.
- Field-based investigations within the Aberdeen Lake map area (NTS 66B) are scarce and there exists a need to build on current knowledge regarding the LIS ice flow history through paleo-ice flow indicator mapping coupled with detailed remote observations.
- Mechanisms to explain the wide-spread occurrence of thick till remain elusive and thorough documentation of till stratigraphy could shed light on possible mechanisms/relative timing of till production. For example, is the majority of till production related to early southerly ice flow phases, purely retreat phases or some combination?

Important research questions regarding this region are:

- Why is there such thick till within this region? The region of interest is postulated to have been a long-standing ice dome for most of the Wisconsinan glaciation, which is more conducive to landscape preservation than one of till production. The presence of thick till on shield terrain within a core region of an ice sheet is intriguing and can provide key information into the glacial dynamics' evolution of ice sheet core regions throughout a glacial cycle.
- What relationships exist between the large landforms occupying vast expanses of the Keewatin Sector (e.g. Greenwood and Kleman 2010) and the stratigraphic record?

Unique opportunities were presented to investigate the glacial geology of this remote region, which includes:

- Access to over 100 drillcores of continuous Quaternary sediments to bedrock from the Aberdeen Lake region provided by Cameco Corporation.
- Helicopter assisted field work to investigate the glacial record through outcrop paleo-ice flow indicator mapping and river bluff logging of Quaternary sediments.
- The collection of both surficial and subsurface Quaternary sediments and sample processing to characterize grain size distribution, clast lithology counts and geochemistry.

1.3 Thesis Objectives

Working Hypotheses:

1. Early-mid Wisconsinan ice flow phases are responsible for the thick till in the region. The study area was possibly in a more ice-marginal setting during these ice flow phases, which is more conducive for till production and these sediments were later preserved under cold-based ice conditions. This was suggested by Greenwood and Kleman (2010) and has been invoked to explain thick till sequences in north-central Sweden (Kleman et al. 2008).
2. Current ice sheet models overestimate the extent of cold-based conditions at times of thick ice in the region. For example, at LGM the study area is suspected to be cold-based, sluggish ice flow (Stokes et al. 2012). This could be due to the incapability of these models to incorporate high order ice stream dynamics into these models. It is possible that future models will show propagation of ice stream catchment areas deeper into ice sheets, such as is observed in Antarctica (Bamber et al. 2000b) and Greenland (Bamber et al. 2000a). This would allow for significant till production under a thick ice sheet in a core region of the LIS.
3. This region is an area of net deposition from a combination of southward ice divide migration and propagation of ice stream catchment areas into the study area. For example if the LIS Keewatin dome was located further to the south at times of thick ice, the extent of cold-based conditions would likely be limited for our study area allowing for warm-based conditions and till production.
4. The large Proterozoic Thelon basin played a significant sediment supply role and/or contributed to the basal thermal regime of the ice sheet. This would allow for the production of large landforms and thick drift throughout the region. The Proterozoic

Athabasca basin of the Canadian Shield is also documented to have thick drift (Campbell 2007).

The main objectives of this thesis include:

- Delineate the surficial paleo-ice flow record through landform mapping and erosional paleo-ice flow indicator mapping in the vicinity of the Aberdeen Lake map area.
    - Reconstruct the paleo-ice flow record through detailed outcrop scale mapping of erosional ice flow indicators.
    - Compare the paleo-ice flow record with the landform record and investigate implications this has for glacial dynamics of the region.
    - Relate the results to the larger context of LIS paleo-ice flow literature.
- Establish the Quaternary stratigraphy through drillcore and till section observations and compare with the surficial record to reconstruct glacial dynamics.
    - Determine the till provenance through clast lithology analysis and geochemical provenance proxies.
    - Estimate the production of successive paleo-ice flow phases in the region (i.e. are early or late ice flow phases more dominant?).
    - Compare the extent and size of depositional features associated to separate ice flow phases and to the till production of each ice flow phase identified within the stratigraphic record.
- Determine whether the surficial till sampled is reflective of the local bedrock over exploration targets or if drillcore samples are necessary to link the subsurface and surficial record for identification of potential dispersal trains.

These research objectives are designed to contribute to both academia and industry and enhance our knowledge regarding the Quaternary record of this remote region and provide a Quaternary framework for present and future mineral exploration within the region.

1.4 Methodology Overview

To understand the glacial geology of the study area and investigate sediment-landform relationships, a combination of remote, field-based and laboratory methods were incorporated. This multi-faceted approach allows for a holistic evaluation of the glacial record of the region.

1.4.1 Mapping the distribution of subglacial landforms and paleo-ice flow indicators

Remote mapping was conducted using SPOT 4/5 satellite imagery and digital elevation data (CDED) available publically from www.geobase.ca. Landform orientation and their corresponding spatial footprint were digitized in ArcGIS 10.0/10.1 software (ESRI). The resolution of the elevation data available inhibited landform height from being investigated and was useful for discerning large-scale features but not small-scale features. The elongation ratio of each mapped landform was conducted using the method of Clark et al. (2009) which involves approximating the landform footprint as an ellipse and calculating length and width using the ellipse area and perimeter that was calculated within the GIS. This calculated elongation ratio was then linked to the mapped polyline for display purposes.

During field traverses and targeted helicopter-assisted investigations, the orientation of outcrop scale paleo-ice flow indicators were mapped, with striae and grooves accounting for the majority of the observations. Paleo-ice flow indicators are often mapped to reconstruct the ice flow history of a region (e.g. Stea and Finck 2001; McMartin et al. 2005; Johnson et al. 2013) and where multiple ice flow phases were observed, the relative age of these ice flow phases was distinguished based upon cross-cutting relationships and the orientation of protected outcrop facets (McMartin and Paulen 2009).

1.4.2 Delineating till stratigraphy through logging and sample characterization

Access to Cameco Corporation drillcores consisting of Quaternary sediments allowed for a unique glimpse at the subsurface stratigraphy of this remote region. Quaternary sediments were recovered from permafrost during diamond drilling for uranium exploration and were continuous NQ (2”) diameter cores to bedrock. On average the first ~5 m of each drillcore was unrecoverable from this drilling method. Discrete intervals throughout drillcores were also not recovered, likely as a result of a change in texture that was not conducive to recovery from this type of drilling method or simply from the drilling effort. Drillcores were logged for lithology,

colour and core recovery with sediment samples taken at desired intervals throughout drillcores. Care was taken to avoid sampling poor core recovery intervals, as well as drillcore that had experienced post drilling "weathering" from exposure to the atmosphere and harsh winters during prolonged periods of storage.

Quaternary sediments were investigated along stream incised exposures south of Qamanaarjuk Lake and slumped regions were avoided. Sediments were logged for lithology and samples were taken at desired intervals to investigate the physical and geochemical properties of the logged Quaternary units present. The fabric of till units identified along till sections were investigated through the orientation (trend and plunge of the A- and B-axis) of elongated clasts (A:B axis ratio of greater than 1.5) as this can provide information regarding the ice flow direction that deposited the unit and depositional nature of the till unit (cf. Evans and Benn 2004, p. 93).

Surficial till samples were collected from mudboils, as these permafrost features are easy to sample and bring unweathered till to the surface (McMartin and McClenaghan 2001). In the few instances where mudboils were absent, till samples were collected from ~ 40-60 cm below the surface of boulder lagged drumlins. Care was taken to avoid oxidized zones within mudboils and reworked sediments within the drumlin samples.

Surficial and drillcore till samples were collected in pairs. One sample of each pair was processed for geochemical analysis of the <63 µm fraction of the till matrix at the Saskatchewan Research Council analytical labs and the other sample processed at the University of Waterloo sedimentology lab for clast counts and grain size analysis. A thorough interpretation of the geochemistry results from till sampling is beyond the scope of this thesis and is being undertaken by a second graduate student at the University of Waterloo. Geochemistry results provided within the text are strictly to support till provenance interpretations. In particular, the <63 µm results of Boron and Rubidium were the only elements utilized to demonstrate the proportion of a rock formation within till. Rubidium was determined by ICP-MS after a total digestion using a $HF\text{-}HNO_3\text{-}HClO_4$ solution. Boron analysis was conducted using ICP-OES following a pulp fusion with $NaO_2/NaCO_3$.

Till samples that were processed in the Sedimentology lab at the University of Waterloo were first dried and sieved into >8, 4-8, 2-4 and <2 mm fractions. The proportion of silt and clay

within till matrix studies is known to affect geochemistry results (e.g. Shilts 1995), which necessitates determination of the proportion of silt and clay within the till matrix of each sample. A sample of the <63 µm fraction was obtained by quick sieving the <2 mm portion to obtain approximately 2-3 grams of material for determination of the proportion of silt and clay using a laser grain size diffractometer, the Fritsch Analysette 22 MicroTec Plus following an overnight distillation in a 4% sodium metaphosphate solution to disaggregate clay particles. The proportion of sand sized particles within till matrix was determined for select samples using wet sieving techniques for till characterization purposes.

In order to investigate the provenance of till lithofacies identified through drillcore logging, the pebble (4-8 mm) and granule (2-4 mm) fraction of drillcore samples were further washed in an ultrasonic bath to remove any till matrix residue and classified according to the lithology classes listed in Appendix E. Drillcore samples were restricted in size and often had an insufficient quantity of pebbles recovered and the granule fraction was analysed in this case. Surficial samples recovered a sufficient quantity of the pebble fraction for till lithology classification. In many cases there were too many pebbles recovered from surficial samples and a sample splitter was used to separate approximately 30 grams (n =100-150) of pebbles to be classified. All till matrix colours are expressed using standard Munsell colour codes and till matrix colours presented within the following text were classified from dried till matrix samples within the lab setting to be eliminate bias attributed to moisture content.

Drillcore logs presented within the following chapters were generated using CorelDRAW X6 and depths were corrected to eliminate the effect of the drilling angle and thus indicate depth below ground surface opposed to depth along drillcore. Subsurface drillcore data was processed using GoCAD software and cross-sections were exported and edited using CorelDRAW X6 for presentation purposes.

1.4.3 Investigating sediment-landform assemblages

Relating observations of the surficial geomorphology to the Quaternary stratigraphy can provide insight into the till production and the relative vigour between ice flow phases. This has a large effect on glacial dispersal, and thus the identification and understanding of dispersal trains. This study allows for a holistic evaluation relating the size of remotely mapped landforms to the suspected till production of the ice flow phase that produced the landforms. Paleo-ice flow

events are also often recognized within the erosional record, but may not have a preserved landform imprint. In this case, paleo-ice flow features mapped at the outcrop-scale are related to the till provenance identified based on clast lithology to assess the preserved imprint of these ice flow phases within the till stratigraphy record.

1.5 Thesis Structure

This thesis includes a thesis abstract, an introduction chapter (Ch. 1), two chapters designed as a two part publishable manuscript (Ch. 2 and 3) and a conclusion chapter (Ch. 4). The first chapter provides a framework for the thesis introducing the research problem, main goals and research methods as well as providing a review of relevant literature to the study region. The thesis is part of a joint collaboration research project designed and organized by Dr. Martin Ross and involves a second masters level graduate student, Aaron Bustard as well as several undergraduate students.

Chapter two is co-authored with supervisor Dr. Martin Ross and was produced as a Part 1 paper investigating the surficial paleo-ice flow record. A landform map is produced and the rationale behind producing the map and an explanation of the main features observed within the region is provided as well. Observations of field-based paleo-ice flow indicators are discussed and the ice flow history for Aberdeen Lake region discussed. Results of the landform mapping are compared with field-based evidence and the glacial history of the study area is discussed. Field work was supported by Cameco Corporation and conducted with Dr. Martin Ross (2012 & 2013), Aaron Bustard (2013) and Rosalind Menzies (2012 field assistant) through the 2012 and 2013 field season. I was responsible for the remote mapping of the glacial features, jointly involved in field-based sample and data collection, interpretation, presentation and writing.

Chapter three investigates the Quaternary stratigraphy of the southeast Aberdeen Lake region and is co-authored with supervisor Dr. Martin Ross. Surficial sample collection, drillcore logging, drillcore sampling and till section investigations were conducted during the 2012 and 2013 summer field seasons with Dr. Martin Ross, Rosalind Menzies, Aaron Bustard and myself. Till fabric measurement were conducted by Dr. Martin Ross, Aaron Bustard and myself. I was responsible for interpretation and presentation of the till fabric data. All of the 4-8 mm clast counts conducted on till samples were conducted by myself and 34/126 clast counts conducted on the 2-4 mm fraction were conducted by Aaron Bustard. I was responsible for interpreting till provenance results, till stratigraphy as well as drillcore logs and cross-section production.

Sieving of till samples and laser grain size analysis was conducted by lab assistants Caroline Karubin and Fidele Ntamwemezi for 2012 samples and supervised by myself. Till samples

collected during the 2013 field season were processed by Aaron Bustard and myself. I was responsible for wet sieving analysis of selected samples.

Chapter 2 : Glacial record of a thick drift region on the Canadian Shield, core of the Laurentide ice sheet: 1. Paleo-ice flow history and geomorphology

2.1 Introduction

Central Kivalliq, mainland Nunavut was located in a core region of the Laurentide Ice Sheet, whose glacial record show evidence of ice divide translocation (Lee et al. 1957; Dyke and Prest 1987; Aylsworth and Shilts 1989; McMartin and Henderson 2004a), but also thick till blanket and landforms that may have developed during either advance or major retreat ice margin phases. The map (Appendix A) associated with this text displays the detailed location and orientation of streamlined subglacial landforms over a broad area northwest of the last known position of the Keewatin Ice Divide (KID; 63°45’ – 65°15’ N, 97°0’ – 100°0’ W). Previous glacial lineation mapping within the study area has been conducted through air photo interpretations with limited ground observations (Aylsworth 1989; Aylsworth et al. 1989; Aylsworth 1990; Aylsworth et al. 1990), detailed air photo interpretation and extensive field observations in the eastern part of the mapping area (McMartin et al. 2008), remote observations of the Dubawnt Lake paleo-ice stream using Landsat imagery (30 m multispectral resolution, 15 m panchromatic resolution; Stokes et al. 2013) and from remote observations at a scale of 1:100 000 or greater (De Angelis 2007; Greenwood and Kleman 2010). Despite this mapping effort, the current surficial geology map of Aberdeen Lake is devoid of large northerly oriented lineations that were identified by Greenwood and Kleman (Group 1 Landforms; 2010), which is likely due to the immense size of these landforms which are not readily identified via air photos. Landform mapping conducted by De Angelis (2007) portrays the general landform trend across the region and is a great tool for understanding the regional landform record; however, the large scale at which mapping was conducted did not allow for the mapping of individual landforms and the current surficial geology map is also absent of large lineaments identified by Greenwood and Kleman (2010) south of Aberdeen that is addressed by this map. Remote landform mapping is supplemented by field-based observations of erosional outcrop scale paleo-ice flow indicators

and glacial dispersal of detritus (Ch. 3), which is commonly undertaken to reconstruct dynamics and evolution of past glacial phases (e.g. McMartin et al. 2006; Trommelen et al. 2013).

The purpose of this map is thus to build on existing maps derived from air photo interpretation and large-scale satellite imagery mapping by supplementing these maps with detailed satellite imagery interpretation. Further field-based mapping of paleo-ice flow indicators and compilation of historical data provides further information regarding the surficial record within the region. GIS-based mapping of the individual landforms also allows the calculation of their statistical characteristics (Clark et al. 2009). This has been partially completed for some aspects of the study area by Stokes et al. (2013) but this study was only concerned with streamlined landforms that are associated with the Dubawnt Lake paleo-ice stream and not of all the glacial lineations present within the area.

2.2 Physiography and Regional Geology

The region of interest is underlain by continuous permafrost with surficial drainage primarily through the Thelon River into Hudson Bay, with some far northern reaches of the map area draining through the Back River into the Arctic Ocean. The region is of low relief, ranging from 72 - 304 m asl, with highlands scattered throughout the study area (Fig. 2-1).

Streamlined “soft-bedded” (sediment) landforms are plentiful throughout the study area and vary in size, with landforms of ‘mega-scale’ classification rather common (Greenwood and Kleman 2010; Stokes et al. 2013). Large eskers are present emanating from the KID (Aylsworth and Shilts 1989; Storrar et al. 2013) and ribbed moraines are present in distinctive fields throughout the region (Aylsworth and Shilts 1989; De Angelis 2007). Despite the relatively continuous cover of till in the study area, bedrock outcrops occur in some areas. The study area is underlain by the Archaen Rae Domain of the Canadian Shield, which primarily consists of meso- to neo-Archean rocks metamorphosed to various degrees and containing outliers of folded sedimentary cover, post-tectonic igneous suites and overlying basins of Proterozoic age throughout the region (Hoffman 1988).

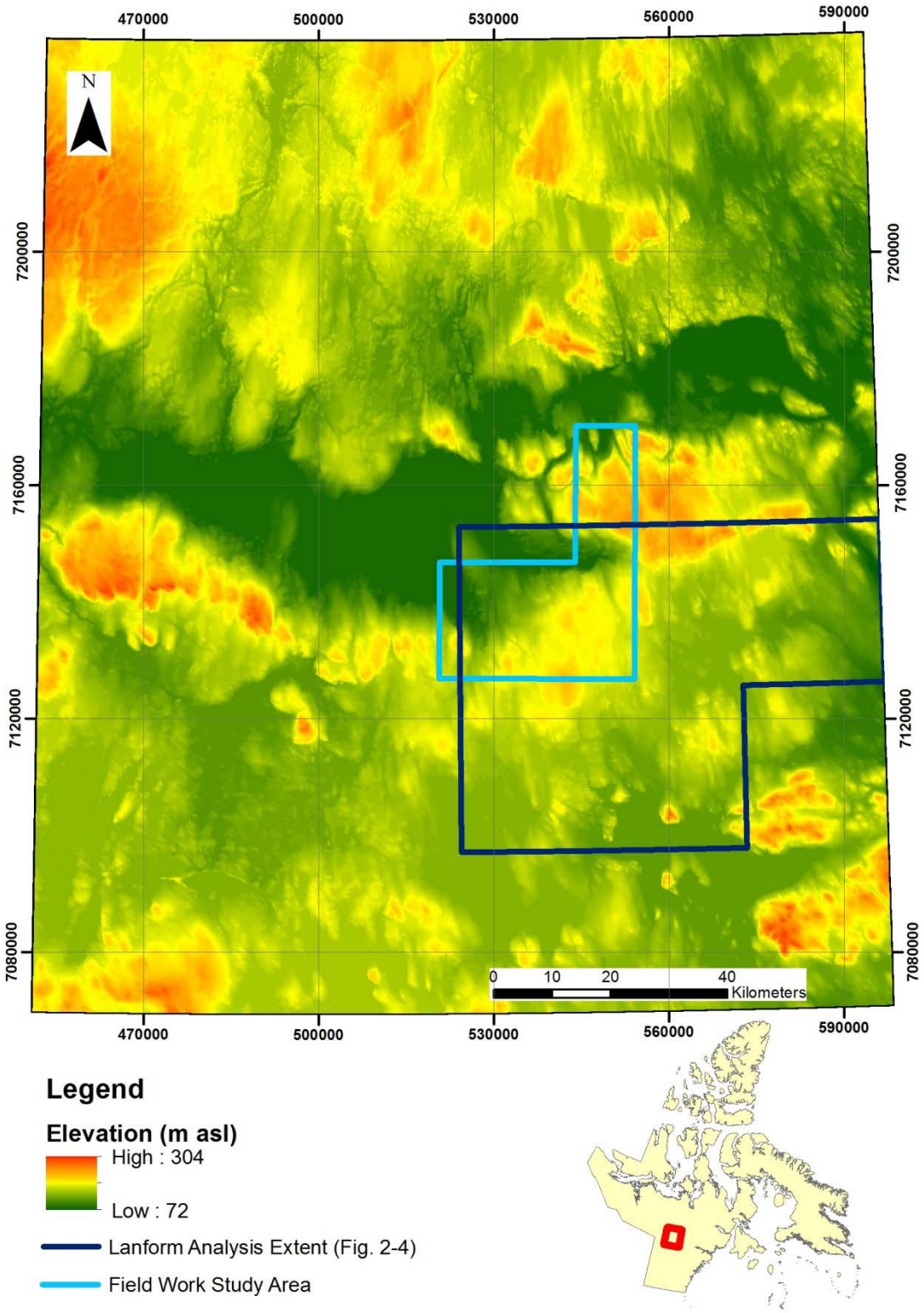

Figure 2-1: Elevation of the remote mapping study area. Relief is generally low ranging from 72-304 m asl. The inset map is of Nunavut Territory, Canada. The field work study area (light blue) and landform analysis (dark blue) extents are indicated.

2.3 Glacial History

Central mainland Nunavut, like most of Canada, has been repeatedly glaciated throughout the Quaternary (Ehlers et al. 2011) and experienced a complex ice flow history during the Wisconsinan glaciation from the KID migration (e.g. McMartin and Henderson 2004a). The landform record of inferred early (pre late-Wisconsinan) ice flows are a result of southerly ice flow phases when the KID was located in northern Kivalliq (Boulton & Clark 1990; Kleman et al. 2002; McMartin and Henderson 2004a; Kleman et al. 2010). During the late Wisconsinan, the KID was southeast of Aberdeen Lake and thus landforms that formed during this period are primarily oriented north, northwest and west (Aylsworth and Shilts 1989; McMartin and Henderson 2004a; McMartin et al. 2008).

Northeast of the study area, there is convincing evidence for a paleo-ice stream (McMartin and Henderson 2004a; De Angelis and Kleman 2005). The age of this paleo-ice stream is unknown, but tentatively proposed to be an onset region for the paleo-ice streams that flowed along the M'Clintock Channel and across Boothia Peninsula (De Angelis and Kleman 2005). During the demise of the LIS, the terrestrial terminating Dubawnt Lake paleo-ice stream was active (Stokes and Clark 2003) and resulted in a strong deglacial westerly overprint in the landform record south of Aberdeen Lake (Stokes et al. 2013).

2.4 Methods

Remote sensing and digital elevation data were used for mapping. SPOT 4/5 panchromatic satellite imagery (10 m resolution, www.geobase.ca) and multispectral imagery (20 m resolution, www.geobase.ca) were the main images utilized for mapping purposes. Google Earth (Landsat 8) images were occasionally used to cross-check mapped landforms. Digital elevation data (8-23 m resolution, www.geobase.ca) was compiled into a mosaic for the study area and used to assist in identifying large-scale features. All mapping was conducted in ESRI ArcMAP 10.1 and figures output through CorelDRAW. False-colour images were generated using SPOT 4/5 multispectral bands 3, 2, 1 (R, G, B) and the pan-sharpening function in ArcMAP utilized to increase the resolution to that similar of the Panchromatic imagery. Examples of the imagery used are exhibited in Fig. 2-2. Regions that were primarily bedrock terrain (left side of Fig. 2-2 B) were mapped out using false-colour imagery in consultation with existing surficial geology maps of the map area.

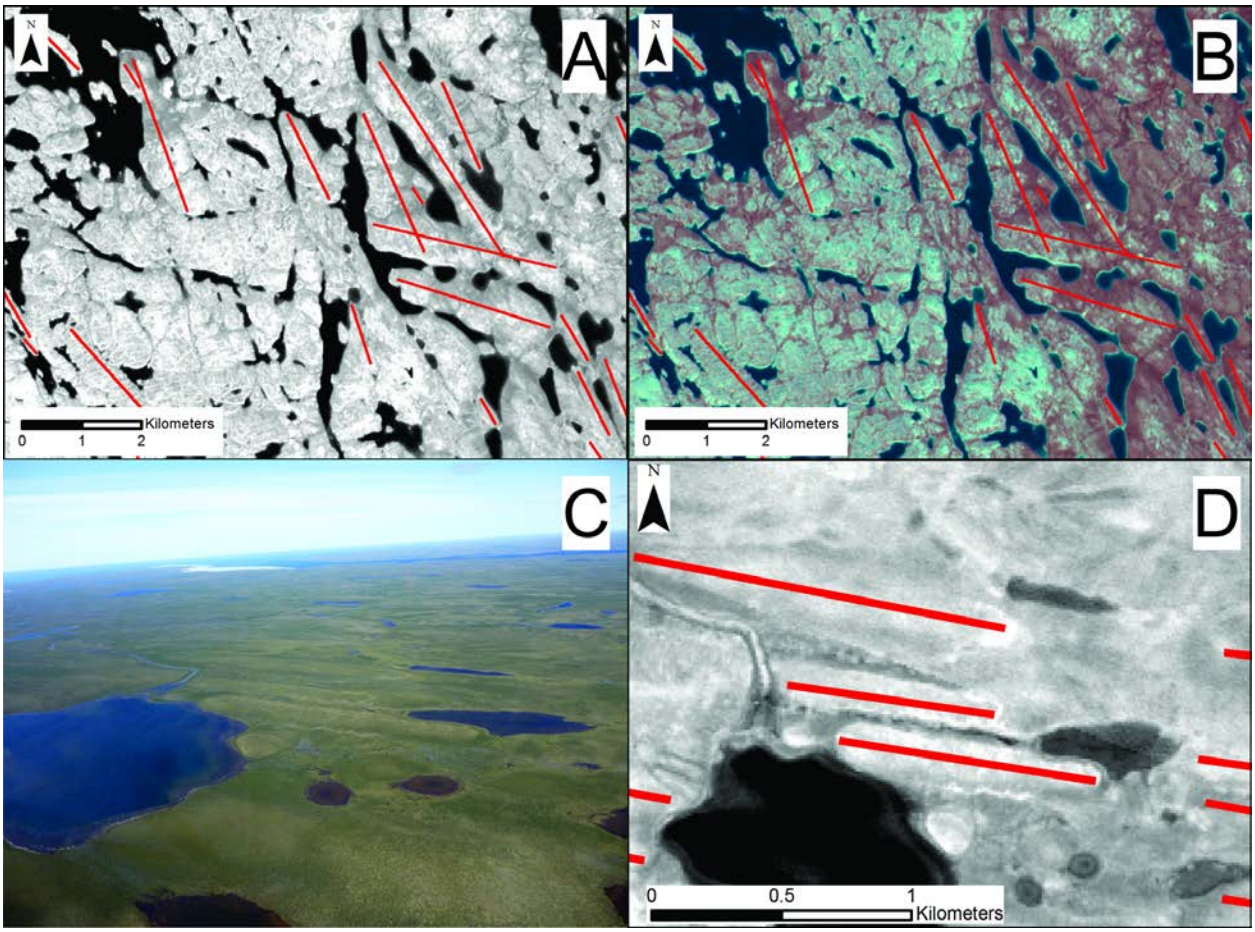

Figure 2-2: Example of the satellite imagery used for mapping landforms. A. Panchromatic SPOT 4/5 imagery. B. Corresponding false-colour image of A generated using SPOT 4/5 imagery. Note the false-colour imagery allows for better distinguishing bedrock terrain (light-tone) in the west from till blanket terrain (darker pink-red) in the east of the image where streamlined landforms are also better developed. C. Aerial photography of drumlins present. D. Corresponding SPOT4/5 imagery of C exhibiting mapped drumlins. Image centered at 7134258N, 540274E, UTM Zone 14N, NAD83.

Landforms that were mapped include sediment drumlins, rock drumlins and crag and tail features. Landforms were mapped by digitizing a polyline along the crest of the landform and mapping their spatial footprint by polygon. This allowed for parameters such as lineation azimuth, perimeter and area to be calculated using ArcGIS, which allowed for the length and width of each landform to be calculated using the ellipse approximation method of Clark et al. (2009). Mapping was conducted at a scale of 1:20 000 to 1:30 000 and larger landforms were mapped at a scale of 1:80 000 to 1:100 000.

Paleo-ice flow indicators are often mapped to reconstruct the ice flow history of a region (e.g. Stea and Finck 2001; McMartin et al. 2005; Johnson et al. 2013). Outcrops encountered during

surficial sampling traverses were investigated as well as targeted outcrops of interest. Erosional outcrop-scale paleo-ice flow indicators such as striae, grooves and crescentic gouges were mapped. The orientation of streamlined outcrops (i.e. small whalebacks and *roches moutonnées*) was also noted. Many encountered outcrops exhibited multiple paleo-ice flow indicators and the relative chronology of these ice flow phases was deciphered using the cross-cutting relationships of facets and striae (e.g. McMartin and Paulen 2009). The associated map displays new observations from this study as well as those published from past field-based studies conducted within the mapped region (Tyrrell 1897; Aylsworth 1990; McMartin et al. 2005).

Due to being limited to only remote sensing data without the support of air photos, the purpose of the map is to provide an overview of the streamlined subglacial landforms present and not meant to be representative of all of the subglacial landforms present.

2.5 Results

2.5.1 Streamlined Landform Mapping

A total of 5 757 streamlined landforms have been mapped over the remote sensing study area study area (Appendix A; Fig. 2-1; ~ 24 000 sq. km). These landforms are interpreted to have formed in the subglacial environment parallel to ice flow. Across the entire map area a complex relationship is observed whereby large km-scale landforms are overprinted by smaller northwest and westerly landforms. These ‘megascale’ landforms, originally identified by Greenwood and Kleman (2010), occupy a large region of Kivalliq, including across this entire map.

In the eastern part of the map area, large km-scale NNW landforms are the dominant glacial lineations present (Fig. 2-3 B, D). These landforms are commonly over-printed by smaller NW oriented landforms in the northern and southeastern portions of the map (e.g. Fig. 2-3 B, C). In the northwest a complex landform pattern exists, whereby large km-scale N-S oriented and large NW-SE landforms are present, with no obvious cross-cutting relationship evident (Fig. 2-3 A). Some of these lineations could be part of the Aberdeen and/or Garry flowset recognized by Kleman et al. (2010). Within the field study area (Fig. 2-3 C) there are three identifiable ice flows recorded in the landform record: NNW, NW and W. The NNW landforms are much larger in size and are overprinted by the later NW and W ice flow phases.

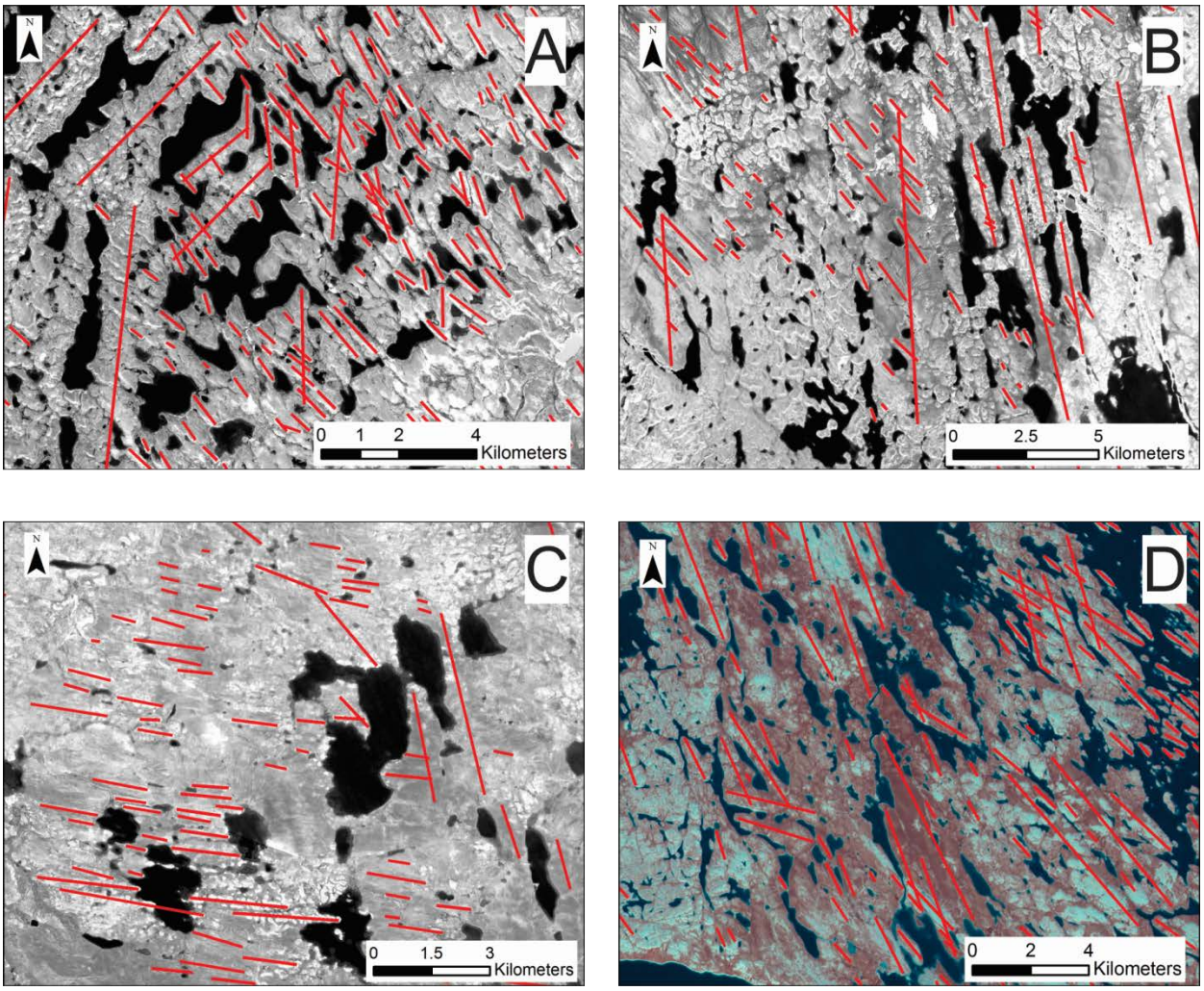

Figure 2-3: Examples of landforms found within map area. Background imagery is SPOT 4/5 imagery panchromatic (A-C) and false colour (D), landforms are indicated by the red polyline. A. Complex landform assemblage in the northwest part of the map. Early N-S and NE-SW oriented landforms are overprinted by later NW oriented landforms. B. Large northerly oriented lineations are over-printed by later NW lineations. C. Landform assemblage over the Tatiggaq uranium prospect (Ch. 3). NNW landforms are overprinted by NW and late W landforms. D. Thin drift area with a complex landform assemblage. NNW landforms are over printed by later NW and W landforms.

2.5.1.1 Landform statistical characteristics

As discussed, in the field study area there are three identifiable ice flows recorded in the landform record: NNW, NW and W. As depicted in Fig. 2-3 C, the NNW landforms are much larger in size and are overprinted by the later NW and W ice flow phases. In order to quantitatively assess the landform characteristics, a sub-region of the map produced was selected (Fig. 2-4) where older NNW landforms are present as well as later NW and W. This region is also absent of SE landforms recognized by McMartin et al. (2008). A 320° landform azimuth

cut-off was used to segregate mapped landforms into two populations consisting of NNW oriented landforms and NW/ W oriented landforms.

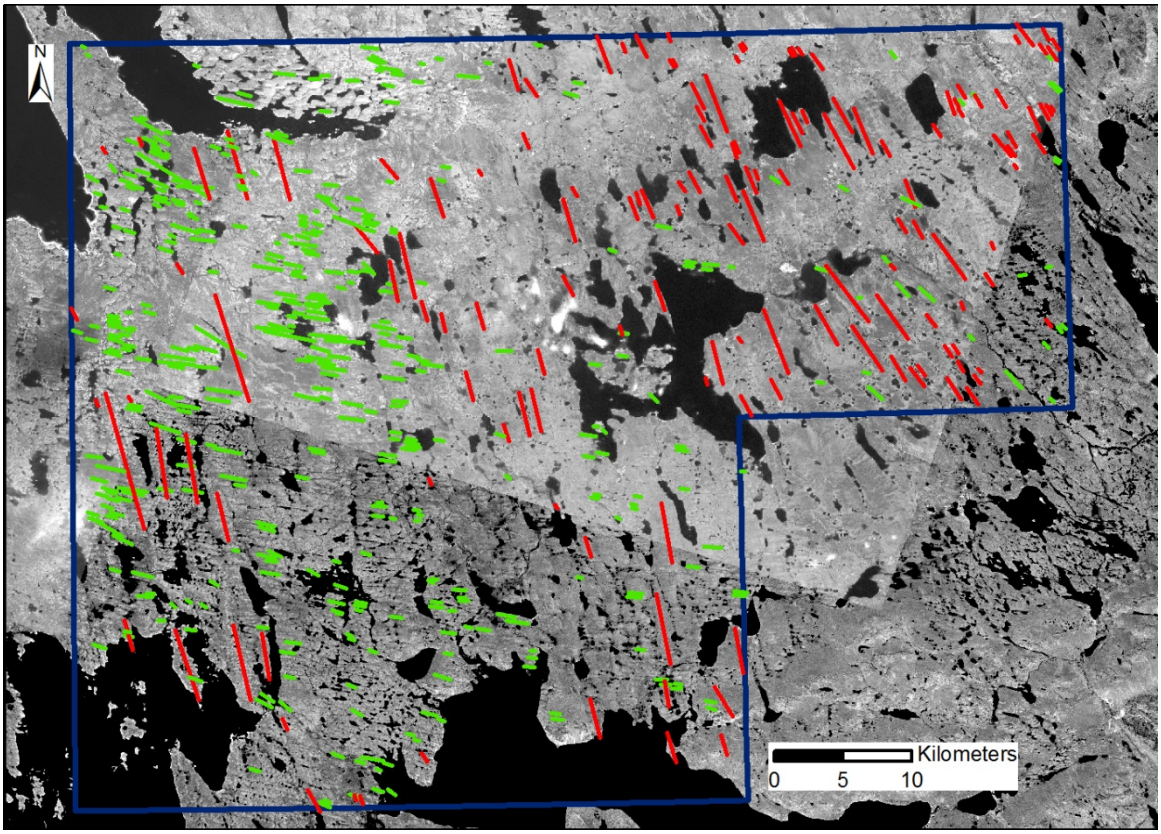

Figure 2-4: Region of glacial lineament statistical analysis. Glacial lineaments are classified according to their segregated population used to calculate landform statistics. Red lineations have an orientation greater than 320°, green lineations less than 320°.

Results show that there is some clear overlap between the two populations, which is expected due to this crude method of separating landform populations; however, there is still a definitive relationship visible. A comparison between the spatial footprint (area) size and the elongation ratio of these two populations confirms that the NNW landforms have a larger spatial footprint on average, but do not exhibit a wide range of elongation ratios, with the majority of the landforms in the 2 - 4 range (Fig. 2-5). The northwesterly and westerly landforms have a wide range of elongation ratios, and generally have a smaller footprint.

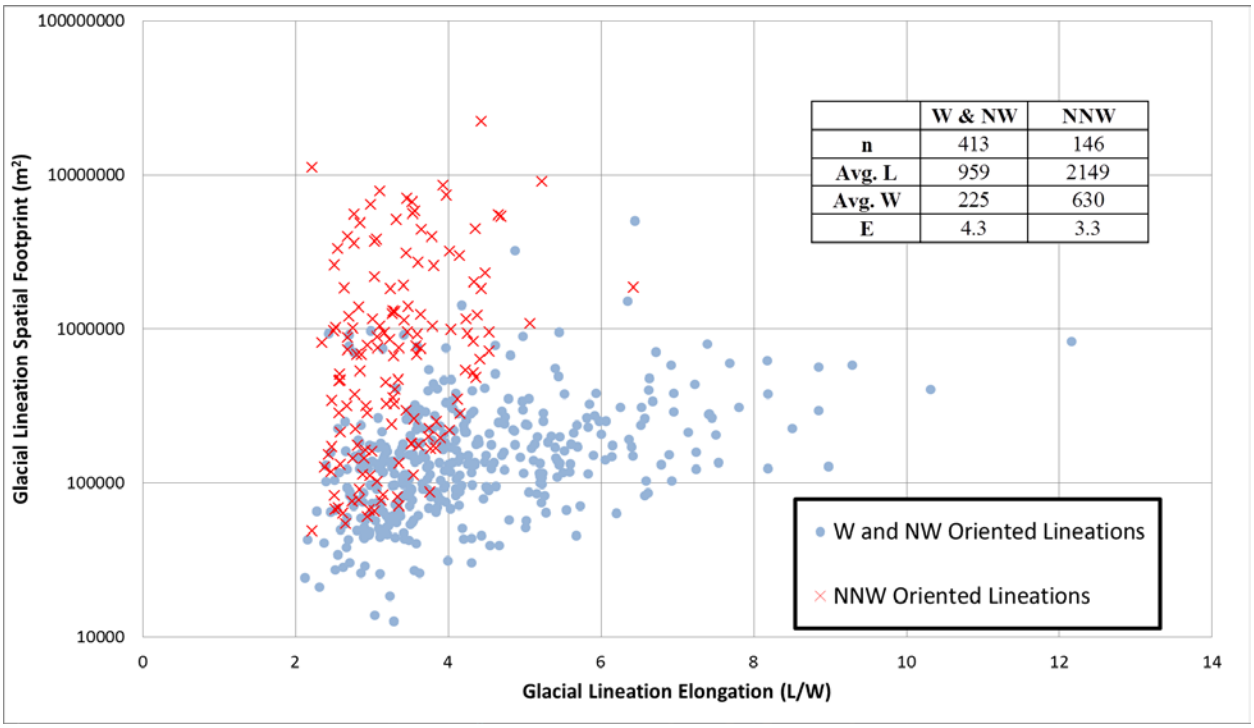

Figure 2-5: Statistics of mapped landforms presented in Fig. 3-7. The calculated landform statistics are summarized in the top right corner of the figure.

Clark et al. (2009) found that the average elongation ratio of drumlins in Britain and Ireland from a large data set (n=37 033) was 2.9 with average landform width and length of 209 m and 629 m, respectively. A comparison with their results shows that the NNW landforms have a very similar average elongation ratio but have a much larger width and length. The NW and W oriented landforms have a similar width, but have a larger length and thus elongation ratio. This is likely due to the incorporation of mapped MSGL's within the region, which are related to the Dubawnt paleo-ice stream flow set, since this region is interpreted to be an on-set region for the paleo-ice stream.

2.5.1.2 Field Area Subglacial Record Variations

Westerly oriented landforms south of Aberdeen Lake (e.g. Fig. 2-3 C) are attributed to the deglacial Dubawnt paleo-ice stream (Stokes and Clark 2003). The northern lateral boundary of this paleo-ice stream has not been distinguished due to the lack of a distinct lateral shear margin (Stokes and Clark 2003). The continuity of similar oriented landforms could represent more of a gradational boundary in this case or lateral migration. The landform and erosional record

southeast of Aberdeen Lake exhibits two varying landscapes within both the erosional and depositional record, suggesting a variable subglacial dynamics record.

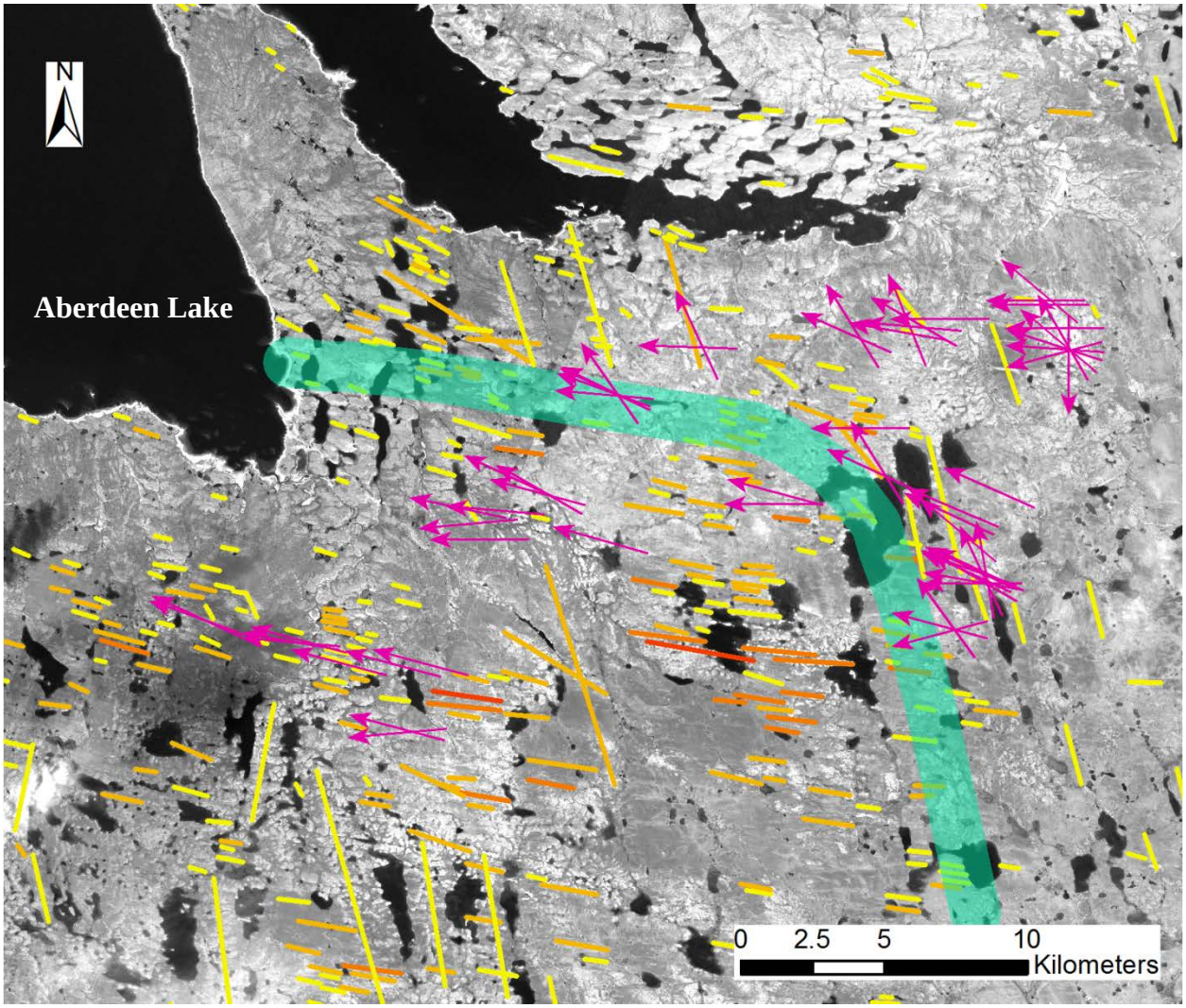

Figure 2-6: Varying glacial record southeast of Aberdeen Lake. Lineations denote mapped landforms, with red and deep orange lineations representing mega-scale lineations. Pink arrows indicate outcrop paleo-ice flow observations, relative age relationships are discussed within the following text. The thick turquoise line denotes an approximate interpreted boundary between two varying landscapes. To the north and east, the landscape contains a higher preservation of older landforms and multiple paleo-ice flow indicators exhibited on outcrops. West of the line the deglacial westerly ice flow phase is more prominent.

From Fig. 2-6, it is evident that all of the outcrops that exhibited multiple paleo-ice flow indicators are concentrated to the north and east of the turquoise line, where they had greater preservation from the deglacial westerly ice flow phase. It was noted in the field that more to the west in the field area investigated, the outcrops generally only exhibited indicators reflecting the last paleo-ice flow phase the region experienced and these outcrops are very well moulded with

meter-scale striae (e.g. Fig. 2-8 E). These observations spatially agree with the landform record as the landscape east of the turquoise line is largely composed of NNW and NW oriented landforms, with some minor W oriented landforms. Within this region the westerly oriented landforms have an average azimuth of ~280°, whereas lineations to the west of Fig. 2-6 in the trunk of the paleo-ice stream are oriented ~295°-300° which attests to convergent ice flow as you travel westward. The presence of mega-scale glacial lineations within the region defined by Fig. 2-6 suggests fast ice flow as well (Stokes and Clark 2002), which likely had a high subglacial vigour and subsequent erosive potential, remoulding the outcrops and eliminating erosional evidence of previous ice flow phases.

2.5.1.3 Northerly landform record

Mapping of the large-scale north-south oriented landforms across the Aberdeen Lake region has exhibited the presence of a large-scale northward converging landform pattern (Fig. 2-7), which is also evident on the DEM for the region (Fig. 2-1). The presence of these landforms continues north of the study area into Chantrey Inlet (Greenwood and Kleman 2010) and is also apparent south of the mapped region. Erosional and depositional evidence for this ice flow phase is widespread across the mapped region (Aylsworth 1990; McMartin et al. 2005; McMartin et al. 2006; McMartin et al. 2013; this study).

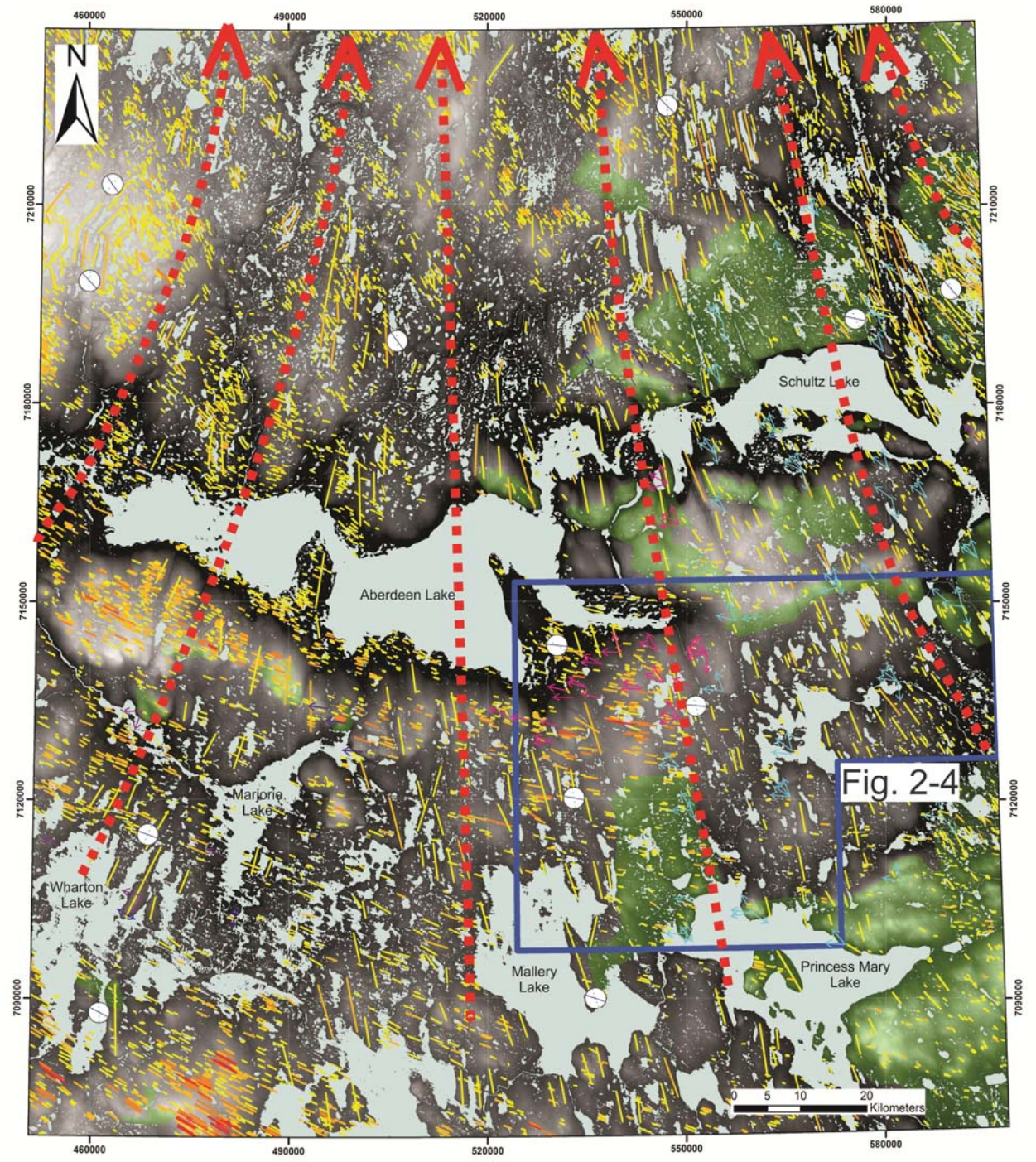

Figure 2-7: The map produced exhibits an apparent convergence of large landforms that are overprinted by later NW and W oriented landforms. Note striae observations near Majorie and Wharton Lake suggest a NNE-SSW paleo-ice flow phase and southeast of Aberdeen Lake a strong NNW paleo-ice flow phase. Lineation colour corresponds to landform elongation (Yellow as low and red as high, refer to Appendix A).

2.5.2 Paleo-ice flow Indicator Mapping

Striae and grooves account for the majority of the outcrop paleo-ice flow observations (77/83 paleo-ice flow indicators). Examples of field-based ice flow indicators mapped are presented in Fig. 2-8 below. An interesting feature encountered during field observations was the presence of large elongated boulders at surface. These boulders had parallel striae on their top surface, which were oriented with the a-axis of the boulder, and a till carapace along the edges of the boulder (Fig. 2-8 A). These boulders are oriented parallel to the last known ice flow phase defined by outcrop striae, suggesting they are lodged boulders within the till plain protruding from the surface and likely a result of the last known ice flow phase over the area. Large quartz clasts within Thelon Fm conglomerate outcrops proved to be useful ice flow indicators as they were commonly striated with better preservation than the rest of the outcrop surface (Fig. 2-8 B). It was also discovered that these clasts can provide insightful directional and relative age indicators. An example of this is a quartz clast that exhibited the appearance of a mini *roche moutonnée*, with the stoss side well-polished and the lee side plucked indicating an old WSW ice flow phase, also preserved on nearby quartz clasts (Fig. 2-8 C). Definitive age relationships were also deciphered from outcrops, such as Fig 2-8 D, where striae associated with an older NNW ice flow are preserved on a facet protected from a subsequent westerly ice flow phase. In the western region of the field area, outcrops were well polished with meter scale striae/grooves and many outcrops were moulded into small-scale *roche moutonnée* (Fig. 2-8 E). Fig. 2-8 F provides an example where all of the ice flow records encountered at other stations were preserved on one outcrop. The outcrop was a mafic dyke within a felsic host rock and contained a plethora of paleo-ice flow indicators on the fine-grained dyke. This outcrop was the only outcrop encountered where evidence of a southerly ice flow phase was distinguished. All of the ice flow indicators mapped during field traverses are depicted on Fig. 2-9.

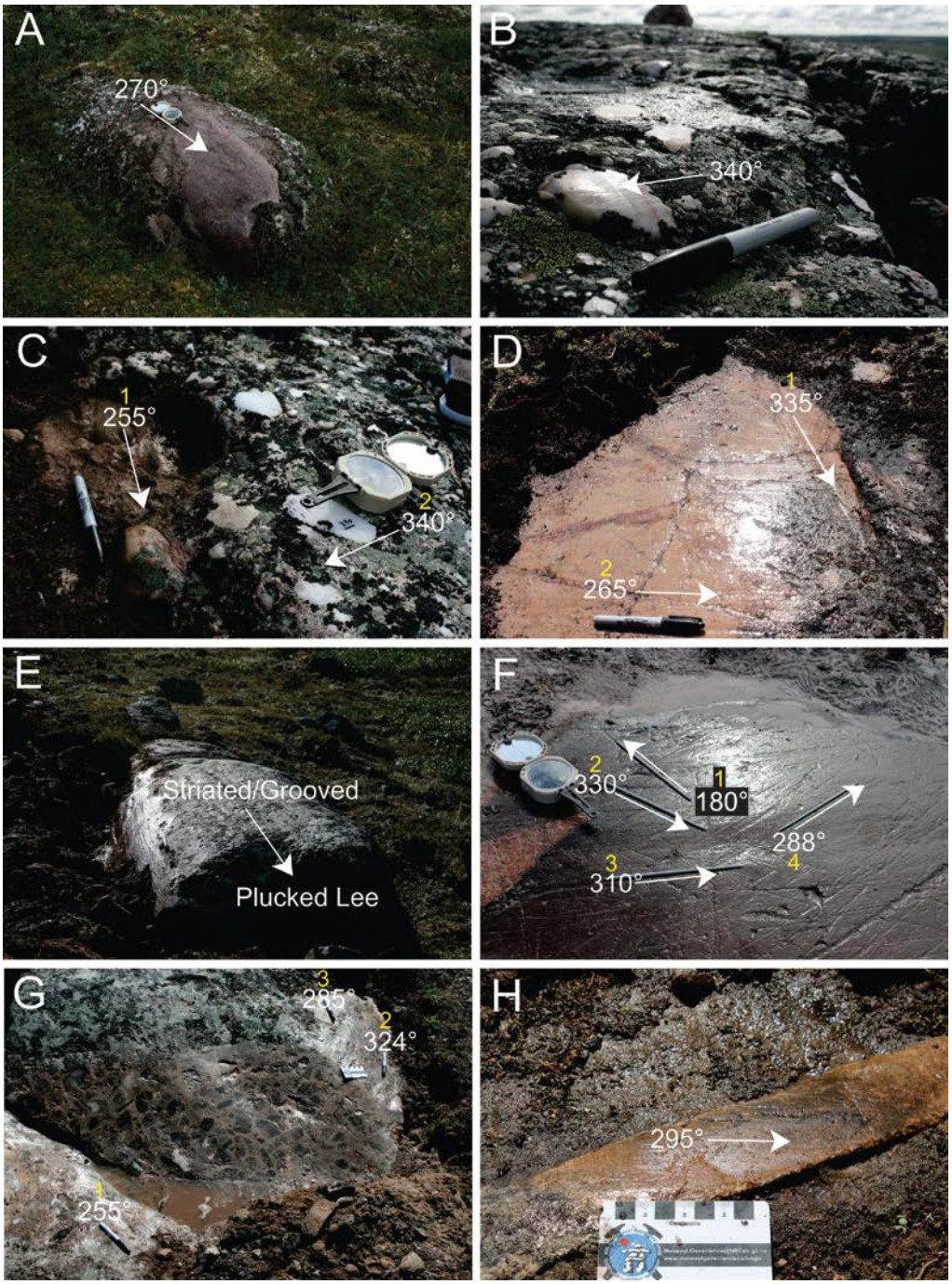

Figure 2-8: Examples of field-based ice flow indicators observed. A. Lodged boulder at the surface of a till plain with parallel striae on its surface indicating the last ice flow the area experienced (270°). B. Striated quartz pebbles within the Thelon Formation indicating NNW (340°) ice flow. C. Pebble within the Thelon Fm that has been eroded into a mini *Roche moutonnée* indicating ice flow towards the WSW (255°). A quartz pebble nearby shows evidence for the same ice flow and a later NNW (340°) ice flow. D. Cross-cutting relationship where the older flow (335°) is protected from the later westerly (265°) ice flow. E. Meter-scale striae and grooves on a westerly-oriented *Roche moutonnée*. F. Mafic dyke preserving a variety of ice flow indicators and ice flow phases. Indicators include striae, grooves, nailhead striae, crescentic gouges. G. Outcrop with three ice flow phases preserved on facets H. Striations preserved on a more resistant vein indicating NW ice flow (295°).

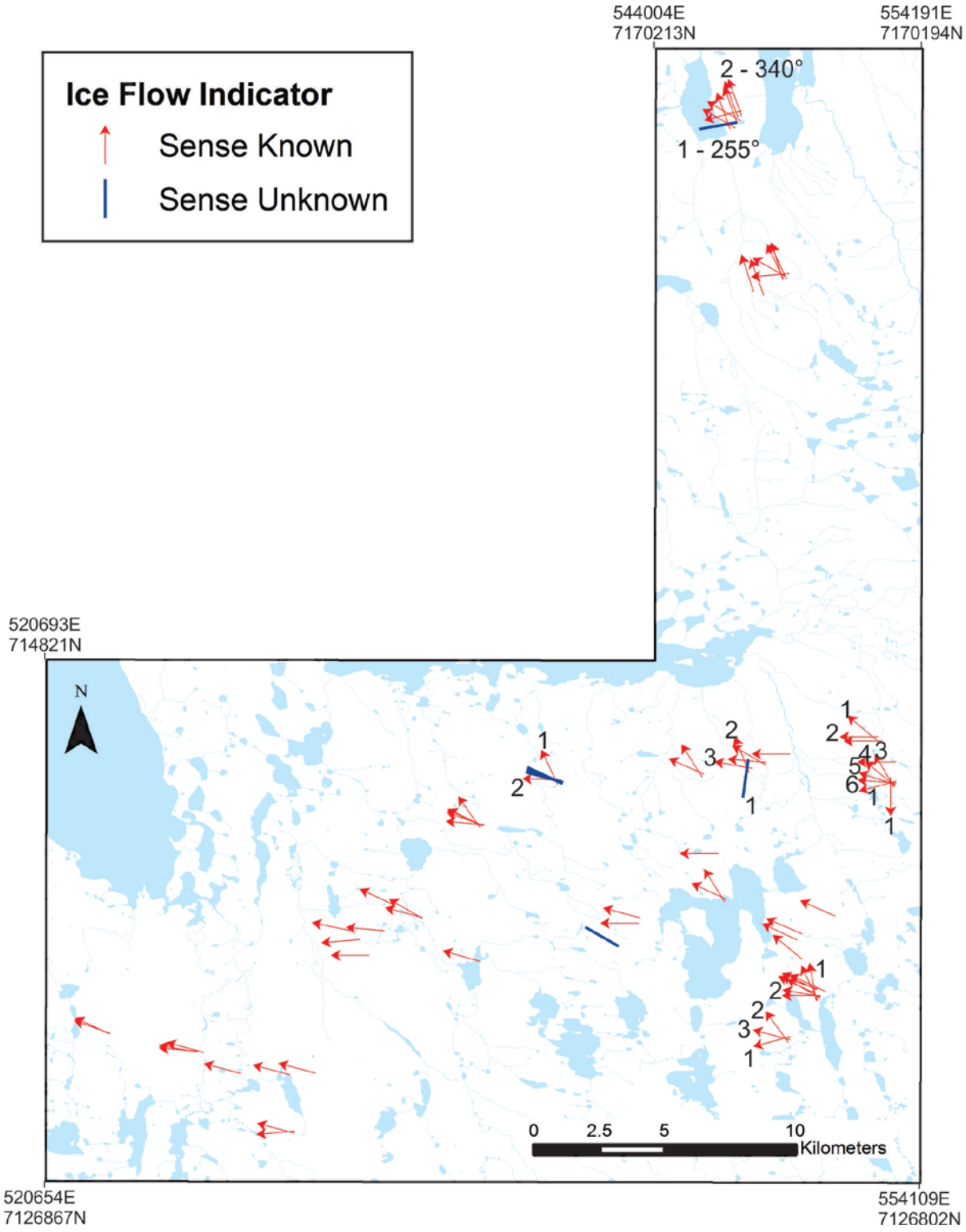

Figure 2-9: Results of paleo-ice flow indicator field observations. The red arrows indicate paleo-ice flow observations with a known directional sense and the blue lines indicate observations where the sense was unknown.

In the northern and eastern part of the field area there was a higher preservation of striae on outcrops of the field area compared with the western part which experienced a more erosive late glacial westerly ice flow phase. This higher preservation of erosional indicators allowed for deciphering paleo-ice flow indicator age relationships. Relative age relationships were observed at 10 of the 48 stations visited and based on these relative age relationships coupled with the landform record, the paleo-ice flow history can be resolved. The earliest ice flow phases recognized are to the west south-west (WSW; 255°) and south (S; 180°). The WSW ice flow phase was recognized at three stations in both the north and eastern portions of the study area and the S ice flow phase was resolved at one outcrop. There was no distinctive age relationship deciphered between these two ice flow phases in the field. McMartin et al. (2005) conducted extensive paleo-ice flow indicator mapping within the Schultz Lake area and based on their work, it appears that the WSW (255°) ice flow phase preceded the S (180°) phase. After these early ice flow phases, there is wide-spread evidence for a north north-west (NNW; 340°) ice flow phase. Paleo-ice flow measurements then suggest a counter-clock wise shift to a northwest (NW; 300°) ice flow phase, before the final westerly (W; 270°) ice flow phase occurred. The shift from NNW to W paleo-ice flow is well preserved at station 13-TH-257 and shown in Appendix G (Photo 12) as well as in Fig. 2-8 F. These ice flow age relationships are synthesized and presented as an ice flow sequence map in Fig. 2-10. The landform record and relative chronology in the field study area corresponds to the last three ice flow phases recorded by cross-cutting relationships between the erosional indicators (Fig. 2-3).

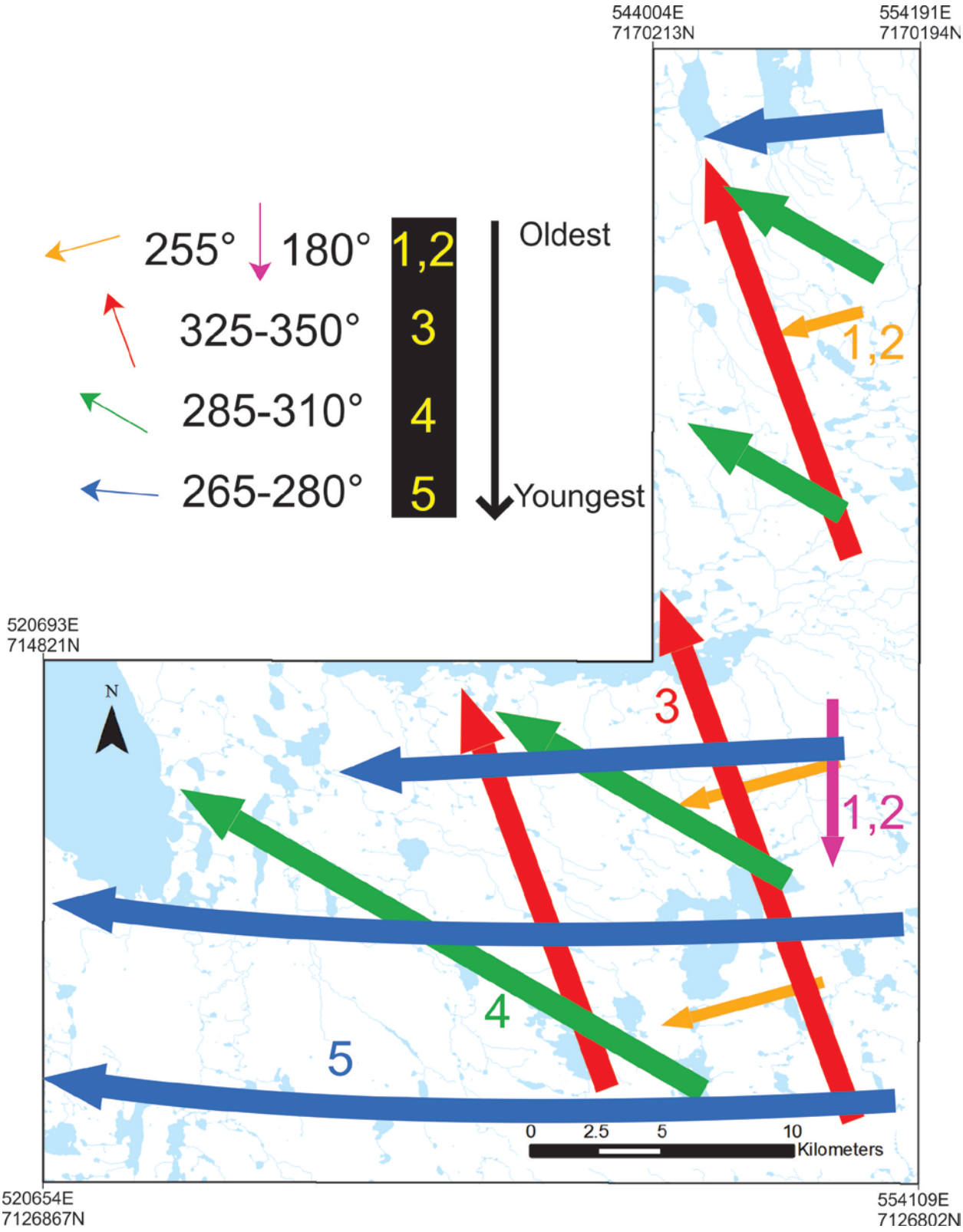

Figure 2-10: Ice flow history interpretation of the study area based upon outcrop-scale paleo-ice flow indicator observations. No age relationship was established between the old S and WSW ice flows (1, 2).

The paleo-ice flow record derived from field work supports work done within the adjacent Schultz Lake map area (McMartin et al. 2005) and across Kivalliq (McMartin and Henderson 2004a), while extending field observations of earlier southerly ice flow phases that have been recognized. The old southeast flow (pre-NNW ice flow phase) recognized by Robinson et al. (2014) near the Kiggavik deposit and by McMartin et al. (2005) in the southeast portion of the map area was not recognized within this study and could represent a northwestern boundary for erosional indicators of this paleo-ice flow as a result of ice-divide migration into the Aberdeen Lake region. It is acknowledged that no late glacial southeast ice flow phase was recognized in the Aberdeen Lake area, supporting McMartin et al. (2006) observations of the western extent of this ice flow phase.

2.6 Discussion

Greenwood and Kleman (2010) segregated mapped mega-scale landforms into two morphological distinct groups. Landforms southwest of Aberdeen Lake in the Marjorie Lake area have been interpreted to have formed as transverse subglacial landforms (Group 2 landforms of Greenwood and Kleman 2010); the second group, in the north and east of our map area is interpreted to be streamlined landforms (Groups 1 and 1B landforms of Greenwood and Kleman 2010). Field-based evidence is sparse at best throughout the majority of the map, with the exception of the Schultz Lake map area (McMartin et al. 2005; McMartin et al. 2006; McMartin et al. 2008); however, more historic field-based investigations have been undertaken in the southwestern portion of the map area. Interestingly, Tyrrell (1897) reported erosional evidence of an early southerly ice flow phase from several of these large landforms. Fyles (1954) later visited this area and although he did not observe evidence for the early southern ice flow phase recognized by Tyrrell, he did observe evidence for a paleo-NNE-SSW ice flow phase as shown by a bidirectional paleo-ice flow indicator presented on the current surficial geology map of the region (Aylsworth 1990). Thus, the erosional evidence suggests the presence of a paleo-ice flow phase parallel to the orientation of the large landforms southwest of Aberdeen Lake and are therefore interpreted to represent streamlined subglacial landforms and not transverse bedforms. Group 1 and 1B and Group 2 landforms of Greenwood and Kleman (2010) alternatively could be part of the same converging ice flow phase with variable degree of remoulding. The majority of the interpreted transverse landforms are overlapping the location of the deglacial Dubawnt paleo-

ice stream (Stokes and Clark 2003; Greenwood and Clark 2010; Stokes et al. 2013), whose landforms are proposed to have been at least partly formed by erosional processes (Ó Cofaigh et al. 2013). These large northerly oriented landforms mapped in the Aberdeen Lake region exhibit a convergent pattern to the north, extending from south of our map area and into northern Kivalliq (Fig. 2-11). Erosional evidence for the north ice flow phase has been reported just south of Yathkyed Lake, extending the southward extent of this paleo-ice flow phase (McMartin and Henderson 2004a). The sheer size of the northerly landforms is impressive and it is hypothesized that a thick ice sheet would be needed to create the landforms.

The north-oriented landform flow set indicates the presence of an east-west oriented KID, likely at some point during the last glaciation. This has been previously proposed by Doornbos et al. (2009) to explain the presence of erratics on Melville Island which have a central Kivalliq provenance. Doornbos et al. (2009) suggest this was likely of LGM in age and predated the presence of the M'Clintock Ice Divide in the late Wisconsinan reconstruction exhibited by Dyke and Prest (1987). The northerly oriented landforms in this study extend into north Kivalliq towards Chantrey Inlet. If the Melville Island erratics and landforms are correlated, i.e. the erratics were emplaced as a result of the last glacial cycle, this would suggest long transport distances from central Kivalliq to Melville Island as a result of a spatially extensive LIS, possibly during the LGM.

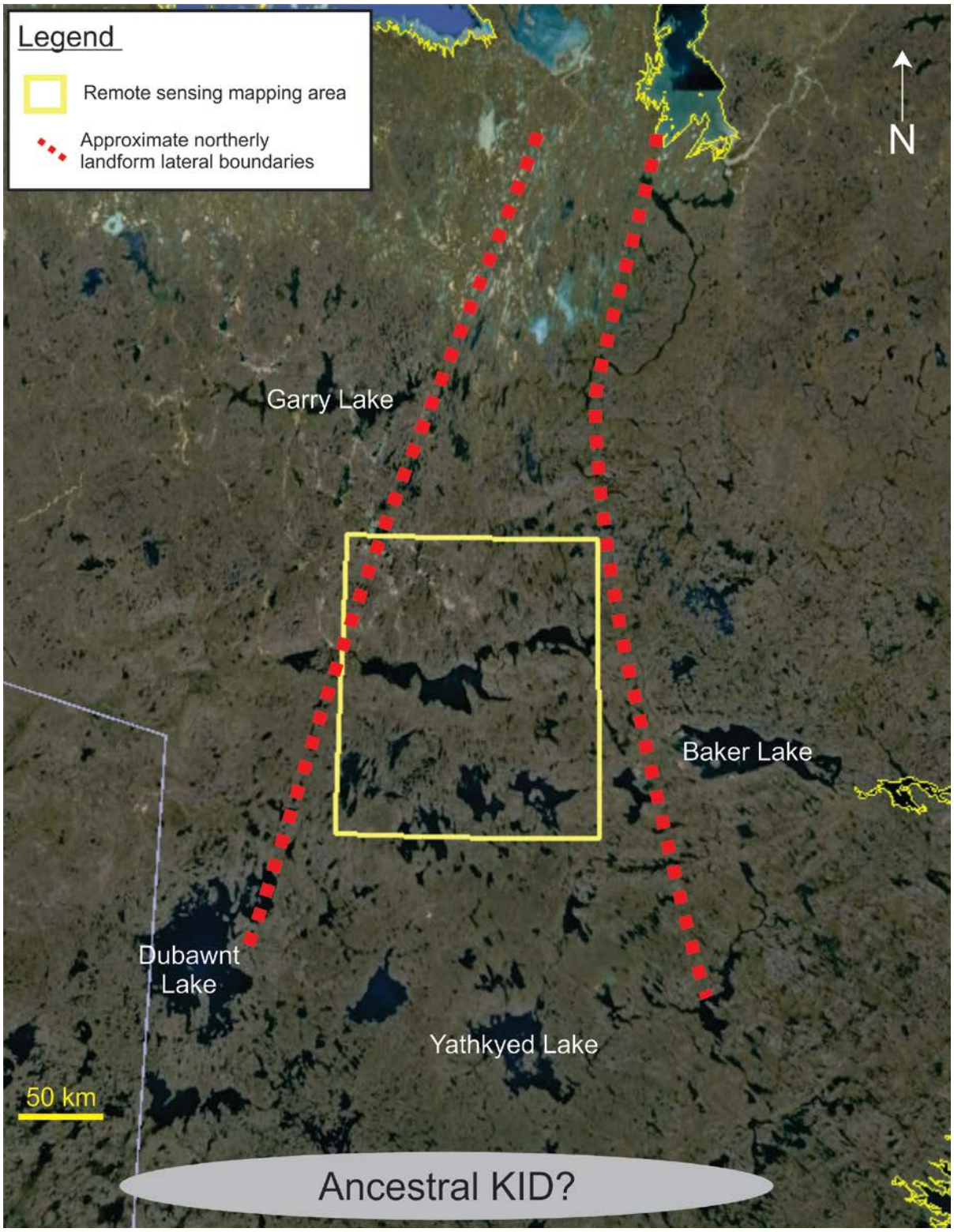

Figure 2-11: Approximate extent of the large northern landforms (cf. Greenwood and Kleman 2010). The mapped region is depicted by the yellow polygon. The landform record suggests the potential for W-E oriented ancestral KID, striae evidence suggests it was situated at some position south of Yathkyed Lake. Image Google Earth (Landsat 8).

It is proposed that the convergent landform pattern observed can be explained by propagation of an ice stream catchment area deep into the LIS, which has previously been proposed in the Kivalliq region for the Hudson Strait Ice Stream (Ross et al. 2011). This would explain the vast convergent landform imprint exhibited in central to northern Kivalliq. This catchment area possible contributed to either the Gulf of Boothia or M'Clintock channel paleo-ice streams (cf. Margold et al. 2014). One possibility is that the KID first experienced a stronger influence from the northern Kivalliq catchment which resulted in a southward migration (e.g. Phase D to E of McMartin and Henderson 2004a) and at a later period of time the Hudson Strait Ice Stream became the dominant drainage catchment in central Kivalliq. This would explain the resultant northward migration of the KID during the late Wisconsinan, and late counter-clockwise rotation (McMartin and Henderson 2004a), as the Hudson Strait Ice Stream catchment propagated onto mainland Nunavut.

Despite the relative wealth of knowledge regarding the surficial record of the region, questions remain as to the proportion of till production that was associated with this northerly ice flow phase. For example, did this ice flow phase simply re-entrained a pre-existing till sheet, or was the ice flow phase responsible for new till production? What is the extent of northward dispersal of Dubawnt Supergroup detritus?

2.7 Conclusion

The southeast Aberdeen Lake region experienced at least five ice flow phases. The earliest of these recognized ice flow phases are south (180°) and west south-west phases (255°). A major ice flow reversal then occurred and resulted in a strong north north-west (340°) phase which was responsible for the production of large streamlined landforms. The depositional and erosional record suggests a counter-clockwise shift to a northwest (300°) ice flow phase and a final deglacial westerly (270°) ice flow phase associated with the Dubawnt paleo-ice stream.

The glacial geomorphology map exhibits the subglacial streamlined landform record of the Aberdeen Lake area building on from previously published maps and can provide assistance when interpreting dispersal patterns in glacial sediments. Within the field study area, the erosional and depositional record exhibits variable reworking by the late glacial westerly ice flow phase. This corresponds to an increase in depositional landforms resulting from the late-glacial westerly ice flow phase, which is also seen in the till stratigraphy (Ch. 3) suggesting the

surficial retreat phase deposition is more prominent in the Aberdeen Lake region than in the Schultz Lake map area to the east (McMartin et al. 2006).

Within the landform record the NNW ice flow phase produced large landforms, typically with elongation ratios between 2 and 4. The landforms are over-printed by smaller NW and W landforms which are suspected to be late-glacial, retreat phase landforms. The northerly extend toward Chantrey Inlet and represent a significant ice flow phase that shaped the Kivalliq landscape. It is suggested this landform imprint represent an ice stream catchment propagation area deep into the LIS and is further discussed in Ch. 3 incorporating the subsurface till stratigraphy.

Chapter 3 : Glacial record of a thick drift region on the Canadian Shield, core of the Laurentide ice sheet: 2. Till stratigraphy and sedimentology

3.1 Introduction

Subglacial erosion and till production under ice divides are considered to be limited due to dominant cold-based conditions and low basal shear stress. For the Laurentide Ice Sheet (LIS), modeling experiments show low basal ice flow velocities and extensive cold-based conditions across its core regions for most of the last glacial cycle (Tarasov and Peltier 2007; Stokes et al. 2012), as well as low erosion rates and sediment production (Melanson et al. 2013). Theoretical reconstructions also predict slight erosion mainly during ice divide migration and a thin till produced during the ice sheet retreat phase (Boulton 1996). However, the slight erosion and prevailing cold-based conditions also favor preservation of a potentially long record of ice advance and retreat, ice divide translocation, and changing basal conditions and glacial dynamics. The Keewatin Sector of the LIS, located in central Nunavut, is considered to be a long standing ice-sheet core region (Dyke et al. 2002) that exhibits a complex paleo-ice flow record (Aylsworth and Shilts 1989; Boulton and Clark 1990; Kleman et al. 2002; Stokes and Clark 2003; McMartin and Henderson 2004a; De Angelis 2007; Kleman et al. 2010). More specifically, remote sensing observations have shown evidence of dynamic shifts of the LIS throughout the last glacial cycle as evidenced by complex landform associations and crosscutting patterns (Boulton and Clark 1990; Kleman et al. 2010). Field-based observations of paleo-ice flow indicators attest to the dynamic nature of the LIS and suggest migration of the Keewatin Ice Divide (KID) by as much as 500 km between ice flow phases (McMartin and Henderson 2004a). However, important uncertainties persist regarding the timing and duration of ice flow and till production phases. For instance, a large central region of the KID is characterized by an extensive till cover (Fulton 1995), but it is unclear whether it was produced during advance and retreat phases or whether the erosion and sediment production record of that area is, in fact, the net effect of several glaciations or, alternatively, evidence that erosion rates in that particular area are underestimated by models.

An important step towards addressing the problem of thick till in ice divide areas is to first thoroughly characterize the stratigraphy, establish sediment provenance, and relate these observations to the surficial ice flow record. Previous Quaternary stratigraphy studies in central mainland Nunavut were restricted to river bluff sections (Tyrrell 1897; Taylor 1956; Klassen 1995; McMartin and Henderson 2004b; McMartin et al. 2006; Stokes et al. 2008; Ó Cofaigh et al. 2013) or shallow drillholes (Shilts 1980; Klassen 1995) with limited coverage of the region (Fig. 1-2).

In this study we focus on an area east and southeast of Aberdeen Lake (Fig. 3-1, 3-2), a region northwest of the last known position of the KID (Aylsworth and Shilts 1989; McMartin and Henderson 2004a). Access to drillcores and helicopter assisted fieldwork offers a unique unprecedented glimpse at the Quaternary stratigraphy of this core region of the LIS. This information is utilized to assess the glacial dynamic evolution of the area, and to provide new insights into the fundamental questions of erosion and till production in former core regions of ice sheets. Results of this study can also be used to assist drift prospecting and related mineral exploration efforts within this region of thick drift.

3.2 Study Location and Geological Setting

3.2.1 Bedrock and Surficial Geology

The study area lies within the Archean Rae Domain of the Western Churchill Province. This Province is primarily composed of variably reworked meso- to neo-Archean rocks with Proterozoic outliers of folded sediments, basins and intrusive suites (Hoffman 1988). The study area is straddled by the Thelon basin to the north and Baker Lake basin to the south (Fig. 3-1). The bedrock present within these basins is part of the Dubawnt Supergroup (Gall 1992). The most distinctive rocks encountered within till is detritus derived from the Thelon Fm and the Pitz Fm volcanics of the Wharton Gp. (Fig. 3-1). The Thelon Fm consists of unmetamorphosed quartz-dominated sandstones and conglomerates (Rainbird et al. 2003). The Pitz volcanics are a purple-mauve rhyolite with distinctive chalky sanidine and quartz phenocrysts (Peterson et al. 2002). The Wharton Gp. is present west and south of the field study area, and represents the best lithological provenance discriminant. The basement rocks typically give limited information regarding till provenance and are not extensively discussed.

The surficial geology of the study area consists primarily of till blanket which is often drumlinized at various scales. Bedrock outcrops are relatively scarce within the field study area and account for approximately <20% of the mapped surficial materials. Glaciofluvial landforms are relatively rare but present as eskers (Aylsworth 1990; McMartin et al. 2008; Storrar et al. 2013). Meltwater channels and raised beaches are also present throughout the field study area (Aylsworth 1990; McMartin et al. 2008).

Quaternary stratigraphy studies have suggested the presence of multi-till stratigraphy throughout the region (Fig. 1-2; Tyrrell 1897; Taylor 1956; Shilts 1980; Klassen 1995; McMartin and Henderson 2004b; McMartin et al. 2006; Ó Cofaigh et al. 2013). Till invoked to be a product of a southern ice flow phase have been reported along the Thelon and Kazan Rivers (Klassen 1995; McMartin et al. 2006). A southern provenance was also invoked based on the geochemical and mineralogical characteristics of drillcore till samples west and south of Pitz Lake (Klassen 1995). Stokes et al. (2008) reported a red till south of Beverly Lake that, based on clast fabrics, was likely emplaced during the last NW-SE ice flow phase the region experienced. Along the Finnie River near the NT-NU border, Ó Cofaigh et al. (2013) observed two subglacial diamicts and through clast fabrics interpreted the upper red diamict to be deposited during the last ice flow phase the region experienced (NW), whereas the lower brown diamict was deposited by a northeasterly ice flow phase of LGM or pre-LGM age.

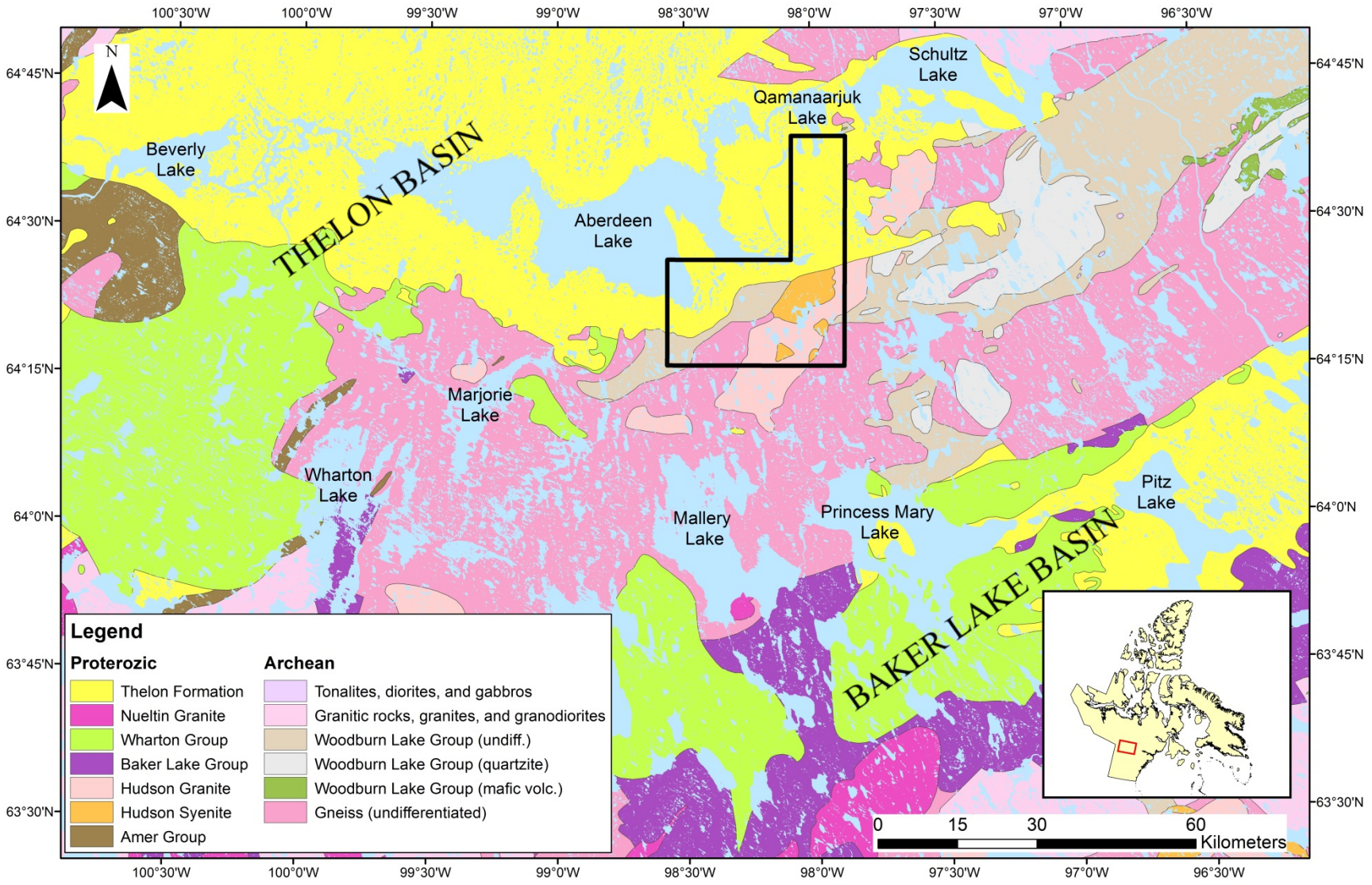

Figure 3-1: Bedrock geology map of study area modified from Paul et al. (2002). Field work and drillcores examined were constrained to the area defined by the black polygon and is shown in Figure 3-2.

3.2.2 Study Area

The study area encompasses parts of Cameco Corporation's Aberdeen and Turqavik projects (Hunter et al. 2011a; 2011b) with sub-surface observations intensified around two uranium exploration targets that have had extensive drilling efforts (Ayra - Fig. 3-2B; Tatiggaq - Fig. 3-2C), while other exploratory drillcores and till sections permit observations of the Quaternary sediments present on a more regional scale. The Qamanaarjuk Quaternary sections investigated are located in the northern part of the field area, where Thelon Fm subcrops and outcrops extensively around the sections (light coloured tones in Fig. 3-2A).

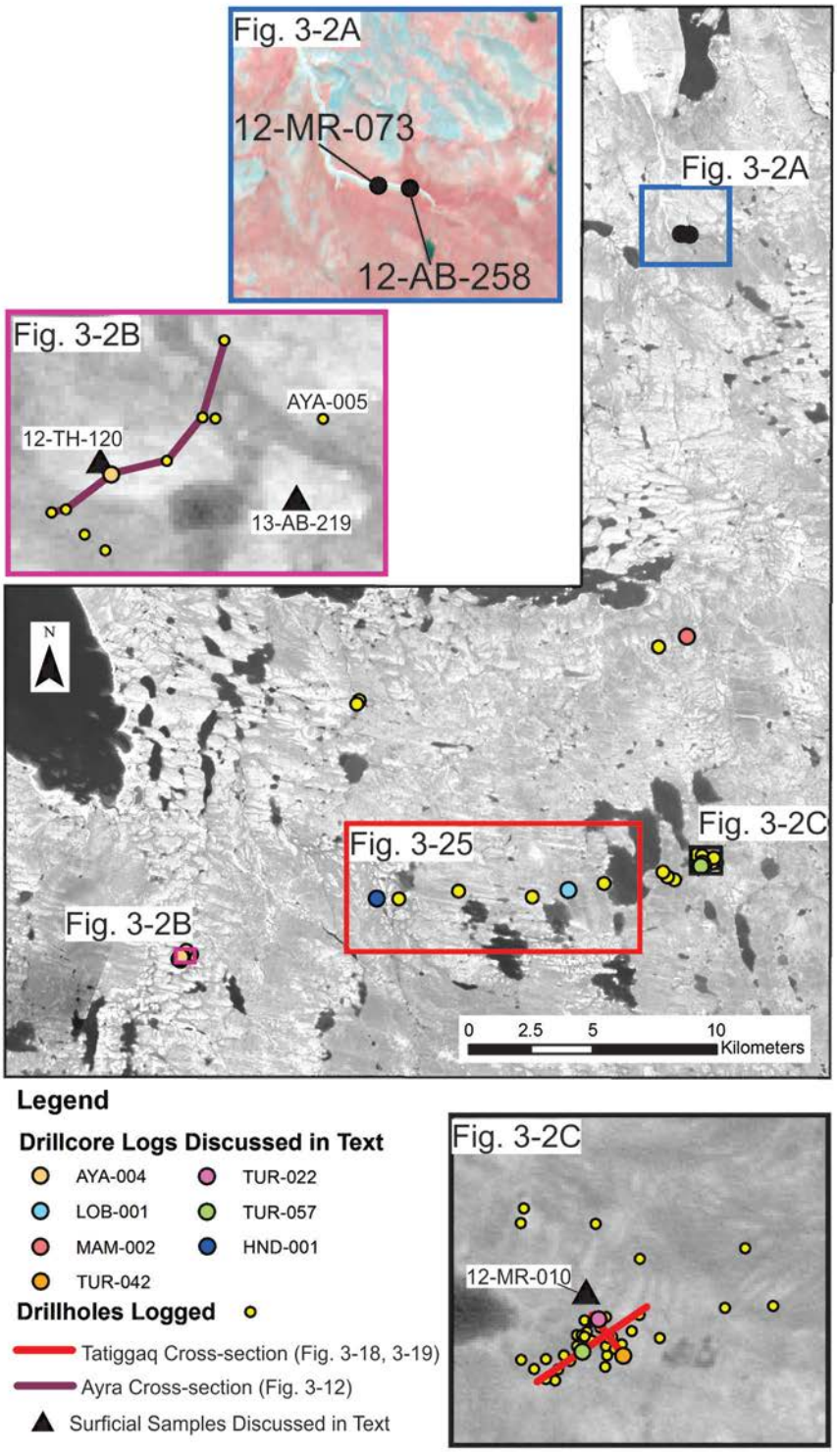

Figure 3-2: Field study area showing the area of the main drilling targets Ayra (3-2B) and Tatiggaq (3-2C). The locations of cross-sections discussed within the text are displayed as polylines. Drillholes logged are identified by the yellow circles and drillcores specifically discussed within the text are individually classified. 3-2A provides the location of the river sections investigated. Note the lighter coloured tones represent bedrock dominated terrain (Thelon Fm).

3.3 Methods

3.3.1 Quaternary Stratigraphy Logging

Drillcore logging was conducted during the 2012 and 2013 field season. A total of 62 drillcores were logged for lithology, colour and core recovery with samples taken at desired intervals. Lithological codes were used to express the lithology throughout the logs (Evans and Benn 2004, p. 30) and standard Munsell codes for the matrix colour. Quaternary sediments were recovered from permafrost terrain during diamond drilling for uranium exploration and were continuous NQ (2 inch) drillcored to bedrock. The first ~2-8 m (avg. 5 m) of each drillcore and discrete intervals throughout the drillcores were unrecoverable due to this drilling method and/or the nature of the sediments present. Drillcore till samples were collected in pairs with approximately 15-20 cm of core submitted for geochemistry analysis and 10-15 cm of core collected for textural and lithological analysis. Logging of the Qamanaarjuk sections was completed in a similar fashion to core logging except lateral observations were permitted. Fabric measurements were conducted using the orientation of elongated (A:B > 1.5) pebbles and cobbles that had an a-axis length of 0.9 – 4.8 cm within till. A bench within the section was cleared to perform unbiased selection of clasts and the orientations of clast A-axis were recorded. In one case, the B-axis was also measured as well for a more complete 3D analysis. Fabric analysis was completed using Rockware StereoStat version 1.5.

3.3.2 Surficial Sampling

Surficial till samples were collected from mudboils (e.g. Appendix G, Photo 9), as these permafrost features are easy to sample and bring unweathered till to the surface (McMartin and McClenaghan 2001). At the Ayra grid where mudboils were absent in some cases, till samples were collected from ~ 40-60 cm below the surface of boulder lagged drumlins (Appendix G, Photos 7, 8). Surficial and section till samples were collected in pairs, with approximately 3-5 kg till samples for geochemical analysis and separate 2-3 kg samples for textural and lithological analysis. Care was taken to avoid oxidized zones within mudboils and reworked sediments within the drumlin samples.

3.3.3 Laboratory Analysis

3.3.3.1 Sedimentology

Till samples were first dried and carefully disaggregated using a rubber mallet, and sieved at the University of Waterloo into >8, 4-8, 2-4 and <2 mm size fractions. For selected samples, the <2 mm portion was divided using a sample splitter to obtain approximately 100-200 grams of material that was then wet sieved to obtain the sand distribution of the <2mm fraction. Otherwise the <2 mm portion of dry material was sieved to obtain approximately 2-3 grams of the <63 μm portion for laser diffractometer grain size analysis, which was completed for every sample using a Fritsch Analysette 22 MicroTec Plus following an overnight distillation in a 4% sodium metaphosphate solution to disaggregate clay particles. Results of grain size analysis for the till samples are presented in Appendix C.

Clast counts were conducted using a 10x magnification binocular microscope after being washed in an ultrasonic bath to remove any matrix residue. Results from clast lithology counts are presented in Appendix E. Lithological classification categories for the size fractions analysed were similar, but the 2-4 mm fraction had more individual mineral grains necessitating additional quartz and feldspar classifications. The classification categories are presented in Table 3-1. For the 4-8 mm clast counts any rounded quartz clasts present were grouped with Thelon Fm classification. Clast counts within the text are expressed in weight percent.

Table 3-1: Lithological classification used during analysis of the 2-4 mm and 4-8 mm fraction of till samples.

4 - 8 and 8+ mm Fraction

Thelon Fm	Pitz Fm	Undiff. Dub. Sed.	Undiff. Dub. Volc	Intrusives	Metased/ Volc	Quartzite	Altered	Other

2 - 4 mm Fraction

Sedimentary	Volcanic	Angular Quartz	Rounded Quartz	Intrusives	Feldspar	Supracrustal	Altered	Other

The altered clasts classification, which is a rather unconventional classification category, had to be incorporated due to the local bedrock around the drillcores which was intensely altered during basin evolution and later incorporated into the local till. The altered bedrock subcrops extensively around the drilling targets and can be a good proxy for mineralization at depth.

Altered clasts are defined as clasts that have experienced intense alteration and the original lithology cannot be distinguished.

Section samples had a sufficient quantity of pebbles recovered to allow clasts counts on the pebble fraction (4-8 mm) and the cobble fraction (>8 mm; 2013 samples only). Drillcore samples were limited to a much smaller sample size and often had an insufficient amount of pebbles recovered and in this case the granule size fraction was identified. At the Ayra grid, 4-8 mm counts were conducted on all of the samples as well as granule counts for the majority of the samples. All the samples from the Tatiggaq grid had the granule size fraction classified and 48 of the 93 samples had the pebble fraction classified. The granule (2-4 mm) fraction had on average 100 clast identified and for the purpose of interpretation only 4-8 mm clast counts that had a minimum of 30 clasts present were incorporated, while the majority of counts had at least 50 clasts identified (Appendix E).

3.3.3.2 Geochemistry

Separate surficial and core till samples had the <63 µm fraction of till matrix processed for geochemistry analysis at the Saskatchewan Research Council. Geochemistry results discussed within the following text are to support till provenance results. A thorough interpretation of the geochemistry results from till samples is beyond the scope of this thesis and is being undertaken by another graduate student at the University of Waterloo. In particular, Boron and Rubidium are utilized herein to demonstrate the influence of Thelon Fm detritus within the till analysed. These elements were utilized since unaltered Thelon Fm is enriched in Boron relative to most bedrock lithologies of the region (with the exception of the Woodburn Lake group) and is depleted in Rubidium relative to every other unaltered regional bedrock unit sampled (Cameco Geochemical Database; Hunter 2013 Pers. Comm.). Rubidium was determined by ICP-MS after a total digestion using a HF-HNO_3-$HClO_4$ solution. Boron analysis was conducted using ICP-OES following a pulp fusion with NaO_2/$NaCO_3$.

3.3.3.3 Till Micromorphology

Eleven drillcore till samples were further processed at Brock University to produce thin sections. The drillcore samples were impregnated with a resin and cut into thin sections following the procedure outlined in Rice et al. (2014). The thin sections produced were observed for micromorphology features following the terminology and practises outlined in Menzies (2000).

3.4 Results

3.4.1 Surficial Till Characteristics and Provenance

Through fieldwork efforts, surficial till was collected from 187 stations and concentrated around three uranium drilling targets (Fig. 3-3). Clast lithology counts conducted on surficial till samples (19/187 stations) suggest that the surficial till is predominately comprised of basement lithologies, mainly intrusive rocks and their metamorphic equivalents (Fig. 3-4; Appendix E). In the western portion of the study area the samples have a higher Dubawnt sedimentary content reflecting incorporation of the local bedrock lithology.

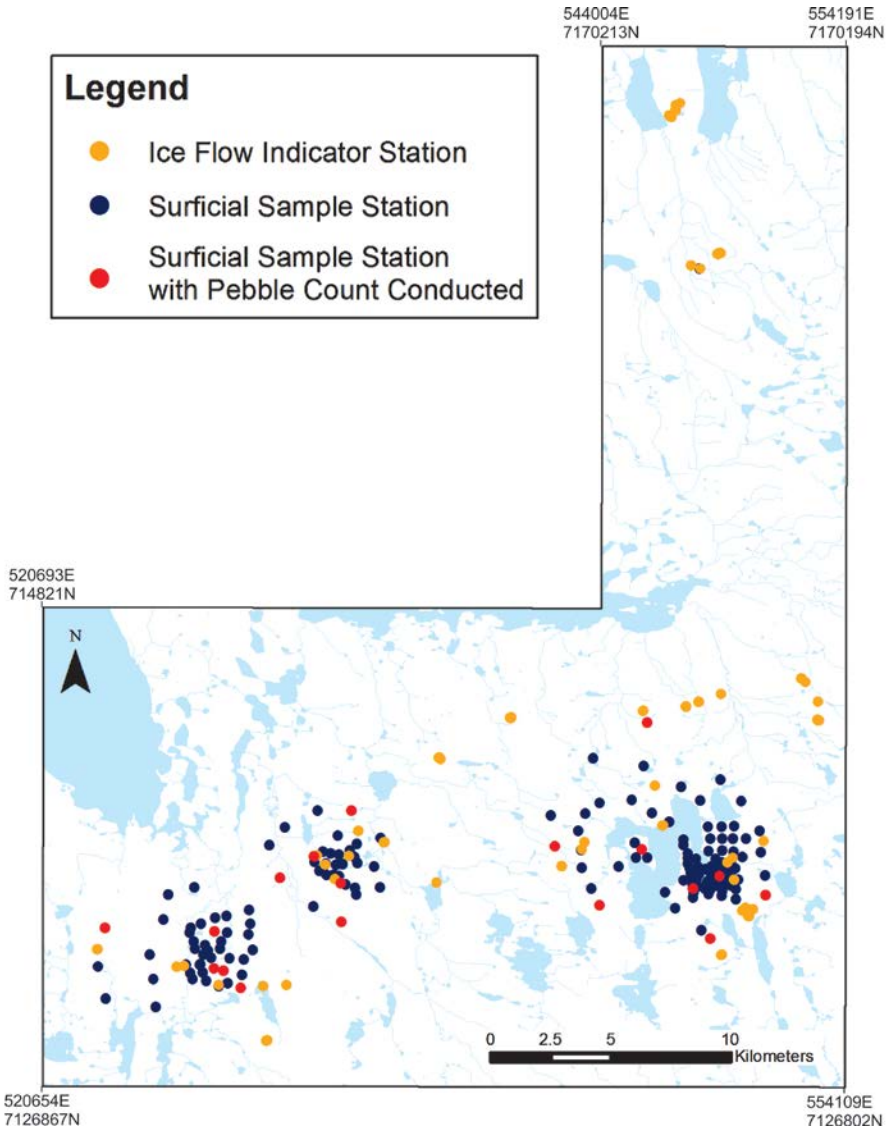

Figure 3-3: Locations of stations visited during the 2012 and 2013 field seasons. Surficial samples that had till lithology clast counts conducted are shown by the red dots.

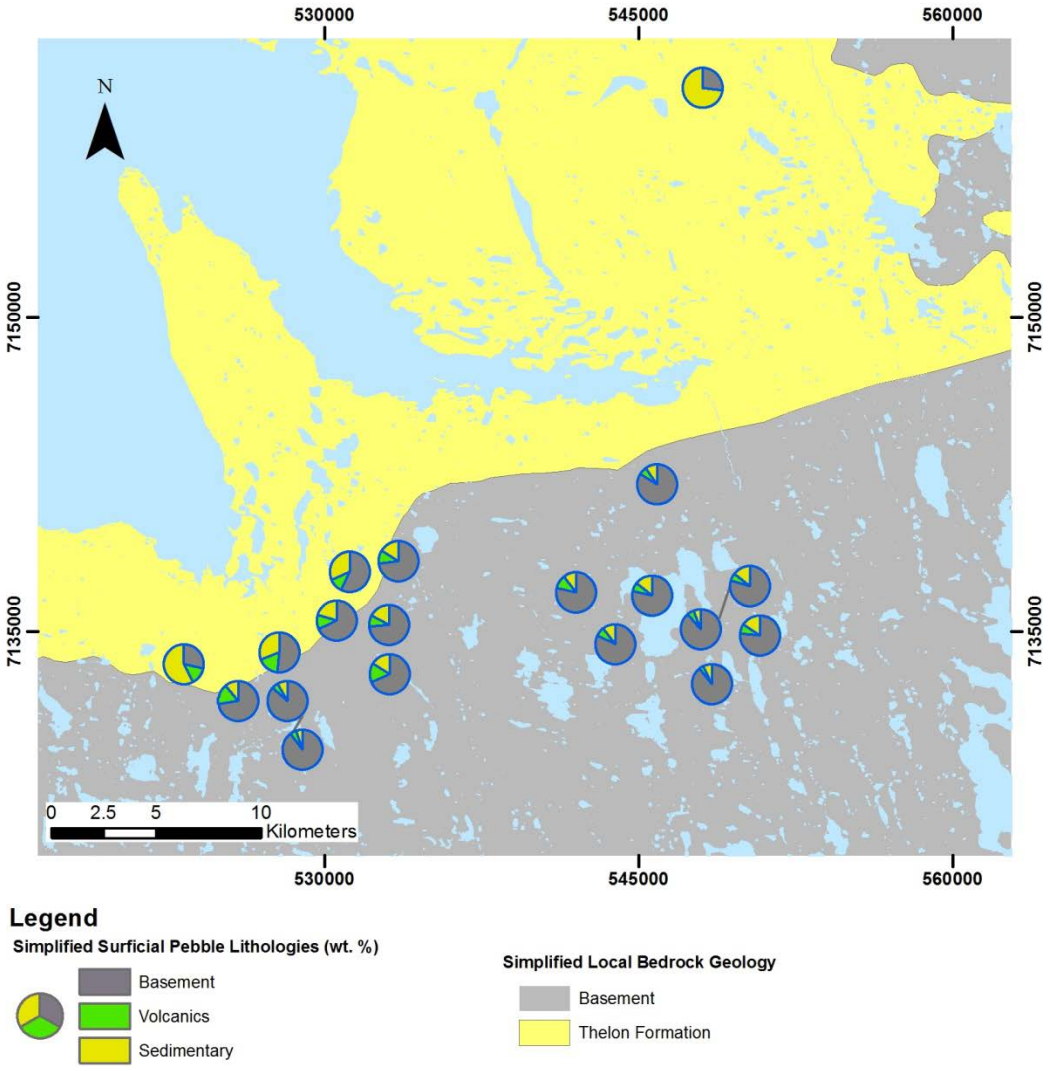

Figure 3-4: Simplified 4-8 mm pebble count results from the surficial till of the study area. Bedrock geology presented is from Paul et al. (2002). Refer to Fig. 3-1 for a broader bedrock geology map.

Dubawnt volcanic rocks outcrop 30 km to the south and 11 km to the west, relative to the field study area (Fig. 3-1). Based on the ice flow record of the region discussed, these pebbles are likely sourced from the south and a result from initial northward dispersal and later incorporation into the late glacial surficial till. A similar situation is suspected for the Dubawnt sedimentary clasts, with the exception of the previously discussed locally derived bedrock component in the west. Dubawnt Supergroup lithologies are more common within the subsurface till units (sections 3.4.3, 3.4.4, 3.4.5) and the occurrence of Dubawnt detritus within till is likely an inheritance signature from the incorporation of earlier deposited till (e.g. Stea and Finck 2001; Trommelen et al. 2013).

The surficial till encountered during field traverses typically has a pinkish grey colour (7.5YR 7/2; dried till matrix colour). Grain size analysis of the <63 µm proportion of the till matrix determined that the samples are dominated by silt in the silt and clay fraction and exhibit a significant range of silt:clay ratios, especially when compared to the relatively small range within drillcore samples (Fig. 3-5), exemplifying the different till characteristics encountered at the surface as opposed to the subsurface. This variations in the silt to clay ratios could be a result of mudboil churning and/or surface winnowing. Wet sieving conducted on surficial samples was limited but ranged from 69-83 weight percent (wt. %) sand (n=3), suggesting that this till is dominantly sandy, similar to subsurface tills.

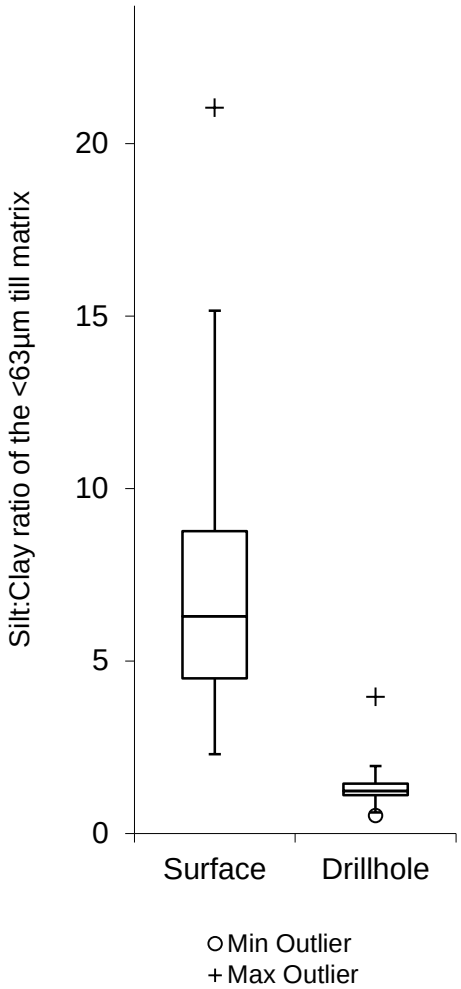

Figure 3-5: Box and whisker plot of surficial and drillcore silt:clay ratio of the less than 63 µm fraction of till matrix (n= 190 for surficial, n = 146 for drillhole). Note the wide range expressed in surficial samples opposed to the narrow range exhibited from drillhole samples. The center line indicates the average for each.

3.4.2 Qamanaarjuk Sections

3.4.2.1 Sedimentology and lithological characteristics

Two sections were logged along a stream south of Cameco's Qamanaarjuk Lake camp (Fig. 3-2), referred to as section 12-MR-073 and 13-AB-258. At section 12-MR-073 (Fig. 3-7) two matrix-supported, massive diamicton (Dmm) units were observed, referred to as Unit 1 (lower) and Unit 2 (upper). Both Dmm units have a pale red colour (1 – 10R 6/2, 2 – 10R 7/2) and are laterally extensive (Fig. 3-7 B). Unit 1 is a stiff diamict, 7 m thick, and has a lower contact with the Thelon Fm bedrock and an upper contact with unit 2. The Thelon Fm at the base of the section is striated and grooved indicating ice flow towards the NNW (340°; Fig. 3-7 C). Near the upper contact within unit 1, cm-scale silty-clay lenses are present that are inclined relative to the lithofacies contact (Fig. 3-7 D). These lenses are interpreted to be either deformed rhythmite stringers or in-filled tensional fractures within the diamicton similar to those documented by Stokes et al. (2008). The laminations did not appear to preserve any primary laminations. Plane orientation measurements of the largest lamination indicate a dip angle of 34° in the NNW direction (350°). The upper diamict is massive throughout and obscured by slumping near the ground surface at the top of the section. Downstream from section 12-MR-073, within diamicton unit 1, a lodged bullet-shaped cobble was uncovered with parallel striae on its top surface (Fig. 3-3). The orientation of the cobble long axis and parallel striations both indicate ice flow in a NNW-SSE orientation (162° - 342°).

Figure 3-6: Lodged elongated cobble, with parallel striae on the upper surface. Cobble and striae indicate ice flow in a NNW-SSE orientation (162° - 342°).

Grain size analysis of unit 1 reveals a silty-sandy texture (avg. 52 wt. % sand, 30 wt. % silt, 18 wt. % clay) with similar results for both samples. Pebble counts from this unit reveal dominant local bedrock (Thelon Fm) influence. Till sample 073D has a higher intrusives component at 28 wt. % as opposed to 10 wt. % observed in 073B (Fig. 3-7), which likely reflects an increase in more distally derived clasts up-unit reflecting a prolonged ice flow phase (Clark 1987). Both samples have volcanic clasts, including Pitz Fm present which represents transport distance of at least 55 km from the closest mapped occurrence to the south (Refer to Fig. 3-1). The upper diamicton unit 2 has an increased proportion of Thelon Fm relative to the upper portion of unit 1 (sample 073D), but similar (78 wt. % vs. 76 wt. %) to that of the lower portion of unit 1 (sample 073B). It is important to note that Thelon Fm outcrops extensively around the stream cut (Fig. 3-2), and this increase in more locally derived detritus was likely a result of a shift in the ice flow direction since the upper portions of unit 1 have a distal lithological signature. Also, no Pitz Fm clasts were observed in Sample -265 of upper unit 2. A nearby mudboil 10 m inland from the top of the section was sampled and found to have similar clast counts to that of sample -265 suggesting unit 2 is continuous to surface. Unit 2 has higher sand and lower clay component (66 wt. % sand, 27 wt. % silt, 7 wt. % clay) relative to unit 1, with slight silt:clay differences experienced between the surficial mudboil and section samples of unit 2 (Fig. 3-7).

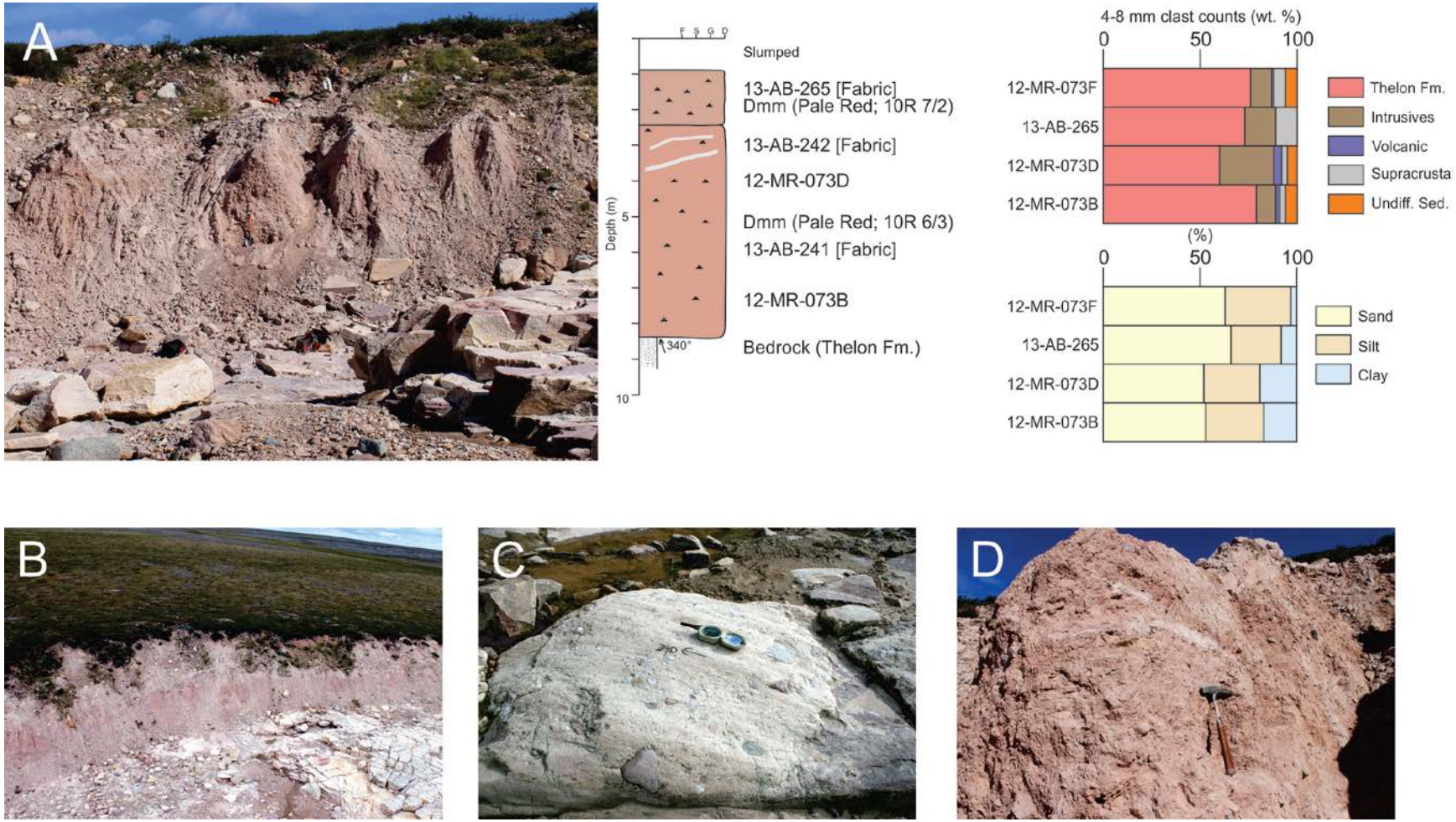

Figure 3-7: A. Photo of section 12-MR-073 investigated with corresponding stratigraphy log and sample properties. Sample 12-MR-073F is from a surficial mudboil located 10 m inland from the river section. B. Aerial photo of the river section 12-MR-073. Note the two till units logged are recognizable by their color difference and are laterally extensive. C. Thelon formation bedrock at the base of the section exhibiting striations and grooves trending NNW (340°) as determined by outcop stoss-lee (abraded-plucked sides) relation. D. Inclined clay lenses present within till unit 1.

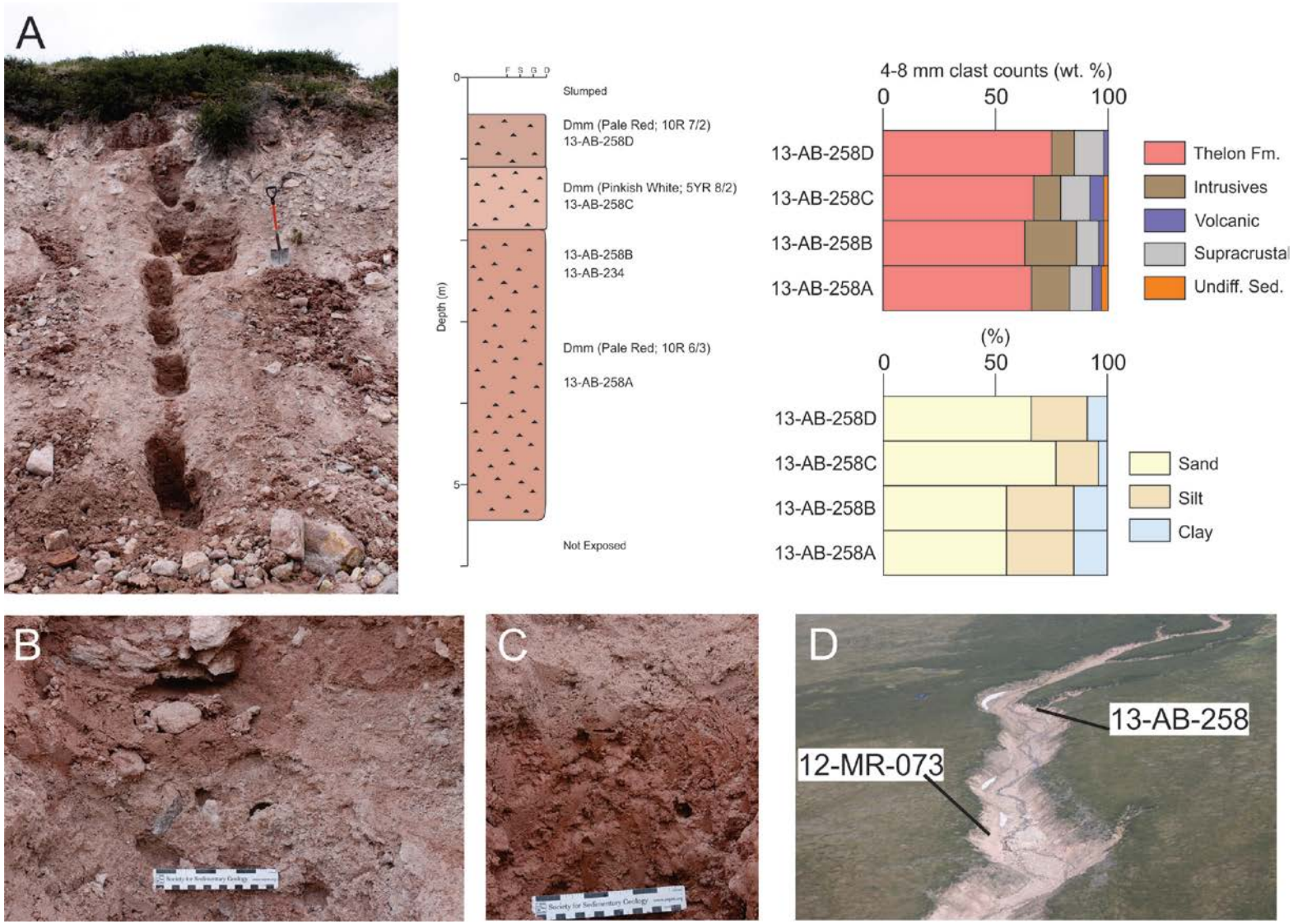

Figure 3-8: Section 13-AB-258. A. Photo of the section that was investigated with the corresponding stratigraphic log generated and sample properties. B. Upper contact of the middle unit displaying a sharp undulatory contact. C. Sharp contact between the lower and middle unit. D. Aerial view depicting the location of the two sections relative to one another. Distance between the two sections is 340 m.

Till section 13-AB-258 was located 340 m upstream of 12-MR-073 at a fork in the stream where a small tributary enters from the south (Fig. 3-8 D). Three diamict units were observed at this section and the bedrock was not exposed. The three units are matrix-supported, massive diamictons, referred to as units 1, 2, and 3 (bottom to top). Unit 1 is a pale red (10R 6/3) stiff diamicton with a minimum thickness of 3.5 m. Unit 2 is in sharp contact (Fig. 3-8 C) with unit 1, and consists of a loosely compacted pinkish-white (5YR 8/2) diamicton that has a thickness of 0.80 m. Unit 3 is a stiff, pale red (10R 7/2) diamicton with a minimum thickness of 0.75 m and has an upper contact that was obscured by slumped material. The contact between unit 2 and 3 is a sharp undulatory contact (Fig. 3-8 B). Textural analysis shows that unit 1 has a silty-sandy matrix (avg. 55 wt. % sand, 30 wt. % silt, 15 wt. % clay) and that the matrix of Unit 2 and 3 predominantly consists of sand (2 – 77 wt. % sand, 19 wt. % silt, 4 wt. % clay; 3 – 66 wt. % sand; 25 wt. % silt, 9 wt. % clay). Samples -A and -B from unit 1 yielded similar textural and clast results, with sample -B having a slightly higher intrusives content. Pitz Fm clasts were recovered from all till samples, but do not exceed 6 wt. % (sample C).

When comparing sedimentology, textural and lithology properties from the two till sections, it is evident that unit 1 of section 12-MR-073 and unit 1 of 13-AB-258 are part of the same till sheet. Unit 2 of section 12-MR-073 and unit 3 of 13-AB-258 are also correlated between the two sections and found to be extensive across the stream cut. Unit 2 of section 13-AB-258 was not observed at section 12-MR-073, suggesting that it is a discontinuous unit along the stream cut.

3.4.2.2 Till Fabric

Till fabric measurements were conducted at section 12-MR-073 within the middle of unit 2 and at two locations within lower unit 1 (refer to Fig. 3-7 for exact locations). The lowermost fabric (13-AB-241) from unit 1 exhibits a north-westward trending clast dip, while the upper fabric (13-AB-242) shows a strong south-eastward a-axis dipping trend. Overall the fabrics of unit 1 exhibit a NW-SE orientation, although dipping in opposite directions. Fabric 13-AB-242 is in agreement with the paleo-ice flow record of the striated bedrock at the section and is stronger than 13-AB-241 (Table 3-2). It is interpreted that the lower till fabric shows local bedrock topography effect, which also led to the weaker fabric strength and resultant down-ice dip. It was noted after taking the fabric that the current bedrock topography in the up-ice direction (SSE) is

above the site of fabric measurements (Appendix G, Photo 11). Therefore, fabric 13-AB-242 is considered more reliable for establishing ice flow during till deposition.

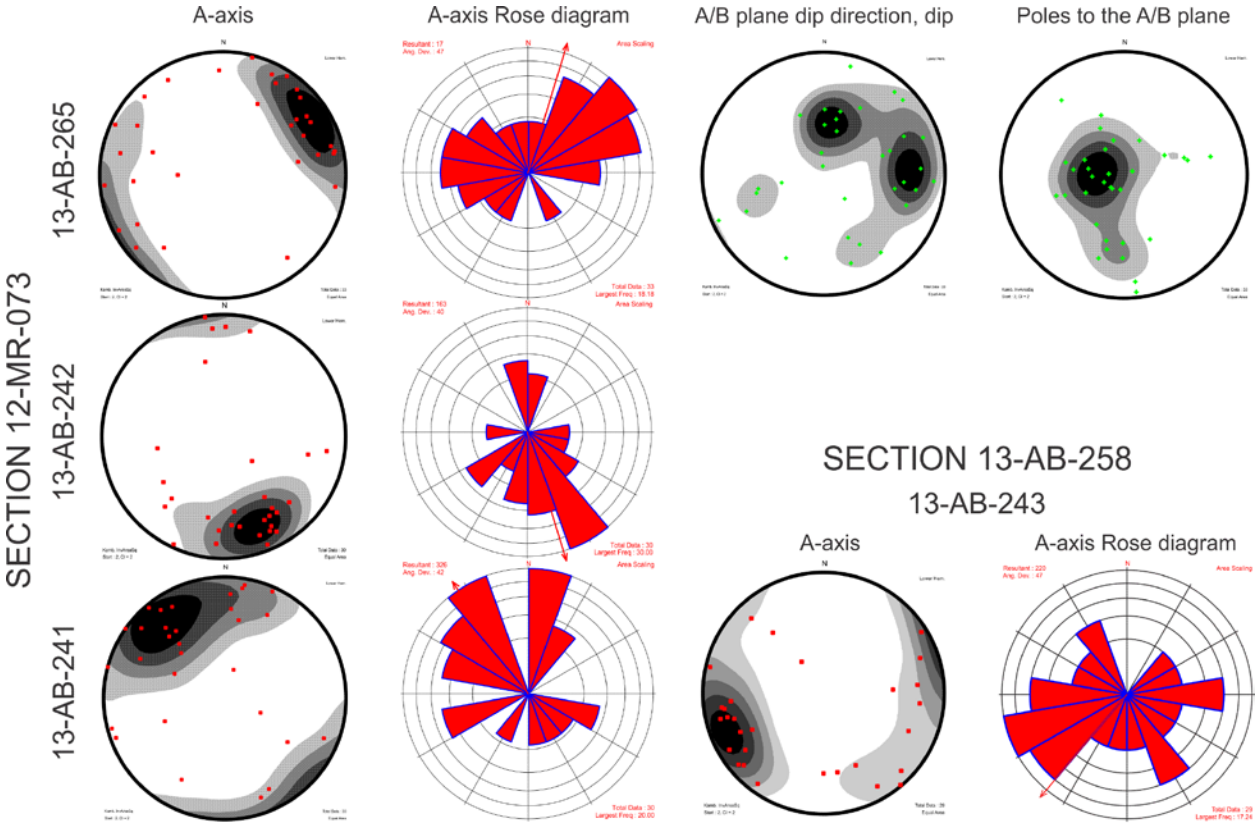

Figure 3-9: Till fabric results from the Qamanaarjuk Quaternary sections investigated, fabric locations are depicted on Figures 3-7 and 3-8 for each respective section.

Clast A- and B-axis measurements were obtained from unit 2 (fabric 13-AB-265) allowing for the calculation of the A/B plane orientation. Clast A-axis was found to be dipping to the east as well as the A/B plane measurements. This suggest a switch to a more westerly ice-flow phase for the deposition of unit 2, which is observed within the depositional and erosional record of the region (Ch. 2).

At section 13-AB-258 one clast fabric was conducted near the top of unit 1 (Fig. 3-8). This fabric (13-AB-243; Fig. 3-9) suggests deposition from ice flowing from the SW towards the NE. This is not supported by ice flow indicators from the landform and outcrop records. Unfortunately, B-axis data was not collected at that site and, therefore, it is unknown whether A/B planes dip in a more consistent way (Table 3-2).

Table 3-2: Fabric statistics from clast A-axis and A/B-axis measurements

Fabric	Axis	n	S1	S2	S3	Isotropy (S3/S1)	Elongation (1-S2/S1)	V1 (°)
13-AB-241	A-Axis	30	0.569	0.259	0.172	0.302	0.545	328
13-AB-242	A-Axis	30	0.702	0.175	0.123	0.175	0.751	167
13-AB-265	A-Axis	33	0.625	0.276	0.099	0.158	0.558	63
13-AB-265	A/B plane	33	0.495	0.272	0.233	0.471	0.451	65
13-AB-243	A-Axis	29	0.590	0.290	0.120	0.203	0.509	259

3.4.2.3 Till Section Interpretation

The presence of angular to sub-angular striated clasts, lodged cobbles with parallel top striations, and stiff nature of these diamicton units together point to a subglacial origin. The lower and upper extensive till units are interpreted to be subglacial traction tills (Evans et al. 2006). The discontinuous thin pinkish-white sandy diamicton present at the upstream section 13-AB-258 is interpreted to be either a subglacial traction till or melt-out till (Evans et al. 2006); however, more work would need to be conducted on this unit to determine its nature and depositional setting (e.g. clast fabrics, micromorphology).

The striated bedrock along with the strong fabric of 13-AB-242 suggests that the lower till unit was deposited during a NW-NNW ice flow phase. This unit also has Pitz Fm clasts whose source is located >55 km to the south. This ice flow phase also correspond to an extensive landform imprint of large elongated till ridges (Ch. 2). Despite the differing ice flow direction suggested by the fabric at section 13-AB-258, the lower unit 1 at that section is also interpreted to be a result of NNW ice flow based on the similar physical properties of this till unit with that observed at section 12-MR-073 (i.e. recovery of Pitz Fm, texture). The upper till unit represents a shift in the ice flow direction to a more westerly ice flow phase and based on a single clast fabric it is interpreted that this traction till was deposited by ice flow towards the SW or W similar to the last known ice flow to affect this region based on the landform record (Ch. 2)

3.4.3 Ayra Stratigraphy

3.4.3.1 Drillcore logging and lithofacies designation

The Ayra exploration target (Fig. 3-2B) has variable cover of Quaternary sediments ranging from 4 to 37 m, and drillcore logging revealed three subsurface diamicton lithofacies and a basal fine-grained sediment lithofacies. A pale red (10R 6/3) matrix-supported, massive diamicton unit (Dmm 3) is the upper unit encountered in drillholes and is laterally extensive, being absent only

in AYA-005 (Fig. 3-2 B). This lithofacies reaches a maximum thickness of 9 m (AYA-003, AYA-010; Fig. 3-12), although it should be noted that this is a minimum as the top of the unit is in contact with intervals of poor core recovery within the drillcores. The base of this diamicton is in sharp contact (Fig. 3-10) with a light brown (7.5YR 6/3) to pinkish grey (7.5YR 6/2) matrix-supported, massive diamicton (Dmm 2).

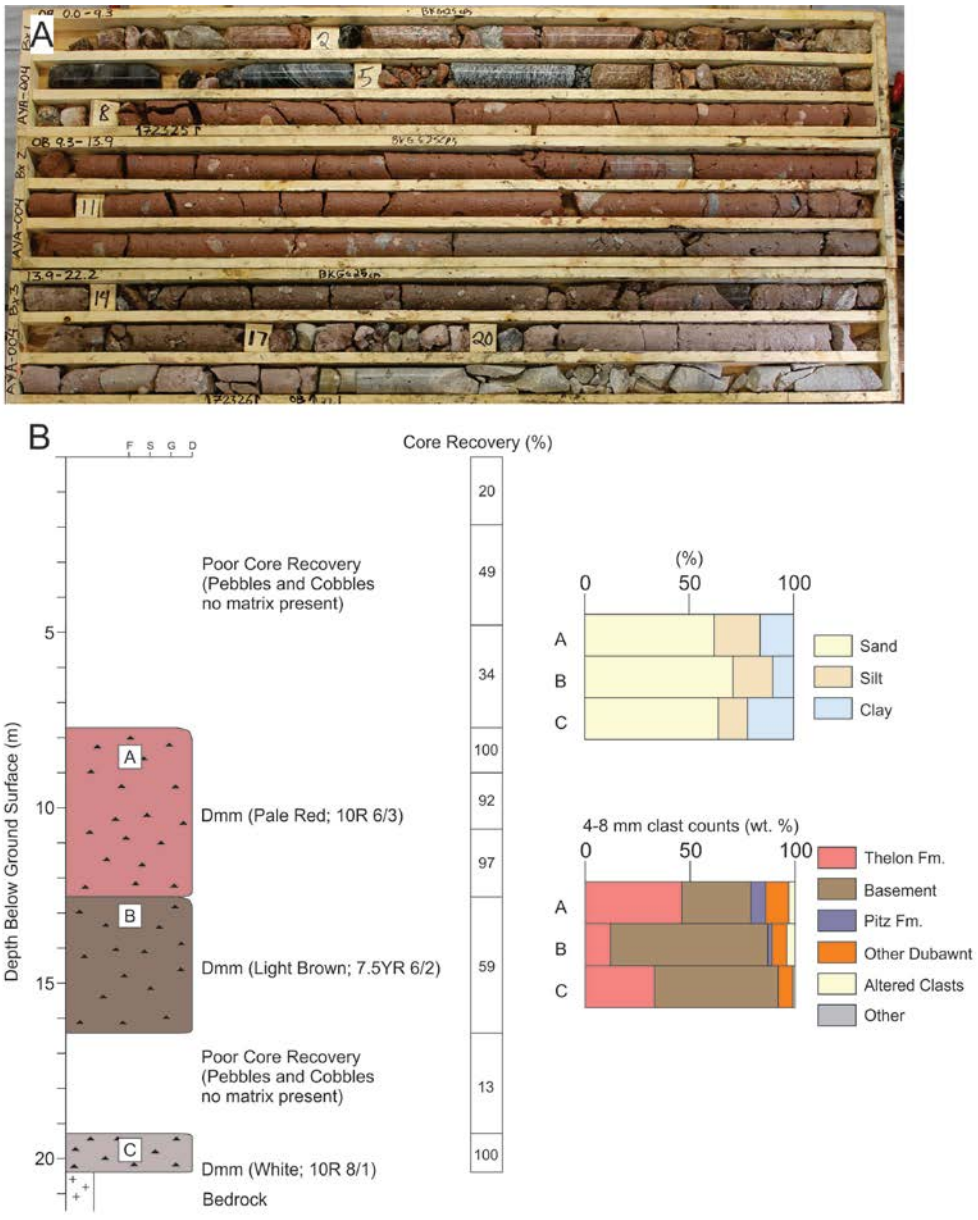

Figure 3-10: A. Drillcore from AYA-004. B. Interpreted stratigraphic log of AYA-004 and till sample properties. Drillcore logging revealed three subsurface units of matrix-supported, massive diamicton. The lower till is separated from the middle till unit by a zone of poor core recovery as seen in the drillcore from the 17-20 m block. Note the depth markers in A differ from the log in B because of inclined drilling path (75° from the horizontal); the log in B is corrected to represent true vertical depth.

The light brown diamict (Dmm 2) is extensive across the target with a minimum thickness of 1 m and a maximum thickness in AYA-009 of 26 m (Fig. 3-12). The lower unit consists of a pale white (10R 8/1) to pinkish-grey (2.5YR 6/2) matrix-supported, massive diamicton (Dmm 1; Fig. 3-10). This unit is discontinuous across the grid and was encountered in three drillholes with a thickness ranging from 1 m (AYA-003, AYA-004) to 13 m (ABR-012). The top contact of this unit is not seen within any of the drillholes logged due to poor recovery. The basal contact was also poorly recovered except in drillhole ABR-012, where it is in contact with fine-grained sediments. The lowermost lithofacies unit is a thin unit (20-30 cm) of laminated fine-grained sediments that was encountered at the bedrock contact in drillhole AYA-009 and above 80 cm of boulders that rested on the bedrock in ABR-012 (Figs 3-11; 3-12). A southwest-northeast cross-section of the Ayra Quaternary stratigraphy is presented in Fig. 3-12.

Figure 3-11: Examples of the laminated fine-grained sediments encountered in drillholes ABR-012 (left) and AYA-009 (right) at Ayra. Note contacts are angled within the drillcore due the inclined path of drilling.

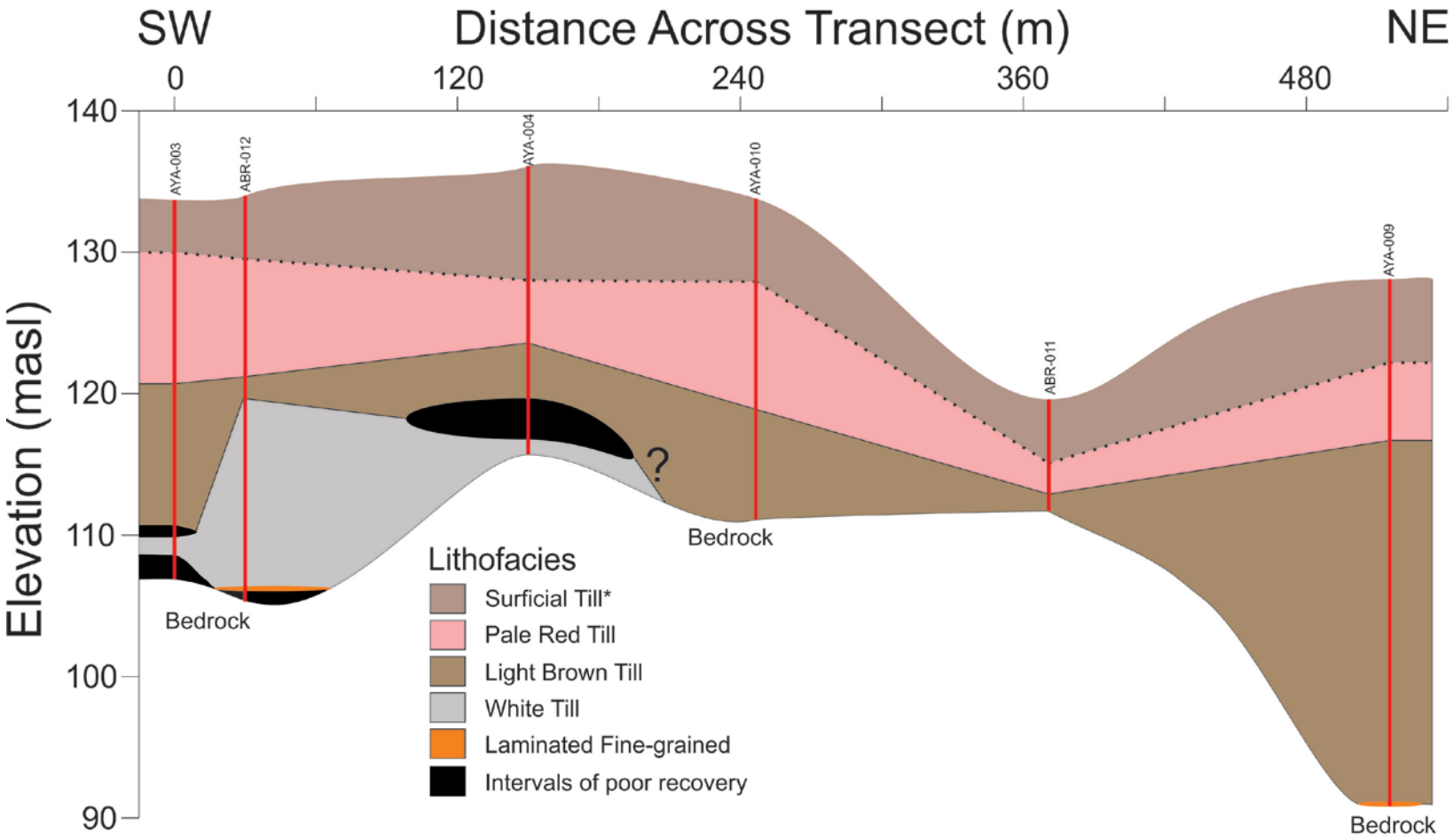

Figure 3-12: Cross-section across the Ayra drilling grid. Refer to Fig. 3-2 for the location of the cross-section. *Note the surficial till is interpreted as being intervals of initial poor recovery in drillcore, therefore the cross-section depicts a maximum thickness for this unit. Vertical exaggeration = 6x.

Matrix textural analysis of the <63µm fraction for each diamicton sample was conducted, which allowed for determination of the silt:clay ratio. As discussed in section 3.4.1, the surficial till (Dmm 4) has a strong basement lithology signature, which is not exhibited within the upper drillcore diamicton unit logged. For discussion purposes the till lithofacies logged within Ayra drillcores (Dmm 1 – 4) will be referred to as "white till, light brown till, pale red till and surficial till". The silt:clay ratio ranges are presented in Table 3-3 for each diamicton lithofacies of the Ayra drillcores. The white till has higher clay content than any of the other till units and the surficial tills has much higher silt content than that of the other till units.

Table 3-3: Silt:Clay ratio of each till lithofacies identified at the Ayra drilling grid.

Lithofacies	Silt:Clay ratio
Surficial Till	11-14
Pale Red Till	1-1.4
Light Brown Till	1.9-2.8
White Till	0.5-0.8

Wet sieving results exhibited that the matrix of the pale red and light brown till units are predominately composed of sand 60-71 wt. % and the white till unit has a variable sand content which ranges from 47-64 wt. % sand. The surficial till is a sand dominated facies over Ayra (83 wt. %) (Refer to Appendix C).

3.4.3.2 Till Provenance

Clast lithology counts conducted on each diamicton lithofacies of the Ayra grid suggest distinct provenances for each lithofacies. The pale red unit has a high Dubawnt Supergroup component with Thelon Fm content ranging from 41 – 72 wt. %, the presence of Pitz Fm observed in every sample (max 8 wt. %) and an intrusive component ranging from 13 – 29 wt. %. The light brown till is an intrusive-rich (59 – 82 wt. %) facies and Pitz Fm clasts were recovered in 8 out of the 12 samples analyzed reaching a maximum of 11 wt. %. Thelon Fm clasts were observed but did not exceed 20 wt % and were absent in the light brown till in some cases. The lower white till has a mixed Dubawnt and basement signature. Thelon Fm clasts range from 20 – 37 wt. % and intrusive clasts are more prevalent ranging from 50 – 72 wt. %. A key finding from the results of the white till is the absence of Pitz Fm clasts. Grouping the individual till sample clast counts

according to their designated logged lithofacies, a composite count was compiled and is summarized in Fig. 3-13.

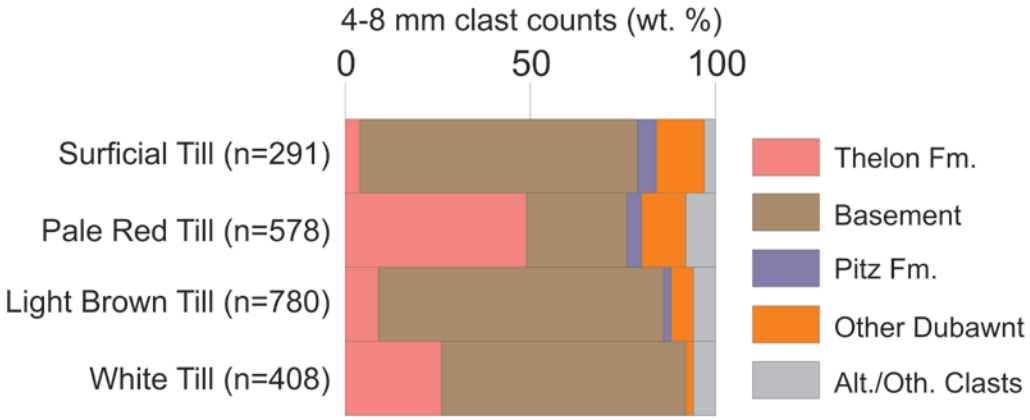

Figure 3-13: Composite summary of sample pebble (4-8 mm) lithology counts for each till lithofacies logged in Ayra drillcores. Note: The surficial till counts presented are from two till samples collected at 40-60 cm below ground surface from a boulder lagged drumlin that is located within 200 meters of the Ayra drillholes (Refer to Fig. 3-2 B).

The lack of Pitz Fm clasts within the white till unit suggests that this till is not derived from a western or southern provenance, where the Pitz Fm is present (Fig. 3-1). Early southerly ice flows have been recorded within the Kivalliq region (Ch. 2; McMartin and Henderson 2004a; Kleman et al. 2010). Based on the proximity of the Ayra drillholes to the Thelon Fm outcrops northward, and the higher abundance of basement material present within the till, this unit is potentially linked to the earliest of these recognized ice flows; the west-southwest ice flow phase (McMartin and Henderson 2004a; Ch 2 – WSW [255°] ice flow phase). The occurrence of fine-grained lithofacies below this unit attests to an advance over non-glacial sediments. The white till lithofacies has more silt and clay within the till matrix relative to any of the tills observed throughout this study, suggesting possible incorporation of the lower lithofacies, regolith and/or altered bedrock during subglacial transport and deposition.

The light brown till is largely derived of basement material but Pitz Fm clasts are present within the till which constrains till provenance to either the west or south. Evidence for east to northeast ice flow phases within the region is patchy but exists (Phase C of McMartin and Henderson 2004a; Ó Cofaigh et al. 2013), although McMartin et al. (2006) found no evidence for easterly ice flow within the Schultz Lake area. To the west of this study near the Nunavut-Northwest

Territories border (Refer to Fig. 1-1), Ó Cofaigh et al. (2013) provide clast fabric evidence for the deposition of a brown diamicton by an easterly/north-easterly ice flow phase. Based on the lack of distinctive bedrock lithologies within the region, this till unit cannot definitively be assigned to a western or southern provenance specifically.

The pale red till has a high Thelon Fm content and the presence of Pitz Fm, constraining the till to either a western or southern provenance. Based on the ice flow record presented in Ch. 2 and the interpretation of sustained northerly ice flows and the stratigraphic position of this subsurface till unit, it is likely sourced from the south. The till may have been produced during the 340° to 300° ice flow phases, although the high content of Thelon clasts suggests that the northwesterly flow (300°, this study) may have been more important for till production since Thelon Fm is more extensive up-ice of the northwesterly ice flow phase (refer to Fig. 3-1).

Based on the landform record presented in Ch. 2, the region surrounding the Ayra grid is streamlined by westerly oriented drumlins. This flowset represents the last ice flow phase the region experienced. Over the Ayra exploration target, westerly drumlins are present and these landforms were sampled at ~40-60 cm below their surface as part of this study (Fig. 3-2B). Clast counts of this surficial till reveal a dominant intrusives lithology signature with relatively minor distal Dubawnt clasts present (Section 3.4.1). The clast counts are consistent with a westerly ice flow as the till is largely comprised of bedrock lithologies that can be found east of the Ayra drillholes with the Dubawnt clast component likely scavenged from the underlying till representing an inheritance signature (e.g. Klassen 2001; Trommelen et al. 2013) or transported from the Thelon Fm outcrops east of the study area. Figure 3-14 shows the unique textural and clast provenance (Dubawnt) characteristics of the three subsurface tills. From this figure, the different lithofacies are clearly discernible by both the Dubawnt pebble component and the silt and clay proportion of the till matrix with no overlap between lithofacies. The lack of a ‘mixing’ signature between the light brown till and the pale red till along with the sharp contact observed between the diamicton units would suggests a high sediment input during deposition of the pale red till resulting in a layered stratigraphy (Trommelen et al. 2013).

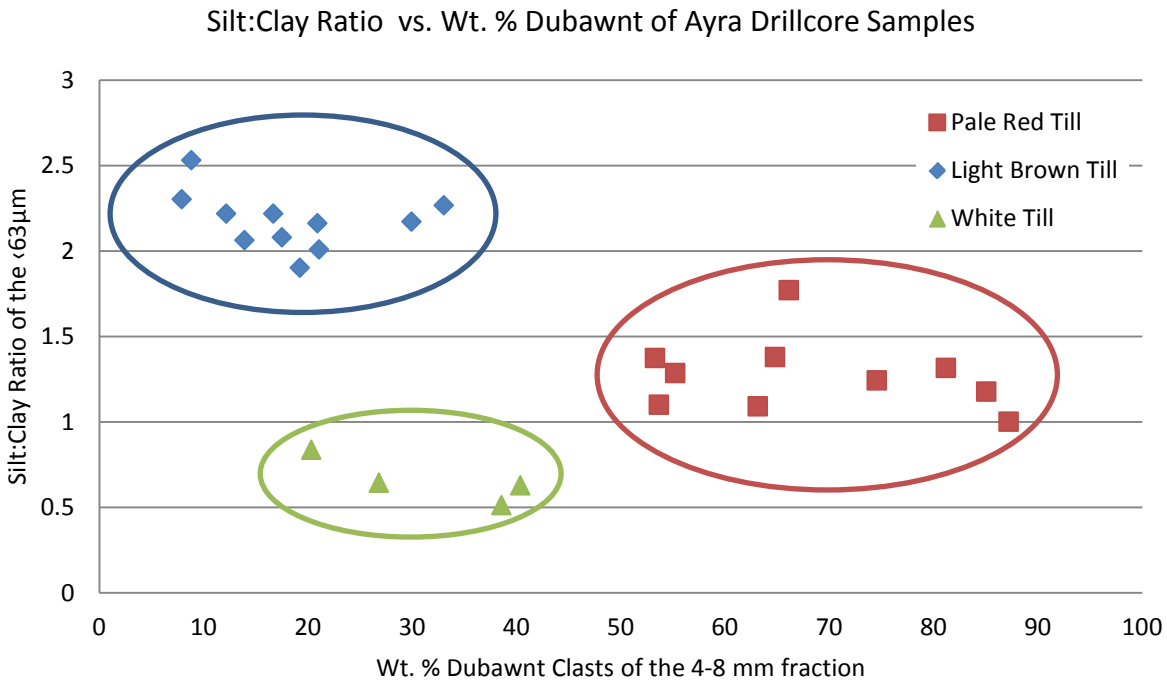

Figure 3-14: Silt:clay ratio and Dubawnt component (wt. %) of pebbles count from Ayra grid drillcore till samples. Surficial clast counts were excluded due to very high and variable silt:clay ratio of this unit (Table 3-3).

3.4.4 Tatiggaq Stratigraphy

3.4.4.1 Drillcore Logging and Lithofacies Designation

At the Tatiggaq drilling target, 38 drillcores were logged (Fig. 3-2C) and 93 diamicton samples collected. Logging and sample analysis identified four diamicton lithofacies (Dmm 1 – 4; lower to upper) present.

Drillcore TUR-022 (Fig. 3-15) has a lower clast-rich, matrix-supported, massive diamicton (Dmm 1) with a large component of locally derived detritus. This is overlain by an upper diamicton unit with no obvious textural or qualitative variations observed throughout the unit; however, it is noted that there is a possible contact at 11.25 m bgs where there is a sharp variation in pale-red colour observed (Appendix G, Photo 4). The presence of a contact is further suggested by lithology counts conducted within the pale red diamicton as there is a large variation between sample C and E. This lithological signature was noted within other drillcores across the exploration target and necessitates the distinction of two separate pale red diamicton lithofacies (Dmm 3 - upper and Dmm 2 - lower). Dmm 2 is defined as having a high proportion of Thelon Fm (>60 wt. % of sedimentary granules in the 2-4 mm range) and devoid of Pitz Fm volcanics (4-8 mm range).

Drillcore TUR-057 exhibits a sandy pale red (10R 6/3 to 10R 7/2) diamicton unit with a minimum thickness of 10.6 m. The lowest unit observed is a massive, matrix-supported, weak red (10R 5/4) clast-rich diamicton (Dmm 1), which reflects the colour of the locally hematized bedrock in this case. The two diamicton units are separated by a thin (10 cm) interval of laminated clayey-silt sediments. The lower diamicton and fine-grained unit observed within TUR-057 are discontinuous units across the Tatiggaq grid. Clast counts and grain size of TUR-057 support the drillcore logging suggesting a homogenous upper till unit as there was very little variance within the properties exhibited in drillcore samples taken above laminated clayey-silt unit (Dmm 3; Fig. 3-16). This suggests that Dmm 2 observed within drillcore TUR-022 is discontinuous across Tatiggaq. Sample TUR057-SK has a higher fine-grained content, which is likely due to incorporation of fine-grained sediments from the unit below during subglacial transport and deposition, as supported by thin section observations of the diamicton (Fig. 3-31 B). The lower diamicton is similar in texture, but has a higher silt content and contrasting clast lithologies. Drillcore TUR-042 (Fig. 3-16) exhibits a two till stratigraphy consisting of Dmm 2

and Dmm 3 resting on bedrock. This drillcore encountered one of the thickest sequences of diamicton across the Tatiggaq target.

Surficial till (Section 3.4.1; Dmm 4) present at the Tatiggaq grid has a strong basement signature and is identified within several drillcores. Drillcores TUR-049 and TUR-059 have an upper diamicton logged (Dmm 4) that exhibits slight colour variations (e.g. Appendix G, Photo 2) from the diamicton below (Dmm 3) and a lithological signature in agreement with till sampled at the surface, suggesting recover of the surficial till in several drillcores.

Figures 3-18 and 3-19 are cross-sections through the main Tatiggaq drilling anomaly with the designated Dmm lithofacies. Fig. 3-18 is near parallel and Fig. 3-19 perpendicular to the large NNW landforms in the region and over the Tatiggaq target. Dmm 2, 3 and 4 are continuous across Fig. 3-18, while Dmm 1 is restricted to drillcore TUR-022. Fig. 3-19 shows that Dmm 2 is discontinuous across the exploration target, and generally restricted to bedrock troughs. The surficial till was sampled in a drillcore across this cross-section, giving an approximate thickness for this unit of 4-5 m. Dmm 3 reaches a maximum thickness of 12 m and Dmm 2 reaches a maximum thickness of 6 m.

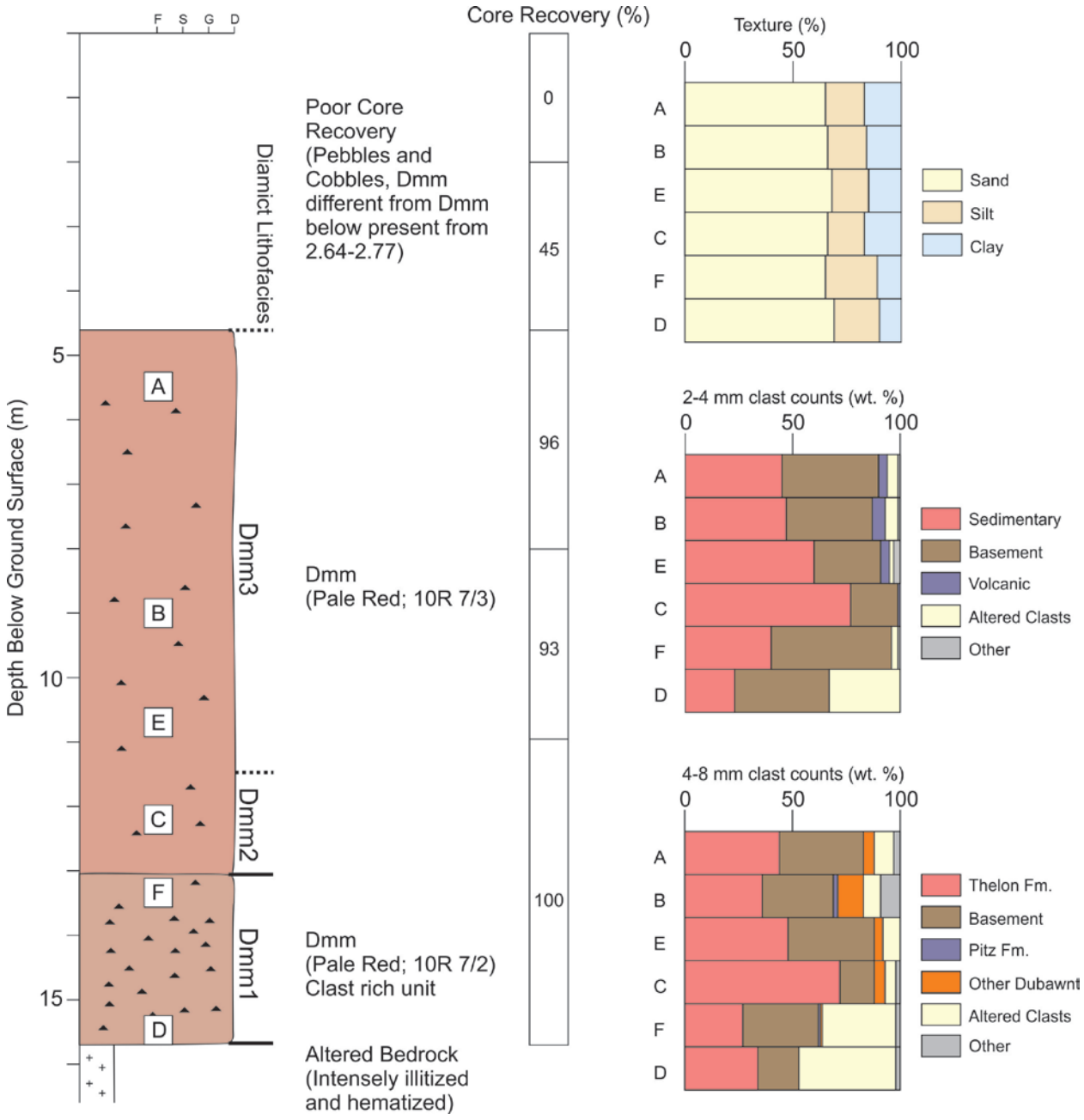

Figure 3-15: Drillcore log of TUR-022 with associated till sample properties. Note the increased altered clast signature within the lower two till samples which is not apparent from sample C upward. The upper pale red till unit has an anomalously high proportion of Thelon Fm at its base which has been interpreted as a separate diamict lithofacies.

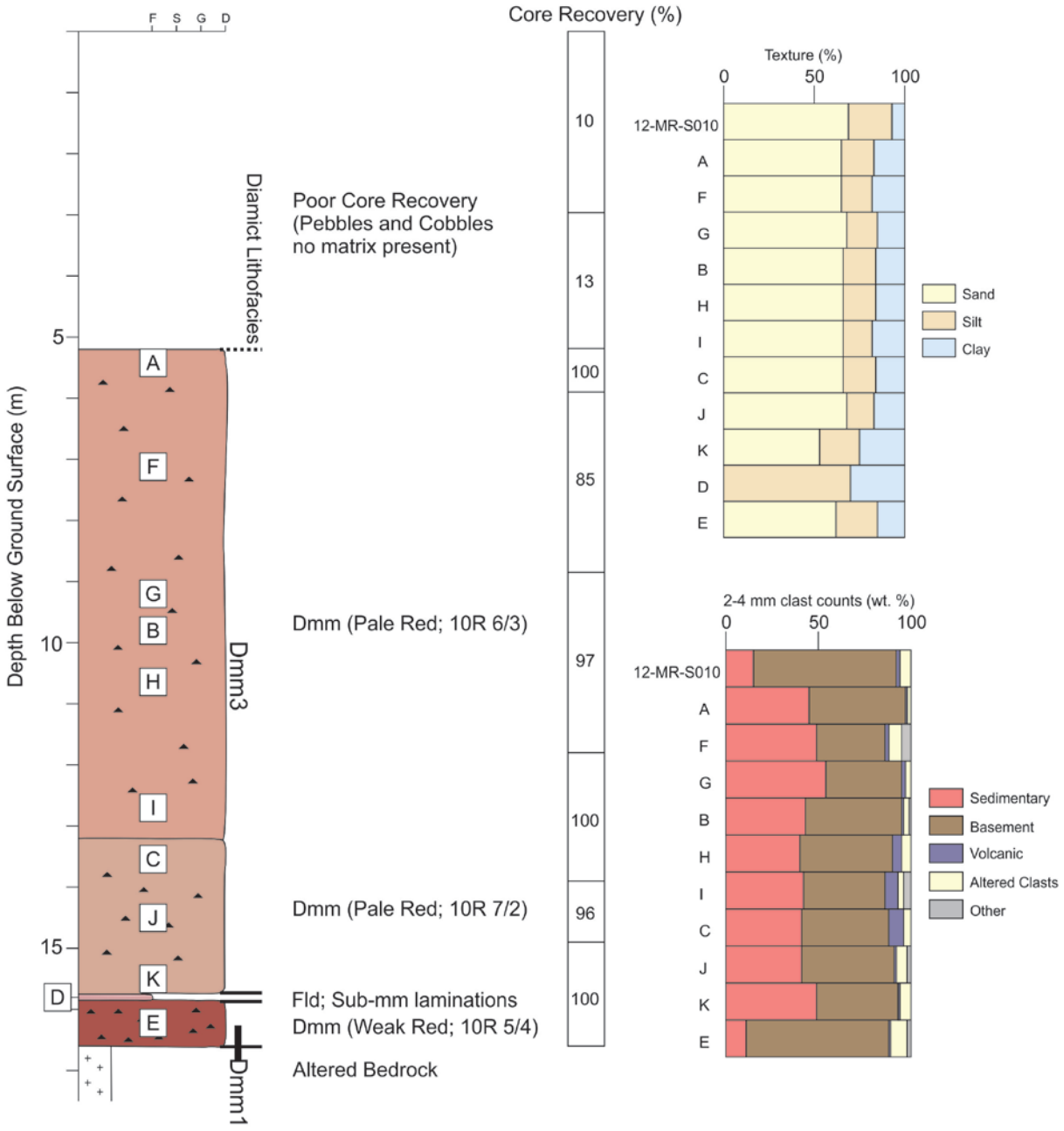

Figure 3-16: Drillcore log of TUR-057 with associated sample properties. Sample 12-MR-S010 is from the closest surficial till sample located 200 m north of drillhole TUR-057 (refer to Fig. 3-2C). Two subsurface diamicton lithofacies are present (Dmm 1 – lower; Dmm 3 – upper). The Thelon Fm rich lithofacies (Dmm 2) observed within TUR-022 is absent in drillcore TUR-057.

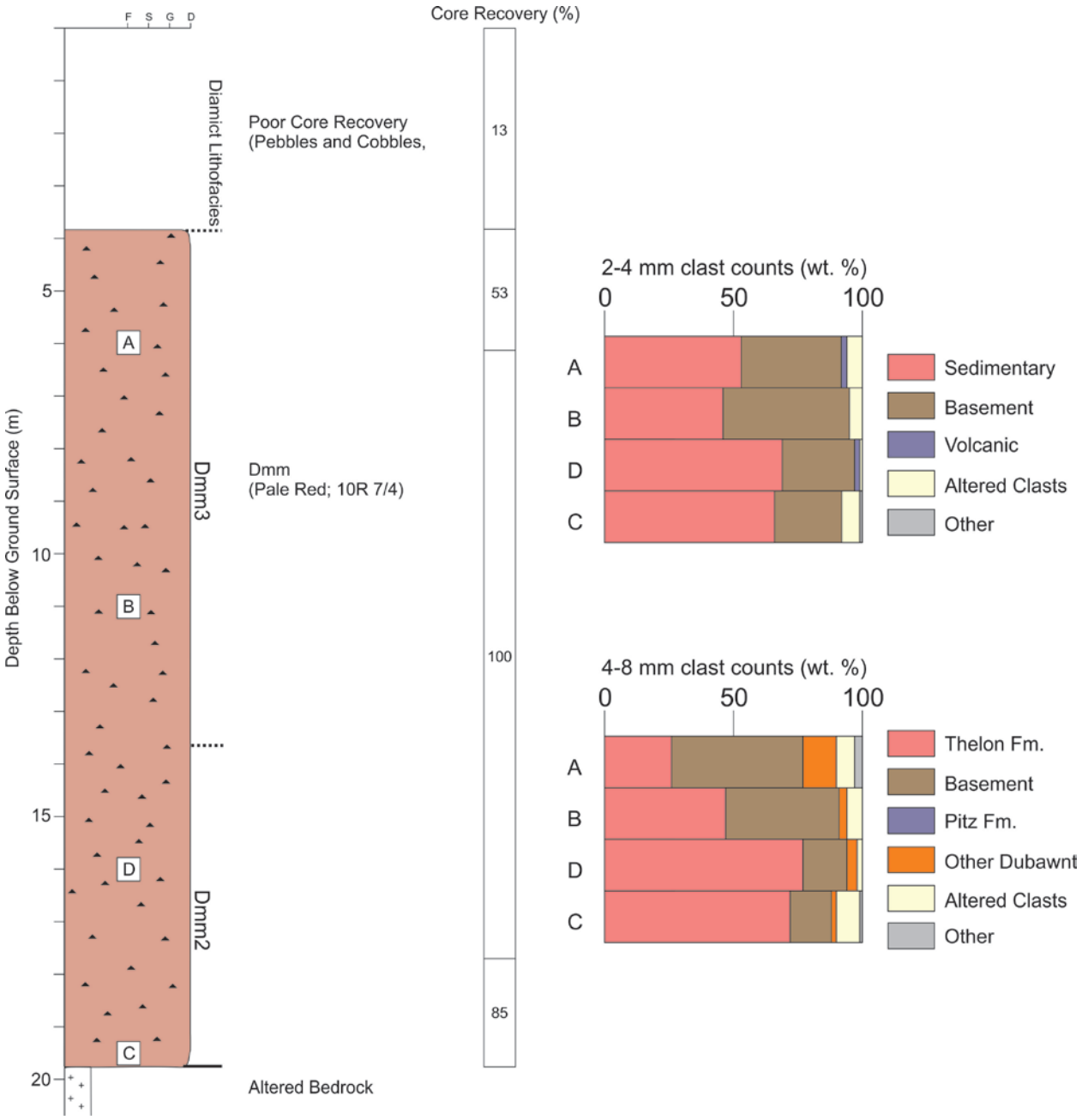

Figure 3-17: Drillcore log TUR-042 with associated sample properties. This drillcores displays two diamicton lithofacies Dmm 2 and Dmm 3.

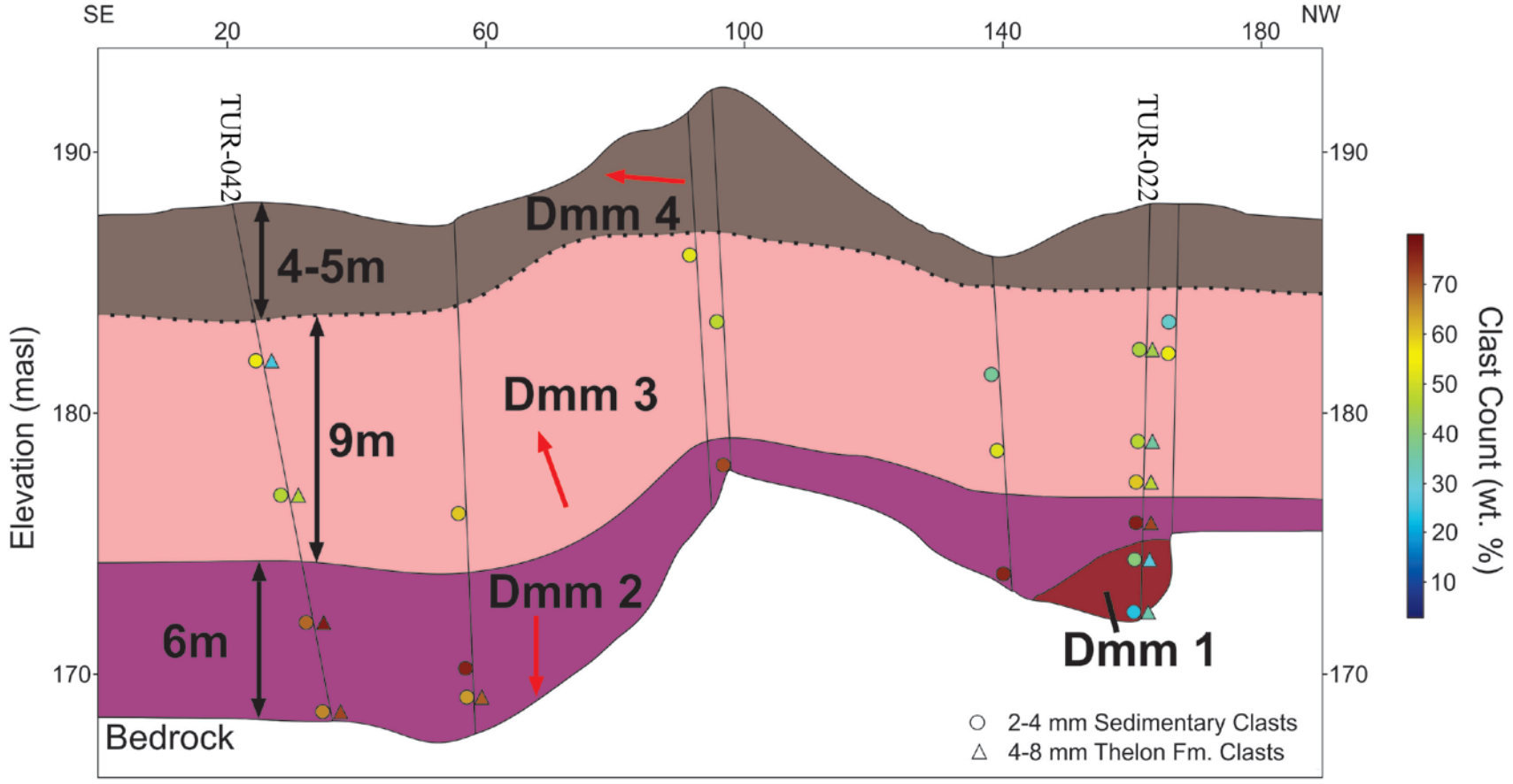

Figure 3-18: SE-NW cross-section through the main Tatiggaq drillcores. Drillcore samples are classified acording to their 2-4 mm Dubawnt sedimentary and 4-8 mm Thelon Fm clast count results. Red arrows indicate the interpreted paleo-ice flow phase responsible for till deposition.Vertical Exaggeration = 4x.

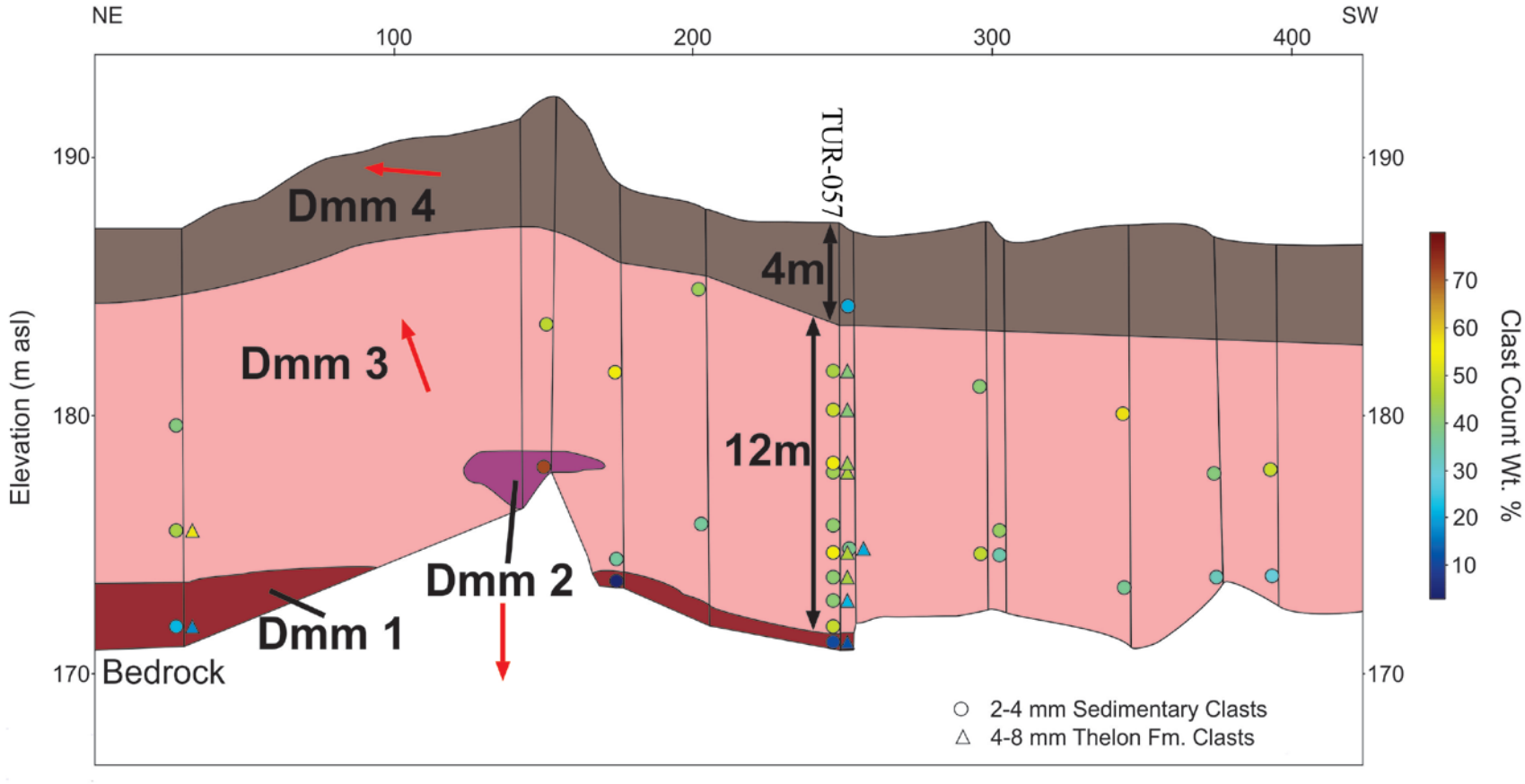

Figure 3-19: NE-SW cross-section through the main Tatiggaq drillcores. Drillcore samples are classified according to their 2-4 mm Dubawnt sedimentary and 4-8 mm Thelon Fm clast count results. Red arrows indicate the interpreted paleo-ice flow phase responsible for till deposition.Vertical Exaggeration = 8.7x.

3.4.4.2 Till Provenance

Lithology clast counts were conducted on all of the samples (n=93) from the Tatiggaq grid for the granule (2-4 mm) fraction and on 48 samples for the pebble (4-8 mm) fraction. Clast counts suggest a varied till provenance between identified lithofacies. Specifically, large variations in the proportion of Thelon Fm are observed between each lithofacies and the presence or absence of Pitz Fm helps constrain till provenance.

The 2-4 mm sedimentary granules were too small to be classified as Thelon Fm with confidence and are thus defined as sedimentary clasts + rounded quartz grains. Comparing the results of the 2-4 mm sedimentary component to that of the 4-8 mm Thelon Fm component (Fig. 3-20), it is evident that there is a strong positive correlation between these two components, suggesting that the 2-4 mm sedimentary granule component is representative of the quantity of the Thelon Fm component in the 4-8 mm range. This is apparent in Fig. 3-20 below where the corresponding trend line has a slope of 0.95 and a correlation coefficient of 0.86. Therefore, for samples where there was an insufficient amount of 4-8 mm clasts recovered to complete the analysis, the sedimentary granule component is a good indicator of the quantity of Thelon Fm clasts present.

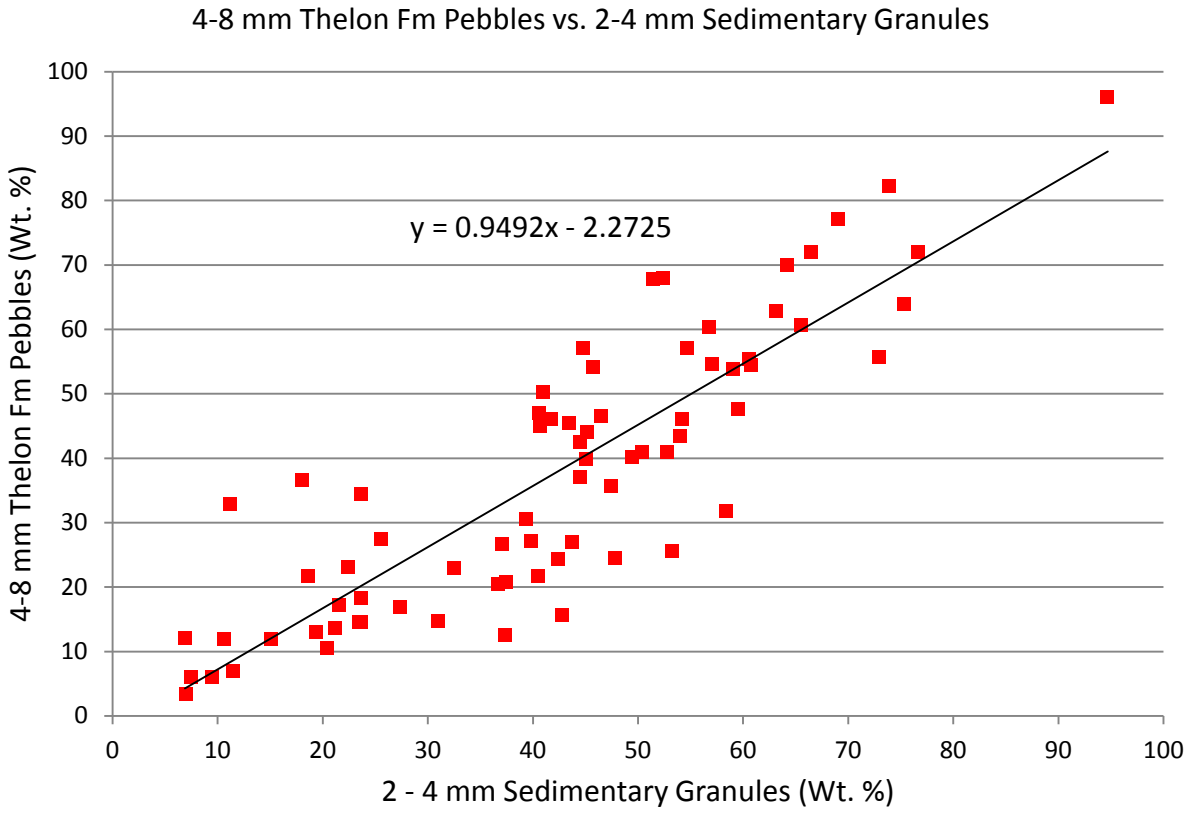

Figure 3-20: Comparison of clast lithology results for all of the drillcore samples analysed across the study area expressed in weight percent of the 4-8 mm Thelon Fm component and the 2-4 mm sedimentary granule component (n=73).

A composite summary of each count for the 4-8 mm fraction is exhibited in Fig. 3-21. The lowermost diamicton observed in several drillholes (Dmm 1; e.g. TUR-057, -022) cannot be confidently assigned to a known ice flow phase from the surficial record. In addition, it is uncertain whether it forms a single till sheet. Nonetheless, the lithological signature of the basal unit of TUR-057 indicates a strong basement component, no volcanic lithologies and a minor component of Thelon Fm, which together could potentially be the result of the earliest identified ice flow phase (WSW; 255°). Alternatively, it could also simply be a short transportation signature. Interestingly, sample F from the Dmm 1 lithofacies at TUR-022 had three Pitz Fm clasts recovered, which suggests either a western or southern provenance for this till unit. This till sheet could potentially be a remnant till sheet from a previous glaciation or correlated to the easterly ice flow phase C of McMartin and Henderson (2004a).

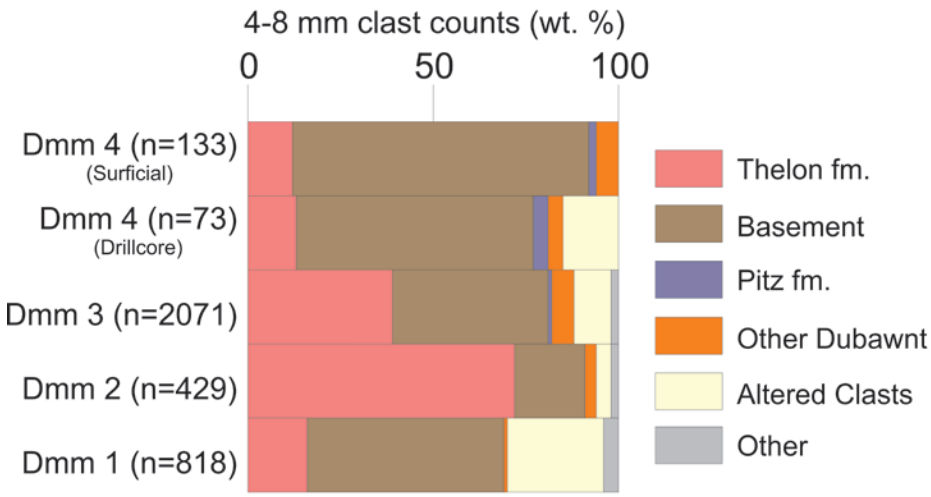

Figure 3-21: Composite clast count for each of the identified diamicton lithofacies of the Tatiggaq grid. Dmm 4 is defined based on drillcore and surficial sample.

The Dmm 2 lithofacies has an anomalously high proportion of Thelon Fm present within the till sheet and no Pitz Fm clasts were recovered from samples that had 4-8 mm counts conducted. The very large proportion of Thelon Fm and lack of Pitz Fm suggests a northern provenance for this lithofacies. A southerly ice flow phase would have eroded large proportion of the relatively soft Thelon Fm which is the dominant bedrock lithology north of the exploration target and is mapped to be present just 9 km to the north.

Lithofacies Dmm 3 has a mixed Thelon Fm and basement lithology signature, however Pitz Fm clasts were recovered from till samples (max 5 wt. %, avg. 1 wt. %). As evidenced by drillcore TUR-057, this till unit has a fairly homogenous textural and lithological signature. Deposition by a northerly ice flow phase suggests a shift in the configuration of the Keewatin ice dome between Dmm 2 and 3, and would require a migration to a location south of the study area which has been documented (Ch. 2; McMartin and Henderson 2004a).

The surficial till sampled in the vicinity of the Tatiggaq exploration target is a basement rich till sheet. Pitz Fm was regularly recovered during sample counts and is generally more numerous than what is observed in Dmm 3. The surficial till (Dmm 4) is interpreted to be a result of NW (300°) to W (270°) ice flow phases. An interpretation of the depositional ice flow phases experienced at the Tatiggaq exploration target are presented in a conceptual reconstruction (Fig. 3-22).

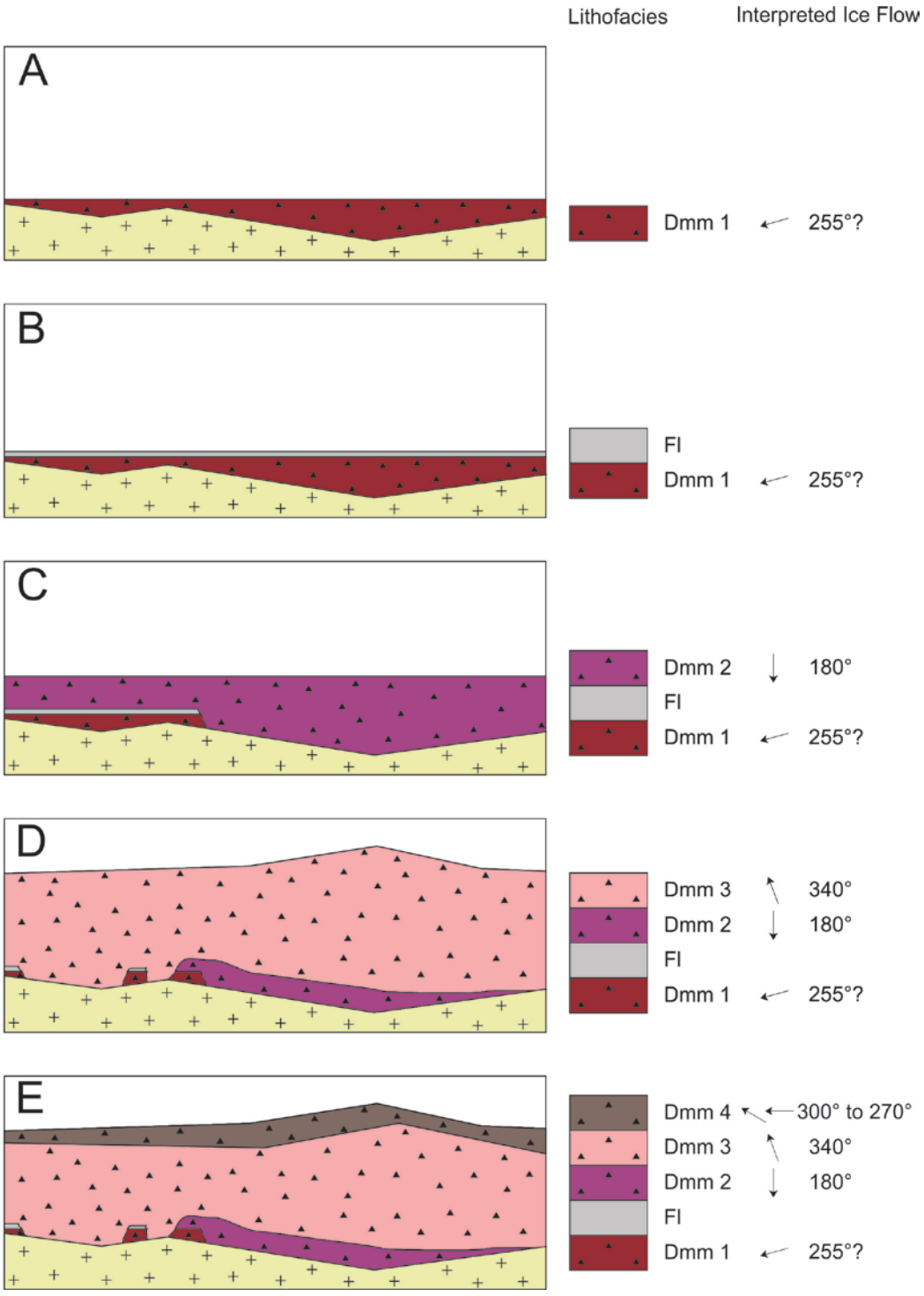

Figure 3-22: Conceptual glacial dynamic reconstruction of the main Tatiggaq exploration target correlated with the surficial paleo-ice flow record. A. Initial till deposition across the exploration target or inheritance from a previous glaciation. B. Period of lacustrine submergence resulting in the deposition of laminated fine-grained sediments. C. Southerly ice flow phase delivering a large quantity of Thelon Fm detritus. D. Near complete re-working and incorporation of early deposited sediment during a strong NNW ice flow phase resulting in a mixed Dubawnt-Basement clast signature. E. Late northwesterly to westerly ice flow phase delivering a large amount of basement detritus.

3.4.5 Regional Drillhole Stratigraphy

3.4.5.1 Mammoth Grid

Drillcore MAM-002 intersected one of the thickest sequences of diamicton sediments throughout the study area with over 30 meters recovered (Fig. 3-23). The first 55 cm of recovered core (5.45 - 6 m below ground surface (bgs) is a pale red (10R 7/2) matrix-supported, massive diamicton. At 6 m bgs, a slight colour variation was observed to a pale red (10R 7/3) matrix-supported, massive diamicton. This unit continues until 28.45 m bgs and is qualitatively homogenous with no variations exhibited in drillcore logging or textural analysis, but exhibits clast lithology count variations. From 28.45 – 36 m bgs, a matrix-supported, massive diamicton is present with various shades of pale red (10R 6/2 to 2.5YR 7/2) colour observed. Textural analysis of samples reveals a dominantly sandy diamict and variance between till samples is minimal with the exception of the upper-most till unit, which has a higher clay component.

Clast lithology counts of the 4-8 mm fraction from MAM-002 were limited for the majority of samples due to subsampling for the production of thin sections. Of the clast counts conducted, no Pitz Fm clasts were found within samples C (n=40), E (n=26), F (n=24) and G (n=32). Sample B had several Pitz Fm clasts recovered but also had the most clasts recovered to identify (n=114). The 2-4 mm fraction exhibited a high proportion of sedimentary granules in the lower till units reflecting the local bedrock of the area. Within the thick pale red till sequence there is an overall decrease in sedimentary granules and an increase in basement lithologies upcore. It is interpreted that at the very least, diamicton deposited after the interval sampled in B can be assigned to a southern provenance due to the recovery of Pitz Fm

From 36 – 38.5 m bgs fine-grained sediments in contact with the Thelon Fm were observed with 100% core recovery of these units. The lowest unit consists of a white (10R 8/1) friable laminated fine-grained sediments. These sediments have a sharp contact at 37.9 m bgs with an overlying unit of white (10R 8/1) fine-grained sediments that are very compacted, generally massive, but locally laminated. The upper fine-grained unit is light olive grey (5Y 6/2) and is laminated with organics at various intervals throughout the unit (Fig. 3-24 B). The contact between the clayey-silt white and laminated light olive grey fine-grained sediments is a gradational contact over ~ 50 cm from 36.97 – 37.47 m bgs.

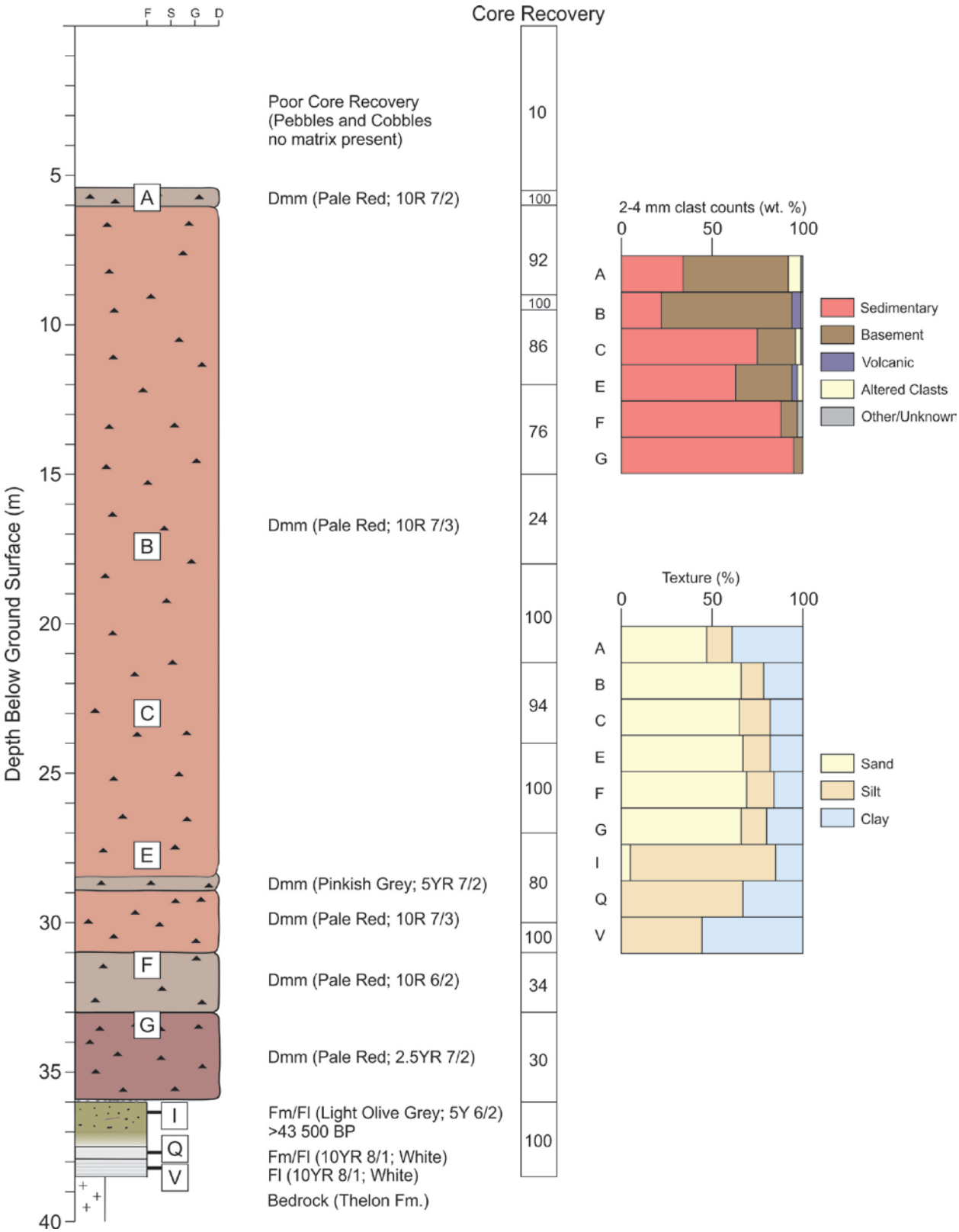

Figure 3-23: Drillcore log of MAM-002 with associated sample properties.

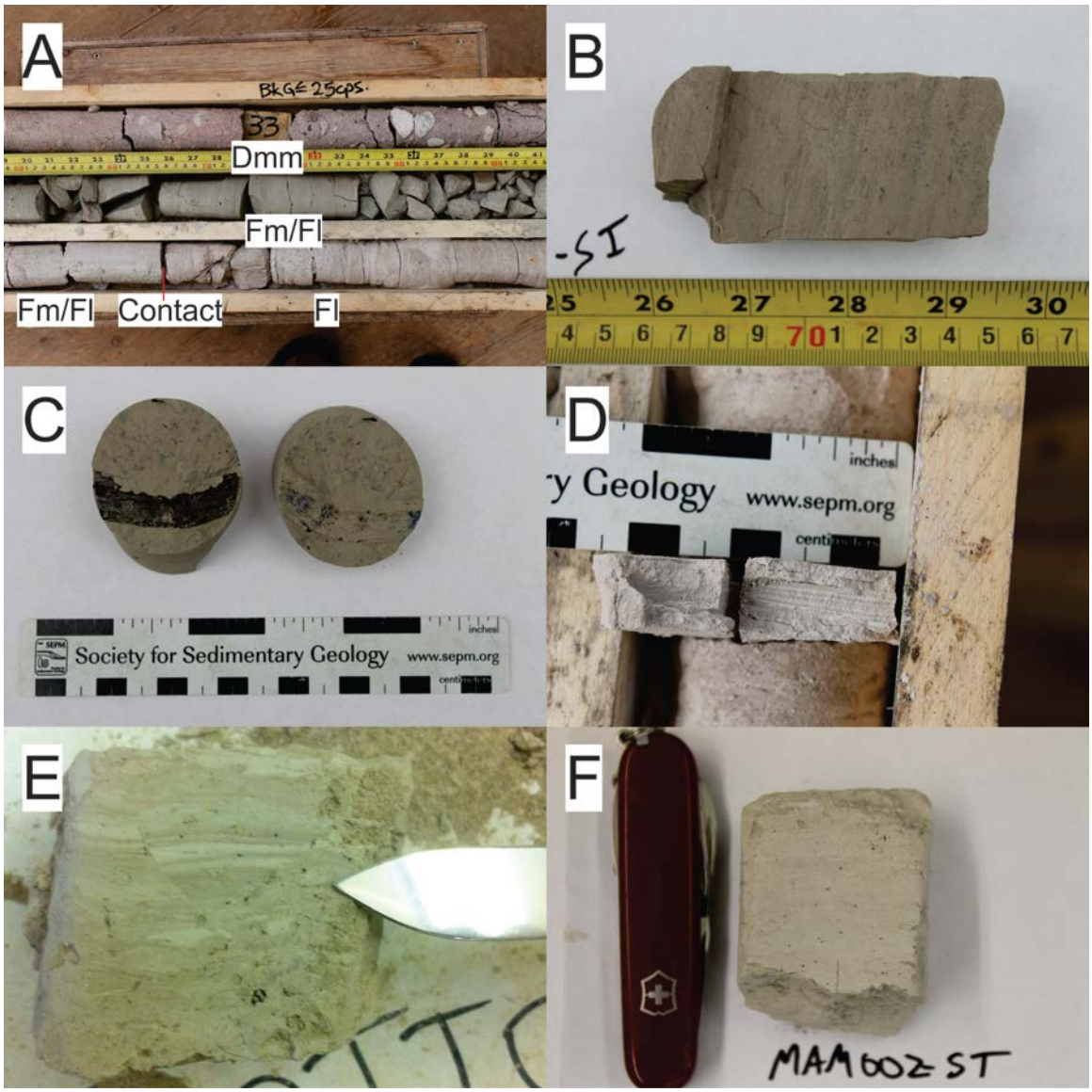

Figure 3-24: A. Part of drillcore MAM-002 from the center of the last Quaternary core box displaying the lower two diamicton units and the three fine-grained units present B. Light olive grey fine-grained unit laminated with black organics. C. Piece of inner bark recovered from the light olive grey fine-grained sediment unit. D. Laminations present within the lower fine-grained silty-clay white unit. E. Laminations present within the clayey-silt white unit. Note the brittle fault within the sediments likely from glacial loading of frozen sediments. F. Clayey-silt white unit that is more massive in appearance. Note the small blue granules within the sediment which are suspected to be vivianite concretions.

Textural analysis of the each fine-grained unit shows a trend of increasing silt content from a silty-clay white fine-grained laminated unit to a clayey-silt light olive grey unit. Within the clayey-silt white unit, laminations were present at intervals throughout the core (Fig. 3-24 E) whereas some intervals were more massive in appearance (Fig. 3-24 F). Within this unit blue granules were identified and concentrated at various depths within the sediments (e.g. Fig 3-24

F). These particles are likely small vivianite concretions within the sediments, indicating reducing and alkaline conditions (Rosenquist 1970). Within the light olive grey unit a piece of wood was recovered (Fig. 3-25 C). Radiocarbon dating of this wood produced a non-finite age date (>43 500 yrs BP) and paleomagnetism suggests a normal polarity signature, likely of the present Brunhes chron (Barendregt pers. comm. 2014; Appendix K).

3.4.5.2 HND, LOB and JSF Grid Drillcores

The HND, LOB and JSF drilling grids are between the Ayra and Tatiggaq drillholes (refer to Fig. 3-2) and consists of six drillholes (Fig. 3-25). Drillcore logging of the Quaternary sediments revealed that the dominant sediment present is a matrix-supported, massive diamicton. The diamicton is generally a pale red colour and varies from Munsell codes 10R 7/2 to 2.5YR 6/2.

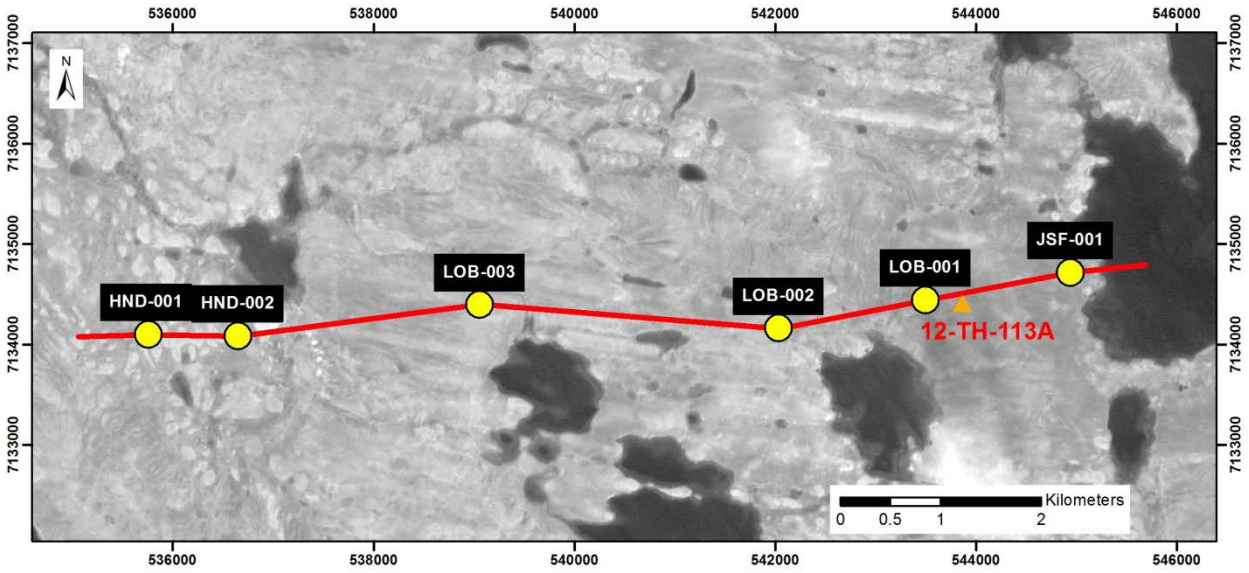

Figure 3-25: HND, LOB, JSF drilling grids displaying the location of drillholes. The red line denotes the location of the cross-section depicted in Appendix G, Fig. 3. Background is SPOT 4/5 imagery. The orange triangle denotes a surficial sample (12-TH-S113) discussed within the text.

Drillhole HND-001 had one of the thickest intersections of Quaternary sediments and encountered bedrock at 59 m bgs. This drillcore consists of two pale red diamicton separated by an interval of fine-grained laminated sediments and laminated diamicton (Fig. 3-26 A, B). The upper pale red diamicton is massive and the lower pale red diamicton is laminated in some intervals and is in contact with sand and fine-grained sediments at a depth of 20 m bgs, which extends to a depth of 22.7 m bgs. The next 36 meters were poorly recovered, consisting mainly of pebbles and cobbles, with little to no matrix recovery. Cobbles recovered from this interval are often rounded to sub-rounded and some intervals display characteristics typical of glaciofluvial clasts, such as rounded iron-shaped cobbles (Fig. 3-26 D). Interestingly, 8 km to the north drillhole SNB-002 intersected a 53 m interval of rounded to sub-rounded cobbles as the basal unit within the drillcore which was overlain by diamict sediments. Due to the drilling method employed not much can be gleaned from these sediments present, but it is evident that

there are likely buried fluvial or glaciofluvial deposits at depth within this region. The potential of buried valleys is important to consider for exploration within this region as thick sequences of Quaternary sediments can influence gravity geophysical surveys, which is a common exploration method employed in unconformity-type uranium exploration.

Clast lithology counts from HND-001 (3-26 E) suggest that the lower till unit has a northern provenance and the upper till unit a southern provenance. This is due to Pitz Fm clasts recovered from the upper unit and proportion of Thelon Fm present within the diamict units. This interpretation is supported by geochemical results (3.4.6) that suggests correlation between the lower till unit (sample E) with that of lithofacies Dmm 2 at Tatiggaq which is interpreted to have a northern provenance; the upper two samples (A and B) are correlated to Dmm 3 at Tatiggaq. Drillcore HND-001 also suggests a period of non-glacial conditions between these two ice flow phases as evidenced by laminated fine-grained sediments with dropstones, indicating a likely proglacial setting.

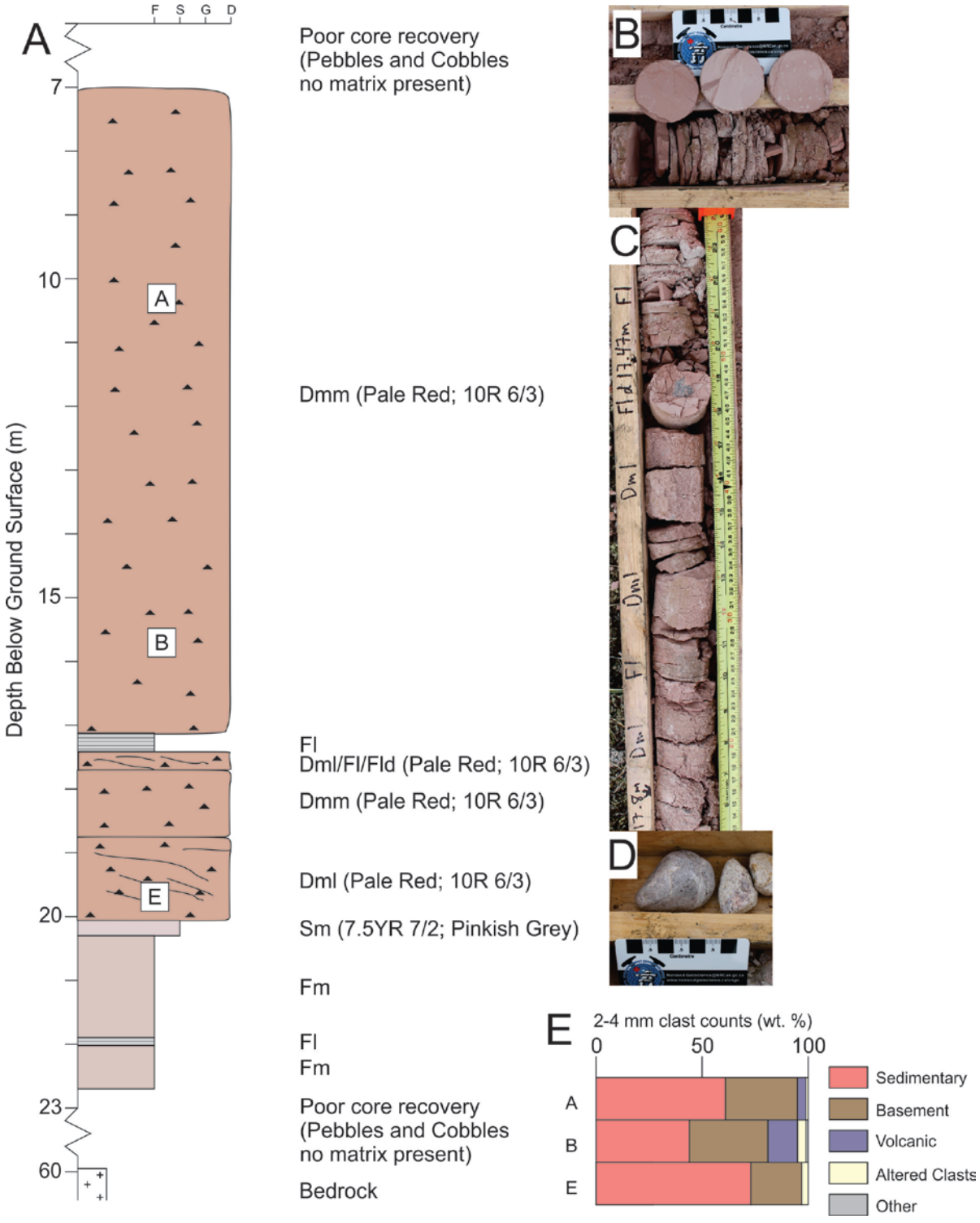

Figure 3-26: A. Drillcore log of HND-001, note the upper and lower zones of poor recovery are not displayed. Core recovery was >90% for the logged interval shown. B. Example of the fine-grained laminated sediments observed above Dml/Fl/Fld. C. Sequence of laminated diamicton and laminated fine-grained sediments with depth along the drillcore is indicated on the core box. Note the presence of a dropstone at 17.47 m. D. Example of a clast from the lower thick sequence of poor core recovery that has the morphology of a rounded iron-shaped clast, typical of a glaciofluvial setting. E. Results of the 2-4 mm clast counts.

Drillcore LOB-001 (Fig. 3-27) had a definitive two till stratigraphy that was identified by a sharp colour change during drillcore logging. Clast counts conducted from within these two units have a large disparity in regards to proportion of Thelon Fm clasts present. The two units present at LOB-001 are texturally very similar, but the lower unit has at least 50 wt. % Thelon Fm clasts whereas the upper unit is dominated by basement lithologies. The presence of Pitz Fm within the lower till unit suggests that this unit was deposited during NNW ice flow phase. The upper till unit clast composition appears to represent a mixing between the lower till unit and surficial counts suggesting it is potentially attributed to the NW ice flow phase or from the W ice flow and having a higher inheritance of the lower till unit than the surficial till samples. From the cross-section (Appendix G, Fig. 3) across the central grid drillcores, it is evident that basal samples in general have a high Thelon Fm component as discussed specifically with LOB-001 and HND-001.

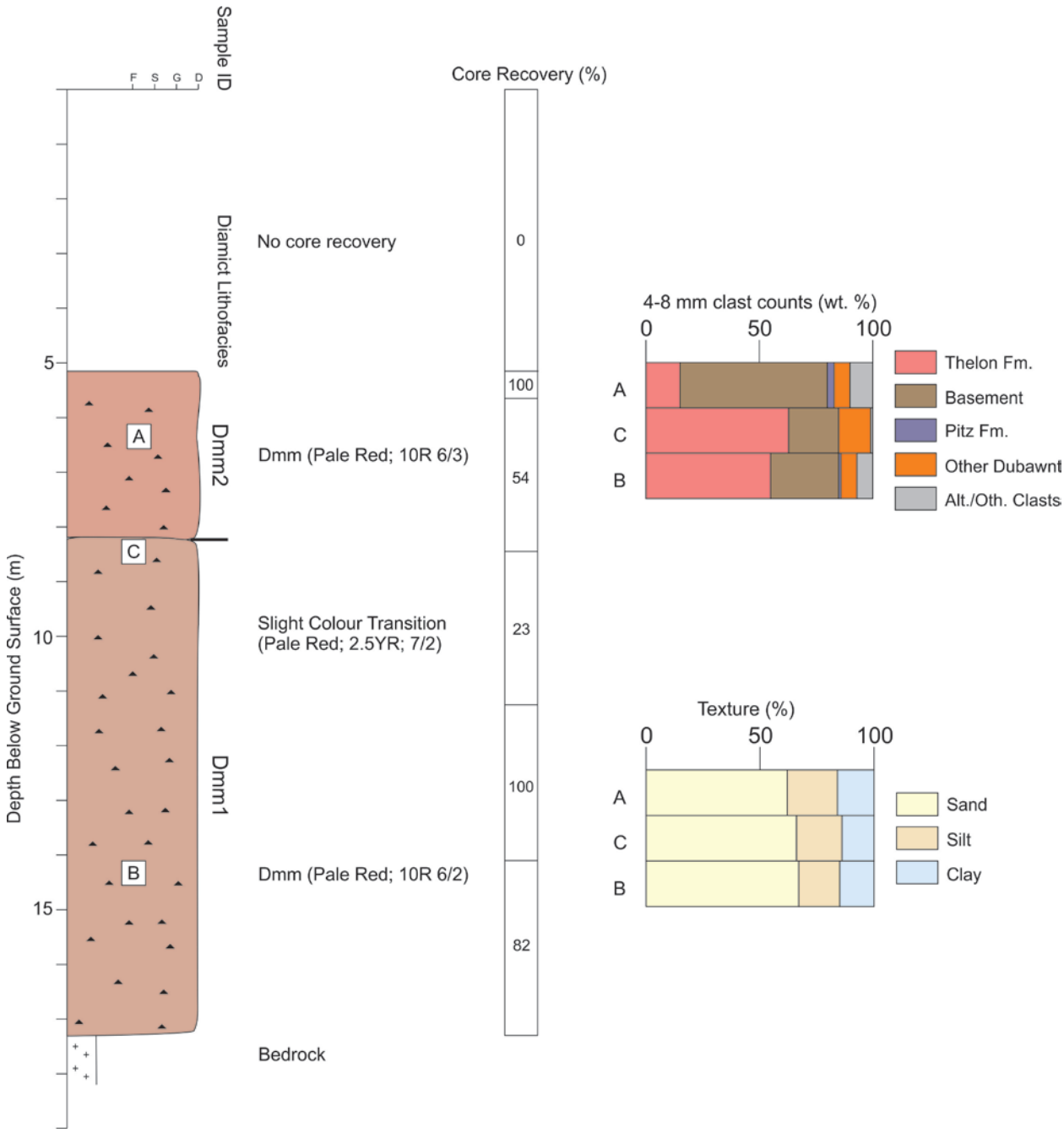

Figure 3-27: Drillcore log of LOB-001 and associated sample properties. Two diamicton units were logged, both consisting of a sandy pale red matrix-supported, massive diamicton. The clast counts show the lower unit is enriched in Thelon Fm clasts relative to the upper diamicton unit.

.

3.4.6 Drillcore Geochemistry as a Proxy for Till Provenance

When assessing Cameco's whole rock geochemistry database, it is evident that the results of unaltered Thelon Fm are enriched in Boron relative to most bedrock lithologies of the region (with the exception of the Woodburn Lake group) and is depleted in Rubidium relative to every other unaltered regional bedrock unit sampled (Hunter pers. comm. 2013). Therefore, the B:Rb ratio of the silt and clay fraction of tills in the area is useful to assess the proportion of Thelon detritus in the till matrix. Despite differences in the composition of the coarse and fine grained size fractions, Fig. 3-28 shows there is a strong relationship between the B:Rb ratio and the proportion of Thelon Fm detritus present within the coarse fraction of tills across the entire study area and that the relationship is independent of sample depth. The B:Rb value was normalized to the proportion of silt and clay, as it is evident that there is fractionation with grain size (Appendix G, Fig. 5).

It is apparent that the high Thelon signature of the Tatiggaq lithofacies Dmm 2 is easily deciphered from the signature of Dmm 3 (Fig. 3-28), which lends support to the interpretation of a till sheet deposited by a separate ice flow phase towards the south. The two till stratigraphy observed at HND-001 is correlated to Dmm 2 and Dmm 3 of the Tatiggaq grid, based on the proportion of Thelon Fm present within each unit and lack/presence of Pitz Fm Shallow drillcore samples at the Tatiggaq grid interpreted to represent the surficial till (Dmm 4) are easily distinguishable from the lower Dmm 3 samples and approach the signature of the surficial till. Lithofacies Dmm 1 of the Tatiggaq displays a more sporadic pattern and has a heightened B:Rb, which is likely due to the incorporation of the locally illitized bedrock which would increase the proportion of B relative to the background values. This is illustrated clearly on Fig. 3-28, as the majority of the Dmm 1 values plot higher than the general trend observed.

The thick pale-red till lithofacies logged in drillcore MAM-002 exhibits a large variation in the proportion of Thelon Fm granules, suggesting the presence of at least two distinct lithofacies. Based on stratigraphic correlation with other drillcores it is likely that the upper part of this drillcore (sample B) is a result of a northern ice flow phase. This is supported by the recovery of Pitz Fm and by the high Thelon signature exhibited in the lower portions of the drillcore, which were likely deposited by a southern ice flow phase (samples C and E).

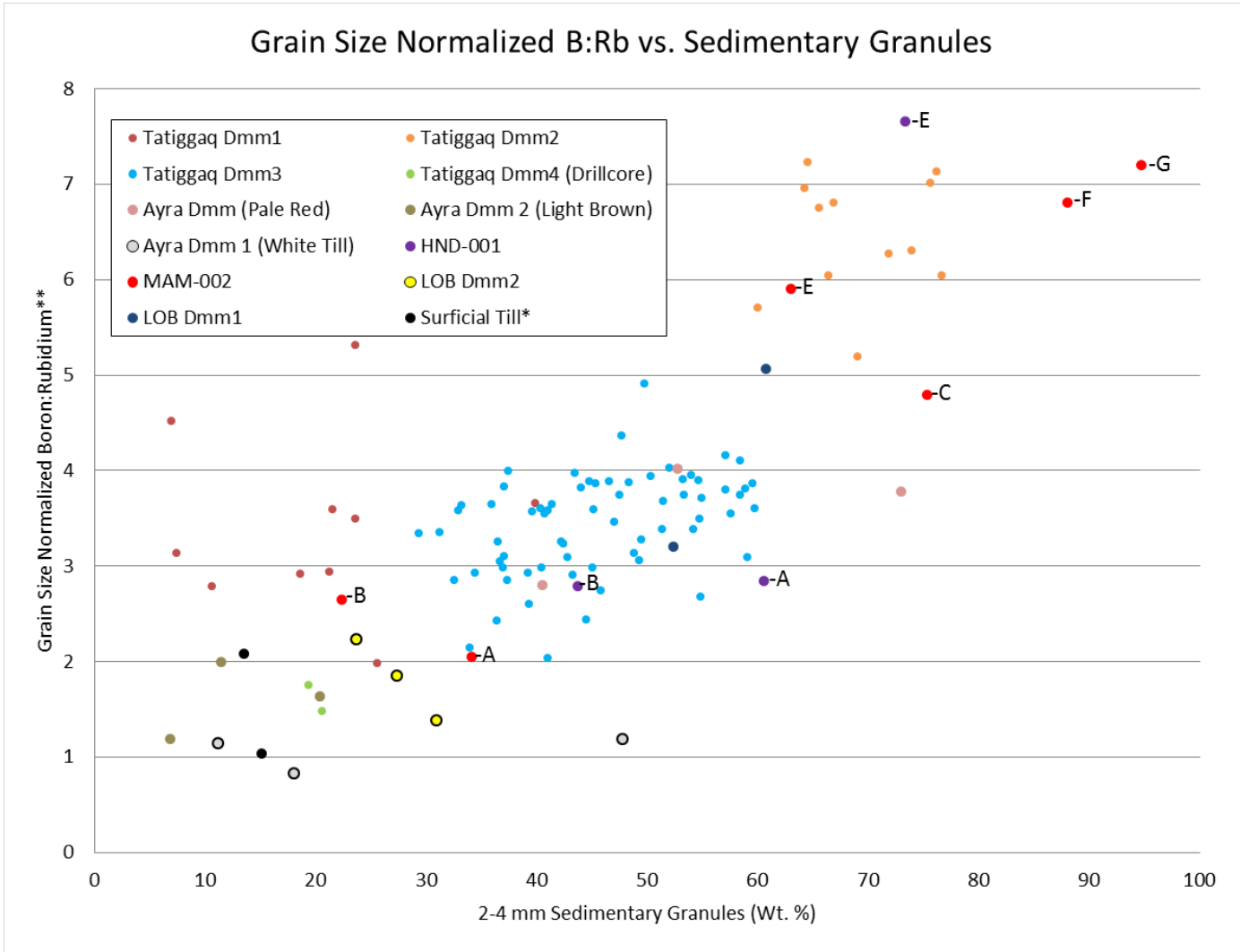

Figure 3-28: B:Rb vs 2-4 mm sedimentary clast component. Samples are classified according to drillcore/lithofacies. The letters (i.e. –A) refer to the samples of specific drillcores. *The surficial till is represented by the only two surficial samples that had 2-4 mm counts conducted, one Tatiggaq surficial (12-MR-010) and one sample near LOB-001 (Fig. 3-26, 13-TH-113). **The B:Rb signature was normalized to the proportion of silt and clay present (B:Rb x silt:clay ratio).

3.4.7 Till Micromorphology

The location of MAM and TUR samples discussed are displayed on figures 3-23 (MAM-002) and 3-16 (TUR-057). The legend for the interpreted features and further annotated figures are located in Appendix L. Note drillcore MAM-002, TUR-057 and AYA-010 were drilled at 90° (perpendicular), 80° and 85° of an incline relative to ground surface, respectively.

3.4.7.1 Thin Section Descriptions

MAM002 (Refer to Fig. 3-23 for sample locations)

Sample A (Fig. 3-29 A) comprises multiple diamicton domains. The predominant domain is a clast-rich domain, while the other consists of a plasma rich domain with primarily fine-sand clasts. Rotational structures and grain lineations are evident within the coarse diamicton domains. The fine-grained domain has a large (1 mm) clast that exhibits a strain cap consisting of clay-rich zonation on either side of the clast. The relatively large fluid escape structure visible within the thin section indicates fluid flow from left to right and is composed of bands of clay, silt and sand cross-cutting the clast-rich diamicton domain. Within the clast rich diamicton domain there is also evidence for a plasma-rich shear zone (Fig. 3-29 B), where a coarser domain (up to 1 mm quartz clasts) is separated from a finer-grained domain (<0.2 mm clasts). Rotational structures are visible within both till domains. Grain stacks and lineations are generally parallel to the inferred shear zone. Evidence of grain crushing was also observed amongst quartz grains.

Sample B displays a single domain of sandy quartz-rich diamicton with sandstone and basement clasts visible. Large clasts are often rimmed by plasma. Rotational structures, lineations and grain stacks are common throughout the diamicton with some minor evidence for grain crushing within quartz grains. Lineations do not experience a multiple preferred orientation and grain stacks are commonly oriented top left to bottom right.

Sample C contains a single domain of sandy quartz-rich diamicton present in the thin-section within ‘hematite’ coloured plasma. Clasts range from well-rounded to very angular, which is a product of the large proportion of Thelon Fm within the diamicton. Microstructures visible include lineations, grain stacks and rotational structures. Lineations are typically having a single preferred orientation (top left to bottom right).

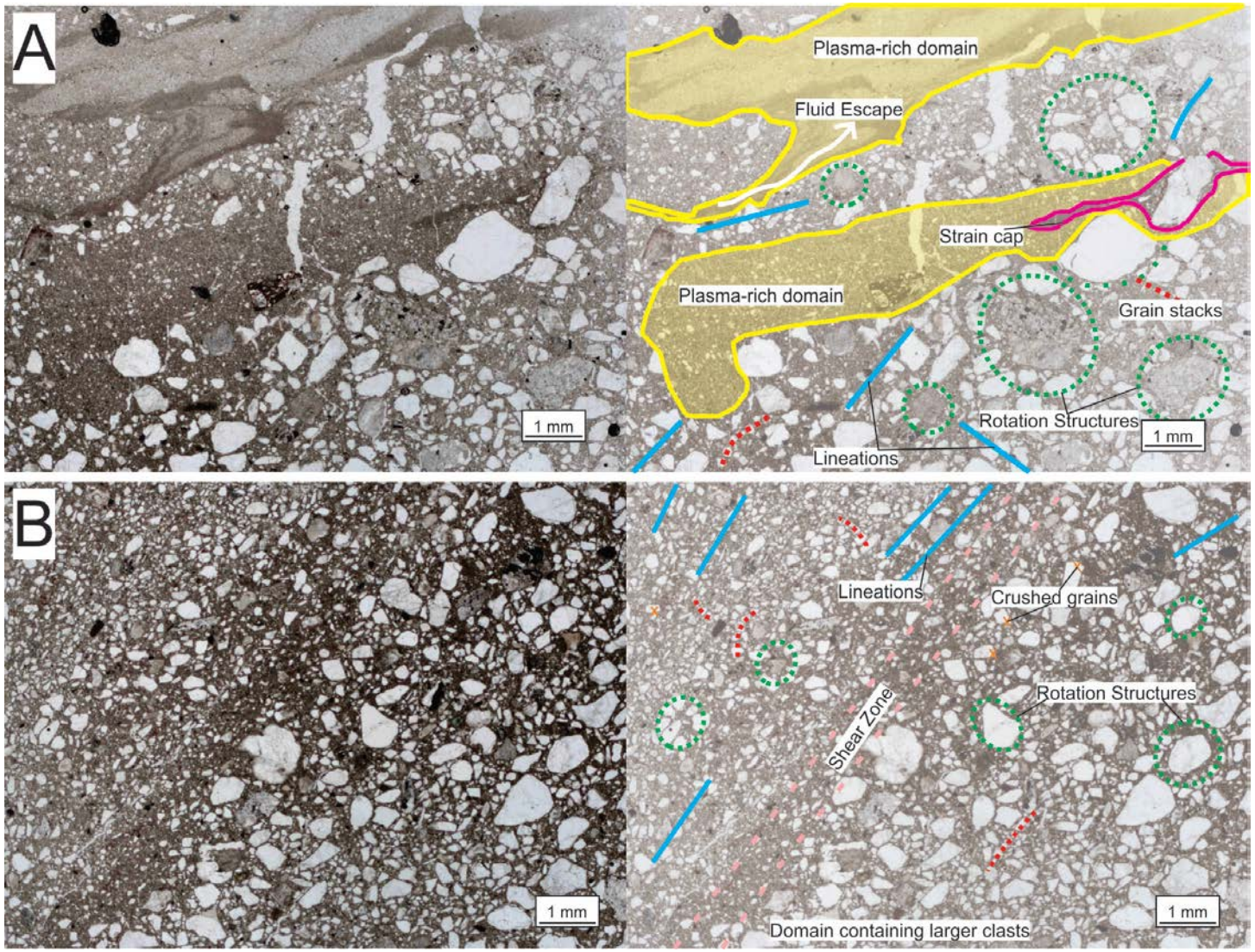

Figure 3-29: Micromorphology interpretation for drillcore sample MAM002-SA. A. Photomicrograph exhibiting multiple diamicton domains, fluid escape structures rotational structures and a strong bottom left to top right lineation sense. B. Photomicrograph showing a distinct plasma-rich shear zone separating two diamicton domains. Images are in plane-polarized light and note the 1 mm scale bar.

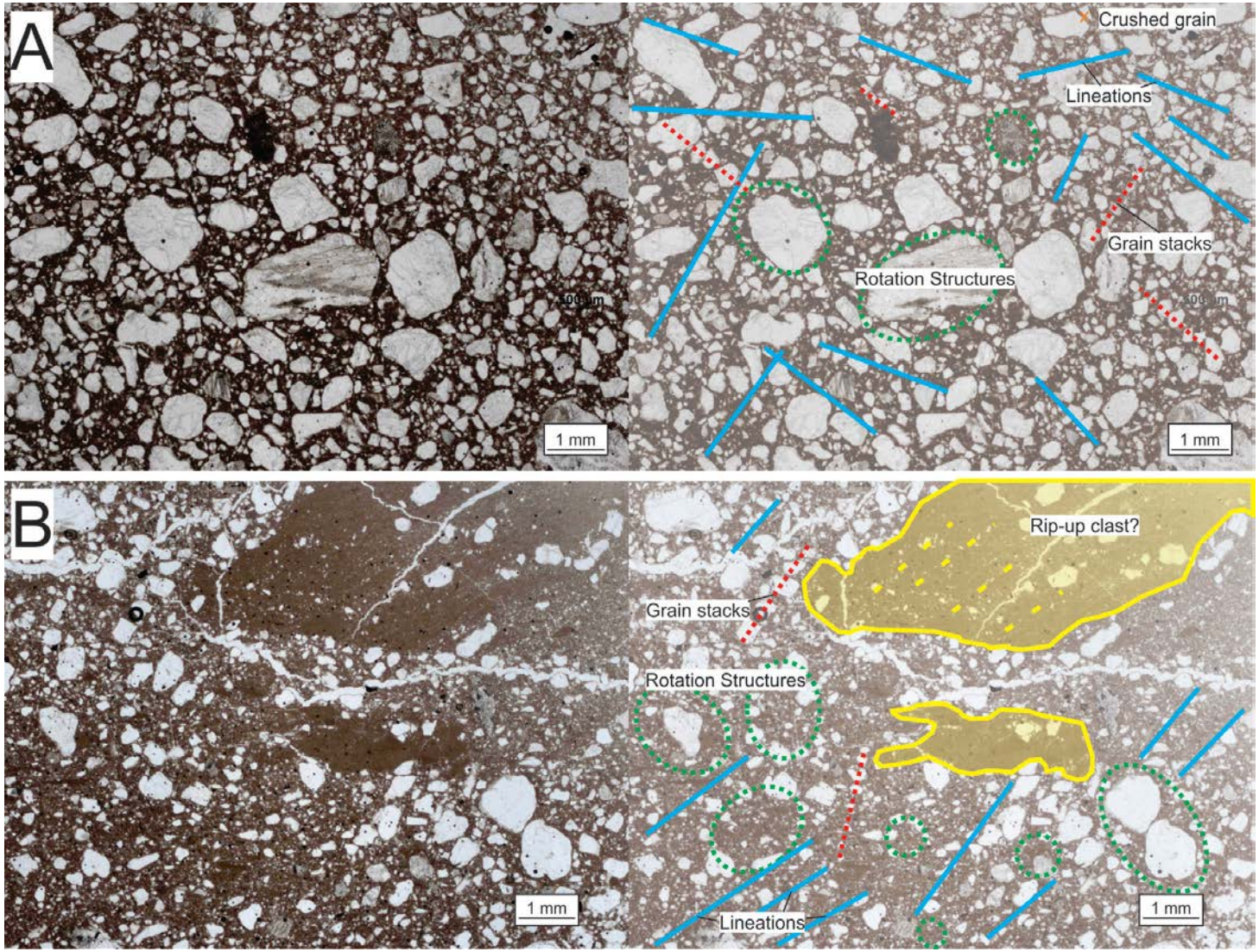

Figure 3-30: Example of micromorphology interpretation from drillcore TUR-057. A. Sample H exhibiting lineations, rotational structures and grain stacks as the dominant microstructures. B. Sample K showing multiple diamicton domains and a dominant bottom left to top right lineation sense, including numerous rotational structures. Images are in plane polarized light and note the 1 mm scale bar.

Sample E exhibited a single till domain almost entirely composed of quartz grains and sandstone clasts with some minor basement clasts present. The plasma is a ‘hematite’ red colour and clasts are rarely in contact. Rotational structures, lineations and grain stacks are the most common microstructures present. Lineations display a strong bottom left to top right orientation, with grain stacks also displaying a similar preferred orientation.

The sample F thin section contains a single diamicton domain composed almost entirely of sandstone and quartz clasts within a ‘hematite’ coloured plasma. The largest skeletal clast in the center of the photomicrography is rimmed by plasma and suggests evidence of rotation, similar to other large skeletal grains. Lineations are oriented in two primary directions (top right to bottom left, and bottom right to top left).

Sample G contains a clast-rich, single domain diamicton composed of quartz and sandstone clasts within reddish-brown coloured plasma. Rotational structures and lineations are present. Rotational structures are abundant and lineations and grain stacks have a dominant top left to bottom right orientation; necking structures are also present.

TUR-057 (Refer to Fig. 3-16 for sample locations)

Sample H (Fig. 3-30 A) has a single diamicton domain evident with lineations, grain stacks and rotational structures present. Lineations have two predominant orientations near perpendicular to one another (top right to bottom left and top left to bottom right).

Sample J contains a single diamicton domain with a ‘hematite’ red colored plasma. The main microstructures visible include grain stacks, lineations and rotation structures. The largest clast within the photomicrograph shows evidence of rotation. Grain stacks are more numerous than lineations and have two preferred orientations.

Sample K (Fig. 3-30 B) contains two domains, one consisting of till and the other of predominantly fine-grained material. Evidence for possible preserved primary structures is evident in some clusters of the fine-grained domains, suggesting that they are interpreted as ‘rip-up’ clasts that have been incorporated into the till from the lower lithofacies (refer to Fig. 3-16), transported and deposited likely in a frozen state. Turbate structures are common. Grain stacks and lineations are also observed throughout the sample.

AYA-010

Thin sections were produced from the two samples (B – 17.4 m bgs, C – 22.0 m bgs) within the light brown diamicton lithofacies (refer to section 3.4.3) of drillcore AYA-010. Both samples appear similar in thin section. Both have lineations and grain stacks present in two preferred orientations, diagonally across the photomicrograph. Rotational structures are evident but less numerous than lineations and grain stacks. Minor evidence for grain crushing and necking structures are present.

3.4.7.2 Micromorpohology Interpretation

MAM-002

Unit 1 (MAM002-SA) has multiple domains within this diamicton suggesting that this unit has experienced incomplete homogenization or experienced a high degree of shearing. The presence of fluid escape structures indicates relatively high pore-water content. Rotational structures indicate ductile matrix deformation within the diamict. Grain lineations primarily oriented in the same direction and the presence of a shear zone parallel to the lineations suggest a high degree of shear was experienced. It is interpreted the multiple domains represent incomplete homogenization of incorporated of the lower diamicton unit.

Three thin sections were produced from the thickest logged unit within drillcore MAM-002, which qualitatively displayed no sedimentological variations throughout the logged interval. The three thin sections samples display a similar suite of microstructures which include rotational structures, lineations, grain stacks and some evidence of grain crushing. Within the lower samples (-SC, -SE) lineations typically have one preferred orientations, while the upper sample (-SB) from the middle of the unit has multiple preferred orientations which could reflect a variation in the shear stress and a possible record overprinting. This sample also displays lithological variations from the other two samples which could represent a change in the dominant ice flow direction responsible for deposition.

Samples F and G were from two lower units rich in Thelon Fm detritus. Sample F exhibits evidence for deformation as indicated by rotational structures throughout the sample. Two distinct lineation orientations are present, suggesting possible variations in the dominant shearing direction throughout deposition. This sample displays evidence for both ductile and brittle

deformation. Sample G has widespread evidence for deformation as evidenced by rotational structures. Lineations appear to have one dominant orientation with oblique lineations occurring in several other orientations. Grain stacks are more numerous than lineations.

TUR-057

All three samples from TUR-057 were from Dmm 3 (refer to section 3.4.4). Samples J and H appear similar exhibiting rotational structures as well as lineations, grain stacks and minor evidence of grain crushing indicative of both brittle and ductile deformation. The main difference observed between the samples is that grain stacks are more numerous in sample J relative to H as well as rotational structures. This suggests ductile deformation was potentially more dominant in J and an increase in brittle deformation up-core from H to J.

The lower sample exhibits the incorporation of a laminated fine-grained unit that is situated stratigraphically below the diamicton sample, in agreement with grain size analysis of the sample which is relatively enriched in silt and clay. The incomplete homogenization of this unit is demonstrated by the distinct domains observed within the thin section. In some cases, it would appear that primary lineations of the incorporated sediment are preserved, which would attest to transport of likely frozen ‘rip-up’ clasts. Rotational structures and lineations suggest a polyphase deformation consisting of both brittle and ductile deformation.

AYA-010

Not much can be gleaned from only two thin sections from the light brown till lithofacies. The similarity between the two samples suggests similar subglacial conditions during deposition. Interestingly the thin sections have a strikingly similar micromorphological signature to Dmm 3 at the Tatiggaq (i.e. TUR-057 samples H and J). This would suggest similar subglacial conditions during deposition and possible correlation, at least based on micromorphological signatures.

3.5 Discussion

3.5.1 Paleoglaciological Interpretation

The earliest ice flow phases recognized within the Keewatin Sector of the LIS are SW and S ice flow phases (McMartin and Henderson 2004a; Kleman et al. 2010). Stratigraphic evidence for early southerly ice flow phases within the Kivalliq region is limited. Klassen (1995) based on drillcore geochemistry and mineralogy suggested that till present in the lower portions of some drillcores had a northerly provenance. Riddler and Shilts (1974) reported a multi-till stratigraphy in the south-central Keewatin Sector near Kaminak Lake, south Kivalliq region, of which the lower grey till was suspected to be a result of southern ice flow. The extent of the early southerly ice flow is unknown, but likely propagated into northern Manitoba, where a multi-till stratigraphy is present within a lower unit of Keewatin provenance and where oscillations between Keewatin and Quebec/Labradorean Sector ice flow influence well documented throughout the main to late Wisconsinan Glaciation (e.g. Dredge and McMartin 2011). Kaszycki and Shilts (1980) identified a dispersal train of Dubawnt detritus emanating from the Baker Lake basin and into Hudson Bay and northern Manitoba. This dispersal train has been interpreted to be evidence of a sustained south-easterly ice flow and long-standing position of the KID (Kaszycki and Shilts (1980) or propagation into the core of the LIS of the Hudson Strait Ice Stream catchments as Dubawnt clasts can be traced to the head of the Hudson Strait (Laymon 1992; Ross et al. 2011). The component of this dispersal train attributed to the early southerly ice flow phase is unknown, but could have been a key contributor to the immense size of the dispersal train in southern Nunavut and the occurrence of Dubawnt erratics in northern Manitoba (e.g. Henderson et al. 1987; Kaszycki et al. 2008; Trommelen et al. 2013). Preliminary investigations by McMartin et al. (2013) in the Chantrey region, northern Kivalliq, have shown northward Dubawnt dispersal in the 8-30 mm fraction of up to 190 km from the nearest outcrops to the south, attesting to extensive northward dispersal of Dubawnt detritus.

Evidence for early WSW (255°) is tentatively recognized within the Ayra grid stratigraphy, although this is based solely on the absence of Pitz Fm and the relative proportion of Thelon Fm and basement lithologies within the till. A depositional signature of the WSW ice flow phase is tentatively recognized at the Tatiggaq grid, although again based on limited proxies. It is also possible that more than one till sheet is represented within lithofacies Dmm 1 at the Tatiggaq

grid (i.e. TUR-022 Dmm 1 vs. TUR-057 Dmm 1). The preserved depositional imprint of an early southern ice flow (Dmm 2) in the southeast Aberdeen Lake region consists of Thelon Fm enriched till (~ 60-80 wt. %) variably preserved across the study area, but best observed at the Tatiggaq grid and drillcore HND-001 (maximum thickness of ~ 6 m). This till unit is tentatively correlated to the pale red till observed by Shilts (1980) and Klassen (1995) at the base of drillcores west and south of Pitz Lake.

Evidence of deposition by northerly ice flow phases is present across the entire study area and in some areas is the dominant till lithofacies present. At the Tatiggaq exploration target and Qamanaarjuk sections, the NNW ice flow phase was responsible for 45-70% of till stratigraphy thickness reaching a maximum of 12 m in thickness. A depositional imprint of the NW (300°) ice flow is potentially recorded in the central grids, where evidence of a 'mixed' Thelon signature was found (Fig. 3-28). A plausible explanation for the thick till present at the Ayra grid remains elusive and it is highly variable across the grid. The thick (>20 m in drillcore AYA-009) sequence of light brown till contains Pitz Fm and therefore constrains provenance from either the W or S/SE (Fig. 3-1). There are two possible origins for this unit: i.) The till is a result of the NNW ice flow phase incorporating a large amount of locally derived basement lithologies. ii.) The till is a product of NE ice flow and correlated to the brown diamicton observed by Ó Cofaigh et al. (2013) near the Nunavut-Northwest Territories border (Fig. 1-2).

The surficial till is rich in basement derived lithologies, typically intrusive rocks and their metamorphic equivalents, and blankets the study area. This till is likely related to the retreat of the Keewatin Sector of the LIS during late Wisconsinan and is interpreted to be a result of NW to W ice flow reflecting the late counter-clockwise rotation observed in the position of KID (McMartin and Henderson 2004a).

Based on the observations collected as part of this study, a regional stratigraphic column is proposed (Fig. 3-31) The stratigraphy of the region suggests oscillations within the LIS between southerly and northerly ice flow phases with the possibility of ice free conditions at times during the Wisconsinan glacial cycle. An example of this is the HND-001 drillcore, where the stratigraphy shows an advance of southerly ice flow over non-glacial sediments followed by a period of laminated fine-grained sediments with dropstones indicative of a pro-glacial setting

prior to till deposited by a northerly ice flow phase. The timing of this non-glacial deposition is unknown.

The stratigraphy of drillcore MAM-002 suggests that the depositional imprint of the Wisonsinan glaciation in this region can reach up to 36 m. This is constrained by basal fine-grained sediments, of which datable material produced an infinite >43 500 ^{14}C yrs BP age, but has a remnant magnetism signature interpreted to be of normal polarity. Pollen analysis suggests Boreal forest like conditions at the time of deposition, warmer than the present climate leading to the interpretation that it is likely interglacial in age (Appendix J).

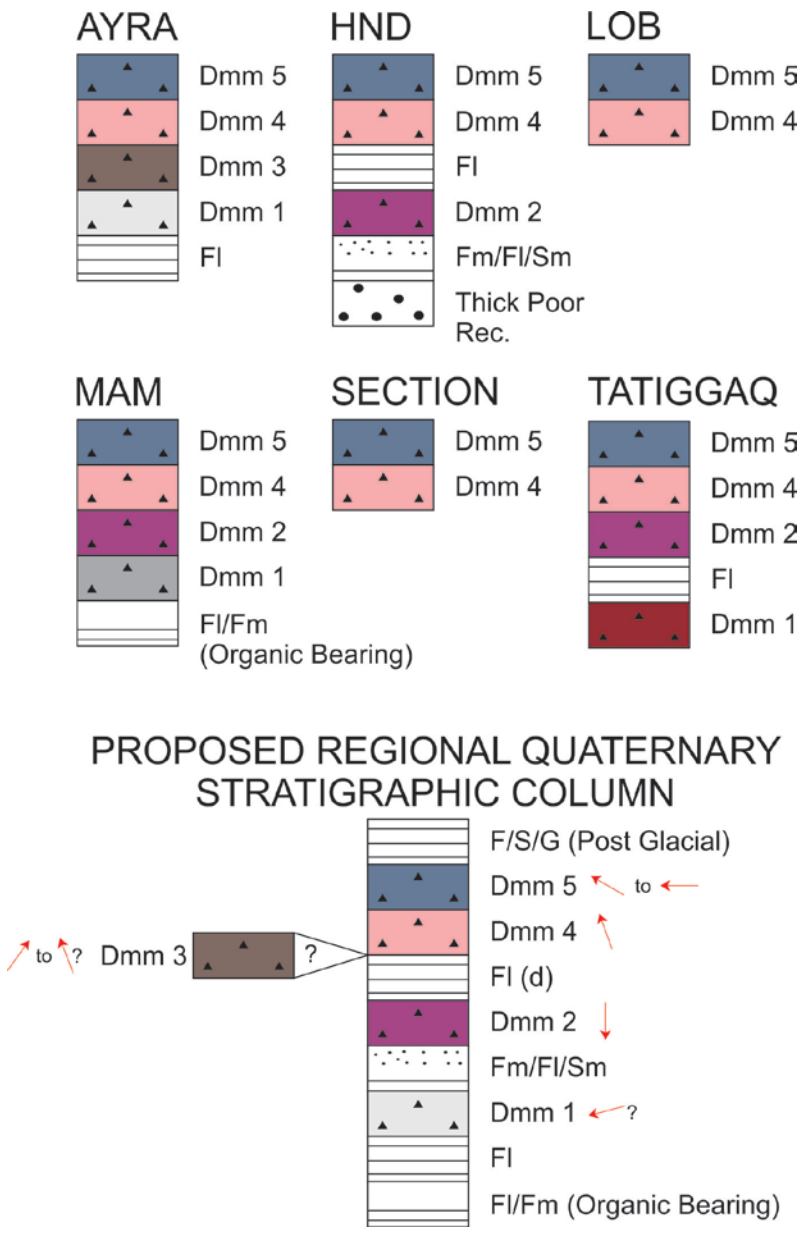

Regional Till Lithofacies	Colour	Lithological Characteristics	Interpreted Ice Flow Phase
Dmm 5	Pinkish Grey	High basement; Dubawnt present (Inc. Pitz fm.)	NW (300°) W (270°)
Dmm 4	Pale Red	Mixed basement-Thelon fm; Pitz fm. present	NNW (340°)
Dmm 3	Light Brown	High basement; Pitz fm. present	NE to NW
Dmm 2	Pale Red	High Thelon fm.; No Pitz fm.	S (180°)
Dmm 1	Varies by grid	Local lithologies	Variable (Ayra - WSW 255°)

Figure 3-31: Proposed regional stratigraphy based on the drillcore and section observations of the southeast Aberdeen Lake region. Interpreted ice flow phases responsible for till deposition are depicted by the red arrows.

3.5.2 Sediment-Landform Relationships

The north-northwest paleo-ice flow phase was a strong ice flow resulting in clast transport of at least 55 km as indicated by the presence of Pitz Fm recovered from the Qamanaarjuk till sections and 190 km in the Chantrey region (McMartin et al. 2013). This ice flow phase also resulted in the formation of large drumlinoid features across much of the Keewatin Sector of the LIS (Ch. 2; McMartin et al. 2008; Greenwood and Kleman 2010). The large landforms, often classified as 'mega-scale' (Greenwood and Kleman 2010), are cross-cut by late glacial NW and W landforms (Ch. 2). The Tatiggaq grid is located on one of these large glacial lineations and offers insight into its composition and related till production. Fig. 2-11 (Ch. 2) depicted the approximate lateral boundaries for the extensive ice flow set, which extends to the north across Kivalliq and into Chantrey Inlet and is reproduced in Fig. 3-32 incorporating known till composition boundaries.

Till lithology counts by McMartin et al. (2006) in the Schultz Lake map area identified a strong NW-SE trending boundary in till composition (approximate boundary represented by green line in Fig. 3-32), between a Dubawnt-rich till in the west and a basement-rich till to the east. This is also reflected in the colour of the surficial till, with the Dubawnt-rich till having a pinkish colour (e.g. Cunningham and Shilts 1977). This dispersal train boundary is a result of both south and north ice flow phases (McMartin et al. 2006); with northern dispersal being predominant in the Schultz Lake map area. This dispersal train boundary is spatially related to the lateral margin for the northerly landform flowset depicted in Fig. 3-32, which has been shown to have resulted in northern dispersal in the Schultz Lake map area (McMartin et al. 2006). In north-central Kivalliq, east of Garry Lake, Taylor (1956) has described a distinct difference in till colour across the study area (lateral bounds depicted by orange lines in Fig. 3-32). Taylor (1956) observed a pink till (10R 8/2) in the west and grey till (2.5Y 8/2) in east regions of his study. It would appear, although not apparent at the time for Taylor (1956), that he is describing an eastern lateral margin for a Dubawnt dispersal train attributed to the northerly ice flow phase, similar to that described by McMartin et al. (2006) in the Schultz Lake map area. Taylor (1956) describes 90-100 ft high drift sections along the Back River attesting to wide-spread thick till along this landform flow set. Previous work has been conducted on investigating the extent of a Dubawnt dispersal train in southern Kivalliq and shown an extensive dispersal train extends eastward into Hudson Bay and southward into northern Manitoba (e.g. Shilts and Kaszycki 1980;

Henderson 1987; Kaszycki et al. 2008; Trommelen et al. 2013). The Dubawnt dispersal train is thought to be indicative of a long-standing south-easterly ice flow phase (Kaszycki and Shilts 1980), or propagation into the core of the LIS of the Hudson Strait Ice Stream catchments as Dubawnt clasts can be traced to the head of the Hudson Strait (Laymon 1992; Ross et al. 2011). Dispersal as a result of the northerly ice flow phase is known to be at least 190 km (McMartin et al. 2013) and the full extent is unknown, but could provide some constraint on subglacial erosion and transport associated with this ice flow phase.

From Fig. 3-32 and 3-33, it is apparent that this northerly ice flow was not an ice-marginal depositional setting, but instead closer to a core region of the LIS. Sedimentation associated with the landforms was responsible for till production in excess of 10 m at HND and Tatiggaq targets (max. 12 m, ~45-70% of till thickness present), which provides a minimum thickness of till production, not accounting for remobilization during the later ice flow phases. The depositional mechanisms behind such a thick till sheet far removed from an ice-marginal setting are intriguing. One hypothesis, is that the till thickness present in the central Keewatin is largely a product of ice-marginal deposition by earlier ice flow phases (Greenwood and Clark 2010) and was subsequently reworked and deposited during the retreat phase of the LIS. The overall high Thelon Fm signature within the NNW ice flow phase sediments, likely suggests some inheritance from an earlier till sheet (Fig. 3-31 - Dmm 2); however, the dispersal train of Dubawnt detritus in the Schultz Lake Map area and likely into north Kivalliq, as well as the dispersal of Pitz Fm in our study area, suggests further erosion and transport during the northern ice flow phase and it would appear this interpretation cannot fully explain the vast expanse of thick till across the region.

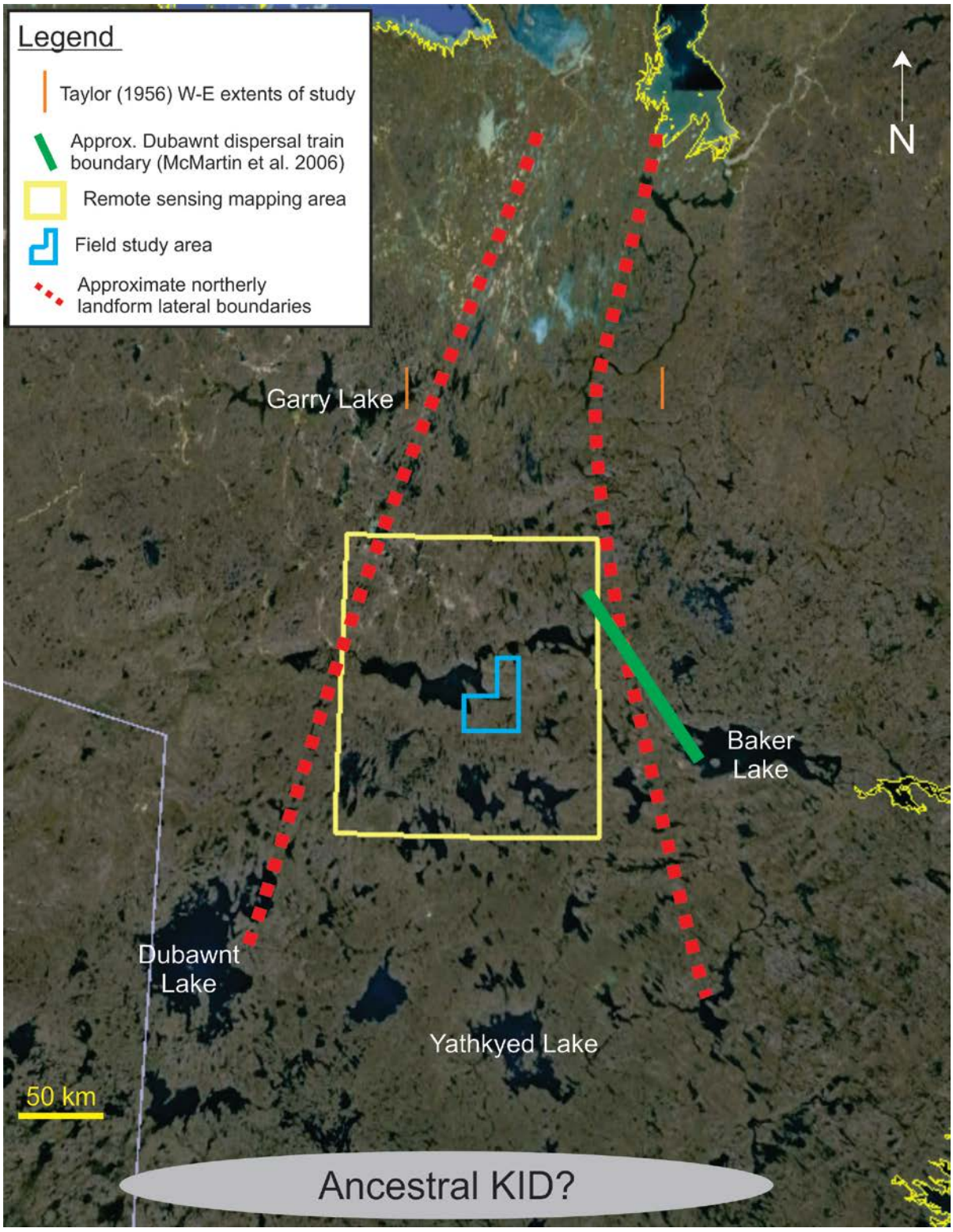

Figure 3-32: Approximate boundaries for the northerly flow set consisting of large landforms. This field study is depicted by the blue polygon and the orange lines depict the east and west margins of the study conducted by Taylor (1956). The approximate eastern boundary of a Dubawnt dispersal train in the Schultz Lake map area identified by McMartin et al. (2006) is depicted by the green line.

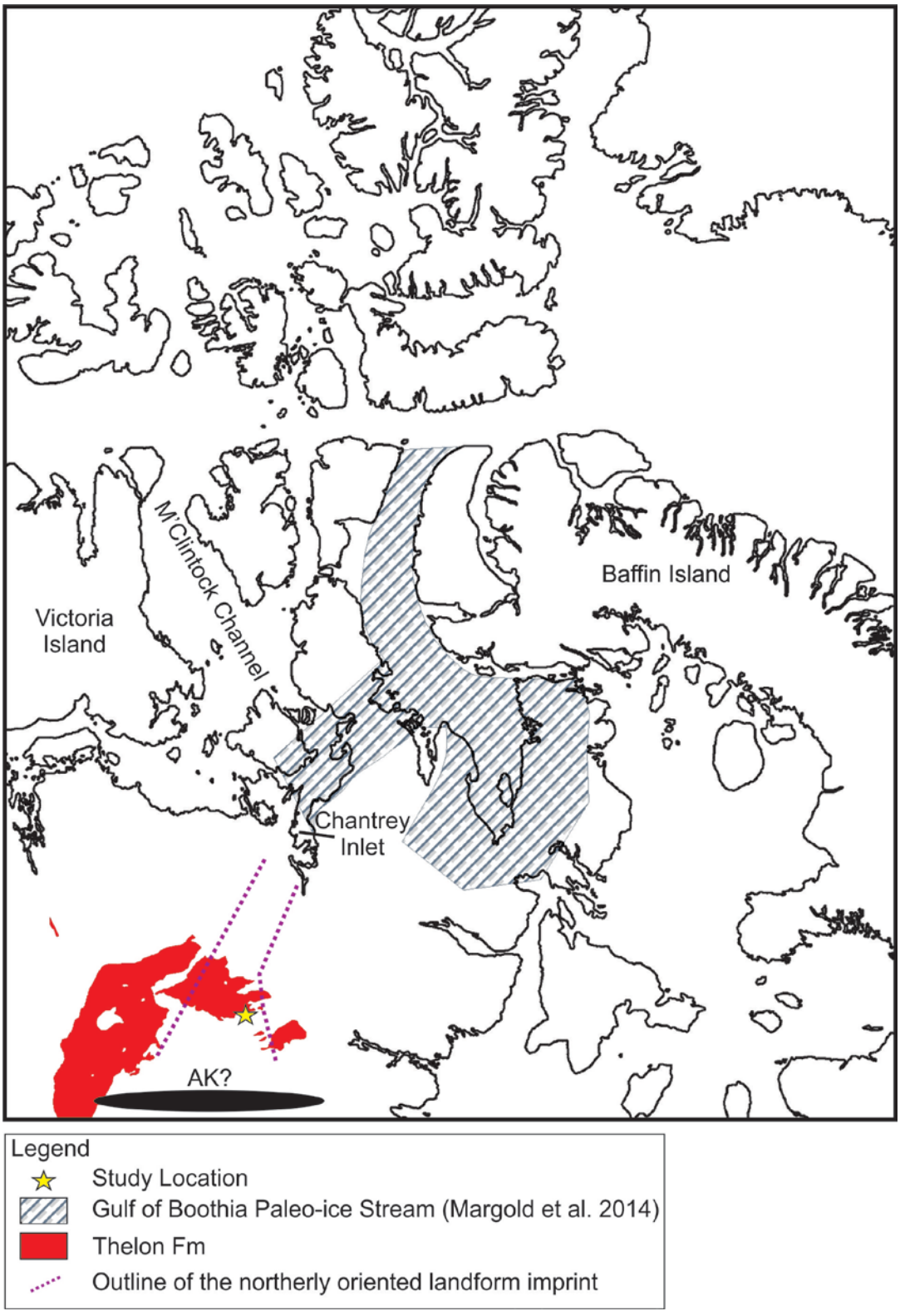

Figure 3-33: Location of the northerly landform imprint of central mainland Nunavut in context with the Boothia paleo-ice stream. It is proposed that this landform imprint represents a catchment region for an arctic paleo-ice stream, possibly the Boothia paleo-ice stream.

An alternative explanation is that at times of thick ice in the region during the Wisconsinan (i.e. LGM) warm-based ice conditions associated with ice-stream catchment areas could have propagated deep into the LIS. The gulf of Boothia paleo-ice stream (Fig. 3-33), is a prospective drainage for this northerly ice flow phase. This is not currently recognized through modelling efforts (e.g. Tarasov and Peltier 2007; Stokes et al. 2012), but it could be a result of the failure to yet incorporate higher order ice dynamics physics to these ice sheet models. A scenario comparable to this would be contemporary Antarctic glaciers which exhibit propagation deep into the ice sheet, in some cases within 200 km of current ice divides (Bamber et al. 2000b) and the northeast Greenland ice stream which propagates deep into the core of the ice sheet (Bamber et al. 2000a). A thick ice sheet with a high subglacial vigour could explain the production of thick, >10 m, till sequences that are observed.

Within our study area the surficial till (Fig. 3-31, Dmm 5) has a pinkish grey colour (7.5YR 7/2) and a basement-rich lithological signature. The surficial till is attributed to late glacial NW to W retreat phases of the LIS, responsible for a depositional imprint of ≤ 5 m at the Tatiggaq grid and ≤ 8 m at the Ayra and LOB grids. To the east, within the Schultz Lake map area, there is little evidence for late glacial westerly transport (McMartin et al. 2006). This suggests an increase in late glacial deposition southeast of Aberdeen Lake, which corresponds to a suspected on-set region of the late-glacial Dubawnt paleo-ice stream (Ch. 2). The late glacial landforms are also much smaller than their northerly counterparts.

A corresponding landform record of the inferred early southerly ice flow phase that deposited the Dmm 2 is not present in the vicinity of the Tatiggaq exploration target. Despite this, the regional erosional record (McMartin and Henderson 2004a) suggests the presence of a widespread southern ice flow phase that could be responsible for the Dmm 2 lithofacies identified in the stratigraphic record at HND, MAM and Tatiggaq grids.

The bedrock of central Kivalliq contains the Baker Lake and Thelon basinal rocks of the Dubawnt Supergroup. These relatively soft Canadian Shield rocks have been shown to be extensive components of till throughout central Kivalliq generating sandy tills, providing a large sediment supply. The soft nature of this bedrock is exemplified by boundaries of the largest lakes in central Kivalliq (i.e. Aberdeen, Schultz and Baker Lakes) which closely follow mapped occurrences of Thelon Fm, indicative of more intense erosion of this bedrock unit. Interestingly

some of thickest till sequences on the Canadian Shield are found in close proximity with the Kivalliq Proterozoic basins (Tyrrell 1897; Taylor 1956; McMartin and Henderson 2004a; Klassen 1995; this study) and the Proterozoic Athabasca basin to the south (e.g. Campbell 2007). The high thermal conductivity of these thick sandstone-conglomerate sequences could also contribute to the basal thermal regime of the LIS, which have been shown to coincide with other paleo-ice stream onset regions (Stokes and Clark 2003; Ross et al. 2009; Ross et al. 2011). The exact associations between these paleo-ice streams and large Proterozoic basins continue to be unknown, but intriguing.

3.6 Conclusion

Drillcore till stratigraphy identified evidence for early southerly ice flow phases as well as wide-spread evidence for north-northwest till deposition and a late glacial westward deposition that blankets the study area. The northward dispersal of detritus is well documented in the Aberdeen Lake stratigraphy, with Pitz Fm clasts suggesting significant transport distances. Sediment-landform assemblages of the Aberdeen Lake region suggest that northerly transport has had the most significant contribution to the landscape and till production. During this ice flow phase, the region is not suspected to have been an ice-marginal depositional setting but instead closer to an ice sheet core region. It is proposed that the Aberdeen Lake region acted as a catchment region feeding an ice stream through Chantrey Inlet, possibly the Gulf of Boothia paleo-ice stream, as a result of a likely W-E oriented ancestral KID located at an unknown locality south of Yathyked Lake. It is proposed that central Kivalliq, likely under a thick ice sheet, experienced warm-based conditions in close proximity to the KID under an extensive LIS. Competition between the northern Kivalliq catchment and Hudson Strait Ice Stream catchment could also have been responsible for the documented migration of the KID during the Late Wisconsinan. This challenges our current view regarding the extent of cold-based conditions within ice sheet core regions, which theoretical reconstructions suggest cold-based, sluggish ice flow with very limited erosion and till production (Tarasov and Peltier 2007; Stokes et al. 2012; Melanson et al. 2013).

Chapter 4 : Conclusions

4.1 Unravelling the Glacial Geology Record of the Aberdeen Lake Region

This thesis focused on the surficial erosional and depositional record of the Aberdeen Lake region, while drillcore logging provided a hitherto glimpse of the stratigraphy recorded in the extensive thick till that blankets the region.

4.1.1 Thesis Contributions

The most significant contributions of this thesis are as follows:

1.) A new map was produced through further mapping of the streamlined subglacial landforms of central Kivalliq. An extensive record of northern landforms is recognized that extends across the vast majority of Kivalliq. Southwest of Aberdeen Lake these features have previously been interpreted to be transverse landforms, but based on previously reported erosional evidence presented it is proposed that at least some of these landforms are streamlined subglacial landforms.

2.) The surficial paleo-ice flow record of the southeast Aberdeen Lake map area (NTS 66B) was resolved through outcrop scale paleo-ice flow observations. Five major paleo-ice flow events are recognized: old WSW (255°) and S (180°) followed by NNW (340°), NW (300°) and W (270°) ice flow phases. These ice flow phases record the migration of the KID throughout the last glacial cycle. The early (pre-NNW) SE ice flow phase recognized to the east (McMartin et al. 2005; Robinson et al. 2014) is not recognized and could reflect migration of the KID into the Aberdeen Lake map area.

3.) The Quaternary stratigraphy of the region was established through subsurface drillcore observations coupled with till section investigations. Till provenance was established through clast lithology counts supplemented with matrix geochemistry and linked to the surficial record. The stratigraphy suggests an extensive depositional record, with multi-till stratigraphy common across the study area and five diamicton lithofacies were recognized. Evidence for early southerly ice flow deposition was recognized. A till unit was correlated with the northward ice flow phase and is the dominant preserved till unit across the region. At the Tatiggaq grid, the north-northwest ice flow phase was

responsible for 45-70% of the till stratigraphy. Other drillcores (e.g. HND-001, LOB-001) and river bluffs investigated attest to a strong ice flow phase. The late glacial westerly ice flow phase deposited a 'blanket' across the study area ~ 5-8 m in thickness.

4.) This study is the first to characterized the till production of successive ice flow phases in the region. The study exhibited that the NNW ice flow phase resulted in significant new till production which is represented in the landform record by large till ridges throughout the map area. The depositional setting during till production is suspected to have been in an interior setting of the LIS. It is proposed that our current estimates of warm-based conditions at times of thick ice in the region are potentially underestimated in models and that ice stream catchment areas likely propagated deep in to the LIS.

5.) The glacial landscape southeast of Aberdeen Lake suggests a higher inheritance of older glacial features north and east of the Tatiggaq target. The Ayra target experienced a higher degree of reworking during the late glacial westerly ice flow phase which is reflected in the surficial glacial record.

6.) A geochemical proxy for the proportion of Thelon Fm was established with the use of B:Rb ratios. This proxy can also be used in collaboration with clast counts to identify regions underlain by altered bedrock in thin drift regions. The stratigraphy of the region suggests that surficial drift prospecting techniques will likely need to be coupled with subsurface samples to be successful, since multi-till stratigraphy is present in regions of till blanket and deposited by nearly opposite ice flow phases in some instances. The use of clast counts and geochemistry is essential to establish till stratigraphy in the region as pale red till is ubiquitous across the region and can be a result of both northern and southern ice flow phases.

7.) It is proposed that the glacial record of central Nunavut can be viewed as a catchment region feeding ice streams in northern Kivalliq and the Arctic islands exhibiting propagation deep into the LIS. It is further proposed that the dynamics of competing catchment areas could have been factors in the late glacial reorganization of the KID.

4.2 Implications of this Work

Prior to this study the Quaternary stratigraphy of the Aberdeen Lake map sheet (NTS 66B) was undocumented. This region was a core region of the LIS during parts of the Wisconsinan glaciation and the stratigraphy suggests a complex pattern of till production and variations in the ice flow phases from migration of the Keewatin ice divide over the region.

4.2.1 Surficial Glacial Geology Record

This thesis suggested that the large lineations present south of Aberdeen Lake are actually streamlined landforms formed parallel to ice flow as opposed to a new classification of transverse 'megascale' landforms (Greenwood and Kleman 2010). This is supported by historical erosional striae near Marjorie and Wharton Lake that appear on the surficial geology map of Aberdeen Lake (Ayslworth 1990). It is noted that the region south and north of Aberdeen Lake could benefit greatly from further field investigations to better understand the sediment-landform relationships, which is currently being conducted in the Chantrey region (McMartin et al. 2013). An example of this is the in north-central Kivalliq, where Taylor (1956) observes distinct till colour variations, possibly indicative of a northward Dubawnt dispersal train, but necessitating further investigations to be sure of the exact origin of this dispersal train. The large northward landforms form a convergent pattern towards Chantrey inlet, typical of catchment ice stream catchment areas.

4.2.2 Sediment-landform Relationships

This study exhibited evidence for deposition by ice flow phases not recognized within the landform record in the field study area. Most notably, evidence for deposition by a southerly ice flow phase is recognized in the stratigraphic record. Erosional evidence for this ice flow has been documented in the Schultz Lake map area (McMartin et al. 2005) as well as in the Aberdeen Lake map area (Ch. 2), and a possible corresponding landform imprint in Kivalliq has been documented (Kleman et al. 2010). This ice flow phase was shown to a have a maximum depositional imprint of 6 m and is variably preserved across the region. Evidence for initial deposition by an early ice flow phase (Dmm 1) was also recognized across the study area (e.g. MAM-002, TUR-057, TUR-022, AYA-004). Based on the high proportion of local bedrock within these units, they cannot be confidently assigned to a known ice flow phase, nor can they be correlated in some cases (e.g. TUR-057 vs TUR-022); however, it is suspected in some cases

they may be associated with the initial advance into the region as a result of a WSW (255°) ice flow phase.

4.2.3 Drift Prospecting Implications and Tracing Clay Alteration Haloes

Klassen (1995) noticed in the Baker Lake area that compositional changes with depth occur in drillcores and stratigraphic sections even within till that appears monolithic. This is reiterated with observations from drillcores across the study area. Drillcore logged as a homogenous pale red diamicton exhibited dramatic variations in the proportion of Thelon Fm clasts interpreted to reflect nearly opposite ice flow phase directions (e.g. MAM-002; HND-001; TUR-042). This necessitates detailed stratigraphic logging to identify till provenance prior to interpreting commodity indicators within till.

The main alteration observed within known drilling targets within the region is intense, nearly obliterating the host-rock lithogeochemistry (Hunter et al. 2011a, 2011b). Several of the main diagenetic phases that affected the Thelon Fm are episodes of illitization (Hiatt et al. 2010), which is also the dominant alteration mineral phase associated with the uranium deposits (Hunter et al. 2011a, 2011b). Thus, some of the main pathfinder elements associated with uranium alteration haloes can be reproduced by the proportion of Thelon Fm detritus within till. The quantity of Dubawnt detritus has also been shown to dilute the signature of the underlying bedrock, inhibiting the geochemical signature of other exploration proxies in till (Klassen 1995; McMartin et al. 2006). Till stratigraphy studies within this region necessitate the use of till clast lithology and/or geochemistry to assist visual observations and distinction of till having similar appearance but distinct provenance. The B:Rb ratio is a good indicator of the proportion of Thelon Fm detritus and can also be used to trace the alteration footprint because till enriched in locally altered bedrock has an even higher B:Rb signature relative to the background input from Thelon Fm Therefore, one approach is to use the B:Rb in combination with clast counts. Samples where there is a departure of the B:Rb ratio from the Thelon clast content (Higher B:Rb than expected from clast counts) could be considered as the footprint of alteration haloes. From this study it would appear that this method can only detect the alteration footprint within the Dmm 1 lithofacies, which consists of local basement and altered bedrock lithologies and is generally only a couple meters in thickness, and thus this approach would likely work only in thin drift regions.

The multi-till stratigraphy across the region also suggests that traditional drift prospecting methods that involve strictly surficial till sampling will likely not work. Till stratigraphy at the Tatiggaq grid also suggests that there is a depositional imprint of early southerly ice flow phases that affected the region. Dispersal trains identified within the region are likely to be complex due to the prolonged ice flow deposition history and will likely need to be coupled with subsurface observations in regions of thick drift. This issue is exhibited to a greater extent at the Ayra exploration target where four diamicton lithofacies with drastically different lithological signatures were identified with sharp contacts observed between till lithofacies. The presence of laminated sediments overlying altered bedrock at the Ayra grid and organic bearing lacustrine sediments within drillhole MAM-002 suggests an even dire situation whereby the alteration signature associated with mineralization is not entrained by the overriding LIS. An in-depth study aimed at tracing the geochemical/mineralogical signature of the alteration haloes near the Ayra and Tatiggaq targets as well as the mineralization signature at the Qavik target is part of an on going project at the University of Waterloo.

References

Aylsworth, J.M. 1989. Surficial Geology, Tebesjuak Lake, District of Keewatin, Northwest Territories. Geological Survey of Canada, Map 35-1989, scale 1:125 000.

Aylsworth, J.M., 1990. Surficial Geology, Aberdeen Lake, District of Keewatin, Northwest Territories. Geological Survey of Canada, Map 43-1989, scale 1:125 000.

Aylsworth, J.M., Cunningham, C.M., Shilts, W.W. 1989. Surficial Geology, Thirty Mile Lake, District of Keewatin, Northwest Territories. Geological Survey of Canada, Map 39-1989, scale 1:125 000.

Aylsworth, J.M., Cunningham, C.M., Shilts, W.W. 1990. Surficial Geology, Schultz Lake, District of Keewatin, Northwest Territories. Geological Survey of Canada, Map 39-1989, scale 1:125 000.

Aylsworth, J.M., Shilts, W.W. 1989. Bedforms of the Keewatin Ice Sheet, Canada. Sedimentary Geology 62, 407-428.

Bamber, J.L., Hardy, R.J., Joughin, I. 2000a. An analysis of balance velocities over the Greenland ice sheet and comparison with synthetic aperture radar interferometry. Journal of Glaciology 46 (152), 67-74.

Bamber, J.L., Vaughn, D.G., Joughin, I. 2000b. Widespread complex flow in the interior of the Antarctic ice sheet. Science 287(5456), 1248-1250.

Bennett, M.R. 2003. Ice streams as the arteries of an ice sheet: their mechanics, stability and significance. Earth-Science Reviews 61, 309-339.

Benn, D.I., Evans, D.J.A. 2010. Glaciers and Glaciation. Hodder Education, London.

Boulton, G.S. 1996. Theory of glacial erosion, transport and deposition as a consequence of subglacial sediment deformation. Journal of Glaciology 42(140), 43-62.

Boulton, G.S., Clark, C.D. 1990. A highly mobile Laurentide ice sheet revealed by satellite images of glacial lineations. Nature 346, 813-817.

Campbell, J.E. 2007. Quaternary geology of the eastern Athabasca Basin, Saskatchewan. *In*: EXTECH IV: Geology and Uranium Exploration TECHnology of the Proterozoic Athabasca Basin, Saskatchewan and Alberta. Jefferson, C.W., Delaney G. (eds.). Geological Survey of Canada Bulletin 588, p. 211-228.

Clark, C.D., Hughes, A.L.C., Greenwood, S.L., Spagnolo, M., Ng, F.S.L., 2009. Size and shape characteristics of drumlins, derived from a large sample, and associated scaling laws. Quaternary Science Reviews 28, 677-692.

Clark, P.U. 1987. Subglacial sediment dispersal and till composition. The Journal of Geology 95(4), 527-541.

Craig, B.G. 1964. Surficial geology of the east-central District of Mackenzie. Geological Survey of Canada, Bulletin 99.

Cunningham, C.M., Shilts, W.W. 1977. Surficial geology of the Baker Lake area, District of Keewatin, Northwest Territories, Canada. Geological Survey of Canada, Report of Activities, B, Paper 77-1B, p. 311-314.

De Angelis, H. 2007. Glacial geomorphology of the east-central Canadian Arctic. Journal of Maps, 323-341.

De Angelis, H., Kleman, J. 2005. Palaeo-ice streams in the northern Keewatin sector of the Laurentide ice sheet. Annals of Glaciology 42, 135-144.

De Angelis, H., Kleman, J. 2008. Palaeo-ice stream onsets: examples from the north-eastern Laurentide Ice Sheet. Earth Surface Processes and Landforms 33, 560-572.

Doornbos, C., Heaman, L.M., Doupé, J.P., England, J., Simonetti, A., Lajeunesse, P. 2009. The first integrated use of in-situ U-Pb geochronology and geochemical analyses to determine long-distance transport of glacial erratics from mainland Canada into the western Arctic Archipelago. Canadian Journal of Earth Science 46, 101-122.

Dredge, L.A., McMartin, I. 2011. Glacial stratigraphy of northern and central Manitoba. Geological Survey of Canada, Bulletin 600.

Dredge, L.A., Thorleifson, L.H. 1987. The middle Wisconsinan history of the Laurentide ice sheet. Géographie physique et Quaternaire 41(2), 215-235.

Dyke, A.S., Andrews, J.T., Clark, P.U., England, J.H., Miller, G.H., Shaw, J., Veillette, J.J. 2002. The Laurentide and Innuitian ice sheets during the Last Glacial Maximum. Quaternary Science Reviews 21, 9-31.

Dyke, A.S., Moore, A., Robertson, L. 2003. Deglaciation of North America. Geological Survey of Canada , Open File 1574.

Dyke, A.S., Prest, V.K. 1987. Paleogeography of northern North America, 18 000 – 5 000 years ago. Geological Survey of Canada, Map 1703A, Scale 1:12 500 000.

Ehlers, J., Gibbard, P.L., Hughes, P.D. (eds.). 2011. Quaternary Glaciations - Extent and Chronology, a closer look. Developments in Quaternary Science, Vol. 15, Elsevier, Amsterdam.

Evans, D.J.A., Benn, D.I. (eds.). 2004. A practical guide to the study of glacial sediments. Hodder Education, London.

Evans, D.J.A., Phillips, E.R., Hiemstra, J.F., Auton, C.A. 2006. Subglacial till: Formation, sedimentary characteristics and classification. Earth-Science Reviews 78, 115-176.

Fulton, R. J. 1995. Surficial materials of Canada Geological Survey of Canada, 'A' Series Map 1880A, Scale 1:5,000,000.

Gall, Q., Peterson, T.D., Donaldson, J.A. 1992. A proposed revision of early Proterozoic stratigraphy of the Thelon and Baker Lake basins, Northwest Territories. Geological Survey of Canada, Current Research, Part C, Paper 92-1C, 129-137.

Greenwood, S.L., Kleman, J. 2010. Glacial landforms of extreme size in the Keewatin sector of the Laurentide Ice Sheet. Quaternary Science Reviews 29, 1894-1910.

Grunksy, E., Harris, J.R., McMartin, I. 2006. Predictive Mapping of Surficial Materials, Schultz Lake Area (NTS 66A), Nunavut, Canada. Geological Survey of Canada, Open File 5153.

Hadlari, T., Rainbird, R.H., Donaldson, J.A. 2006. Alluvial, eolian and lacustrine sedimentology of a Paleoproterozoic half-graben, Baker Lake Basin, Nunavut, Canada.

Henderson, P.J. 1987. Data report description and composition of cores and grab samples, Hudson 87-028 Hudson Bay. Geological Survey of Canada, Open File 2081.

Hiatt, E.E., Palmer, S.E., Kyser, T.K., O'Connor, T.K. 2010. Basin evolution, diagenesis and uranium mineralization in the Paleoproterozoic Thelon Basin, Nunavut , Canada. Basin Research 22, 302-323.

Hoffman, P.F. 1988. United plates of America, the birth of a craton: Early Proterozoic assembly and growth of Laurentia. Annual Review of Earth and Planetary Sciences 16, 543-603.

Hunter, R., Black, R., Zaluski, G. 2011a. Cameco Corporation 2010 Geological, Geophysical, Geochemical & Diamond Drilling Exploration Report. Aberdeen Project, Nunavut (NTS 66B-1, 2, 3, 6, 7, 8, 9, 10).

Hunter, R., Black, R., Lesperance, J., Zaluski, G. 2011b. Cameco Corporation 2010 Geological, Geophysical, Geochemical & Diamond Drilling Exploration Report. Turqavik Project, Nunavut (NTS 66A-5, 12 & 66B-8, 9, 15, 16).

Johnson, C., Ross, M., Tremblay, T. 2013. Glacial geomorphology of north-central Hall Peninsula, Southern Baffin Island, Nunavut. Geological Survey of Canada, Open File 7413.

Kaszycki, C.A., Dredge, L.A., Groom, H. 2008. Surficial geology and glacial history, Lynn Lake – Leaf Rapids are, Manitoba. Geological Survey of Canada, Open File 5873.

Kaszycki, C.A., Shilts, W.W. 1980. Glacial erosion of the Canadian Shield - calculation of average depths. Atomic Energy of Canada Limited, Technical Record TR-106.

King, E.C., Hindmarsh, R.C.A., Stokes, C.R. 2009. Formation of mega-scale glacial lineations observed beneath a West Antarctica ice stream. Nature Geoscience 2, 585-588.

Klassen, R.A. 1995. Drift composition and glacial dispersal trains, Baker Lake area, District of Keewatin, Northwest Territories. Geological Survey of Canada, Bulletin 485.

Kleman, J., Glasser, N.F. 2007. The subglacial thermal organisation (STO) of ice sheets. Quaternary Science Reviews 26, 585-597.

Kleman, J., Fastook, J., Stroeven, A.P. 2002. Geologically and geomorphologically constrained numerical model of Laurentide Ice Sheet inception and build-up. Quaternary International 95-96, 87-98.

Kleman, J., Jansson, K.N., De Angelis, H., Stroeven, A., Hättestrand, C., Alm, G. and Glasser, N.F., 2010. North American Ice Sheet build-up during the last glacial cycle, 115-21 kyr. Quaternary Science Reviews 29, 2036-2051.

Kleman, J., Stroeven, A.P., Lundqvist, J. 2008. Patterns of Quaternary ice sheet erosion and deposition in Fennoscandia and a theoretical framework for explanation. Geomorphology 97, 73-90.

Laymon, C.A. 1992. Glacial geology of western Hudson Strait, Canada, with reference to Laurentide Ice Sheet dynamics. Geological Society of America Bulletin 104, 1169-1177.

Lee, H.A., Craig, B.G., Fyles, J.G. 1957. Keewatin Ice Divide. Geological Society of America Bulletin 68, 1760-1761.

Livingstone, S.J., Ó Cofiagh, C., Stokes, C.R., Hillenbrand, C.D., Vieli, A., Jamieson, S.S.R. 2012. Antarctic paleo-ice streams. Earth-Science Reviews 111, 90-128.

Margold, M., Stokes, C.R., Clark, C.D., Kleman, J. 2014. Ice streams in the Laurentide Ice Sheet: a new mapping inventory. Journal of Maps 1-16.

McMartin, I., Berman, R.G., Normandeau, P.X., Percival, J.A. 2013. Till composition of a transect across the Thelon tectonic zone, Queen Maud block, and adjacent Rae craton: results from the Geo-Mapping Frontiers' Chantrey project. Geological Survey of Canada, Open File 7418.

McMartin, I., Dredge, L.A. and Aylsworth, J.M., 2008. Surficial Geology, Schultz Lake south, Nunavut. Geological Survey of Canada, Map 2120A, scale 1:100 000.

McMartin, I., Dredge, L.A., Ford, K.L., Kjarsgaard, I.M. 2006. Till composition, provenance and stratigraphy beneath the Keewatin Ice Divide, Schultz Lake area (NTS 66A), mainland Nunavut. Geological Survey of Canada, Open File 5312.

McMartin, I., Dredge, L.A., Robinson, L. 2005. Ice flow maps and datasets: Schultz Lake (NTS 66A) and Wager Bay (NTS 56G) area, Kivalliq Region, Nunavut. Geological Survey of Canada, Open File 4926.

McMartin, I., Henderson, P.J. 2004a. Evidence from Keewatin (Central Nunavut) for paleo-ice divide migration. Géographie physique et Quaternaire 58(2-3), 163-186.

McMartin, I., Henderson, P.J. 2004b. Ice flow history and glacial stratigraphy, Kivalliq Region, Nunavut (NTS 55J,K,L,M,N,O; 65I and P): complete datasets, maps and photographs from the Western Churchill NATMAP Project. Geological Survey of Canada, Open File 4595.

McMartin, I., McClenaghan, B. 2001. Till geochemistry and sampling techniques in glaciated shield terrain: a review. *In:* Drift Exploration in Glaciated Terrain. McClenaghan, M.B., Bobrowsky, P.T., Hall, G.E.M., Cook, S.J. (eds.). Geological Society Special Publication 185, p. 19-43.

McMartin, I., Paulen, R.C. 2009. Ice-flow indicators and the importance of ice-flow mapping for drift prospecting. *In*: Paulen, R.C., McMartin I. (eds.). Application of till and stream sediment heavy mineral and geochemical methods to mineral exploration in western and northern Canada. Geological Association of Canada, GAC Short Course Notes 18, p. 15-34.

Melanson, A., Bell, T., Tarasov, L. 2013. Numerical modelling of subglacial erosion and sediment transport and its application to the North American ice sheets over the last glacial cycle. Quaternary Science Reviews 68, 154-174.

Ó Cofaigh, C., Stokes, C.R., Lian, O.B., Clark,C.D., Tulaczyk, S. 2013. Formation of mega-scale glacial lineations on the Dubawnt Lake Ice Stream bed: 2. Sedimentology and stratigraphy. Quaternary Science Review 77, 210-227.

Parent, M., Paradis, S.J., Doiron, A. 1996. Palimpsest glacial dispersal trains and their significance for drift prospecting. Journal of Geochemical Exploration 56, 123-140.

Patterson, J., LeCheminant, A.N. 1985. A preliminary geological compilation of the northeastern Barrens Grounds, parts of the Districts of Keewatin and Franklin. Geological Survey of Canada, Open File 1138, Scale 1:1 000 000.

Paul, D., Hanmer, S., Tella, S., Peterson, T.D., LeCheminant, A.N. 2002. Geology, Compilation, bedrock geology of the Western Churchill Province, Nunavut-Northwest Territories. Geological Survey of Canada, Open File 4236, Scale 1:1 000 000.

Paulen, R.C. 2009. Drift Prospecting in Northern Alberta – A unique Glacial Terrain for Exploration. *In*: Paulen, R.C., McMartin I. (eds.). Application of till and stream sediment heavy mineral and geochemical methods to mineral exploration in western and northern Canada. Geological Association of Canada, GAC Short Course Notes 18, p. 185-205.

Peterson, T.D., Van Breeman, O., Sandeman, H., Cousens, B. 2002. Proterozic (1.85 – 1.75 Ga) igneous suites of the Western Churchill Province: granitoid and ultrapotassic magmatism in a reworked Archean hinterland. Precambrian Research 119, 73-100.

Rainbird, R.H., Davis, W.J., Pehrsson, S.J., Wodicka, N., Rayner, N., Skulski, T. 2010. Early Paleoproterozoic supracrustal assemblages of the Rae domain, Nunavut, Canada: Intracratonic basin development during supercontinent break-up and assembly. Precambrian Research 181, 167-186.

Rainbird, R.H., Hadlari, T., Aspler, L.B., Donaldson, J.A., LeCheminant, A.N., Peterson, T.D. 2003. Sequence stratigraphy and evolution of the Paleoproterozoic intracontinental Baker Lake and Thelon basins, western Churchill Province, Nunavut, Canada. Precambrian Research 125, 21-53.

Rice, J.M., Paulen, R.C., Menzies, J., McClenaghan, M.B. 2014. Micromorphological descriptions of till from pit K-62, Pine Point mining district, Northwest Territories. Geological Survey of Canada, Open File 7256.

Riddler, R.H., Shilts, W.W. 1974. Exploration for Archean polymetallic sulphide deposits in permafrost terrains, Kaminak Lake area, District of Keewatin. Geological Survey of Canada, Paper 73-34.

Robinson, S.V.J., Paulen, R.C., Jefferson, C.W., McClenaghan, M.B., Layton-Matthews, D., Quirt, D., Wollenberg, P. 2014. Till geochemical signatures of the Kiggavik uranium deposit, Nunavut. Geological Survey of Canada, Open File 7550.

Rosenquist, I.T. 1970. Formation of vivianite in Holocene clay sediments. Lithos 3, 327-334.

Ross, M., Campbell, J.E., Parent, M., Adams, R.S. 2009. Paleo-ice streams and the subglacial landscape mosaic of the North American mid-continental prairies. Boreas 38, 421-439.

Ross, M., Lajeunesse, P., Kosar, K. 2011. The subglacial record of northern Hudson Bay: insights into the Hudson Strait Ice Stream catchment. Boreas 40, 73-91.

Shilts, W.W. Cunningham, C.M., Kaszycki, C.A. 1979. Keewatin Ice Sheet – Re-evaluation of the traditional concept of the Laurentide Ice Sheet. Geology 7, 537-541.

Shilts, W.W. 1980. Geochemical profile of till from Longlac, Ontario to Somerset Island. Canadian Institute of Mining Bulletin 73, 85-94.

Shilts, W.W. 1995. Geochemical Partitioning in Till. *In*: Drift exploration in the Canadian Cordillera. Bobrowsky , P.T., Sibbick, S.J., Newell, J.M., Matysek, P.F. (eds.). British Columbia Ministry of Energy, Mines and Petroleum Resources, Paper 1995-2, 149-163.

Smith, A.M., Murray, T., Nicholls, K.W., Makinson, K., Aðalgeirsdóttier, G., Behar, A.E., Vaughan, D.G. 2007. Rapid erosion, drumlin formation, and changing hydrology beneath an Antarctic ice stream. Geology 35 (2), 127-130.

Stea, R.R., Finck, P.W. 2001. An evolutionary model of glacial dispersal and till genesis in Maritime Caanda. *In:* Drift Exploration in Glaciated Terrain. McClenaghan, M.B., Bobrowsky, P.T., Hall, G.E.M., Cook, S.J. (eds.). Geological Society Special Publication 185, p. 237-265.

Stokes, C.R., Clark, C.D. 2002. Are long subglacial bedforms indicative of fast ice flow? Boreas 31, 239-249.

Stokes, C.R., Clark, C.D., 2003. The Dubawnt Lake palaeo-ice stream: evidence for dynamic ice sheet behaviour on the Canadian Shield and insights regarding the controls on ice-stream location and vigour. Boreas 32, 263-279.

Stokes, C.R., Tarasov, L., Dyke, A.S. 2012. Dynamics of the North American Ice Sheet Complex during its inception and build-up to the Last Glacial Maximum. Quaternary Science Reviews 50, 86-104.

Stokes, C.R., Lian, O.B., Tulaczyk, S., Clark, C.D. 2008. Superimposition of ribbed moraines on a palaeo-ice-stream bed: implications for ice stream dynamics and shutdown. Earth Surface Processes and Landforms 33, 593-609.

Stokes, C.R., Spagnola, M., Clark,C.D., Ó Cofaigh, C., Lian, O.B., Dunstone, R.B. 2013. Formation of mega-scale glacial lineations on the Dubawnt Lake Ice Stream bed: 1. size, shape and spacing from a large remote sensing dataset. Quaternary Science Reviews 77, 190-209.

Storarr, R.D., Stokes, C.R., Evans, D.J.A. 2013. A map of large Canadian eskers from Landsat satellite imagery. Journal of Maps 9-3, 456-473.

Storarr, R.D., Stokes, C.R., Evans, D.J.A. 2014. Increased channelization of subglacial drainage during deglaciation of the Laurentide Ice Sheet. Geology 42(3), 239-242.

Tarasov, L., Peltier, W.R. 2007. Coevolution of continental ice cover and permafrost extent over the last glacial-interglacial cycle in North America. Journal of Geophysical Research 112 (F2), F02S08.

Taylor, R.S. 1956. Glacial geology of North-central Keewatin, Northwest Territories, Canada. Bulletin of the Geological Society of America 67, 943-956.

Thorleifson, L.H., Wyatt, P.H., Shilts, W.W., Nielson, E. 1992. Hudson Bay lowland Quaternary stratigraphy: Evidence for early Wisconsinan glaciation centered in Quebec. *In*: Clark, P.U., Lea, P.D. (eds.). The last interglacial-glacial transition in North America. Geological Society of America Special Paper 270.

Trommelen, M.S., Ross, M., Campbell, J.E. 2013. Inherited clast dispersal patterns: Implications for palaeoglaciology of the SE Keewatin Sector of the Laurentide Ice Sheet. Boreas 42, 693-713.

Tyrrell, J.B., 1897. Report on the Doobaunt, Kazan, and Ferguson rivers and the northwest coast of Hudson Bay. Geological Survey of Canada, Annual Report 618: 1F-218F.

Winsborrow, M.C.M., Clark, C.D., Stokes, C.R. 2004. Ice Streams of the Laurentide Ice Sheet. Géographie physique et Quaternaire 58(2-3), 269-280.

Zaleski, E., Pehrsson, S., Duke, N., Davis, W.J., L'Heureuz, R., Greiner, E., Kerswill, J.A. 2000. Geological Survey of Canada, Current Research 2000-C7.

Appendix A – Map: of Subglacial Streamlined Landforms of central Kivalliq, Nunavut

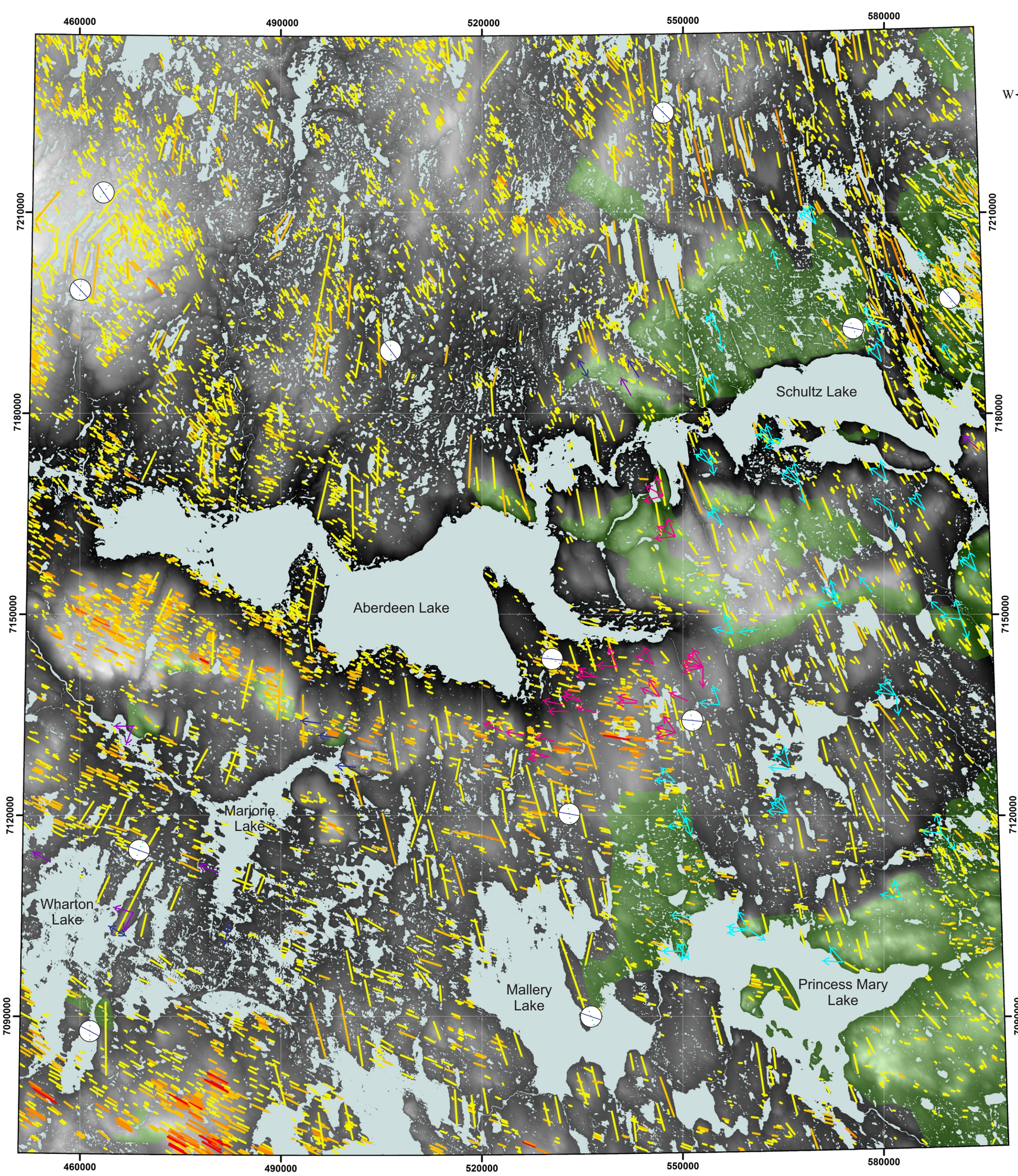

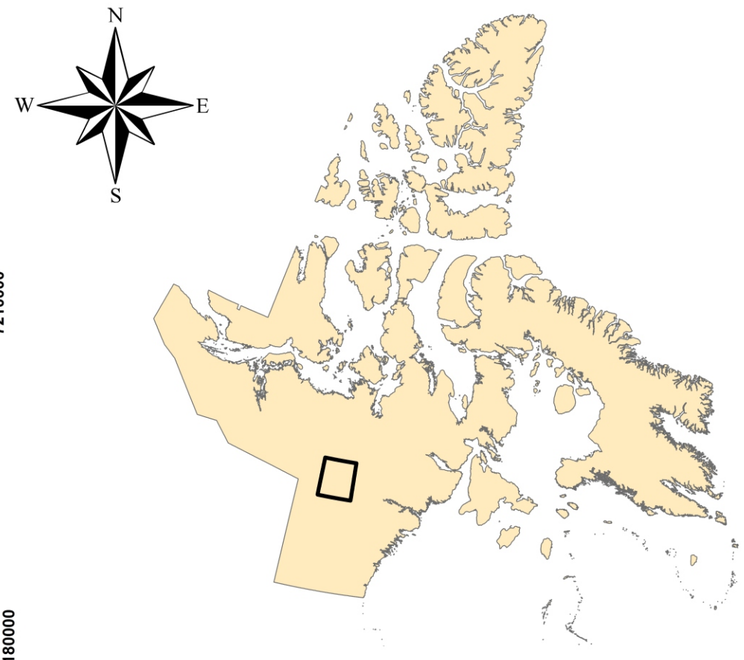

066G04	066G03	066G02	066G01	066H04	066H03
066B13	066B14	066B15	066B16	066A13	066A14
066B12	066B11	066B10	066B09	066A12	066A11
066B05	066B06	066B07	066B08	066A05	066A06
066B04	066B03	066B02	066B01	066A04	066A03
065O13	065O14	065O15	065O16	065P13	065P14

Index to Canadian National Topographic System

Legend

- Subglacial Streamlined Lineation
- Landform Elongation Ratio
  - 1.8 - 4.5
  - 4.5 - 7.0
  - 7.0 - 10.0
  - 10.0 - 12.0
  - 12.0 - 15.3
- Primarily Bedrock Terrain
- Paleo-ice Flow Indicator (Bidirectional)
- Paleo-ice Flow Indicator (Unidirectional)
  - This Study
  - McMartin et al. 2005
  - Aylsworth 1990
  - Tyrrell 1897

Landform Cross-cutting Relationships

- -Younger (Blue, Solid)
- - Older (Green, Dashed)

0 5 10 20 Kilometers

Scale: 1:500 000
Datum: North American Datum 1983
Projection: UTM 14N

Elevation (m asl)
High: 304
Low: 72

Subglacial Streamlined Landforms of the Aberdeen Lake Area, Kivalliq Region, Nunavut

Tyler J. Hodder & Martin Ross
Department of Earth & Environmental Sciences
University of Waterloo, Ontario, Canada

Subglacial streamlined landforms were digitized from SPOT 4/5 satellite imagery combined with elevation data from the Canadian digital elevation data (CDED). Paleo-ice flow indicators mapped in the field from this study are presented as well that of other field-based investigations within the mapped region. This map was produced as part of a M.Sc. project at the University of Waterloo which receives funding from Cameco Corporation and the National Science and Engineering Research Council (NSERC).

References

Aylsworth, J.M., 1990. Surficial Geology, Aberdeen Lake, District of Keewatin, Northwest Territories. Geological Survey of Canada, Map 43-1989, scale 1:125 000.
McMartin, I., Dredge, L.A., Robinson, L. 2005. Ice flow maps and datasets: Schultz Lake (NTS 66A) and Wager Bay (NTS 56G) area, Kivalliq Region, Nunavut. Geological Survey of Canada, Open File 4926.
Tyrrell, J.B., 1897. Report on the Doobaunt, Kazan, and Ferguson rivers and the northwest coast of Hudson Bay. Geological Survey of Canada, Annual Report 618: 1F-218F.

Appendix B – Paleo-Ice Flow Indicator Measurements

Station_ID	Date	Datum	UTM Zone	Northing	Easting	Elevation	Azimuth	Type	Age Relationship (1 - Oldest)	Sense	Comments
12-MR-001	17-Jul-12	NAD83	14	7161567	548782	197	343	Striae	--	Known	
12-MR-001	17-Jul-12	NAD83	14	7161567	548782	197	300	Striae	--	Known	Strong directional sense, polished stoss and abraded lee offer good directional sense
12-MR-001	17-Jul-12	NAD83	14	7161567	548782	197	335	Striae	--	Known	Plucked lee face depicts sense
12-MR-002	17-Jul-12	NAD83	14	7161579	548883	203	335	Striae	1	Known	Definitive cross-cutting relationship, with the E-W flow being younger
12-MR-002	17-Jul-12	NAD83	14	7161579	548883	203	265	Striae	2	Known	
12-MR-003	17-Jul-12	NAD83	14	7142210	540150	155	290	Striae	--	Unknown	Unsure regarding directional sense
12-MR-003	17-Jul-12	NAD83	14	7142210	540150	155	335	Striae	1	Known	Older flow protected on sloping face
12-MR-003	17-Jul-12	NAD83	14	7142210	540150	155	272	Striae	2	Known	
12-MR-003	17-Jul-12	NAD83	14	7142210	540150	155	285	Striae	--	Unknown	Directional sense unkown, very well polished, but weak striae
12-MR-003	17-Jul-12	NAD83	14	7142210	540150	155	295	Striae	--	Unknown	
12-MR-005	17-Jul-12	NAD83	14	7140543	537177	159	290	Striae	--	Known	Up to 300; Plucked lee face, great directional sense. Bedrock hill also streamlined in same direction with plucked face
12-MR-005	17-Jul-12	NAD83	14	7140543	537177	159	325	Striae	--	Known	Westward of 290 measurement, different direction possibly due to location on side of hill
12-MR-005	17-Jul-12	NAD83	14	7140543	537177	159	295	Striae	--	Known	Near 12-MR-005B but on top of bedrock high, intero to be more rep. of flow direction
12-MR-005	17-Jul-12	NAD83	14	7140543	537177	159	296	Striae	--	Known	Another measurement from top of outcrop
12-MR-006	17-Jul-12	NAD83	14	7140498	537223	158	275	Striae	--	Known	Up to 280; Longer striae than found at this outcrop, very well polished surface
12-MR-037	19-Jul-12	NAD83	14	7135474	549448	187	310	Lodged Boulder	--	Known	Lodged boulder, striae on side indicate ice flow in the direction of 300, top striae 310. General shape of lodged clast indicates 270 ice flow.
12-MR-054	22-Jul-12	NAD83	14	7167837	547198	172	340	Striae/Grooves	--	Known	Sense known by outcrop; plucked lee faces down-ice
12-MR-055	22-Jul-12	NAD83	14	7167762	547063	172	255	Striae	1	Known	Excellent relationship between the two ice flow phases. Mini rouche moutonee supports the 255 ice flow direction and it is on a protected face
12-MR-055	22-Jul-12	NAD83	14	7167762	547063	172	340	Striae	2	Known	
12-MR-056	22-Jul-12	NAD83	14	7167539	547036	158	300	Elongated Rouche Moutonee	--	Known	
12-MR-056	22-Jul-12	NAD83	14	7167539	547036	158	340	Striae/Grooves	--	Known	
12-MR-057	22-Jul-12	NAD83	14	7167322	546770	148	260	Striae	--	Unknown	Suspected that 260 flow is in that direction due to previous observations of that relationship at another outcrop, but no directional indicator at this outcrop
12-MR-057	22-Jul-12	NAD83	14	7167322	546770	148	340	Striae	--	Known	
12-MR-058	22-Jul-12	NAD83	14	7167256	546860	151	300	Striae	--	Known	Up to 305; Occur in a slight bedrock depression; landform shape suggests 300 flow direction
12-MR-065	23-Jul-12	NAD83	14	7139392	546180	189	270	Lodged Boulder	--	Known	Lodged boulder (Bullet-Shaped); polished with striations and till cover in the up-ice direction
12-MR-073	24-Jul-12	NAD83	14	7160954	548054	170	340	Striated/Grooved Bedrock	--	Known	Bedrock is Thelon formation

Station_ID	Date	Datum	UTM Zone	Northing	Easting	Elevation	Azimuth	Type	Age Relationship (1 - Oldest)	Sense	Comments
12-MR-075	24-Jul-12	NAD83	14	7161094	547662	162	342	Lodged Bullet-Shaped Clast	--	Known	Lodged bullet shaped clast found at till section where fabric measurements were conducted; Boulder with striae on top of it parallel and oriented at 342
12-MR-081	25-Jul-12	NAD83	14	7132328	548943	187	285	Striae	3	Known	285 flow cross-cuts 324 flow, older 255 flow on a protected surface from both flows; host rock a brecciated volcanic rock
12-MR-081	25-Jul-12	NAD83	14	7132328	548943	187	324	Striae	2	Known	
12-MR-081	25-Jul-12	NAD83	14	7132328	548943	187	255	Striae	1	Known	
12-MR-082	25-Jul-12	NAD83	14	7133953	550089	176	350	Striae	1	Known	
12-MR-082	25-Jul-12	NAD83	14	7133953	550089	176	280	Striae	2	Known	
12-MR-082	25-Jul-12	NAD83	14	7133953	550089	176	335	Striae	1	Known	
12-MR-082	25-Jul-12	NAD83	14	7133953	550089	176	270	Striae	2	Known	
12-MR-082	25-Jul-12	NAD83	14	7133953	550089	176	300	Striae	--	Known	
12-MR-083	25-Jul-12	NAD83	14	7134220	550278	181	295	Striae	--	Known	
12-MR-084	25-Jul-12	NAD83	14	7134283	549966	184	289	Striae	--	Known	Striae on felsic portion of outcrop, majority of outcop is mafic
12-MR-084	25-Jul-12	NAD83	14	7134283	549966	184	295	Striae	--	Known	
12-MR-085	25-Jul-12	NAD83	14	7134172	549825	181	295	Striae	--	Known	Striae on felsic rock; plucked lee depicts sense
12-MR-088	25-Jul-12	NAD83	14	7136396	549389	180	293	Striae	--	Known	Striae on felsic outcrop
12-MR-089	25-Jul-12	NAD83	14	7136179	549220	183	295	Lodged Boulder	--	Known	Boulder oriented at 295; striae on top are parallel and oriented at 295; boulder morphometry depicts ice-flow sense
12-MR-090	26-Jul-12	NAD83	14	7128756	529975	171	265	Large Grooves/Striae	--	Known	Measurement from top of outcrop; outcrop appears to have potentially had a 340 flow along it's side but it was erased by the 265 flow
12-MR-090	26-Jul-12	NAD83	14	7128756	529975	171	285	Striae	--	Known	Measurement from side of outcrop; 265 measurement most likely a more true ice flow direction measurement
12-MR-091	26-Jul-12	NAD83	14	7131048	530788	177	285	Striae	--	Known	Up to 288; Sense known by plucked faces
12-MR-092	26-Jul-12	NAD83	14	7130994	529817	163	285	Striae	--	Known	Sense knowned by stoss-lee relationship
12-MR-096	26-Jul-12	NAD83	14	7131042	527942	133	285	Striae	--	Known	Sense knowned by plucked lee faces and outcrop morphometry; felsic coarse-grained outcrop
12-MR-097	26-Jul-12	NAD83	14	7131849	526510	120	285	Striae	--	Known	Probable grooves present as well but not definitively clear
12-MR-098	26-Jul-12	NAD83	14	7131839	526243	152	280	Grooves	--	Known	Volcanic rock, poor preservation but grooves are present; bedrock outcrop face plucked lee's depict sense of ice flow
12-MR-098	26-Jul-12	NAD83	14	7131839	526243	152	275	Grooves	--	Known	Measured just west at another face of the outcrop
12-MR-099	28-Jul-12	NAD83	14	7137005	534871	143	285	Grooves	--	Known	Up to 290
12-MR-099	28-Jul-12	NAD83	14	7137005	534871	143	300	Grooves	--	Known	
12-MR-100	28-Jul-12	NAD83	14	7137503	533834	141	295	Grooves on Lodged Boulder	--	Known	Boulder oriented at 285, a single groove is poorly preserved, but discernable

Station_ID	Date	Datum	UTM Zone	Northing	Easting	Elevation	Azimuth	Type	Age Relationship (1 - Oldest)	Sense	Comments
12-MR-101	28-Jul-12	NAD83	14	7136454	533401	140	275	Whaleback/Rock Drumlin	--	Known	Sense is known because the one end of the whaleback is plucked and it is sort of a hybrid landform between a whaleback and a rock
12-MR-102	28-Jul-12	NAD83	14	7136490	532070	127	282	Grooves	--	Known	Known by plucked lee relationshiop
12-TH-108	29-Jul-12	NAD83	14	7136997	543202	208	285	Grooves/Striae	--	Known	Up to 290; Sense known by bedrock plucked lee
12-TH-109	29-Jul-12	NAD83	14	7136725	543142	208	270	Small Grooves/Striae	--	Known	Striae on side of outcrop on more resistant porphyroclasts within volcanic rock; Plucked lee depicts direction
12-TH-115	29-Jul-12	NAD83	14	7136005	542286	204	300	Small Grooves/Striae	--	Unknown	Up to 305; Felsic outcrop
12-TH-136	1-Aug-12	NAD83	14	7135497	532842	139	270	Grooves	--	Known	Grooves are on side of streamlined outcrop; ice flow direction known by outcrop scale
12-TH-177	5-Aug-12	NAD83	14	7136084	532452	129	265	Striae	--	Known	Striae are on side of outcrop; known by stoss-lee relationship
12-TH-179	6-Aug-12	NAD83	14	7132574	522930	202	295	Small Grooves/Striae	--	Known	Measurements on top of outcrop, very well polished surface; Plucked lee depicts sense
12-TH-179	6-Aug-12	NAD83	14	7132574	522930	202	290	Striae	--	Known	Bedrock very elongated and almost bullet-shaped, striae on side; plucked lee depicts sense
13-AB-198	4-Jul-13	NAD 83	14	7135328	537050	154	286	Grooves	--	Known	284 on top, 286 on south side, 290 on north side, bedrock striking 290
13-TH-238	7-Jul-13	NAD 83	14	7137086	550669	188	294	Striae	--	Known	
13-TH-251	12-Jul-13	NAD 83	14	7137727	546515	183	295	Grooves	--	Known	
13-TH-251	12-Jul-13	NAD 83	14	7137727	546515	183	328	Striae	--	Known	Outcrop Streamlined at 280; Outcrop may have shifted, but not considered to significantly affect measurement
13-TH-255	15-Jul-13	NAD 83	14	7142513	545655	206	328	Grooves	--	Known	m scale grooves on W side of outcrop
13-TH-255	15-Jul-13	NAD 83	14	7142513	545655	206	294	Striae	--	Known	Striae on a xenolith
13-TH-256	15-Jul-13	NAD 83	14	7142683	547484	198	280	Striae	3	Known	285 on top of outcrop
13-TH-256	15-Jul-13	NAD 83	14	7142683	547484	198	338	Striae	2	Known	338 flow protected from 285 flow
13-TH-256	15-Jul-13	NAD 83	14	7142683	547484	198	188	Striae	1	Unknown	Faint striae on a protected face from previous ice flow events. Face is very well polished. Directional sense indicated by plucked clast; but not the strongest directional indicator
13-TH-257	15-Jul-13	NAD 83	14	7142108	552976	185	255	Striae	--	Known	Nail head striae define directional sense; Older than 330 flow no correlation with 180 flow
13-TH-257	15-Jul-13	NAD 83	14	7142108	552976	185	180	Striae	--	Known	Single striae that becomes wider to the south suggesting a 'nail head' appearance and flow from the north. 288 and 274 flows cross-cut the striae; older than 330 flow but no correlation with 255 flow
13-TH-257	15-Jul-13	NAD 83	14	7142108	552976	185	330	Striae	3	Known	Cross-cutting relationships suggest this flow is older than 288 and 274
13-TH-257	15-Jul-13	NAD 83	14	7142108	552976	185	310	Striae/Grooves	4	Known	
13-TH-257	15-Jul-13	NAD 83	14	7142108	552976	185	288	Striae/Grooves	5	Known	Crescentic gouges define directional sense
13-TH-257	15-Jul-13	NAD 83	14	7142108	552976	185	274	Striae/Grooves	6	Known	Nail head striae define directional sense
13-TH-260	19-Jul-13	NAD 83	14	7142894	552970	191	270	Striae	--	Known	Striae on intrusive rock
13-TH-261	19-Jul-13	NAD 83	14	7143701	552448	189	270	Striae	--	Known	
13-TH-262	19-Jul-13	NAD 83	14	7143859	552293	188	270	Striae	2	Known	

Station_ID	Date	Datum	UTM Zone	Northing	Easting	Elevation	Azimuth	Type	Age Relationship (1 - Oldest)	Sense	Comments
13-TH-262	19-Jul-13	NAD 83	14	7143859	552293	188	310	Grooves	1	Known	
13-TH-263	19-Jul-13	NAD 83	14	7143203	548941	147	270	Striae	--	Known	
13-TH-264	19-Jul-13	NAD 83	14	7142879	547994	170	300	Striae/Grooves	1	Known	Up to 310
13-TH-264	19-Jul-13	NAD 83	14	7142879	547994	170	275	Striae	2	Known	270-275

Appendix C – Grain Size Results

LASER GRAIN SIZE ANALYSIS RESULTS						
Sample_ID	**%_Clay (<4 µm)**	**%_Silt (4-63 µm)**	**Norm_Clay**	**Norm_Silt**	**Silt:Clay**	**Comments**
Drillcore Samples						
ABR011-SA	42.04	57.77	42.12	57.88	1.37	
ABR011-SB	31.46	68.30	31.53	68.47	2.17	
ABR012-SA	30.42	67.43	31.08	68.92	2.22	
ABR012-SB	66.12	33.87	66.13	33.87	0.51	
ABR012-SD	43.16	56.78	43.19	56.81	1.32	
ABR012-SE	54.42	45.49	54.47	45.53	0.84	No Geochem Sample
AYA001-SA	47.54	52.34	47.60	52.40	1.10	
AYA001-SB	45.87	54.00	45.93	54.07	1.18	
AYA002-SA	49.98	50.01	49.99	50.01	1.00	
AYA003-SA	43.58	56.04	43.74	56.26	1.29	
AYA003-SB	44.34	55.12	44.58	55.42	1.24	
AYA003-SC	32.24	66.51	32.65	67.35	2.06	
AYA003-SD	60.87	39.14	60.87	39.13	0.64	
AYA004-SA	42.00	57.97	42.02	57.98	1.38	
AYA004-SB	33.20	66.68	33.24	66.76	2.01	
AYA004-SC	61.42	38.59	61.42	38.58	0.63	
AYA005-SA	32.44	67.44	32.48	67.52	2.08	
AYA006-SA	31.41	67.88	31.64	68.36	2.16	
AYA006-SB	30.94	68.60	31.08	68.92	2.22	
AYA009-SA	36.07	63.90	36.08	63.92	1.77	
AYA009-SB	28.29	71.60	28.32	71.68	2.53	
AYA009-SC	34.40	65.42	34.46	65.54	1.90	
AYA009-SD	30.25	69.64	30.28	69.72	2.30	
AYA009-SE	26.28	73.58	26.32	73.68	2.80	
AYA010-SA	47.82	52.20	47.81	52.19	1.09	
AYA010-SB	30.09	63.40	32.19	67.81	2.11	
AYA010-SC	30.58	69.33	30.61	69.39	2.27	
GEX001-SA	43.53	56.44	43.54	56.46	1.30	
GEX002-SA	29.46	70.33	29.52	70.48	2.39	
GEX002-SB	30.94	68.60	31.08	68.92	2.22	
GEX003-SA	27.28	72.51	27.34	72.66	2.66	
GEX003-SB	40.95	58.88	41.02	58.98	1.44	
HND001-SA	45.38	54.44	45.46	54.54	1.20	
HND001-SB	42.58	57.05	42.74	57.26	1.34	
HND001-SE	46.83	53.10	46.86	53.14	1.13	
HND002-SA	44.90	55.09	44.90	55.10	1.23	
HND002-SB	46.87	53.09	46.89	53.11	1.13	
JSF001-SA	45.56	54.19	45.67	54.33	1.19	
LOB001-SA	42.01	57.81	42.09	57.91	1.38	
LOB001-SB	44.67	54.70	44.95	55.05	1.22	
LOB001-SC	42.22	57.68	42.26	57.74	1.37	No Geochem Sample
LOB002-SA	41.48	58.38	41.54	58.46	1.41	
LOB002-SB	43.65	56.35	43.65	56.35	1.29	
LOB002-SC	25.42	74.55	25.43	74.57	2.93	No Geochem Sample
LOB003-SA	39.15	60.68	39.22	60.78	1.55	
LOB003-SB	44.36	55.49	44.42	55.58	1.25	
MAM002-SA	26.58	73.36	26.59	73.41	2.76	
MAM002-SB	33.86	65.85	33.96	66.04	1.94	

LASER GRAIN SIZE ANALYSIS RESULTS						
Sample_ID	**%_Clay (<4 µm)**	**%_Silt (4-63 µm)**	**Norm_Clay**	**Norm_Silt**	**Silt:Clay**	**Comments**
MAM002-SC	47.50	52.47	47.51	52.49	1.10	
MAM002-SE	46.59	53.38	46.61	53.39	1.15	
MAM002-SF	41.78	58.16	41.81	58.19	1.39	
MAM002-SG	37.64	62.29	37.67	62.33	1.65	
SNB002-SA	30.52	69.45	30.53	69.47	2.28	No Geochem Sample
TUR020-SA	56.76	43.20	56.79	43.21	0.76	
TUR021-SA	48.63	51.23	48.70	51.30	1.05	
TUR021-SB	45.30	54.42	45.43	54.57	1.20	
TUR021-SC	44.39	55.50	44.44	55.56	1.25	
TUR022-SA	48.48	51.41	48.54	51.46	1.06	
TUR022-SB	46.20	53.41	46.38	53.62	1.16	
TUR022-SC	50.26	49.73	50.27	49.73	0.99	
TUR022-SD	32.65	67.18	32.71	67.29	2.06	
TUR022-SE	46.89	53.08	46.90	53.10	1.13	
TUR022-SF	31.65	68.16	31.71	68.29	2.15	
TUR024-SA	48.27	51.60	48.33	51.67	1.07	
TUR025-SA	47.19	52.62	47.28	52.72	1.12	
TUR029-SA	42.80	56.90	42.93	57.07	1.33	
TUR031-SA	43.75	54.89	44.35	55.65	1.25	
TUR031-SB	40.97	58.60	41.15	58.85	1.43	
TUR031-SC	47.39	52.57	47.41	52.59	1.11	
TUR031-SD	40.71	59.19	40.75	59.25	1.45	
TUR031-SF	39.78	60.14	39.81	60.19	1.51	
TUR032-SA	49.67	50.22	49.73	50.27	1.01	
TUR032-SB	44.59	54.94	44.80	55.20	1.23	
TUR032-SC	38.88	60.93	38.95	61.05	1.57	
TUR034-SA	47.46	52.12	47.66	52.34	1.10	
TUR034-SB	47.24	52.63	47.30	52.70	1.11	
TUR034-SD	39.28	60.26	39.46	60.54	1.53	
TUR035-SA	46.11	53.82	46.14	53.86	1.17	
TUR035-SB	49.30	50.66	49.32	50.68	1.03	
TUR036-SA	45.53	54.37	45.58	54.42	1.19	
TUR038-SA	47.60	52.25	47.68	52.32	1.10	
TUR039-SA	20.14	79.55	20.20	79.80	3.95	
TUR039-SB	42.77	57.09	42.83	57.17	1.33	
TUR039-SC	48.67	51.18	48.74	51.26	1.05	
TUR040-SA	48.22	51.60	48.31	51.69	1.07	
TUR041-SA	46.61	53.03	46.78	53.22	1.14	
TUR041-SB	46.98	52.86	47.06	52.94	1.13	
TUR042-SA	47.97	51.89	48.04	51.96	1.08	
TUR042-SB	47.08	52.82	47.12	52.88	1.12	
TUR042-SC	46.41	53.41	46.49	53.51	1.15	
TUR042-SD	44.98	54.98	45.00	55.00	1.22	
TUR043-SA	48.41	51.42	48.49	51.51	1.06	
TUR043-SB	41.08	58.26	41.35	58.65	1.42	
TUR044-SA	47.41	52.50	47.45	52.55	1.11	
TUR044-SB	43.23	56.52	43.34	56.66	1.31	
TUR045B-SA	45.81	54.07	45.86	54.14	1.18	
TUR045B-SB	46.88	53.03	46.92	53.08	1.13	

LASER GRAIN SIZE ANALYSIS RESULTS						
Sample_ID	**%_Clay (<4 µm)**	**%_Silt (4-63 µm)**	**Norm_Clay**	**Norm_Silt**	**Silt:Clay**	**Comments**
TUR045B-SC	42.83	57.04	42.89	57.11	1.33	
TUR046-SA	47.34	52.47	47.43	52.57	1.11	
TUR046-SB	47.77	52.07	47.85	52.15	1.09	
TUR046-SC	41.77	58.14	41.81	58.19	1.39	
TUR047-SA	49.11	50.80	49.15	50.85	1.03	
TUR047-SB	42.14	57.30	42.38	57.62	1.36	
TUR048-SA	48.30	51.50	48.40	51.60	1.07	
TUR048-SB	42.21	57.75	42.23	57.77	1.37	
TUR048-SC	43.91	55.49	44.17	55.83	1.26	
TUR049-SA	39.43	48.52	44.83	55.17	1.23	
TUR049-SB	37.99	61.97	38.00	62.00	1.63	
TUR049-SC	40.77	59.10	40.83	59.17	1.45	
TUR050-SA	48.92	50.92	49.00	51.00	1.04	
TUR050-SB	38.51	61.33	38.57	61.43	1.59	
TUR050-SC	46.07	53.81	46.13	53.87	1.17	
TUR051-SA	47.01	52.84	47.08	52.92	1.12	
TUR051-SB	46.02	53.78	46.11	53.89	1.17	
TUR052-SA	48.68	51.18	48.74	51.26	1.05	
TUR052-SB	41.99	57.78	42.09	57.91	1.38	
TUR053-SA	44.75	55.09	44.82	55.18	1.23	
TUR053-SB	44.79	54.92	44.92	55.08	1.23	
TUR053-SC	36.07	63.50	36.22	63.78	1.76	
TUR054-SA	48.75	51.10	48.82	51.18	1.05	
TUR054-SB	46.46	53.10	46.67	53.33	1.14	
TUR054-SE	43.10	56.73	43.17	56.83	1.32	
TUR055-SA	42.96	56.70	43.10	56.90	1.32	
TUR056-SA	47.69	52.07	47.81	52.19	1.09	
TUR056-SB	47.32	52.62	47.35	52.65	1.11	
TUR057-SA	48.48	51.39	48.54	51.46	1.06	
TUR057-SB	46.68	53.04	46.81	53.19	1.14	
TUR057-SC	44.18	55.35	44.39	55.61	1.25	
TUR057-SE	38.79	60.97	38.88	61.12	1.57	
TUR057-SF	47.76	52.19	47.78	52.22	1.09	
TUR057-SG	45.06	54.81	45.12	54.88	1.22	
TUR057-SH	46.80	53.19	46.80	53.20	1.14	
TUR057-SI	46.10	53.86	46.12	53.88	1.17	
TUR057-SJ	42.23	51.71	44.96	55.04	1.22	
TUR057-SK	46.14	53.84	46.15	53.85	1.17	
TUR058-SA	46.68	53.11	46.78	53.22	1.14	
TUR058-SC	41.85	58.12	41.86	58.14	1.39	
TUR059-SA	43.91	55.66	44.10	55.90	1.27	
TUR059-SB	32.69	67.14	32.74	67.26	2.05	
TUR060-SA	45.35	54.25	45.53	54.47	1.20	
TUR060-SB	44.77	55.13	44.81	55.19	1.23	
TUR060-SD	49.78	50.21	49.79	50.21	1.01	
TUR060-SE	40.11	59.80	40.15	59.85	1.49	
TUR060-SF	47.79	52.20	47.79	52.21	1.09	
TUR061-SA	48.59	51.31	48.64	51.36	1.06	
TUR061-SB	51.30	48.61	51.34	48.66	0.95	

LASER GRAIN SIZE ANALYSIS RESULTS						
Sample_ID	**%_Clay (<4 µm)**	**%_Silt (4-63 µm)**	**Norm_Clay**	**Norm_Silt**	**Silt:Clay**	**Comments**
Surficial Samples						
12-MR-007	23.99	75.21	24.18	75.82	3.14	
12-MR-008	16.92	82.49	17.02	82.98	4.88	
12-MR-009	8.34	90.45	8.44	91.56	10.85	
12-MR-010	23.81	75.87	23.89	76.11	3.19	
12-MR-011	20.91	78.99	20.93	79.07	3.78	
12-MR-012	14.75	83.45	15.02	84.98	5.66	
12-MR-013	20.72	79.07	20.76	79.24	3.82	
12-MR-014	23.64	76.24	23.67	76.33	3.22	
12-MR-015	18.76	80.80	18.85	81.15	4.31	
12-MR-016	11.59	87.73	11.67	88.33	7.57	
12-MR-017	12.43	86.75	12.54	87.46	6.98	
12-MR-018	18.40	80.61	18.58	81.42	4.38	
12-MR-020	12.51	86.28	12.66	87.34	6.90	
12-MR-021	24.32	75.51	24.36	75.64	3.10	
12-MR-022	18.38	81.36	18.43	81.57	4.43	
12-MR-023	21.21	78.54	21.26	78.74	3.70	
12-MR-024	21.12	78.28	21.24	78.76	3.71	
12-MR-025	19.02	80.72	19.07	80.93	4.24	
12-MR-026	11.72	86.82	11.89	88.11	7.41	
12-MR-027	13.92	85.18	14.04	85.96	6.12	
12-MR-028	18.23	81.45	18.29	81.71	4.47	
12-MR-029	6.59	90.76	6.77	93.23	13.76	
12-MR-030	19.63	80.11	19.68	80.32	4.08	
12-MR-032	14.24	85.09	14.34	85.66	5.98	
12-MR-033	13.46	85.38	13.62	86.38	6.34	
12-MR-033	13.46	85.38	13.62	86.38	6.34	
12-MR-034	20.96	78.70	21.03	78.97	3.76	
12-MR-035	6.59	90.76	6.77	93.23	13.76	
12-MR-036	17.91	81.44	18.03	81.97	4.55	
12-MR-038	15.40	82.54	15.72	84.28	5.36	
12-MR-039	17.57	81.77	17.68	82.32	4.65	
12-MR-040	14.11	83.70	14.43	85.57	5.93	
12-MR-041	20.92	78.99	20.94	79.06	3.78	
12-MR-042	10.06	89.61	10.09	89.91	8.91	
12-MR-042	10.06	89.61	10.09	89.91	8.91	
12-MR-043	10.13	87.43	10.38	89.62	8.63	
12-MR-044	11.36	86.66	11.59	88.41	7.63	
12-MR-045	11.27	86.99	11.47	88.53	7.72	
12-MR-046	22.73	76.13	23.00	77.00	3.35	
12-MR-047	16.10	82.02	16.41	83.59	5.09	
12-MR-048	22.65	76.95	22.74	77.26	3.40	
12-MR-049	16.17	83.00	16.30	83.70	5.13	
12-MR-049	16.17	83.00	16.30	83.70	5.13	
12-MR-050	13.26	85.80	13.39	86.61	6.47	
12-MR-051	13.69	85.71	13.77	86.23	6.26	
12-MR-052	16.82	82.92	16.87	83.13	4.93	
12-MR-053	15.41	83.74	15.54	84.46	5.44	
12-MR-060	17.92	81.60	18.01	81.99	4.55	

LASER GRAIN SIZE ANALYSIS RESULTS						
Sample_ID	**%_Clay (<4 µm)**	**%_Silt (4-63 µm)**	**Norm_Clay**	**Norm_Silt**	**Silt:Clay**	**Comments**
12-MR-061	22.76	76.70	22.89	77.11	3.37	
12-MR-063	15.31	83.66	15.47	84.53	5.46	
12-MR-069	9.39	89.19	9.53	90.47	9.50	
12-MR-070	15.31	83.78	15.45	84.55	5.47	
12-MR-071	11.16	86.74	11.39	88.61	7.78	
12-MR-072	14.46	83.96	14.69	85.31	5.81	
12-MR-076	10.41	87.04	10.68	89.32	8.36	
12-MR-077	10.57	87.57	10.77	89.23	8.28	
12-MR-078	25.18	74.45	25.27	74.73	2.96	
12-MR-079	18.85	79.45	19.18	80.82	4.21	
12-MR-086	18.10	80.41	18.37	81.63	4.44	
12-MR-087	17.42	81.47	17.61	82.39	4.68	
12-MR-094	3.95	71.51	5.24	94.76	18.09	
12-MR-095	19.18	79.92	19.35	80.65	4.17	
12-TH-103	14.26	84.55	14.43	85.57	5.93	
12-TH-104	14.53	84.69	14.64	85.36	5.83	
12-TH-105	22.28	77.27	22.38	77.62	3.47	
12-TH-106	16.98	82.36	17.09	82.91	4.85	
12-TH-110	15.74	83.10	15.92	84.08	5.28	
12-TH-111	10.66	87.76	10.83	89.17	8.24	
12-TH-112	15.64	82.14	16.00	84.00	5.25	
12-TH-113	9.67	89.24	9.78	90.22	9.23	
12-TH-116	19.76	79.30	19.95	80.05	4.01	
12-TH-117	15.89	83.31	16.02	83.98	5.24	
12-TH-118	11.65	81.46	12.51	87.49	6.99	
12-TH-119	3.71	77.97	4.54	95.46	21.03	
12-TH-120	5.60	76.54	6.82	93.18	13.67	
12-TH-121	9.02	79.00	10.25	89.75	8.76	
12-TH-122	15.02	82.72	15.37	84.63	5.51	
12-TH-124	4.69	76.59	5.77	94.23	16.33	
12-TH-125	10.19	86.74	10.52	89.48	8.51	
12-TH-126	9.40	89.50	9.51	90.49	9.52	
12-TH-127	13.10	86.30	13.18	86.82	6.59	
12-TH-128	10.92	88.27	11.01	88.99	8.08	
12-TH-129	6.86	92.20	6.93	93.07	13.43	
12-TH-130	8.50	90.28	8.60	91.40	10.63	
12-TH-131	7.09	91.15	7.21	92.79	12.86	
12-TH-132	10.72	88.23	10.83	89.17	8.23	
12-TH-133	15.40	84.41	15.43	84.57	5.48	
12-TH-134	10.64	88.04	10.78	89.22	8.27	
12-TH-135	7.74	90.33	7.89	92.11	11.67	
12-TH-137	10.22	89.52	10.25	89.75	8.76	
12-TH-138	11.68	87.64	11.76	88.24	7.50	
12-TH-140	12.52	87.12	12.57	87.43	6.96	
12-TH-141	14.14	85.18	14.24	85.76	6.02	
12-TH-142	7.29	91.94	7.34	92.66	12.62	
12-TH-143	8.18	90.63	8.28	91.72	11.08	
12-TH-144	8.76	89.10	8.95	91.05	10.17	
12-TH-145	10.61	88.52	10.70	89.30	8.34	

LASER GRAIN SIZE ANALYSIS RESULTS						
Sample_ID	**%_Clay (<4 µm)**	**%_Silt (4-63 µm)**	**Norm_Clay**	**Norm_Silt**	**Silt:Clay**	**Comments**
12-TH-147	18.71	78.82	19.19	80.81	4.21	
12-TH-148	21.82	77.10	22.06	77.94	3.53	
12-TH-149	12.78	85.76	12.97	87.03	6.71	
12-TH-149	12.78	85.76	12.97	87.03	6.71	
12-TH-150	22.09	77.68	22.14	77.86	3.52	
12-TH-151	19.67	80.07	19.72	80.28	4.07	
12-TH-152	11.91	87.36	11.99	88.01	7.34	
12-TH-154	10.87	88.63	10.93	89.07	8.15	
12-TH-155	7.88	85.24	8.46	91.54	10.82	
12-TH-155	8.00	85.56	8.55	91.45	10.69	
12-TH-156	9.77	89.23	9.87	90.13	9.13	
12-TH-157	9.09	89.49	9.22	90.78	9.85	
12-TH-158	13.53	86.05	13.58	86.42	6.36	
12-TH-159	9.35	89.40	9.47	90.53	9.57	
12-TH-160	9.85	88.23	10.05	89.95	8.96	
12-TH-161	5.65	93.07	5.72	94.28	16.48	
12-TH-162	7.04	89.76	7.27	92.73	12.75	
12-TH-163	8.96	89.89	9.06	90.94	10.04	
12-TH-163	8.96	89.89	9.06	90.94	10.04	
12-TH-164	23.17	76.41	23.27	76.73	3.30	
12-TH-165	15.99	83.75	16.03	83.97	5.24	
12-TH-166	15.79	83.63	15.88	84.12	5.30	
12-TH-167	12.87	86.27	12.98	87.02	6.70	
12-TH-168	18.24	81.61	18.27	81.73	4.47	
12-TH-169	21.85	78.15	21.85	78.15	3.58	
12-TH-171	11.74	87.84	11.79	88.21	7.48	
12-TH-172	10.82	88.58	10.88	89.12	8.19	
12-TH-173	4.79	90.24	5.04	94.96	18.83	
12-TH-174	19.54	80.43	19.55	80.45	4.12	
12-TH-175	13.21	86.66	13.23	86.77	6.56	
12-TH-176	8.50	90.55	8.58	91.42	10.65	
12-TH-178	5.21	93.95	5.26	94.74	18.02	
12-TH-181	17.31	82.55	17.33	82.67	4.77	
12-TH-182	10.03	89.19	10.11	89.89	8.90	
12-TH-183	30.16	69.22	30.35	69.65	2.30	
12-TH-184	20.87	78.21	21.06	78.94	3.75	
12-TH-185	17.73	80.94	17.97	82.03	4.56	
12-TH-186	9.87	89.58	9.92	90.08	9.08	
12-TH-187	13.58	85.85	13.66	86.34	6.32	
12-TH-188	17.06	82.09	17.21	82.79	4.81	
12-TH-190	14.10	85.46	14.16	85.84	6.06	
12-TH-191	24.10	75.81	24.12	75.88	3.15	
12-TH-192	11.13	87.55	11.28	88.72	7.86	
12-TH-193	12.19	87.26	12.26	87.74	7.16	
12-TH-194	9.24	90.16	9.29	90.71	9.76	
13-AB-196	15.11	84.59	15.16	84.84	5.60	
13-AB-197	9.76	89.01	9.88	90.12	9.12	
13-AB-199	11.84	87.94	11.87	88.13	7.43	
13-AB-200	11.81	87.62	11.88	88.12	7.42	

LASER GRAIN SIZE ANALYSIS RESULTS						
Sample_ID	**%_Clay (<4 µm)**	**%_Silt (4-63 µm)**	**Norm_Clay**	**Norm_Silt**	**Silt:Clay**	**Comments**
13-AB-201	11.60	87.55	11.70	88.30	7.55	
13-AB-202	13.91	85.92	13.93	86.07	6.18	
13-AB-203	18.56	81.27	18.59	81.41	4.38	
13-AB-204	18.08	81.71	18.12	81.88	4.52	
13-AB-205	23.38	76.51	23.41	76.59	3.27	
13-AB-206	12.62	87.16	12.65	87.35	6.90	
13-AB-207	14.55	85.32	14.57	85.43	5.86	
13-AB-209	23.97	76.00	23.98	76.02	3.17	
13-AB-210	14.29	85.64	14.30	85.70	5.99	
13-AB-211	10.06	89.61	10.09	89.91	8.91	
13-AB-212	18.76	81.17	18.77	81.23	4.33	
13-AB-213	10.10	89.58	10.13	89.87	8.87	
13-AB-214	26.22	73.57	26.27	73.73	2.81	
13-AB-215	15.36	84.37	15.40	84.60	5.49	
13-AB-216	9.02	90.62	9.05	90.95	10.04	
13-AB-217	18.76	81.17	18.77	81.23	4.33	
13-AB-218	15.31	84.67	15.31	84.69	5.53	
13-AB-219	7.58	86.05	8.10	91.90	11.35	
13-AB-221	6.57	92.04	6.67	93.33	14.00	
13-AB-222	5.94	85.61	6.48	93.52	14.42	
13-AB-223	8.01	89.93	8.18	91.82	11.22	
13-AB-224	6.50	88.72	6.83	93.17	13.65	
13-AB-225	9.82	87.79	10.06	89.94	8.94	
13-AB-226	7.50	90.62	7.64	92.36	12.09	
13-AB-227	7.15	88.32	7.49	92.51	12.35	
13-AB-228	14.10	85.15	14.21	85.79	6.04	
13-AB-229	13.34	86.36	13.38	86.62	6.47	
13-AB-230	12.27	87.22	12.34	87.66	7.11	
13-AB-231	12.99	86.70	13.03	86.97	6.68	
13-AB-232	8.13	90.99	8.20	91.80	11.19	
13-AB-234	13.74	85.88	13.80	86.20	6.25	
13-AB-235	16.86	82.93	16.90	83.10	4.92	
13-AB-236	12.01	87.52	12.06	87.94	7.29	
13-AB-237	18.72	81.12	18.75	81.25	4.33	
13-AB-239	18.76	81.17	18.77	81.23	4.33	
13-AB-240	10.97	88.78	10.99	89.01	8.10	
13-AB-244	14.21	85.62	14.23	85.77	6.03	
13-AB-245	14.57	85.13	14.61	85.39	5.84	
13-AB-246	14.75	85.04	14.79	85.21	5.76	
13-AB-247	10.59	89.10	10.62	89.38	8.42	
13-AB-249	14.16	85.44	14.21	85.79	6.03	
13-AB-250	7.42	91.32	7.52	92.48	12.30	
13-AB-252	14.98	84.88	15.00	85.00	5.67	
13-AB-253	16.35	83.59	16.36	83.64	5.11	
Till Section Samples						
13-AB-258D	26.82	72.97	26.88	73.12	2.72	
13-AB-258C	17.06	82.42	17.15	82.85	4.83	
13-AB-258B	34.62	65.35	34.63	65.37	1.89	
13-AB-258A	34.80	65.04	34.86	65.14	1.87	

LASER GRAIN SIZE ANALYSIS RESULTS						
Sample_ID	**%_Clay (<4 µm)**	**%_Silt (4-63 µm)**	**Norm_Clay**	**Norm_Silt**	**Silt:Clay**	**Comments**
12-MR-073F	8.62	89.97	8.75	91.25	10.43	
13-AB-265	21.79	76.87	22.08	77.92	3.53	
12-MR-073D	39.22	60.59	39.30	60.70	1.54	
12-MR-073B	36.13	63.70	36.20	63.80	1.76	

DRY SIEVING RESULTS					
Sample ID	**>8**	**4-8**	**2-4**	**<2**	**Comments**
Surficial Till Samples					
12-MR-S007	54.08	38.1	42.42	714.37	
12-MR-S008	35.49	33.87	36.96	667.9	
12-MR-S009	26.28	39.35	28.91	685.81	
12-MR-S010	48.24	45.05	62.52	1291.51	
12-MR-S011	104.28	68.2	64.6	1043.94	
12-MR-S012	69.17	39.36	55.37	1047.62	
12-MR-S013	71.84	49.51	45.83	731.23	
12-MR-S014	87.3	54.32	60.94	1312.39	
12-MR-S015	124.34	52.64	43.26	734.96	
12-MR-S016	128.36	50.92	34.22	562.22	
12-MR-S017	146.59	30.06	26.02	579.41	
12-MR-S018	99.28	62.13	60.2	1159.06	
12-MR-S020	27.59	28.05	38.37	952.04	
12-MR-S021	22.07	28.99	45.9	1151.26	
12-MR-S022	61.85	40.15	43.78	914.91	
12-MR-S023	69.39	33.27	38.42	846.23	
12-MR-S024	38.76	40.69	43.4	864.1	
12-MR-S025	54.12	44.67	54.29	1081.28	
12-MR-S026	32.39	43.38	44.45	729.85	
12-MR-S027	48.37	34.72	34.08	849.68	
12-MR-S028	109.37	61.41	58.6	955.28	
12-MR-S029	73.35	31.13	31.4	665.81	
12-MR-S030	87.66	65.85	62.59	915.92	
12-MR-S032	52.61	55.79	55.87	872.07	
12-MR-S033	38.69	29.37	39.27	673.56	
12-MR-S034	105.06	43.46	50.25	806.41	
12-MR-S035	7.3	30.59	34.23	924.43	
12-MR-S036	253.2	35.98	38.98	689.54	
12-MR-S038	24.36	45.41	31.66	723.27	
12-MR-S039	34.28	37.91	38.37	811.61	
12-MR-S040	97.77	25.08	31	858.3	
12-MR-S041	120.61	59.42	67.7	1551.82	
12-MR-S042	160.97	37.35	37.86	1063.29	
12-MR-S043	7.6	26.76	36.37	895.06	
12-MR-S044	16.85	28.3	50.02	1186.67	
12-MR-S045	33.68	51.66	63.05	1356.38	
12-MR-S046	122.3	67.88	64.58	1422.8	
12-MR-S047	40.07	53.31	61.58	1118.45	
12-MR-S048	66.87	82.84	80.7	1764.37	
12-MR-S049	126.76	47.04	46.62	944.65	
12-MR-S050	12.98	26.69	36.89	1151.44	
12-MR-S051	253.48	66.58	55.78	1206.17	
12-MR-S052	66.01	62.72	44.77	1087.18	

DRY SIEVING RESULTS					
Sample ID	**>8**	**4-8**	**2-4**	**<2**	**Comments**
12-MR-S053	55.22	32.12	36	776.51	
12-MR-S060	82.34	81.69	78.46	1278.3	
12-MR-S061	173.64	54.44	67.55	907.55	
12-MR-S063	64.16	58.65	38.76	622.06	
12-MR-S069	11.2	39.05	32.89	972.75	
12-MR-S070	60.67	46.85	24.59	716.85	
12-MR-S071	48.48	29.74	24.25	725.39	
12-MR-S072	87.84	54.04	42.27	753.17	
12-MR-S073	191.76	82.75	82.32	1230.53	
12-MR-S073D	39.86	24.74	26.83	436.99	
12-MR-S073F	51.29	76.91	101.11	1413.89	
12-MR-S076	4.81	18.53	23.56	849.98	
12-MR-S077	96.21	28.57	29.14	637.01	
12-MR-S078	709.33	46.69	56.47	1390.15	
12-MR-S079	92.72	53.43	60.12	910.81	
12-MR-S086	116.79	37.72	48.68	824.86	
12-MR-S087	9.34	30.1	43.38	972.43	
12-MR-S094	135.4	60.59	59.94	913.59	
12-MR-S095	286.88	65.02	55.9	728.04	
12-TH-S103	45.74	45.32	49.69	786.74	
12-TH-S104	211.55	59.11	66.01	699.82	
12-TH-S105	177.98	46.99	52.94	734.54	
12-TH-S106	26.03	37.38	40.77	677.33	
12-TH-S110	53.97	48.02	50.76	667.5	
12-TH-S111	48.76	58.86	60.56	994.72	
12-TH-S112	10.82	35.42	43.33	908.82	
12-TH-S113	7.71	46.67	71.73	1468.12	
12-TH-S116	53.85	52.9	47.17	792.65	
12-TH-S117	14.86	34.35	47.56	854.44	
12-TH-S118	302.46	76.04	68.41	752.7	
12-TH-S119	93.31	65.17	60.12	865.22	
12-TH-S120	276.94	94.51	93.99	944.32	
12-TH-S121	261.98	82.85	94.66	990.43	
12-TH-S122	219.51	202.2	186.11	2712.15	
12-TH-S124	537.2	97.45	84.46	1280.44	
12-TH-S125	94.62	95.24	100.6	2218.56	
12-TH-S126	8.17	58.23	112.46	2286.1	
12-TH-S127	7.06	31.56	58.95	1232.99	
12-TH-S128	50.71	122.3	143.71	2219.01	
12-TH-S129	72.35	91.53	82.54	1495.2	
12-TH-S130	45	53.64	77.78	1644.24	
12-TH-S131	43.65	23.63	45.52	1691.82	
12-TH-S132	253.16	68.86	88.06	2422.38	
12-TH-S133	94.85	95.64	116.23	1992.1	

DRY SIEVING RESULTS					
Sample ID	**>8**	**4-8**	**2-4**	**<2**	**Comments**
12-TH-S134	25.23	62.65	90.57	1649.62	
12-TH-S135	1.61	5.39	47.74	1953.38	
12-TH-S137	166.65	92.93	95.57	1460.24	
12-TH-S138	5.97	44.19	71.31	2266.86	
12-TH-S140	41.38	43.91	52.84	1925.27	
12-TH-S141	332.31	68.25	79.67	1872.64	
12-TH-S142	1.93	33.9	74.63	1968.13	
12-TH-S143	10.69	34.63	50.89	974.27	
12-TH-S144	56.66	40.81	50.66	1158.93	
12-TH-S145	137.17	64.71	63.87	1190.51	
12-TH-S147	41.89	40.52	48.81	1009.28	
12-TH-S148	96.81	66.67	61.14	899.29	
12-TH-S149	28.77	80.25	89.24	1264.67	
12-TH-S150	65.81	47.62	49.28	827.28	
12-TH-S151	58.7	47.89	52.13	887.53	
12-TH-S152	72.98	54.25	61.04	895.45	
12-TH-S154	13.75	41.85	51.36	981.99	
12-TH-S155	240.37	61.31	69.37	734.48	
12-TH-S156	41.92	46.67	48.66	858.71	
12-TH-S157	7.27	23.96	21.45	1370.46	
12-TH-S158	34.02	35.93	42.34	811.5	
12-TH-S159	14.76	25.33	28.97	1042.38	
12-TH-S160	13.87	40.71	24.31	1103.77	
12-TH-S161	7.09	29.77	47.24	1151.36	
12-TH-S162	23.64	36.62	38.94	1146.4	
12-TH-S163	18.5	49.73	81.2	1118.43	
12-TH-S164	57.11	64.95	91.07	1179.83	
12-TH-S165	26.28	62.92	90.57	2050.71	
12-TH-S166	29.57	51.69	85.18	2085.9	
12-TH-S167	47.65	51.27	62.13	1502.23	
12-TH-S168	243.27	150.32	131.39	2227.91	
12-TH-S169	87.93	92.79	200.32	2948.22	
12-TH-S171	39.53	83.71	102.63	1683.58	
12-TH-S172	52.92	53.91	76.84	1697.97	
12-TH-S173	131.55	58.51	71.18	1325.04	
12-TH-S174	72.42	81.07	85.89	1844.61	
12-TH-S175	72.69	77.18	95.43	1947.03	
12-TH-S176	16.44	30.4	41.72	946.04	
12-TH-S178	22.47	38.49	52.6	910.92	
12-TH-S181	54.06	62.59	61.8	806.53	
12-TH-S182	30.92	39.07	44.86	815.14	
12-TH-S183	33.34	39.12	54.54	955.6	
12-TH-S184	64.48	64.68	83.44	1165.13	
12-TH-S185	4.66	40.93	44.38	1255.9	

DRY SIEVING RESULTS					
Sample ID	**>8**	**4-8**	**2-4**	**<2**	**Comments**
12-TH-S186	26.97	41.45	39.33	691.18	
12-TH-S187	174.35	54.98	39.2	742.11	
12-TH-S188	59.27	31.48	21.35	1311.08	
12-TH-S190	93.09	83.15	80.4	1499.59	
12-TH-S191	81.11	60.34	50.97	1183.14	
12-TH-S192	9.12	39.34	30.79	873.67	
12-TH-S193	30.97	55.36	57.68	1170.69	
12-TH-S194	15.88	43.74	55.24	993.56	
13-AB-196	--	--	--	640.35	
13-AB-197	--	--	--	604.73	
13-AB-199	--	--	--	652.89	
13-AB-200	--	--	--	723.28	
13-AB-201	--	--	--	1241.74	
13-AB-202	--	--	--	--	Laser only recorded
13-AB-203	--	--	--	1056.78	
13-AB-204	--	--	--	896.7	
13-AB-205	--	--	--	704.2	
13-AB-206	--	--	--	558.25	
13-AB-207	--	--	--	--	Laser only recorded
13-AB-208	--	--	--	--	Duplicate Sample
13-AB-209	--	--	--	750.04	
13-AB-210	--	--	--	--	Laser only recorded
13-AB-211	--	--	--	--	Laser only recorded
13-AB-212	--	--	--	--	Laser only recorded
13-AB-213	--	--	--	--	Laser only recorded
13-AB-214	18.09	30.4	42.5	761.38	
13-AB-215	17.58	41.98	49.46	1125.8	
13-AB-216	--	--	--	--	Laser only recorded
13-AB-217	--	--	--	--	Laser only recorded
13-AB-218	--	--	--	--	Laser only recorded
13-AB-219	--	--	--	--	Laser only recorded
13-AB-220	--	--	--	--	Duplicate Sample
13-AB-221	--	--	--	--	
13-AB-222	--	--	--	1060.78	
13-AB-223	--	--	--	1514.42	
13-AB-224	--	--	--	822.31	
13-AB-225	--	--	--	864.39	
13-AB-226	100.41	73.2	84.64	990.36	
13-AB-227	--	--	--	1027.18	
13-AB-228	--	--	--	967.87	
13-AB-229	--	--	--	1265.78	
13-AB-230	--	--	--	1070.39	
13-AB-231	--	--	--	1028.47	
13-AB-232	--	--	--	808.23	

DRY SIEVING RESULTS					
Sample ID	**>8**	**4-8**	**2-4**	**<2**	**Comments**
13-AB-233	--	--	--	--	Duplicate Sample
13-AB-234	--	--	--	1490.54	
13-AB-235	--	--	--	952.39	
13-AB-236	--	--	--	1453.08	
13-AB-237	--	--	--	1330.91	
13-AB-239	--	--	--	--	Laser only recorded
13-AB-240	--	--	--	--	Laser only recorded
13-AB-244	--	--	--	1534.12	
13-AB-245	--	--	--	1408.75	
13-AB-246	35.74	43.36	42.45	1019.7	
13-AB-247	--	--	--	1273.88	
13-AB-248	--	--	--	--	Duplicate Sample
13-AB-249	--	--	--	1495.09	
13-AB-250	--	--	--	1008.58	
13-AB-252	--	--	--	1137.77	
13-AB-253	11.32	48.46	54.64	1217	
13-AB-254	--	--	--	--	Duplicate Sample
13-AB-258A	451.96	133.74	131.63	2092.52	
13-AB-258B	308.78	162.52	171.48	2712.26	
13-AB-258C	483.66	253.2	238.21	2922.53	
13-AB-258D	579.99	160.54	213.85	2589.4	
13-AB-258E	79.34	49.42	73.41	918.7	
13-AB-265	--	--	--	--	Laser only recorded
Drillcore Samples					
ABR011-SA	31.06	22.1	15.59	387.35	
ABR011-SB	48.04	11.5	11.39	259.3	
ABR012-SA	52.87	21.11	20.67	501.97	
ABR012-SB	13.03	10.36	10.35	366.39	
AYA001-SA	3.86	11.73	10.78	338.13	
AYA001-SB	182.89	10.28	9.69	317.8	
AYA002-SA	51.54	6.93	8.09	333.91	
AYA003-SA	24.56	11.73	9.82	247.44	
AYA003-SB	74.28	4.34	8.47	302.38	
AYA003-SC	49.08	14.92	17.51	300.56	
AYA003-SD	30.66	7.88	11.33	406.71	
AYA004-SA	29.05	13.44	14.99	452.92	
AYA004-SB	40.95	22.47	17.95	465.37	
AYA004-SC	6.98	14.22	11.89	411.07	
AYA005-SA	170.96	13.38	13.89	361.59	
AYA006-SA	217.74	9.56	12.51	290.8	
AYA006-SB	43.31	14.95	14.39	343.15	
GEX001-SA	96.76	19.71	17.19	397.54	
GEX002-SA	8.63	15.88	15	366.65	
GEX002-SB	139.78	23.69	24.53	368.72	

DRY SIEVING RESULTS					
Sample ID	**>8**	**4-8**	**2-4**	**<2**	**Comments**
GEX003-SB	31.25	15.97	13.13	302.52	
GEX003-SA	15.67	9.27	10.38	120.62	
HND001-SA	40.59	8.45	9.29	378.76	
HND001-SB	52.34	17.92	16.63	503.43	
HND001-SE	1.64	3.63	7.06	236.92	
JSF001-SA	79	3.49	8.52	256.93	
TUR020-SA	4.27	10.91	12.61	438.17	
TUR021-SA	10.56	8.56	10.83	333.75	
TUR021-SB	21.81	7.95	9.52	288.24	
TUR022-SA	21.41	12.6	10.86	345.08	
TUR022-SB	14.93	6.72	10.89	365.21	
TUR022-SC	34.79	7.84	9.34	260.21	
TUR022-SD	34.31	17.95	17.45	262.59	
TUR024-SA	14.18	14.11	14.24	419.07	
TUR025-SA	22.92	13.47	10.39	328.61	
TUR029-SA	46.34	10.66	9.15	279.3	
TUR031-SA	42.95	12.4	13.87	406.95	
TUR031-SB	30.88	15.6	15.6	302.62	
TUR032-SA	33.93	13.7	11.09	333.79	
TUR032-SB	32.38	8.27	8.75	258.99	
TUR034-SA	37.77	11.29	8.63	293.29	
TUR034-SB	28.23	10.23	9.26	291.58	
TUR034-SD	12.26	8.79	8.22	270.09	
TUR035-SA	17.15	11.27	12.29	338.73	
TUR035-SB	47.23	11.48	11.57	302.09	
TUR036-SA	48.96	11.57	12.97	457.24	
TUR038-SA	28.25	16.16	14.13	409.83	
TUR040-SA	23.17	9.11	10.94	306.93	
TUR041-SA	26.95	10.9	11.29	356.16	
TUR041-SB	64.38	18.17	21.81	550.56	
TUR042-SA	10.71	11.86	14.43	494.05	
TUR042-SB	33.38	19.73	15.3	377.44	
TUR042-SC	47.26	18.38	20.92	502.93	
TUR043-SB	85.05	8.48	7.7	258.54	
TUR043-SA	19.95	10.64	11.93	345.67	
TUR044-SA	61	12.04	12.14	382.33	
TUR044-SB	94.97	13.39	17.3	407.63	
TUR045B-SA	16.48	20.81	19.93	433.09	
TUR045B-SB	38.8	12.4	11.27	268.29	
TUR046-SA	62.84	9.92	10.97	345.06	
TUR047-SA	15.73	7.31	11.27	361.45	
TUR047-SB	28.36	9.88	12.36	302.77	
TUR048-SA	108.73	14.05	15.1	435.52	
TUR048-SB	44.24	16.67	10.56	352.02	

DRY SIEVING RESULTS					
Sample ID	**>8**	**4-8**	**2-4**	**<2**	**Comments**
TUR048-SC	181.72	9.23	7.82	201.08	
TUR049-SA	73.32	16.03	12.48	267.43	
TUR049-SB	2.97	2.16	1.94	107.7	
TUR050-SA	13.04	9.24	8.05	220.07	
TUR050-SB	43.24	14.46	15.46	268.66	
TUR051-SA	26.91	15.17	13.4	305.27	
TUR051-SB	70.44	6.91	9.23	179.2	
TUR052-SA	57.71	8.5	8.82	288.26	
TUR052-SB	27.81	5.74	8.16	230.59	
TUR053-SA	21.26	17.05	12.65	328.68	
TUR053-SB	143.89	15.74	16.98	382.35	
TUR053-SC	104.72	28.4	29.09	301.3	
TUR054-SA	76.46	13.21	9.26	297.06	
TUR054-SB	54.11	9.26	11.28	288.51	
TUR055-SA	70.08	7.99	7.86	194.19	
TUR056-SA	33.11	14.15	12.73	396.89	
TUR056-SB	160.42	8.9	9.61	252.86	
TUR057-SA	44.63	5.38	7.3	204.14	
TUR057-SB	89.4	6.01	6.28	203.18	
TUR057-SC	12.04	5.7	9.84	309.24	
TUR057-SE	46.92	20.95	19.61	234.01	
TUR059-SA	27.94	18.76	16.41	494.33	
LOB001-SA	67.42	15.32	13.49	344.57	
LOB001-SB	15.99	4.88	7.77	313	
TUR060-SA	22.39	12.65	12.18	317.63	
TUR060-SB	25.93	8.68	11.67	332.79	
TUR060-SD	70.05	7.13	5.84	201.7	
TUR061-SA	11.78	5.72	7.06	214.57	
TUR061-SB	5.02	2.13	8.75	352.36	
TUR058-SA	16.64	9.5	9.08	260.08	
LOB002-SA	3.16	13.16	13.06	335.41	
LOB002-SB	49.31	0.33	0.96	192.27	
ABR012-SD	29.17	12.57	18.19	601.35	
ABR012-SE	69.3	34.49	54.96	1299.72	
AYA009-SA	68.26	10.04	5.12	206.47	
AYA009-SB	2.65	12.78	7.97	176.09	
AYA009-SC	148.1	11.61	13.86	276.16	
AYA009-SD	97.31	21.39	24.17	318.44	
AYA009-SE	--	--	--	--	
AYA010-SA	18.67	11.53	14.07	360.79	
AYA010-SB	32.7	4.7	10.95	162.05	
AYA010-SC	39.38	12.17	11.56	181.36	
HND002-SA	12.03	6.8	8.79	283.97	
HND002-SB				267.56	

DRY SIEVING RESULTS					
Sample ID	**>8**	**4-8**	**2-4**	**<2**	**Comments**
LOB003-SA	92.85	25.37	24.19	482.93	
LOB003-SB	72.72	15.64	20.31	629.35	
LOB003-SC	123.29	32.12	17.41	508.68	
MAM002-SA	8.84	6.5	8.21	448.5	
MAM002-SB	125.7	29.31	29.18	513.82	
MAM002-SC	118.41	7.63	10.66	298.62	
MAM002-SE	209.63	5.44	10.53	301.1	
MAM002-SF	25.24	6.08	11.14	400.35	
MAM002-SG	18.71	11.21	8.33	231.27	
TUR021-SC	78.48	24.11	23.73	623.27	
TUR022-SE	163.96	19.36	20.96	646.96	
TUR022-SF	119.91	37.86	33.57	487.71	
TUR031-SC	129.02	11.26	14.87	453.79	
TUR031-SD	144.38	17.01	24.8	405.13	
TUR031-SF	117.6	28.6	25.7	405.9	
TUR032-SC	234.09	28.56	27.36	623.18	
TUR039-SC	38.87	24.14	24.48	690.32	
TUR042-SD	204.27	17.3	25.39	697.5	
TUR045B-SC	56.91	27.13	23.84	470.13	
TUR046-SB	20.43	16.64	16.89	455.59	
TUR049-SC	77.42	18.63	16.8	440.21	
TUR050-SC	14.35	16.76	22.89	321.48	
TUR054-SE	125.88	16.52	18.17	400.76	
TUR057-SF	53.44	12	14.68	509.29	
TUR057-SG	73.62	12.1	16.06	485.41	
TUR057-SH	26.45	11.36	13.09	343.8	
TUR057-SI	42.7	19.33	20.31	491.91	
TUR057-SJ	33.95	15.81	15.23	418.12	
TUR057-SK	0	6.65	7.32	287.72	
TUR058-SC	106.05	23.59	26.61	628.13	
TUR059-SB	--	--	--	97.85	
TUR060-SF	67.54	15.59	15.58	607.05	
TUR060-SE	95.26	7.57	10.15	254.63	
SNB002-SA	206.18	24.71	23.49	523.53	
LOB001-SC	34.31	8.6	14.17	566.27	
TUR039-SB	--	--	--	259.71	

WET SIEVE RESULTS					
Sample_ID	Initial_Weight	Final_Weight	**Wt_%_Sand**	**Wt_%_Silt**	**Wt_%_Clay**
Surficial Till Samples					
13-AB-246	126.5	80.52	**63.65**	**30.97**	**5.37**
12-MR-010	321.82	221.54	**68.84**	**23.72**	**7.44**
13-AB-219	321.83	265.76	**82.58**	**16.01**	**1.41**
12-TH-120	123.59	102.17	**82.67**	**16.15**	**1.18**
Till Section Samples					
13-AB-258A	159.34	87.19	**54.72**	**29.45**	**15.76**
13-AB-258B	149.8	81.93	**54.69**	**29.61**	**15.68**
13-AB-258C	246.31	188.77	**76.64**	**19.25**	**3.98**
13-AB-258D	144.7	95.05	**65.69**	**25.04**	**9.20**
13-AB-265	193.7	127.54	**65.84**	**26.61**	**7.54**
12-MR-073B	154.39	81.08	**52.52**	**30.30**	**17.19**
12-MR-073D	215.71	113.01	**52.39**	**28.90**	**18.71**
12-MR-073F	140.64	88.21	**62.72**	**34.02**	**3.26**
Drillcore Samples					
ABR012-SA	105.75	70.14	**66.33**	**23.21**	**10.47**
ABR012-SB	88.83	45.43	**51.14**	**16.55**	**32.31**
ABR012-SD	140.82	63.54	**45.12**	**31.18**	**23.70**
ABR012-SE	180.35	111.66	**61.91**	**17.34**	**20.75**
AYA003-SA	71.63	47.99	**67.00**	**18.57**	**14.44**
AYA003-SB	74.86	52.88	**70.64**	**16.27**	**13.09**
AYA003-SC	74.00	51.41	**69.47**	**20.56**	**9.97**
AYA003-SD	97.85	46.65	**47.68**	**20.36**	**31.96**
AYA004-SA	210.39	131.23	**62.37**	**21.82**	**15.81**
AYA004-SB	112.80	80.15	**71.05**	**19.32**	**9.62**
AYA004-SC	91.74	59.27	**64.61**	**13.66**	**21.74**
AYA010-SA	87.57	53.40	**60.98**	**20.37**	**18.66**
LOB001-SA	166.01	102.77	**61.91**	**22.06**	**16.03**
LOB001-SB	154.95	104.08	**67.17**	**18.07**	**14.76**
LOB001-SC	133.10	88.04	**66.15**	**19.55**	**14.31**
MAM002-SA	111.8	52.21	**46.70**	**14.17**	**39.13**
MAM002-SB	123.4	80.9	**65.56**	**11.70**	**22.75**
MAM002-SC	145.82	95.04	**65.18**	**16.55**	**18.28**
MAM002-SE	141.93	94.86	**66.84**	**15.46**	**17.71**
MAM002-SF	92.1	63.81	**69.28**	**14.32**	**16.40**
MAM002-SG	86.28	56.53	**65.52**	**14.42**	**20.07**
TUR022-SA	86.83	56.59	**65.17**	**17.92**	**16.90**
TUR022-SB	88.93	58.28	**65.53**	**18.48**	**15.99**
TUR022-SC	61.64	40.74	**66.09**	**16.86**	**17.04**
TUR022-SD	59.33	40.62	**68.46**	**21.22**	**10.31**
TUR022-SE	117.4	79.68	**67.87**	**17.06**	**15.07**
TUR022-SF	157.31	101.98	**64.83**	**24.02**	**11.15**
TUR053-SA	162.10	105.53	**65.10**	**19.37**	**15.53**
TUR053-SB	93.46	59.75	**63.93**	**19.87**	**16.20**
TUR053-SC	73.96	52.28	**70.69**	**18.69**	**10.62**

WET SIEVE RESULTS					
Sample_ID	Initial_Weight	Final_Weight	**Wt_%_Sand**	**Wt_%_Silt**	**Wt_%_Clay**
TUR057-SA	99.66	65.01	**65.23**	**17.84**	**16.93**
TUR057-SB	104.31	68.95	**66.10**	**18.03**	**15.87**
TUR057-SC	148.16	100.44	**67.79**	**17.91**	**14.30**
TUR057-SE	115.35	71.25	**61.77**	**23.37**	**14.87**
TUR057-SF	121.16	79.2	**65.37**	**16.55**	**18.08**
TUR057-SG	116.12	79.15	**68.16**	**17.47**	**14.36**
TUR057-SH	157.65	103.42	**65.60**	**16.10**	**18.30**
TUR057-SI	118.10	77.33	**65.48**	**18.60**	**15.92**
TUR057-SJ	180.51	121.97	**67.57**	**14.58**	**17.85**
TUR057-SK	118.83	63.48	**53.42**	**21.50**	**25.08**
TUR060-SA	156.00	101.93	**65.34**	**18.88**	**15.78**
TUR060-SB	162.20	104.83	**64.63**	**19.52**	**15.85**
TUR060-SD	98.78	48.44	**49.04**	**25.59**	**25.37**

Appendix D – Surficial Sample Stations

Station_ID	Date	Datum	UTM Zone	Northing	Easting	Elevation (m)	Sample Medium	Field Till Matrix Colour	Comments
12-MR-007	19-Jul-12	NAD83	14	7135524	548883	178	Mudboil	10R 7/2; Pale Red	
12-MR-008	19-Jul-12	NAD83	14	7135902	548749	182	Mudboil	10R 7/2; Pale Red	
12-MR-009	19-Jul-12	NAD83	14	7135750	548860	188	Mudboil	10R 7/2; Pale Red	
12-MR-010	19-Jul-12	NAD83	14	7135606	548867	185	Mudboil	10R 7/2; Pale Red	
12-MR-011	19-Jul-12	NAD83	14	7135443	549007	185	Mudboil	10R 7/3; Pale Red	
12-MR-012	19-Jul-12	NAD83	14	7135764	548487	181	Mudboil	10R 7/3; Pale Red	
12-MR-013	19-Jul-12	NAD83	14	7135658	548655	182	Mudboil	2.5YR 6/4; Light Reddish Brown	
12-MR-014	19-Jul-12	NAD83	14	7135614	548766	182	Mudboil	10R 6/3; Pale Red	
12-MR-015	19-Jul-12	NAD83	14	7135530	548872	184	Mudboil	10R 6/3; Pale Red	
12-MR-016	19-Jul-12	NAD83	14	7135390	548367	183	Mudboil	10R 6/3; Pale Red	
12-MR-017	19-Jul-12	NAD83	14	7135384	548576	188	Mudboil	10R 6/3; Pale Red	
12-MR-018	19-Jul-12	NAD83	14	7135414	548677	186	Mudboil	10R 6/3; Pale Red	
12-MR-020	19-Jul-12	NAD83	14	7135380	548790	187	Mudboil	10R 7/2; Pale Red	
12-MR-021	19-Jul-12	NAD83	14	7135052	548496	184	Mudboil	10R 7/2; Pale Red	
12-MR-022	19-Jul-12	NAD83	14	7135230	548741	185	Mudboil	10R 6/1; Reddish Grey	
12-MR-023	19-Jul-12	NAD83	14	7135355	548888	183	Mudboil	10R 6/3; Pale Red	Some Pockets of more redder material (10R 6/4)
12-MR-024	19-Jul-12	NAD83	14	7134797	548970	183	Mudboil	10R 6/2; Pale Red	
12-MR-025	19-Jul-12	NAD83	14	7134998	548987	186	Mudboil	10R 6/2; Pale Red	
12-MR-026	19-Jul-12	NAD83	14	7135087	548984	184	Mudboil	10R 6/2; Pale Red	
12-MR-027	19-Jul-12	NAD83	14	7135321	548988	185	Mudboil	10R 6/2; Pale Red	
12-MR-028	19-Jul-12	NAD83	14	7135383	549000	188	Mudboil	10R 6/2; Pale Red	
12-MR-029	19-Jul-12	NAD83	14	7135077	549560	185	Mudboil	10R 6/2; Pale Red	
12-MR-030	19-Jul-12	NAD83	14	7135219	549369	185	Mudboil	10R 6/2; Pale Red	
12-MR-032	19-Jul-12	NAD83	14	7135269	549281	188	Mudboil	10R 6/2; Pale Red	
12-MR-033	19-Jul-12	NAD83	14	7135329	549178	188	Mudboil	10R 6/2; Pale Red	
12-MR-034	19-Jul-12	NAD83	14	7135416	549058	187	Mudboil	10R 6/2; Pale Red	
12-MR-035	19-Jul-12	NAD83	14	7135466	549658	187	Mudboil	10R 7/2; Pale Red	
12-MR-036	19-Jul-12	NAD83	14	7135477	549455	187	Mudboil	10R 7/2; Pale Red	
12-MR-038	19-Jul-12	NAD83	14	7135481	549348	186	Mudboil	10R 6/2; Pale Red	
12-MR-039	19-Jul-12	NAD83	14	7135497	549225	184	Mudboil	10R 6/2; Pale Red	
12-MR-040	21-Jul-12	NAD83	14	7137120	547387	188	Mudboil	Pale Red	
12-MR-041	21-Jul-12	NAD83	14	7136918	547384	186	Mudboil	Pale Red	
12-MR-042	21-Jul-12	NAD83	14	7136556	547540	189	Mudboil	Pale Red	
12-MR-043	21-Jul-12	NAD83	14	7136353	547559	187	Mudboil	Pale Red	
12-MR-044	21-Jul-12	NAD83	14	7136142	547541	187	Mudboil	Pale Red	
12-MR-045	21-Jul-12	NAD83	14	7135955	547619	186	Mudboil	Pale Red	
12-MR-046	21-Jul-12	NAD83	14	7135761	547667	185	Mudboil	Pale Red	
12-MR-047	21-Jul-12	NAD83	14	7135563	547685	193	Mudboil	--	
12-MR-048	21-Jul-12	NAD83	14	7135305	547735	190	Mudboil	Pale Red	
12-MR-049	21-Jul-12	NAD83	14	7135102	547769	192	Mudboil	Pale Red	
12-MR-050	21-Jul-12	NAD83	14	7134925	547794	191	Mudboil	Pale Red	
12-MR-051	21-Jul-12	NAD83	14	7134720	547782	192	Mudboil	Pale Red	
12-MR-052	21-Jul-12	NAD83	14	7134882	548416	185	Mudboil	Pale Red	
12-MR-053	21-Jul-12	NAD83	14	7135092	548280	186	Mudboil	--	
12-MR-060	23-Jul-12	NAD83	14	7142011	545868	183	Mudboil	10R 7/3; Pale Red	
12-MR-061	23-Jul-12	NAD83	14	7140213	545707	194		10R 7/3; Pale Red	Frost upheaved till (look up proper name); Cobble and pebble content higher than the till recovered from
12-MR-063	23-Jul-12	NAD83	14	7138789	545218	195	Mudboil	10R 7/2; Pale Red	

Station_ID	Date	Datum	UTM Zone	Northing	Easting	Elevation (m)	Sample Medium	Field Till Matrix Colour	Comments
12-MR-069	23-Jul-12	NAD83	14	7138776	548073	181	Mudboil	10R 7/3; Pale Red	
12-MR-070	23-Jul-12	NAD83	14	7137678	548391	182	Mudboil	10R 7/3; Pale Red	
12-MR-071	23-Jul-12	NAD83	14	7137172	548486	183	Mudboil	10R 7/3; Pale Red	
12-MR-072	23-Jul-12	NAD83	14	7136335	548724	180	Mudboil	10R 7/3; Pale Red	
12-MR-073	24-Jul-12	NAD83	14	7160954	548054	170	Mudboil	--	
12-MR-076	25-Jul-12	NAD83	14	7134937	546614	183	Mudboil	Pale Red	
12-MR-077	25-Jul-12	NAD83	14	7134275	547039	184	Mudboil	Pale Red	
12-MR-078	25-Jul-12	NAD83	14	7133355	548117	190	Mudboil	Pale Red	
12-MR-079	25-Jul-12	NAD83	14	7133010	548491	192	Mudboil	Pale Red	
12-MR-086	25-Jul-12	NAD83	14	7135930	549535	183	Mudboil	Pale Red	
12-MR-087	25-Jul-12	NAD83	14	7136239	549360	181	Mudboil	Pale Red	
12-MR-094	26-Jul-12	NAD83	14	7131146	528367	141	Mudboil	Pale Red	Boulder lag at surface, below marine limit
12-MR-095	26-Jul-12	NAD83	14	7131039	527994	137	Mudboil	Pale Red	
12-TH-103	29-Jul-12	NAD83	14	7140534	543595	176	Mudboil	Pale Red	
12-TH-104	29-Jul-12	NAD83	14	7138669	543867	187	Mudboil	Light Brown	Dry
12-TH-105	29-Jul-12	NAD83	14	7138217	543286	191	Mudboil	Pale Red	
12-TH-106	29-Jul-12	NAD83	14	7137514	542995	199	Mudboil	Pale Red	
12-TH-110	29-Jul-12	NAD83	14	7136699	543104	208	Mudboil	Pale Red/Light Brown	Dry
12-TH-111	29-Jul-12	NAD83	14	7135952	543141	200	Mudboil	Pale Red/Light Brown	Appears sandier
12-TH-112	29-Jul-12	NAD83	14	7135090	543525	194	Mudboil	Light Brown	Appears sandier
12-TH-113	29-Jul-12	NAD83	14	7134409	543870	189	Mudboil	Pale Red	
12-TH-116	29-Jul-12	NAD83	14	7136862	542012	199	Mudboil	Pale Brown	Dry
12-TH-117	29-Jul-12	NAD83	14	7138154	541837	191	Mudboil	Pale Brown	Dry
12-TH-118	30-Jul-12	NAD83	14	7131251	527471	142	Boulder Lagged Drumlin	--	Boulder lagged drumlin
12-TH-119	30-Jul-12	NAD83	14	7131599	527327	138	Mudboil	7.5YR 7/2; Pinkish Grey	Mudboil on boulder lagged drumlin; dry
12-TH-120	30-Jul-12	NAD83	14	7131760	527812	127	Boulder Lagged Drumlin	--	Boulder lagged drumlin
12-TH-121	30-Jul-12	NAD83	14	7131938	527222	132	Boulder Lagged Drumlin	7.5YR 6/3; Light Brown	Boulder lagged drumlin; moist
12-TH-122	30-Jul-12	NAD83	14	7132219	527677	120	Mudboil	5YR 8/2; Pinkish White	Mudboil on top of boulder lagged drumlin; dry
12-TH-124	30-Jul-12	NAD83	14	7133301	527819	116	Boulder Lagged Drumlin	5YR 7/2; Pinkish Grey	Boulder lagged drumlin; coarse sand near surface, dug to till and sampled with trowel
12-TH-125	30-Jul-12	NAD83	14	7133249	528354	105	Mudboil	5YR 7/2; Pinkish Grey	Mudboil on flank of reworked drumlin
12-TH-126	1-Aug-12	NAD83	14	7136673	533455	135	Mudboil	5YR 5/2; Reddish Grey	Wet
12-TH-127	1-Aug-12	NAD83	14	7136953	533749	142	Mudboil	5YR 5/2; Reddish Grey	Moist
12-TH-128	1-Aug-12	NAD83	14	7136413	533663	134	Mudboil	5YR 6/3; Light Reddish Brown	Dry
12-TH-129	1-Aug-12	NAD83	14	7136157	533794	139	Mudboil	7.5YR 6/3; Light Brown	Dry
12-TH-130	1-Aug-12	NAD83	14	7136023	534471	140	Mudboil	5YR 6/2; Pinkish Grey	Dry
12-TH-131	1-Aug-12	NAD83	14	7134842	533735	152	Mudboil	5YR 6/3; Light Reddish Brown	Dry
12-TH-132	1-Aug-12	NAD83	14	7135111	533690	147	Mudboil	5YR 6/2; Pinkish Grey	Dry; a little moist
12-TH-133	1-Aug-12	NAD83	14	7135259	533290	143	Mudboil	5YR 6/2; Pinkish Grey	Dry
12-TH-134	1-Aug-12	NAD83	14	7135312	533078	141	Mudboil	5YR 6/3; Light Reddish Brown	Dry
12-TH-135	1-Aug-12	NAD83	14	7135622	533018	134	Mudboil	5YR 7/2; Pinkish Grey	Dry
12-TH-137	1-Aug-12	NAD83	14	7135663	532784	135	Mudboil	5YR 6/2; Pinkish Grey	Dry
12-TH-138	1-Aug-12	NAD83	14	7135675	532495	133	Mudboil	5YR 6/2; Pinkish Grey	Moist
12-TH-140	1-Aug-12	NAD83	14	7135845	532200	131	Mudboil	2.5YR 6/2; Pinkish Grey	Moist
12-TH-141	1-Aug-12	NAD83	14	7136219	531991	126	Mudboil	5YR 6/2; Pinkish Grey	Dry
12-TH-142	1-Aug-12	NAD83	14	7136437	531977	124	Mudboil	5YR 6/2; Pinkish Grey	Dry
12-TH-143	1-Aug-12	NAD83	14	7136640	532333	124	Mudboil	5YR 6/3; Light Reddish Brown	
12-TH-144	1-Aug-12	NAD83	14	7136564	532675	125	Mudboil	5YR 6/3; Light Reddish Brown	Moist

Station_ID	Date	Datum	UTM Zone	Northing	Easting	Elevation (m)	Sample Medium	Field Till Matrix Colour	Comments
12-TH-145	1-Aug-12	NAD83	14	7136509	533024	135	Mudboil	5YR 6/2; Pinkish Grey	Moist
12-TH-147	3-Aug-12	NAD83	14	7130956	528930	148	Mudboil	5YR 7/3; Pink	Moist
12-TH-148	3-Aug-12	NAD83	14	7131488	528981	142	Mudboil	10R 6/2; Pale Red; Pale Red	Moist
12-TH-149	3-Aug-12	NAD83	14	7132149	529039	137	Mudboil	5YR 6/3; Light Reddish Brown	Moist
12-TH-150	3-Aug-12	NAD83	14	7132540	529404	138	Mudboil	5YR 7/3; Pink	Moist
12-TH-151	3-Aug-12	NAD83	14	7133178	529241	134	Mudboil	5YR 6/3; Light Reddish Brown	Moist
12-TH-152	3-Aug-12	NAD83	14	7133645	529328	133	Mudboil	2.5YR 7/2; Pinkish Grey	Moist
12-TH-154	3-Aug-12	NAD83	14	7134193	529269	128	Mudboil	5YR 6/2; Pinkish Grey	Moist
12-TH-155	3-Aug-12	NAD83	14	7133958	528315	108	Boulder Lagged Drumlin	10R 7/2; Pale Red; Pale Red	Approx. 14" of sand overlying reworked till
12-TH-156	3-Aug-12	NAD83	14	7133874	527847	112	Mudboil	5YR 6/2; Pinkish Grey	Mudboil on the flank of a drumlin. More enriched in silt and clay than other areas
12-TH-157	3-Aug-12	NAD83	14	7133626	527254	115	Mudboil	5YR 6/3; Light Reddish Brown	Dry
12-TH-158	3-Aug-12	NAD83	14	7133457	526839	116	Mudboil	10R 7/2; Pale Red; Pale Red	Dry
12-TH-159	3-Aug-12	NAD83	14	7133254	526782	116	Mudboil	5YR 6/2; Pinkish Grey	Moist
12-TH-160	3-Aug-12	NAD83	14	7132884	526953	115	Mudboil	10R 6/3; Pale Red	Moist
12-TH-161	3-Aug-12	NAD83	14	7132579	527014	121	Mudboil	10R 6/2; Pale Red; Pale Red	Moist
12-TH-162	3-Aug-12	NAD83	14	7131922	526631	118	Mudboil	5YR 6/2; Pinkish Grey	Mudboil on the side of a boulder lagged drumlin
12-TH-163	3-Aug-12	NAD83	14	7131579	526809	128	Mudboil	5YR 6/3; Light Reddish Brown	Moist
12-TH-164	3-Aug-12	NAD83	14	7131337	526916	133	Mudboil	5YR 6/3; Light Reddish Brown	Moist
12-TH-165	5-Aug-12	NAD83	14	7138345	533522	129	Mudboil	5YR 5/3; Reddish Brown	Wet
12-TH-166	5-Aug-12	NAD83	14	7138336	532129	119	Mudboil	5YR 6/3; Light Reddish Brown	Moist
12-TH-167	5-Aug-12	NAD83	14	7137651	530760	108	Mudboil	7.5YR 6/3; Light Brown	Moist
12-TH-168	5-Aug-12	NAD83	14	7136906	530100	106	Mudboil	5YR 6/3; Light Reddish Brown	Moist
12-TH-169	5-Aug-12	NAD83	14	7135533	530557	113	Mudboil	5YR 6/3; Light Reddish Brown	Moist
12-TH-171	5-Aug-12	NAD83	14	7134353	531942	140	Mudboil	5YR 6/2; Pinkish Grey	Just above palaeo-shoreline; moist
12-TH-172	5-Aug-12	NAD83	14	7133707	533103	171	Mudboil	5YR 6/2; Pinkish Grey	Moist
12-TH-173	5-Aug-12	NAD83	14	7135153	534723	147	Boulder Lagged Drumlin	5YR 5/3; Reddish Brown	Dug ~50 cm to till. Bullet-shaped glacial clasts found when digging.
12-TH-174	5-Aug-12	NAD83	14	7136124	533166	133	Mudboil	5YR 7/2; Pinkish Grey	Mudboil is on side of boulder lagged drumlin
12-TH-175	5-Aug-12	NAD83	14	7136077	532895	132	Mudboil	5YR 7/2; Pinkish Grey	
12-TH-176	5-Aug-12	NAD83	14	7136144	532468	126	Mudboil	5YR 6/2; Pinkish Grey	
12-TH-178	6-Aug-12	NAD83	14	7133457	523265	198	Mudboil	5YR 6/2; Pinkish Grey	Moist
12-TH-181	6-Aug-12	NAD83	14	7131836	522977	175	Mudboil	5YR 6/3; Light Reddish Brown	Moist
12-TH-182	6-Aug-12	NAD83	14	7130514	523287	172	Mudboil	5YR 6/2; Pinkish Grey	Moist
12-TH-183	6-Aug-12	NAD83	14	7130158	525369	157	Mudboil	10R 6/3; Pale Red	Moist
12-TH-184	6-Aug-12	NAD83	14	7131328	525278	185	Mudboil	5YR 5/2; Reddish Grey	Moist
12-TH-185	6-Aug-12	NAD83	14	7132343	525134	192	Mudboil	5YR 5/3; Reddish Brown	Moist
12-TH-186	6-Aug-12	NAD83	14	7133803	525693	136	Mudboil	5YR 6/3; Light Reddish Brown	Wet
12-TH-187	6-Aug-12	NAD83	14	7134855	525899	115	Mudboil	7.5YR 6/3; Light Brown	Moist
12-TH-188	6-Aug-12	NAD83	14	7135135	526991	94	Mudboil	--	Wet; more swampy terrain
12-TH-190	7-Aug-12	NAD83	14	7134180	550145	171	Mudboil	5YR 6/3; Light Reddish Brown	Moist
12-TH-191	7-Aug-12	NAD83	14	7134829	550794	166	Mudboil	--	Wet; more swampy terrain
12-TH-192	7-Aug-12	NAD83	14	7135633	550767	173	Mudboil	5YR 7/2; Pinkish Grey	Moist
12-TH-193	7-Aug-12	NAD83	14	7136603	550606	178	Mudboil	5YR 6/2; Pinkish Grey	Moist
12-TH-194	7-Aug-12	NAD83	14	7137500	550554	180	Mudboil	7.5YR 5/2; Brown	Moist
13-AB-196	4-Jul-13	NAD 83	14	7137299	532969	124	Mud Boil	2.5YR 5/2; Weak Red	Till veneer interspersed with boulder fields
13-AB-197	4-Jul-13	NAD 83	14	7137212	534750	138	Mudboil	2.5YR 6/1; Reddish Grey	Sandy till in bouldery terrain

Station_ID	Date	Datum	UTM Zone	Northing	Easting	Elevation (m)	Sample Medium	Field Till Matrix Colour	Comments
13-AB-199	5-Jul-13	NAD 83	14	7134642	549563	178	Mudboil	5YR 6/2; Pinkish Grey	Till blanket, numerous fsc (syenite) boulders at surface, potentially explaining strong K radiometrics
13-AB-200	5-Jul-13	NAD 83	14	7135190	548005	185	Mudboil	5YR 6/2; Pinkish Grey	On east side of drumlin
13-AB-201	5-Jul-13	NAD 83	14	7135473	547928	185	Mudboil	5YR 6/2; Pinkish Grey	east side of drumlin
13-AB-202	5-Jul-13	NAD 83	14	7135439	547372	183	Mudboil	--	West side of drumlin
13-AB-203	5-Jul-13	NAD 83	14	7135696	548024	185	Mudboil	5YR 5/2; Reddish Grey	Mudboil in low area between drumlin and small lake. Ground is wet
13-AB-204	5-Jul-13	NAD 83	14	7136015	547979	185	Mudboil	5YR 6/2; Pinkish Grey	Between drumlin and big lake
13-AB-205	5-Jul-13	NAD 83	14	7136324	547899	185	Mudboil	--	Northernmost sample on point between lake and drumlin
13-AB-206	5-Jul-13	NAD 83	14	7135911	548298	184	Mudboil	2.5YR 5/2; Weak Red	Stretch of land between the big lake and small lake
13-AB-207	5-Jul-13	NAD 83	14	7135837	548626	184	Mudboil	2.5YR 6/2; Pinkish Grey	
13-AB-207	5-Jul-13	NAD 83	14	7135837	548626	184	Mudboil	2.5YR 6/2; Pinkish Grey	
13-AB-209	5-Jul-13	NAD 83	14	7135683	548771	184	Mudboil	2.5YR 5/2; Weak Red	
13-AB-210	5-Jul-13	NAD 83	14	7135598	549050	184	Mudboil	2.5YR 5/2; Weak Red	
13-AB-211	5-Jul-13	NAD 83	14	7135816	549393	182	Mudboil	--	Dry till
13-AB-212	5-Jul-13	NAD 83	14	7136064	549359	182	Mudboil	5YR 5/3; Reddish Brown	
13-AB-213	5-Jul-13	NAD 83	14	7136193	548955	185	Mudboil	5YR 5/2; Reddish Grey	Wet
13-AB-214	5-Jul-13	NAD 83	14	7136133	548724	184	Mudboil	5YR 5/2; Reddish Grey	Near small puddle
13-AB-215	5-Jul-13	NAD 83	14	7136009	548551	180	Mudboil	5YR 5/3; Reddish Brown	Sandy
13-AB-216	5-Jul-13	NAD 83	14	7135893	549075	182	Mudboil	5YR 6/2; Pinkish Grey	Dry, compact, and sandy
13-AB-217	5-Jul-13	NAD 83	14	7135857	548890	179	Mudboil	5YR 5/2; Reddish Grey	
13-AB-218	5-Jul-13	NAD 83	14	7135896	548760	180	Mudboil	2.5YR 5/2; Weak Red	
13-AB-219	6-Jul-13	NAD 83	14	7131685	528208	125	Boulder Lagged Drumlin	5YR 6/2; Pinkish Grey	
13-AB-221	6-Jul-13	NAD 83	14	7132190	528447	127	Boulder Lagged Drumlin	2.5YR 5/3; Reddish Brown	
13-AB-222	6-Jul-13	NAD 83	14	7132580	528043	111	Boulder Lagged Drumlin	5YR 6/2; Pinkish Grey	
13-AB-223	6-Jul-13	NAD 83	14	7132898	528102	113	Boulder Lagged Drumlin	5YR 6/2; Pinkish Grey	
13-AB-224	6-Jul-13	NAD 83	14	7132733	527425	118	Boulder Lagged Drumlin	5YR 6/2; Pinkish Grey	
13-AB-225	6-Jul-13	NAD 83	14	7132526	527563	119	Boulder Lagged Drumlin	5YR 6/2; Pinkish Grey	
13-AB-226	6-Jul-13	NAD 83	14	7132331	527365	119	Boulder Lagged Drumlin	5YR 6/2; Pinkish Grey	
13-AB-227	6-Jul-13	NAD 83	14	7131922	527207	133	Boulder Lagged Drumlin	5YR 6/2; Pinkish Grey	
13-AB-228	7-Jul-13	NAD 83	14	7136662	548414	181	Mudboil	2.5YR 6/2; Pinkish Grey	
13-AB-229	7-Jul-13	NAD 83	14	7136679	548986	185	Mudboil	5YR 6/2; Pinkish Grey	
13-AB-230	7-Jul-13	NAD 83	14	7136639	549466	182	Mudboil	5YR 6/2; Pinkish Grey	
13-AB-231	7-Jul-13	NAD 83	14	7136412	549827	176	Mudboil	5YR 6/2; Pinkish Grey	
13-AB-232	7-Jul-13	NAD 83	14	7137183	549430	184	Mudboil	5YR 6/2; Pinkish Grey	
13-AB-232	7-Jul-13	NAD 83	14	7137183	549430	184	Mudboil	5YR 6/2; Pinkish Grey	
13-AB-234	7-Jul-13	NAD 83	14	7137169	548982	185	Mudboil	5YR 5/2; Reddish Grey	
13-AB-235	7-Jul-13	NAD 83	14	7137674	548956	184	Mudboil	5YR 6/2; Pinkish Grey	
13-AB-236	7-Jul-13	NAD 83	14	7137692	549482	183	Mudboil	5YR 6/2; Pinkish Grey	
13-AB-237	7-Jul-13	NAD 83	14	7137187	549973	183	Mudboil	5YR 6/2; Pinkish Grey	
13-AB-239	7-Jul-13	NAD 83	14	7138749	549792	181	Mudboil	5YR 5/2; Reddish Grey	
13-AB-240	7-Jul-13	NAD 83	14	7139639	548918	176	Mudboil	5YR 5/2; Reddish Grey	
13-AB-244	12-Jul-13	NAD 83	14	7136377	545393	183	Mudboil	2.5YR 7/2; Pinkish Grey	
13-AB-245	12-Jul-13	NAD 83	14	7136388	545871	183	Mudboil	5YR 5/3; Reddish Brown	
13-AB-246	12-Jul-13	NAD 83	14	7136733	545644	183	Mudboil	5YR 6/2; Pinkish Grey	
13-AB-247	12-Jul-13	NAD 83	14	7137015	545330	184	Mudboil	5YR 6/2; Pinkish Grey	
13-AB-249	12-Jul-13	NAD 83	14	7136023	544674	187	Mudboil	5YR 6/2; Pinkish Grey	

Station_ID	Date	Datum	UTM Zone	Northing	Easting	Elevation (m)	Sample Medium	Field Till Matrix Colour	Comments
13-AB-250	12-Jul-13	NAD 83	14	7138248	546057	188	Mudboil	5YR 5/2; Reddish Grey	
13-AB-252	12-Jul-13	NAD 83	14	7137877	546770	185	Mudboil	5YR 5/2; Reddish Grey	
13-AB-253	12-Jul-13	NAD 83	14	7139335	547274	190	Mudboil	5YR 5/3; Reddish Brown	

Appendix E – Till Lithological Clast Counts

2-4 mm Till Lithology Clast Counts

			SS + Cong.			Volcanic			Intrusive			Rounded Qtz			Angular Qtz			Feldspar			Supracrustal			Other/Unknown			Altered			Conducted
Sample ID	**n tot.**	**wt. tot. (g)**	**n**	***wt.***	***wt. %***	***n***	***wt.***	***wt. %***	***n***	***wt.***	***wt. %***	***n***	***wt.***	***wt. %***	***n***	***wt.***	***wt. %***	***n***	***wt.***	***wt. %***	***n***	***wt.***	***wt. %***	***n***	***wt.***	***wt. %***	***n***	***wt.***	**wt. %**	**By:**
12-MR-S010	128	3.763	18	0.425	11.29	3	0.089	2.37	73	2.206	58.62	8	0.143	3.80	3	0.053	1.41	1	0.025	0.66	16	0.577	15.33	1	0.014	0.37	5	0.231	6.14	TH
12-TH-S113	127	3.951	16	0.434	10.98	9	0.238	6.02	75	2.614	66.16	5	0.102	2.58	6	0.155	3.92	3	0.063	1.59	9	0.260	6.58	3	0.060	1.52	1	0.025	0.63	TH
ABR012-SA	137	4.182	12	0.358	8.56	3	0.168	4.02	91	2.845	68.03	5	0.120	2.87	13	0.365	8.73	8	0.243	5.81	2	0.039	0.93	0	0.000	0.00	3	0.044	1.05	TH
ABR012-SB	105	3.136	13	0.454	14.48	0	0.000	0.00	54	1.671	53.28	6	0.111	3.54	18	0.475	15.15	8	0.257	8.20	0	0.000	0.00	2	0.096	3.06	4	0.072	2.30	TH
AYA003-SA	152	4.584	49	1.446	31.54	12	0.319	6.96	27	0.993	21.66	41	0.971	21.18	6	0.211	4.60	2	0.074	1.61	2	0.120	2.62	0	0.000	0.00	13	0.450	9.82	TH
AYA003-SB	130	4.124	51	1.591	38.58	15	0.536	13.00	9	0.324	7.86	47	1.417	34.36	2	0.072	1.75	1	0.018	0.44	1	0.061	1.48	3	0.064	1.55	1	0.041	0.99	TH
AYA003-SC	142	4.523	10	0.351	7.76	3	0.129	2.85	84	2.658	58.77	18	0.572	12.65	11	0.344	7.61	12	0.253	5.59	0	0.000	0.00	3	0.195	4.31	1	0.021	0.46	TH
AYA003-SD	187	4.991	30	0.852	17.07	0	0.000	0.00	58	1.724	34.54	63	1.533	30.72	18	0.479	9.60	12	0.268	5.37	1	0.015	0.30	3	0.042	0.84	2	0.078	1.56	TH
AYA004-SA	151	4.274	38	1.064	24.89	14	0.410	9.59	24	0.771	18.04	30	0.669	15.65	10	0.233	5.45	23	0.753	17.62	1	0.018	0.42	8	0.220	5.15	3	0.136	3.18	TH
AYA004-SB	133	4.242	5	0.172	4.05	4	0.084	1.98	84	2.921	68.86	5	0.120	2.83	17	0.398	9.38	10	0.279	6.58	3	0.107	2.52	2	0.064	1.51	3	0.097	2.29	TH
AYA004-SC	219	6.341	17	0.401	6.32	0	0.000	0.00	147	4.590	72.39	11	0.310	4.89	20	0.384	6.06	15	0.358	5.65	4	0.175	2.76	3	0.053	0.84	2	0.070	1.10	TH
GEX003-SA	132	4.018	14	0.343	8.54	7	0.237	5.90	69	2.217	55.18	2	0.037	0.92	15	0.309	7.69	3	0.090	2.24	6	0.308	7.67	3	0.085	2.12	13	0.392	9.76	TH
GEX003-SB	119	3.678	20	0.673	18.30	6	0.229	6.23	51	1.653	44.95	7	0.189	5.14	11	0.311	8.46	4	0.065	1.77	5	0.121	3.29	3	0.056	1.51	12	0.381	10.36	TH
HND001-SA	119	3.437	48	1.333	38.78	3	0.151	4.39	23	0.662	19.26	26	0.750	21.82	11	0.298	8.67	1	0.036	1.05	4	0.157	4.57	0	0.000	0.00	3	0.050	1.45	TH
HND001-SB	142	3.970	47	1.395	35.14	17	0.543	13.68	26	0.802	20.20	18	0.341	8.59	16	0.455	11.46	0	0.000	0.00	6	0.211	5.31	2	0.050	1.26	10	0.173	4.36	TH
HND001-SE	140	3.241	70	1.592	49.12	0	0.000	0.00	6	0.152	4.69	36	0.786	24.25	13	0.311	9.60	1	0.021	0.65	9	0.272	8.39	0	0.000	0.00	5	0.107	3.30	TH
HND002-SA	153	3.979	52	1.216	30.56	10	0.404	10.15	35	1.067	26.82	27	0.555	13.95	15	0.392	9.85	2	0.055	1.38	5	0.119	2.99	2	0.039	0.98	5	0.132	3.32	TH
HND002-SB	165	4.038	80	2.025	50.15	2	0.087	2.15	5	0.124	3.07	63	1.473	36.48	11	0.257	6.36	0	0.000	0.00	3	0.056	1.39	1	0.016	0.40	0	0.000	0.00	TH
JSF001-SA	139	3.429	54	1.321	38.52	3	0.089	2.60	25	0.754	21.99	27	0.625	18.23	19	0.358	10.44	1	0.028	0.82	1	0.056	1.63	0	0.000	0.00	9	0.198	5.77	TH
LOB001-SA	112	3.045	23	0.722	23.71	4	0.111	3.65	46	1.245	40.89	12	0.221	7.26	9	0.233	7.65	2	0.046	1.51	4	0.140	4.60	1	0.020	0.66	11	0.307	10.08	TH
LOB001-SB	138	3.507	55	1.480	42.20	1	0.011	0.31	20	0.648	18.48	32	0.652	18.59	18	0.465	13.26	1	0.017	0.48	2	0.046	1.31	4	0.088	2.51	5	0.100	2.85	TH
LOB001-SC	128	3.734	52	1.560	41.78	3	0.135	3.62	20	0.706	18.91	30	0.798	21.37	13	0.341	9.13	1	0.011	0.29	6	0.112	3.00	1	0.044	1.18	2	0.027	0.72	TH
LOB002-SA	120	3.180	23	0.495	15.57	7	0.123	3.87	48	1.429	44.94	14	0.374	11.76	10	0.220	6.92	2	0.088	2.77	8	0.291	9.15	3	0.074	2.33	5	0.086	2.70	TH
LOB003-SA	104	3.363	16	0.601	17.87	2	0.082	2.44	44	1.503	44.69	7	0.195	5.80	10	0.220	6.54	4	0.084	2.50	15	0.513	15.25	1	0.040	1.19	5	0.125	3.72	TH
LOB003-SB	105	3.366	35	1.109	32.95	3	0.106	3.15	22	0.791	23.50	21	0.653	19.40	10	0.254	7.55	1	0.017	0.51	8	0.292	8.67	2	0.038	1.13	3	0.106	3.15	TH
MAM002-SA	96	2.902	23	0.799	27.53	0	0.000	0.00	47	1.497	51.59	9	0.191	6.58	3	0.045	1.55	0	0.000	0.00	7	0.150	5.17	1	0.014	0.48	6	0.206	7.10	TH
MAM002-SB	111	3.371	19	0.430	12.76	3	0.151	4.48	57	1.848	54.82	13	0.325	9.64	10	0.292	8.66	2	0.084	2.49	4	0.189	5.61	1	0.013	0.39	2	0.039	1.16	TH
MAM002-SC	126	3.180	52	1.391	43.74	0	0.000	0.00	17	0.394	12.39	38	1.005	31.60	11	0.211	6.64	0	0.000	0.00	2	0.051	1.60	1	0.021	0.66	5	0.107	3.36	TH
MAM002-SE	125	3.683	52	1.517	41.19	1	0.100	2.72	22	0.853	23.16	36	0.805	21.86	9	0.176	4.78	1	0.016	0.43	2	0.108	2.93	0	0.000	0.00	2	0.108	2.93	TH
MAM002-SF	141	3.548	65	1.720	48.48	0	0.000	0.00	3	0.103	2.90	59	1.405	39.60	11	0.213	6.00	0	0.000	0.00	0	0.000	0.00	3	0.107	3.02	0	0.000	0.00	TH
MAM002-SG	137	3.734	73	2.184	58.49	1	0.007	0.19	2	0.026	0.70	52	1.352	36.21	8	0.141	3.78	1	0.024	0.64	0	0.000	0.00	0	0.000	0.00	0	0.000	0.00	TH
TUR020-SA	123	3.655	23	0.711	19.45	4	0.073	2.00	50	1.500	41.04	17	0.530	14.50	12	0.256	7.00	2	0.025	0.68	3	0.206	5.64	3	0.068	1.86	9	0.286	7.82	TH
TUR021-SA	95	2.851	33	0.992	34.79	1	0.037	1.30	24	0.735	25.78	20	0.526	18.45	7	0.268	9.40	1	0.015	0.53	7	0.224	7.86	0	0.000	0.00	2	0.054	1.89	TH
TUR021-SB	136	3.847	50	1.478	38.42	1	0.013	0.34	16	0.472	12.27	35	1.005	26.12	21	0.626	16.27	0	0.000	0.00	4	0.080	2.08	1	0.037	0.96	8	0.136	3.54	AB
TUR021-SC	96	3.234	19	0.495	15.31	1	0.044	1.36	46	1.741	53.83	18	0.516	15.96	2	0.024	0.74	0	0.000	0.00	10	0.414	12.80	0	0.000	0.00	0	0.000	0.00	AB
TUR022-SA	140	4.126	39	1.269	30.76	4	0.170	4.12	40	1.212	29.37	25	0.594	14.40	19	0.424	10.28	2	0.057	1.38	3	0.139	3.37	3	0.063	1.53	5	0.198	4.80	TH
TUR022-SB	137	3.949	45	1.257	31.83	4	0.223	5.65	30	0.946	23.96	21	0.617	15.62	21	0.423	10.71	3	0.139	3.52	3	0.055	1.39	2	0.047	1.19	8	0.242	6.13	TH
TUR022-SC	158	3.921	74	1.836	46.82	1	0.049	1.25	11	0.307	7.83	47	1.170	29.84	23	0.499	12.73	1	0.012	0.31	1	0.048	1.22	0	0.000	0.00	0	0.000	0.00	TH
TUR022-SD	123	3.346	20	0.551	16.47	0	0.000	0.00	36	1.062	31.74	10	0.240	7.17	11	0.248	7.41	6	0.112	3.35	2	0.029	0.87	0	0.000	0.00	38	1.104	6.70	TH
TUR022-SE	110	2.871	36	0.957	33.33	3	0.105	3.66	19	0.432	15.05	34	0.753	26.23	4	0.156	5.43	3	0.089	3.10	6	0.231	8.05	2	0.092	3.20	3	0.056	1.95	TH
TUR022-SF	94	3.154	21	0.671	21.27	0	0.000	0.00	40	1.386	43.94	16	0.586	18.58	8	0.292	9.26	1	0.007	0.22	4	0.094	2.98	1	0.027	0.86	3	0.091	2.89	AB
TUR024-SA	101	3.001	32	0.967	32.22	0	0.000	0.00	19	0.613	20.43	35	0.785	26.16	5	0.113	3.77	1	0.021	0.70	6	0.280	9.33	1	0.180	6.00	2	0.042	1.40	TH

			SS + Cong.			Volcanic			Intrusive			Rounded Qtz			Angular Qtz			Feldspar			Supracrustal			Other/Unknown			Altered			Conducted
Sample ID	**n tot.**	**wt. tot. (g)**	**n**	***wt.***	***wt. %***	***n***	***wt.***	***wt. %***	***n***	***wt.***	***wt. %***	***n***	***wt.***	***wt. %***	***n***	***wt.***	***wt. %***	***n***	***wt.***	***wt. %***	***n***	***wt.***	***wt. %***	***n***	***wt.***	***wt. %***	***n***	***wt.***	**wt. %**	**By:**
TUR025-SA	138	4.094	36	0.984	24.04	3	0.091	2.22	35	1.159	28.31	36	0.817	19.96	12	0.250	6.11	2	0.050	1.22	6	0.382	9.33	5	0.292	7.13	3	0.069	1.69	TH
TUR029-SA	116	3.174	38	1.059	33.36	2	0.090	2.84	27	0.735	23.16	23	0.520	16.38	12	0.330	10.40	0	0.000	0.00	11	0.355	11.18	0	0.000	0.00	3	0.085	2.68	AB
TUR031-SA	125	3.201	45	1.333	41.64	1	0.007	0.22	32	0.770	24.05	23	0.535	16.71	11	0.302	9.43	1	0.024	0.75	2	0.029	0.91	3	0.060	1.87	7	0.141	4.40	TH
TUR031-SB	146	3.652	23	0.588	16.10	0	0.000	0.00	79	2.140	58.60	11	0.187	5.12	10	0.200	5.48	8	0.251	6.87	2	0.033	0.90	0	0.000	0.00	13	0.253	6.93	TH
TUR031-SC	123	3.503	35	0.883	25.21	5	0.173	4.94	46	1.400	39.97	24	0.720	20.55	5	0.090	2.57	0	0.000	0.00	8	0.237	6.77	0	0.000	0.00	0	0.000	0.00	AB
TUR031-SD	92	2.753	14	0.298	10.82	2	0.043	1.56	48	1.673	60.77	10	0.215	7.81	5	0.128	4.65	2	0.063	2.29	8	0.245	8.90	0	0.000	0.00	3	0.088	3.20	AB
TUR031-SF	102	2.877	15	0.428	14.88	1	0.019	0.66	33	1.126	39.14	13	0.251	8.72	7	0.121	4.21	5	0.116	4.03	7	0.238	8.27	0	0.000	0.00	21	0.578	20.09	TH
TUR032-SA	122	3.209	37	1.005	31.32	1	0.038	1.18	39	1.046	32.60	26	0.643	20.04	3	0.106	3.30	2	0.028	0.87	3	0.132	4.11	1	0.027	0.84	10	0.184	5.73	TH
TUR032-SB	111	3.369	44	1.333	39.57	2	0.069	2.05	15	0.499	14.81	41	1.216	36.09	7	0.209	6.20	2	0.043	1.28	0	0.000	0.00	0	0.000	0.00	0	0.000	0.00	TH
TUR032-SC	92	3.318	20	0.743	22.39	2	0.116	3.50	36	1.341	40.42	18	0.468	14.10	2	0.092	2.77	4	0.124	3.74	5	0.164	4.94	2	0.112	3.38	3	0.158	4.76	TH
TUR034-SA	118	3.257	32	0.835	25.64	4	0.096	2.95	30	1.106	33.96	25	0.573	17.59	11	0.235	7.22	2	0.021	0.64	9	0.253	7.77	1	0.014	0.43	4	0.124	3.81	AB
TUR034-SB	128	3.615	28	0.691	19.11	2	0.126	3.49	48	1.381	38.20	23	0.624	17.26	9	0.219	6.06	2	0.110	3.04	11	0.295	8.16	1	0.046	1.27	4	0.123	3.40	AB
TUR034-SD	119	3.434	38	0.917	26.70	1	0.096	2.80	39	1.290	37.57	19	0.484	14.09	2	0.050	1.46	3	0.080	2.33	9	0.382	11.12	0	0.000	0.00	8	0.135	3.93	TH
TUR035-SA	112	3.219	28	0.995	30.91	2	0.026	0.81	41	1.230	38.21	9	0.207	6.43	18	0.429	13.33	0	0.000	0.00	8	0.203	6.31	0	0.000	0.00	6	0.129	4.01	AB
TUR035-SB	103	2.953	20	0.606	20.52	1	0.009	0.30	40	1.340	45.38	21	0.556	18.83	6	0.113	3.83	2	0.033	1.12	8	0.201	6.81	2	0.057	1.93	3	0.038	1.29	AB
TUR036-SA	115	3.267	31	0.994	30.43	3	0.108	3.31	26	0.811	24.82	24	0.541	16.56	20	0.463	14.17	0	0.000	0.00	5	0.181	5.54	1	0.021	0.64	5	0.148	4.53	AB
TUR038-SA	121	3.284	30	0.986	30.02	0	0.000	0.00	45	1.071	32.61	32	0.813	24.76	4	0.134	4.08	0	0.000	0.00	5	0.190	5.79	0	0.000	0.00	5	0.090	2.74	TH
TUR039-SA	104	2.652	3	0.077	2.90	0	0.000	0.00	14	0.359	13.54	1	0.016	0.60	13	0.281	10.60	1	0.013	0.49	1	0.019	0.72	2	0.027	1.02	69	1.860	70.14	AB
TUR039-SB	109	3.235	22	0.589	18.21	3	0.064	1.98	25	0.941	29.09	22	0.574	17.74	13	0.348	10.76	4	0.068	2.10	10	0.428	13.23	0	0.000	0.00	10	0.223	6.89	AB
TUR039-SC	106	3.049	28	0.883	28.96	1	0.021	0.69	23	0.790	25.91	34	0.789	25.88	6	0.172	5.64	1	0.045	1.48	8	0.258	8.46	4	0.081	2.66	1	0.010	0.33	TH
TUR040-SA	114	3.239	31	0.806	24.88	2	0.038	1.17	30	0.765	23.62	30	0.880	27.17	9	0.261	8.06	1	0.063	1.95	6	0.186	5.74	1	0.033	1.02	4	0.207	6.39	TH
TUR041-SA	120	3.548	35	1.033	29.11	6	0.158	4.45	30	1.090	30.72	27	0.659	18.57	12	0.270	7.61	2	0.076	2.14	3	0.077	2.17	1	0.049	1.38	4	0.136	3.83	AB
TUR041-SB	132	3.859	62	1.833	47.50	3	0.086	2.23	15	0.429	11.12	33	0.940	24.36	12	0.220	5.70	1	0.032	0.83	5	0.289	7.49	0	0.000	0.00	1	0.030	0.78	TH
TUR042-SA	130	3.692	41	1.273	34.48	3	0.060	1.63	31	0.941	25.49	24	0.694	18.80	14	0.262	7.10	4	0.088	2.38	3	0.138	3.74	0	0.000	0.00	10	0.236	0.68	TH
TUR042-SB	125	3.680	35	1.105	30.03	1	0.013	0.35	38	1.256	34.13	24	0.607	16.49	18	0.471	12.80	2	0.039	1.06	0	0.000	0.00	0	0.000	0.00	7	0.189	0.63	TH
TUR042-SC	140	3.859	61	1.859	48.17	0	0.000	0.00	22	0.503	13.03	27	0.705	18.27	19	0.395	10.24	3	0.112	2.90	0	0.000	0.00	1	0.051	1.32	7	0.234	0.49	TH
TUR042-SD	116	3.462	57	1.613	46.59	2	0.066	1.91	11	0.417	12.05	27	0.778	22.47	15	0.510	14.73	0	0.000	0.00	3	0.062	1.79	0	0.000	0.00	1	0.016	0.46	TH
TUR043-SA	148	3.927	50	1.222	31.12	4	0.084	2.14	26	0.755	19.23	37	1.091	27.78	17	0.417	10.62	3	0.078	1.99	8	0.245	6.24	2	0.025	0.64	1	0.010	0.25	AB
TUR043-SB	110	3.306	26	0.880	26.62	1	0.015	0.45	36	0.991	29.98	17	0.487	14.73	7	0.175	5.29	0	0.000	0.00	9	0.375	11.34	0	0.000	0.00	14	0.383	11.58	AB
TUR044-SA	135	3.856	35	0.996	25.83	4	0.100	2.59	44	1.338	34.70	21	0.530	13.74	17	0.399	10.35	0	0.000	0.00	9	0.360	9.34	1	0.017	0.44	4	0.116	3.01	AB
TUR044-SB	110	3.239	21	0.552	17.04	0	0.000	0.00	41	1.364	42.11	21	0.515	15.90	10	0.280	8.64	2	0.035	1.08	5	0.126	3.89	0	0.000	0.00	10	0.367	11.33	TH
TUR045B-SA	133	3.562	22	0.516	14.49	0	0.000	0.00	57	1.695	47.59	25	0.643	18.05	7	0.171	4.80	9	0.179	5.03	8	0.209	5.87	2	0.057	1.60	3	0.092	2.58	TH
TUR045B-SB	123	3.747	61	2.008	53.59	2	0.020	0.53	11	0.304	8.11	28	0.762	20.34	17	0.436	11.64	1	0.014	0.37	3	0.203	5.42	0	0.000	0.00	0	0.000	0.00	AB
TUR045B-SC	99	3.251	34	1.082	33.28	0	0.000	0.00	34	1.062	32.67	8	0.251	7.72	12	0.359	11.04	0	0.000	0.00	2	0.129	3.97	0	0.000	0.00	9	0.368	11.32	TH
TUR046-SA	120	3.261	50	1.429	43.82	0	0.000	0.00	18	0.516	15.82	17	0.354	10.86	9	0.195	5.98	1	0.012	0.37	14	0.406	12.45	2	0.102	3.13	9	0.247	7.57	AB
TUR046-SB	132	3.817	46	1.208	31.65	1	0.013	0.34	37	1.289	33.77	19	0.490	12.84	17	0.467	12.23	0	0.000	0.00	9	0.273	7.15	1	0.037	0.97	2	0.040	1.05	AB
TUR046-SC	127	3.516	41	1.206	34.30	2	0.082	2.33	30	0.933	26.54	37	0.801	22.78	10	0.286	8.13	4	0.116	3.30	1	0.058	1.65	0	0.000	0.00	2	0.034	0.97	TH
TUR047-SA	120	3.560	27	0.718	20.17	6	0.180	5.06	39	1.176	33.03	23	0.597	16.77	12	0.481	13.51	1	0.036	1.01	8	0.214	6.01	1	0.079	2.22	3	0.079	2.22	AB
TUR047-SB	119	3.153	47	1.236	39.20	2	0.038	1.21	22	0.591	18.74	27	0.656	20.81	8	0.300	9.51	1	0.025	0.79	4	0.132	4.19	2	0.037	1.17	6	0.138	4.38	TH
TUR048-SA	125	3.631	43	1.301	35.83	0	0.000	0.00	29	0.815	22.45	34	0.843	23.22	5	0.204	5.62	2	0.058	1.60	3	0.104	2.86	3	0.157	4.32	6	0.149	4.10	TH
TUR048-SB	106	3.255	47	1.477	45.38	1	0.013	0.40	15	0.541	16.62	24	0.657	20.18	14	0.445	13.67	1	0.035	1.08	2	0.044	1.35	0	0.000	0.00	2	0.043	1.32	AB
TUR048-SC	137	3.597	49	1.277	35.50	1	0.083	2.31	19	0.504	14.01	49	1.127	31.33	14	0.391	10.87	0	0.000	0.00	3	0.145	4.03	0	0.000	0.00	2	0.070	1.95	TH
TUR049-SA	121	3.394	30	0.705	20.77	2	0.040	1.18	40	1.295	38.16	22	0.554	16.32	5	0.138	4.07	2	0.026	0.77	9	0.252	7.42	2	0.039	1.15	9	0.345	10.16	TH
TUR049-SB	135	3.304	7	0.155	4.69	0	0.000	0.00	64	1.738	52.60	5	0.076	2.30	5	0.160	4.84	3	0.053	1.60	3	0.083	2.51	3	0.147	4.45	45	0.892	27.00	TH

			SS + Cong.			Volcanic			Intrusive			Rounded Qtz			Angular Qtz			Feldspar			Supracrustal			Other/Unknown			Altered			Conducted
Sample ID	**n tot.**	**wt. tot. (g)**	**n**	***wt.***	***wt. %***	***n***	***wt.***	***wt. %***	***n***	***wt.***	***wt. %***	***n***	***wt.***	***wt. %***	***n***	***wt.***	***wt. %***	***n***	***wt.***	***wt. %***	***n***	***wt.***	***wt. %***	***n***	***wt.***	***wt. %***	***n***	***wt.***	**wt. %**	**By:**
TUR049-SC	105	3.842	19	0.565	14.71	3	0.130	3.38	48	1.920	49.97	8	0.180	4.69	7	0.229	5.96	1	0.051	1.33	6	0.258	6.72	3	0.110	2.86	10	0.399	10.39	TH
TUR050-SA	124	3.548	37	0.867	24.44	7	0.290	8.17	30	0.924	26.04	27	0.721	20.32	12	0.304	8.57	1	0.026	0.73	4	0.170	4.79	0	0.000	0.00	6	0.246	6.93	TH
TUR050-SB	142	3.896	19	0.520	13.35	2	0.093	2.39	65	1.842	47.28	16	0.319	8.19	10	0.263	6.75	7	0.256	6.57	4	0.133	3.41	0	0.000	0.00	19	0.470	12.06	TH
TUR050-SC	125	3.511	30	0.759	21.62	2	0.037	1.05	43	1.422	40.50	26	0.619	17.63	8	0.267	7.60	1	0.017	0.48	5	0.123	3.50	4	0.132	3.76	6	0.135	3.85	TH
TUR051-SA	136	3.428	41	0.895	26.11	2	0.085	2.48	30	0.810	23.63	36	0.795	23.19	15	0.408	11.90	1	0.011	0.32	8	0.271	7.91	1	0.027	0.79	2	0.126	3.68	AB
TUR051-SB	111	3.507	22	0.573	16.34	1	0.013	0.37	46	1.742	49.67	20	0.457	13.03	10	0.330	9.41	3	0.079	2.25	1	0.043	1.23	2	0.038	1.08	6	0.232	6.62	TH
TUR052-SA	129	3.681	50	1.538	41.78	2	0.044	1.20	23	0.444	12.06	22	0.581	15.78	8	0.234	6.36	3	0.079	2.15	12	0.386	10.49	0	0.000	0.00	9	0.375	10.19	AB
TUR052-SB	129	3.886	26	0.641	16.50	1	0.067	1.72	49	1.478	38.03	25	0.800	20.59	10	0.250	6.43	4	0.082	2.11	12	0.433	11.14	2	0.135	3.47	0	0.000	0.00	AB
TUR053-SA	122	3.511	25	0.744	21.19	3	0.060	1.71	48	1.442	41.07	23	0.543	15.47	7	0.178	5.07	1	0.017	0.48	4	0.242	6.89	1	0.078	2.22	10	0.207	5.90	TH
TUR053-SB	134	3.535	40	1.030	29.14	4	0.098	2.77	43	1.205	34.09	21	0.483	13.66	11	0.225	6.36	2	0.033	0.93	4	0.091	2.57	2	0.093	2.63	7	0.277	7.84	TH
TUR053-SC	111	3.262	2	0.028	0.86	0	0.000	0.00	64	2.040	62.54	7	0.215	6.59	3	0.044	1.35	12	0.266	8.15	5	0.144	4.41	0	0.000	0.00	18	0.525	16.09	TH
TUR054-SA	115	3.070	44	1.072	34.92	1	0.025	0.81	20	0.567	18.47	24	0.762	24.82	12	0.258	8.40	1	0.063	2.05	6	0.179	5.83	2	0.035	1.14	5	0.109	3.55	TH
TUR054-SB	101	3.004	38	1.319	43.91	1	0.152	5.06	12	0.240	7.99	36	0.970	32.29	10	0.261	8.69	0	0.000	0.00	1	0.014	0.47	0	0.000	0.00	3	0.048	1.60	TH
TUR054-SE	117	3.427	50	1.466	42.78	0	0.000	0.00	15	0.459	13.39	29	0.734	21.42	13	0.454	13.25	0	0.000	0.00	4	0.146	4.26	0	0.000	0.00	6	0.168	4.90	TH
TUR055-SA	117	3.340	43	1.304	39.04	0	0.000	0.00	32	0.849	25.42	19	0.531	15.90	10	0.230	6.89	1	0.012	0.36	7	0.166	4.97	1	0.108	3.23	4	0.140	4.19	AB
TUR056-SA	127	3.501	39	0.920	26.28	3	0.041	1.17	32	1.020	29.13	23	0.491	14.02	9	0.260	7.43	1	0.021	0.60	9	0.322	9.20	0	0.000	0.00	11	0.426	12.17	AB
TUR056-SB	128	3.846	43	1.225	31.85	3	0.075	1.95	35	1.484	38.59	31	0.634	16.48	6	0.128	3.33	0	0.000	0.00	8	0.231	6.01	0	0.000	0.00	2	0.069	1.79	AB
TUR057-SA	127	3.746	34	1.223	32.65	1	0.017	0.45	43	1.389	37.08	20	0.466	12.44	16	0.370	9.88	3	0.041	1.09	5	0.147	3.92	1	0.011	0.29	4	0.082	2.19	TH
TUR057-SB	158	4.428	45	1.311	29.61	2	0.046	1.04	47	1.500	33.88	24	0.612	13.82	22	0.501	11.31	4	0.092	2.08	8	0.197	4.45	1	0.062	1.40	5	0.107	2.42	TH
TUR057-SC	129	3.744	33	0.874	23.34	7	0.291	7.77	49	1.486	39.69	26	0.649	17.33	2	0.030	0.80	1	0.055	1.47	7	0.214	5.72	0	0.000	0.00	4	0.145	3.87	TH
TUR057-SE	166	4.629	12	0.261	5.64	1	0.054	1.17	81	2.588	55.91	11	0.231	4.99	14	0.340	7.34	18	0.487	10.52	6	0.159	3.43	2	0.098	2.12	21	0.411	8.88	TH
TUR057-SF	120	3.753	33	1.096	29.20	2	0.059	1.57	34	1.122	29.90	32	0.759	20.22	5	0.172	4.58	0	0.000	0.00	4	0.100	2.66	3	0.172	4.58	7	0.273	7.27	TH
TUR057-SG	152	4.011	47	1.116	27.82	4	0.090	2.24	42	1.232	30.72	34	1.051	26.20	12	0.228	5.68	1	0.018	0.45	8	0.170	4.24	0	0.000	0.00	4	0.106	2.64	AB
TUR057-SH	121	3.313	28	0.677	20.43	4	0.150	4.53	32	1.013	30.58	24	0.680	20.53	18	0.407	12.28	2	0.052	1.57	6	0.191	5.77	0	0.000	0.00	7	0.143	4.32	AB
TUR057-SI	134	3.749	39	1.234	32.92	4	0.153	4.08	45	1.300	34.68	32	0.797	21.26	5	0.095	2.53	0	0.000	0.00	6	0.115	3.07	3	0.055	1.47	0	0.000	0.00	AB
TUR057-SI	109	3.667	30	1.099	29.97	5	0.249	6.79	32	1.073	29.26	19	0.432	11.78	12	0.247	6.74	0	0.000	0.00	5	0.297	8.10	2	0.166	4.53	4	0.104	2.84	AB
TUR057-SJ	114	3.193	23	0.774	24.24	1	0.013	0.41	40	1.190	37.27	23	0.518	16.22	14	0.332	10.40	2	0.048	1.50	3	0.049	1.53	2	0.079	2.47	6	0.190	5.95	TH
TUR057-SK	102	2.831	26	0.825	29.14	1	0.020	0.71	32	0.911	32.18	24	0.557	19.68	7	0.138	4.87	0	0.000	0.00	7	0.193	6.82	1	0.017	0.60	4	0.170	6.00	AB
TUR058-SA	118	3.410	26	0.709	20.79	1	0.045	1.32	42	1.237	36.28	17	0.466	13.67	11	0.245	7.18	1	0.040	1.17	8	0.299	8.77	3	0.088	2.58	9	0.281	8.24	TH
TUR058-SC	104	3.125	42	1.069	34.21	4	0.152	4.86	19	0.730	23.36	13	0.252	8.06	10	0.316	10.11	2	0.042	1.34	5	0.220	7.04	1	0.014	0.45	8	0.330	10.56	AB
TUR059-SA	119	3.456	24	0.626	18.11	4	0.164	4.75	43	1.154	33.39	23	0.667	19.30	9	0.311	9.00	2	0.106	3.07	8	0.250	7.23	0	0.000	0.00	6	0.178	5.15	TH
TUR059-SB	100	3.464	13	0.510	14.72	4	0.151	4.36	47	1.715	49.51	9	0.202	5.83	9	0.206	5.95	1	0.037	1.07	9	0.327	9.44	4	0.185	5.34	4	0.131	3.78	TH
TUR060-SA	102	2.903	26	0.870	29.97	2	0.077	2.65	37	1.053	36.27	16	0.362	12.47	13	0.248	8.54	1	0.029	1.00	3	0.098	3.38	0	0.000	0.00	4	0.166	5.72	TH
TUR060-SB	148	4.078	56	1.578	38.70	2	0.040	0.98	34	0.964	23.64	21	0.475	11.65	19	0.576	14.12	3	0.073	1.79	5	0.143	3.51	1	0.032	0.78	7	0.197	4.83	TH
TUR060-SD	146	4.051	27	0.827	20.41	1	0.015	0.37	67	1.849	45.64	9	0.210	5.18	15	0.414	10.22	4	0.114	2.81	5	0.097	2.39	2	0.060	1.48	16	0.465	11.48	TH
TUR060-SE	84	2.469	23	0.633	25.64	1	0.022	0.89	31	0.901	36.49	6	0.186	7.53	11	0.372	15.07	1	0.016	0.65	5	0.207	8.38	2	0.030	1.22	4	0.102	4.13	TH
TUR060-SF	97	3.203	44	1.377	42.99	0	0.000	0.00	24	0.867	27.07	11	0.272	8.49	13	0.525	16.39	1	0.053	1.65	4	0.109	3.40	0	0.000	0.00	0	0.000	0.00	TH
TUR061-SA	133	3.126	35	0.750	23.99	0	0.000	0.00	29	0.697	22.30	47	1.034	33.08	11	0.310	9.92	0	0.000	0.00	7	0.256	8.19	2	0.040	1.28	2	0.039	1.25	TH
TUR061-SB	126	3.040	27	0.638	20.99	1	0.012	0.39	33	0.997	32.80	36	0.739	24.31	13	0.251	8.26	0	0.000	0.00	10	0.277	9.11	3	0.068	2.24	3	0.058	1.91	TH

4-8 mm Till Lithology Clast Counts

			Thelon Fm.			Pitz Fm.			Undiff. Sed.			Intrusives			Undiff. Volc.			Metased/Volc			Quartzite			Altered Clasts			Other		
Sample ID	**n tot.**	**wt. tot. (g)**	**n**	***wt.***	***wt. %***	***n***	***wt.***	***wt. %***	***n***	***wt.***	***wt. %***	***n***	***wt.***	***wt. %***	***n***	***wt.***	***wt. %***	***n***	***wt.***	***wt. %***	***n***	***wt.***	***wt. %***	***n***	***wt.***	***wt. %***	***n***	***wt.***	***wt. %***
Surficial Samples																													
12-TH-S147	123	29.68	7	1.25	4.21	3	0.40	1.35	1	0.29	0.98	96	24.86	83.76	6	1.04	3.50	0	0.00	0.00	3	0.45	1.52	6	0.92	3.10	1	0.47	1.58
12-TH-S116	98	23.59	5	1.11	4.71	4	1.01	4.28	5	1.35	5.72	70	15.78	66.89	6	1.56	6.61	1	0.21	0.89	2	0.75	3.18	3	1.31	5.55	2	0.51	2.16
12-MR-S060	131	29.55	13	2.47	8.36	1	0.11	0.37	2	0.38	1.29	91	20.52	69.44	5	1.67	5.65	5	0.76	2.57	6	1.41	4.77	0	0.00	0.00	8	2.23	7.55
12-MR-S079	111	26.37	10	1.86	7.05	5	0.87	3.30	0	0.00	0.00	81	20.26	76.83	1	0.13	0.49	6	1.47	5.57	2	0.54	2.05	6	1.24	4.70	0	0.00	0.00
12-TH-S172	123	29.72	14	3.58	12.05	10	2.72	9.15	6	1.20	4.04	71	17.26	58.08	9	1.90	6.39	2	1.04	3.50	7	1.11	3.73	0	0.00	0.00	4	0.91	3.06
12-TH-S134	140	29.92	13	2.95	9.86	9	1.86	6.22	10	2.16	7.22	84	18.18	60.76	6	0.87	2.91	9	1.58	5.28	8	2.15	7.19	0	0.00	0.00	1	0.17	0.57
12-TH-S142	180	33.78	40	8.27	24.48	12	1.94	5.74	10	2.40	7.10	89	15.42	45.65	10	1.89	5.60	6	1.11	3.29	10	2.30	6.81	0	0.00	0.00	3	0.45	1.33
12-TH-S169	227	44.88	31	5.99	13.35	11	1.57	3.50	19	3.24	7.22	126	25.81	57.51	16	3.63	8.09	9	1.74	3.88	12	2.41	5.37	0	0.00	0.00	3	0.49	1.09
12-TH-S165	130	31.81	19	3.80	11.95	4	0.87	2.73	7	1.30	4.09	80	21.44	67.40	11	2.60	8.17	4	0.93	2.92	3	0.48	1.51	0	0.00	0.00	2	0.39	1.23
12-TH-S124	179	46.77	50	11.10	23.73	16	5.41	11.57	11	3.44	7.36	74	18.89	40.39	12	2.77	5.92	9	3.14	6.71	5	1.32	2.82	0	0.00	0.00	2	0.70	1.50
12-MR-S010	133	31.35	14	3.76	11.99	4	0.46	1.47	4	0.71	2.26	85	20.99	66.95	8	1.44	4.59	7	2.27	7.24	11	1.72	5.49	0	0.00	0.00	0	0.00	0.00
12-TH-S178	176	38.47	79	15.34	39.88	9	2.48	6.45	28	6.64	17.26	33	7.36	19.13	14	3.07	7.98	0	0.00	0.00	5	1.48	3.85	2	0.52	1.35	6	1.58	4.11
12-TH-S191	106	29.54	12	2.74	9.28	4	1.06	3.59	7	1.91	6.47	58	17.85	60.43	7	1.34	4.54	5	1.18	3.99	4	1.01	3.42	7	2.45	8.29	2	0.00	0.00
12-TH-S120	173	46.70	10	2.34	5.01	15	3.61	7.73	8	2.86	6.12	116	30.22	64.71	11	3.95	8.46	1	0.10	0.21	3	1.13	2.42	6	1.64	3.51	3	0.85	1.82
12-TH-S113	106	23.62	8	1.88	7.96	5	1.33	5.63	5	0.57	2.41	69	14.80	62.66	3	0.47	1.99	6	1.63	6.90	5	1.34	5.67	1	0.12	0.51	4	1.48	6.27
12-MR-S049	89	24.46	4	1.03	4.21	2	0.37	1.51	1	0.44	1.80	66	17.69	72.32	4	0.96	3.92	3	0.43	1.76	3	1.27	5.19	4	0.93	3.80	2	1.34	5.48
13-AB-246	93	21.58	13	2.33	10.80	2	0.71	3.29	2	0.76	3.52	61	14.38	66.64	3	0.87	4.03	0	0.00	0.00	7	1.68	7.78	5	0.85	3.94	0	0.00	0.00
13-AB-219	118	32.15	4	0.83	2.58	1	0.18	0.57	6	1.72	5.35	96	26.20	81.49	5	1.64	5.10	4	1.28	3.98	2	0.30	0.93	0	0.00	0.00	0	0.00	0.00
12-TH-S120	173	46.70	10	2.34	5.01	15	3.61	7.73	8	2.86	6.12	116	30.22	64.71	11	3.95	8.46	1	0.10	0.21	3	1.13	2.42	6	1.64	3.51	3	0.85	1.82
Drillhole Samples																													
Ayra Study																													
AYA002-SA	32	6.80	23	4.86	71.47	1	0.18	2.65	1	0.14	2.06	4	0.87	12.79	3	0.75	11.03	0	0.00	0.00	0	0.00	0.00	0	0.00	0.00	0	0.00	0.00
AYA001-SB	40	9.84	27	6.17	62.70	1	0.29	2.95	3	1.53	15.55	6	1.46	14.84	2	0.38	3.86	0	0.00	0.00	1	0.01	0.10	0	0.00	0.00	0	0.00	0.00
AYA001-SA	37	11.22	18	5.13	45.72	2	0.34	3.03	2	0.39	3.48	8	2.68	23.88	1	0.16	1.43	1	1.11	9.89	1	0.01	0.08	1	0.01	0.11	3	1.39	12.39
AYA003-SA	124	31.95	51	13.10	40.99	6	1.85	5.79	10	1.76	5.50	31	9.22	28.87	6	0.94	2.94	2	0.37	1.16	2	0.33	1.05	11	2.77	8.67	5	1.61	5.04
AYA003-SB	85	18.20	50	10.14	55.71	2	0.22	1.21	6	1.53	8.41	9	2.64	14.51	7	1.68	9.23	1	0.11	0.60	1	0.22	1.21	8	1.52	8.35	1	0.14	0.77
AYA004-SA	56	13.18	24	6.19	46.97	3	0.96	7.28	4	1.11	8.42	15	2.65	20.11	2	0.28	2.12	1	0.51	3.87	4	1.10	8.35	3	0.38	2.88	0	0.00	0.00
AYA009-SA	40	9.95	20	5.19	52.16	3	0.81	8.14	2	0.37	3.72	7	1.76	17.69	1	0.21	2.11	1	0.10	1.01	2	0.37	3.72	2	0.35	3.52	2	0.79	7.94
ABR012-SD	47	12.55	28	8.02	63.90	1	0.82	6.53	6	1.22	9.72	9	2.11	16.81	1	0.13	1.04	0	0.00	0.00	0	0.00	0.00	2	0.25	1.99	0	0.00	0.00
ABR011-SA	76	21.64	23	7.00	32.35	2	0.34	1.57	9	2.36	10.91	24	6.34	29.30	5	1.83	8.46	0	0.00	0.00	4	1.41	6.52	6	1.74	8.04	3	0.62	2.87
AYA010-SA	41	11.15	23	5.45	48.88	3	0.62	5.56	0	0.00	0.00	8	2.69	24.13	3	0.97	8.70	1	0.70	6.28	1	0.36	3.23	2	0.36	3.23	0	0.00	0.00
AYA003-SC	149	42.52	20	4.44	10.44	0	0.00	0.00	4	1.37	3.22	106	30.94	72.76	1	0.11	0.26	4	1.57	3.70	5	1.75	4.12	4	1.20	2.82	5	1.14	2.68
AYA006-SB	58	14.43	5	1.27	8.80	1	0.47	3.26	2	0.67	4.64	47	11.43	79.21	0	0.00	0.00	0	0.00	0.00	0	0.00	0.00	0	0.00	0.00	3	0.59	4.09
ABR012-SA	74	20.27	7	1.42	7.01	0	0.00	0.00	1	1.05	5.18	57	15.18	74.89	0	0.00	0.00	2	0.35	1.73	2	1.24	6.12	3	0.62	3.06	2	0.41	2.02

			Thelon Fm.			Pitz Fm.			Undiff. Sed.			Intrusives			Undiff. Volc.			Metased/Volc			Quartzite			Altered Clasts			Other		
Sample ID	**n tot.**	**wt. tot. (g)**	**n**	***wt.***	***wt. %***	***n***	***wt.***	***wt. %***	***n***	***wt.***	***wt. %***	***n***	***wt.***	***wt. %***	***n***	***wt.***	***wt. %***	***n***	***wt.***	***wt. %***	***n***	***wt.***	***wt. %***	***n***	***wt.***	***wt. %***	***n***	***wt.***	***wt. %***
ABR011-SB	48	11.05	5	0.80	7.24	3	0.47	4.25	2	1.17	10.59	29	6.58	59.55	4	0.87	7.87	1	0.28	2.53	0	0.00	0.00	2	0.51	4.62	2	0.37	3.35
AYA010-SB	23	4.61	3	0.36	7.81	1	0.14	3.04	0	0.00	0.00	13	2.33	50.54	3	1.26	27.33	2	0.32	6.94	0	0.00	0.00	0	0.00	0.00	1	0.20	4.34
AYA010-SC	46	11.59	0	0.00	0.00	5	1.25	10.79	2	0.43	3.71	27	7.39	63.76	10	2.15	18.55	1	0.15	1.29	0	0.00	0.00	1	0.22	1.90	0	0.00	0.00
AYA004-SB	88	21.68	14	2.61	12.04	2	0.49	2.26	1	0.71	3.27	58	14.96	69.00	4	0.76	3.51	0	0.00	0.00	4	1.26	5.81	5	0.89	4.11	0	0.00	0.00
AYA009-SB	51	12.11	2	0.39	3.22	2	0.27	2.23	0	0.00	0.00	35	8.75	72.25	3	0.41	3.39	1	0.13	1.07	1	0.12	0.99	5	1.75	14.45	2	0.29	2.39
AYA009-SC	56	11.39	11	2.19	19.23	0	0.00	0.00	0	0.00	0.00	35	7.21	63.30	0	0.00	0.00	0	0.00	0.00	1	0.16	1.40	6	1.22	10.71	3	0.61	5.36
AYA009-SD	92	20.19	8	1.60	7.91	0	0.00	0.00	0	0.00	0.00	73	16.62	82.33	0	0.00	0.00	5	0.88	4.36	2	0.32	1.59	3	0.63	3.12	1	0.14	0.69
AYA005-SA	52	12.97	7	1.34	10.33	2	0.52	4.01	3	0.41	3.16	33	9.30	71.70	0	0.00	0.00	4	0.63	4.86	1	0.10	0.77	0	0.00	0.00	2	0.67	5.17
AYA006-SA	43	9.42	2	0.31	3.29	3	0.79	8.39	0	0.00	0.00	32	6.73	71.44	2	0.87	9.24	1	0.13	1.38	1	0.12	1.27	2	0.47	4.99	0	0.00	0.00
AYA003-SD	133	35.36	31	8.67	24.52	0	0.00	0.00	3	0.81	2.29	84	21.39	60.50	0	0.00	0.00	0	0.00	0.00	6	1.35	3.82	4	2.32	6.57	5	0.81	2.30
ABR012-SB	83	18.20	31	6.66	36.58	0	0.00	0.00	1	0.36	1.98	42	9.13	50.17	0	0.00	0.00	3	0.58	3.19	1	0.20	1.09	1	0.10	0.56	4	1.17	6.43
ABR012-SE	131	34.50	25	6.93	20.09	0	0.00	0.00	0	0.00	0.00	97	24.99	72.43	1	0.09	0.26	1	0.92	2.67	0	0.00	0.00	6	0.93	2.70	1	0.64	1.86
AYA004-SC	61	14.61	23	4.79	32.79	0	0.00	0.00	4	1.11	7.60	31	8.15	55.78	0	0.00	0.00	0	0.00	0.00	2	0.43	2.94	1	0.13	0.89	0	0.00	0.00
Tatiggaq Study																													
TUR060-SA	47	12.44	15	3.03	24.36	1	0.13	1.05	4	0.98	7.88	18	5.47	43.97	3	1.53	12.30	1	0.19	1.53	1	0.15	1.21	2	0.49	3.94	2	0.47	3.78
TUR060-SB	66	16.25	28	6.66	40.99	2	0.37	2.28	4	1.30	8.00	20	5.03	30.95	2	0.34	2.09	1	0.31	1.91	0	0.00	0.00	7	1.78	10.95	2	0.46	2.83
TUR060-SD	100	24.53	34	6.71	27.37	1	0.26	1.06	2	0.32	1.30	45	12.8	51.98	3	0.91	3.71	2	0.95	3.87	3	0.6	2.45	5	0.06	0.24	5	1.43	5.83
TUR060-SF	58	14.75	41	10.01	67.86	0	0.00	0.00	2	0.90	6.10	8	2.16	14.64	1	0.13	0.88	4	1.26	8.54	0	0.00	0.00	2	0.29	1.97	0	0.00	0.00
TUR053-SA	68	16.75	18	3.43	20.48	1	0.13	0.78	4	0.51	3.04	30	7.99	47.70	4	1.13	6.75	6	2.44	14.57	0	0.00	0.00	4	1.00	5.97	1	0.12	0.72
TUR053-SB	64	15.45	13	2.42	15.66	2	0.40	2.59	2	0.43	2.78	24	6.16	39.87	3	0.72	4.66	4	1.06	6.86	3	0.70	4.53	11	2.50	16.18	2	1.06	6.86
TUR053-SC	107	27.72	8	1.67	6.02	0	0.00	0.00	1	0.14	0.51	41	10.34	37.30	0	0.00	0.00	5	2.16	7.79	1	0.81	2.92	42	10.26	37.01	9	2.34	8.44
TUR042-SA	50	11.38	14	2.90	25.48	0	0.00	0.00	5	1.56	13.71	22	5.27	46.31	0	0.00	0.00	0	0.00	0.00	2	0.59	5.18	5	0.77	6.77	2	0.29	2.55
TUR042-SB	65	19.38	26	9.01	46.49	0	0.00	0.00	2	0.29	1.50	25	6.66	34.37	1	0.31	1.60	1	0.56	2.89	6	1.44	7.43	4	1.11	5.73	0	0.00	0.00
TUR042-SC	79	17.93	55	12.92	72.06	0	0.00	0.00	1	0.35	1.95	13	2.47	13.78	0	0.00	0.00	0	0.00	0.00	2	0.47	2.62	7	1.56	8.70	1	0.16	0.89
TUR042-SD	78	16.66	61	12.85	77.13	0	0.00	0.00	0	0.00	0.00	10	2.43	14.59	2	0.70	4.20	0	0.00	0.00	2	0.32	1.92	3	0.36	2.16	0	0.00	0.00
TUR059-SA	82	17.79	18	3.69	20.74	1	0.19	1.07	8	1.21	6.80	39	8.76	49.24	0	0.00	0.00	3	0.68	3.82	5	1.71	9.61	5	0.94	5.28	3	0.61	3.43
TUR057-SA	69	14.61	28	5.83	39.92	0	0.00	0.00	3	0.54	3.70	24	5.68	38.89	3	0.30	2.02	2	0.36	2.46	1	0.12	0.82	8	1.78	12.19	0	0.00	0.00
TUR057-SB	67	15.03	24	6.84	45.52	0	0.00	0.00	2	0.29	1.93	25	4.63	30.79	3	0.31	2.04	2	0.50	3.35	3	1.03	6.84	8	1.43	9.54	0	0.00	0.00
TUR057-SC	49	11.49	19	5.17	45.00	0	0.00	0.00	2	0.50	4.35	20	4.14	36.02	2	0.28	2.44	1	0.55	4.79	1	0.30	2.61	4	0.55	4.79	0	0.00	0.00
TUR057-SF	49	11.69	21	4.70	40.21	0	0.00	0.00	4	1.58	13.52	16	3.38	28.91	0	0.00	0.00	1	0.24	2.05	0	0.00	0.00	7	1.79	15.31	0	0.00	0.00
TUR057-SG	52	11.51	23	5.00	43.44	0	0.00	0.00	2	0.64	5.56	22	4.82	41.88	1	0.33	2.87	1	0.12	1.04	1	0.28	2.43	2	0.32	2.78	0	0.00	0.00
TUR057-SI	71	18.77	31	8.65	46.08	1	0.16	0.85	5	1.76	9.38	28	6.44	34.31	0	0.00	0.00	0	0.00	0.00	2	1.00	5.33	4	0.76	4.05	0	0.00	0.00
TUR057-SJ	60	14.80	17	3.20	21.62	0	0.00	0.00	1	0.10	0.68	32	8.07	54.53	3	0.89	6.01	1	0.65	4.39	1	0.17	1.15	4	1.63	11.01	1	0.09	0.61
TUR057-SK	21	5.07	8	1.90	37.44	0	0.00	0.00	1	0.31	6.12	10	2.37	46.77	1	0.12	2.37	0	0.00	0.00	0	0.00	0.00	1	0.37	7.30	0	0.00	0.00
TUR049-SA	62	15.82	13	4.22	26.68	1	0.18	1.14	5	1.61	10.18	30	6.48	40.96	0	0.00	0.00	1	0.20	1.26	0	0.00	0.00	11	2.49	15.74	1	0.64	4.05
TUR049-SC	73	17.35	10	2.26	13.03	2	0.71	4.09	2	0.55	3.17	41	9.70	55.91	1	0.21	1.21	4	1.02	5.88	2	0.36	2.07	11	2.54	14.64	0	0.00	0.00
TUR022-SA	54	12.34	24	5.44	44.08	0	0.00	0.00	3	0.62	5.02	20	4.86	39.38	0	0.00	0.00	0	0.00	0.00	0	0.00	0.00	6	1.11	9.00	1	0.31	2.51

			Thelon Fm.			Pitz Fm.			Undiff. Sed.			Intrusives			Undiff. Volc.			Metased/Volc			Quartzite			Altered Clasts			Other		
Sample ID	**n tot.**	**wt. tot. (g)**	**n**	***wt.***	***wt. %***	***n***	***wt.***	***wt. %***	***n***	***wt.***	***wt. %***	***n***	***wt.***	***wt. %***	***n***	***wt.***	***wt. %***	***n***	***wt.***	***wt. %***	***n***	***wt.***	***wt. %***	***n***	***wt.***	***wt. %***	***n***	***wt.***	***wt. %***
TUR022-SB	104	23.40	44	8.35	35.66	2	0.43	1.84	9	2.48	10.60	32	6.92	29.57	2	0.29	1.24	2	0.36	1.54	2	0.50	2.14	6	1.90	8.11	5	2.18	9.32
TUR022-SC	97	23.88	70	17.18	71.96	0	0.00	0.00	3	0.98	4.10	14	2.92	12.23	2	0.36	1.49	1	0.57	2.39	2	0.29	1.21	4	0.93	3.90	1	0.65	2.72
TUR022-SD	84	17.36	27	5.98	34.45	0	0.00	0.00	0	0.00	0.00	18	3.04	17.51	0	0.00	0.00	1	0.07	0.40	1	0.12	0.69	35	7.82	45.05	2	0.33	1.90
TUR022-SE	71	18.59	35	8.84	47.55	0	0.00	0.00	3	0.66	3.55	22	6.79	36.53	1	0.13	0.70	4	0.75	4.03	0	0.00	0.00	6	1.42	7.64	0	0.00	0.00
TUR022-SF	156	35.82	44	9.74	27.19	2	0.28	0.78	0	0.00	0.00	50	12.01	33.53	0	0.00	0.00	2	0.64	1.79	0	0.00	0.00	56	12.35	34.48	2	0.80	2.23
TUR048-SA	55	13.46	31	7.25	53.86	0	0.00	0.00	5	1.39	10.33	13	3.41	25.33	1	0.28	2.08	0	0.00	0.00	0	0.00	0.00	5	1.13	8.40	0	0.00	0.00
TUR048-SB	54	16.19	41	9.83	60.72	0	0.00	0.00	4	0.72	4.45	0	3.90	24.09	0	0.00	0.00	0	0.00	0.00	2	0.27	1.67	5	1.11	6.86	2	0.36	2.22
TUR045B-SA	91	20.53	19	4.70	22.89	2	0.46	2.24	0	0.00	0.00	56	12.57	61.23	0	0.00	0.00	1	0.16	0.78	0	0.00	0.00	13	2.64	12.86	0	0.00	0.00
TUR045B-SB	52	11.81	44	9.71	82.22	0	0.00	0.00	0	0.00	0.00	7	1.86	15.75	0	0.00	0.00	1	0.24	2.03	0	0.00	0.00	0	0.00	0.00	0	0.00	0.00
TUR045B-SC	96	26.40	47	13.25	50.19	0	0.00	0.00	0	0.00	0.00	36	9.65	36.55	0	0.00	0.00	0	0.00	0.00	0	0.00	0.00	13	3.50	13.26	0	0.00	0.00
TUR031-SA	58	11.58	18	3.69	31.87	0	0.00	0.00	4	0.94	8.12	27	5.40	46.63	1	0.33	2.85	0	0.00	0.00	1	0.22	1.90	4	0.58	5.01	3	0.42	3.63
TUR031-SB	64	14.73	10	2.01	13.65	0	0.00	0.00	1	0.16	1.09	40	9.88	67.07	0	0.00	0.00	2	0.31	2.10	0	0.00	0.00	7	1.26	8.55	4	1.11	7.54
TUR031-SC	45	10.67	22	5.77	54.08	0	0.00	0.00	1	0.11	1.03	14	3.05	28.58	1	0.26	2.44	2	0.59	5.53	0	0.00	0.00	4	0.65	6.09	1	0.24	2.25
TUR031-SD	82	16.15	19	3.49	21.61	0	0.00	0.00	1	0.16	0.99	44	9.28	57.46	1	0.14	0.87	6	1.33	8.24	0	0.00	0.00	11	1.75	10.84	0	0.00	0.00
TUR031-SF	99	23.45	15	4.29	18.29	0	0.00	0.00	0	0.00	0.00	44	10.27	43.80	3	0.34	1.45	2	1.06	4.52	0	0.00	0.00	34	7.21	30.75	1	0.28	1.19
TUR054-SE	69	16.15	50	11.29	69.93	0	0.00	0.00	1	0.22	1.36	14	3.39	21.00	0	0.00	0.00	1	0.52	3.22	1	0.27	1.67	1	0.09	0.53	1	0.37	2.29
TUR050-SA	32	8.96	18	5.12	57.14	0	0.00	0.00	0	0.00	0.00	9	2.54	28.35	1	0.30	3.35	0	0.00	0.00	2	0.32	3.57	2	0.68	7.59	0	0.00	0.00
TUR050-SB	67	13.72	14	2.37	17.27	0	0.00	0.00	0	0.00	0.00	33	6.74	49.13	0	0.00	0.00	2	0.38	2.77	2	0.33	2.41	16	3.90	28.43	0	0.00	0.00
TUR035-SA	52	10.83	8	1.36	12.56	3	0.54	4.99	1	0.21	1.94	32	6.12	56.51	0	0.00	0.00	3	1.52	14.04	0	0.00	0.00	5	1.08	9.97	0	0.00	0.00
TUR035-SB	54	11.08	18	3.39	30.60	0	0.00	0.00	3	0.77	6.95	22	4.33	39.08	0	0.00	0.00	1	0.42	3.79	0	0.00	0.00	9	2.00	18.05	1	0.17	1.53
TUR057-SE	88	20.42	11	2.43	11.90	0	0.00	0.00	0	0.00	0.00	57	13.65	66.85	0	0.00	0.00	0	0.00	0.00	3	0.40	1.96	15	3.23	15.82	2	0.71	3.48
TUR049-SB	127	33.89	4	1.13	3.33	0	0.00	0.00	0	0.00	0.00	62	17.77	52.43	0	0.00	0.00	0	0.00	0.00	0	0.00	0.00	59	14.01	41.34	2	0.98	2.89
TUR046-SA	43	9.72	21	5.55	57.10	0	0.00	0.00	3	0.40	4.12	15	2.86	29.42	1	0.12	1.23	3	0.79	8.13	0	0.00	0.00	0	0.00	0.00	0	0.00	0.00
TUR046-SB	61	15.51	23	5.76	37.14	2	0.25	1.61	5	1.21	7.80	27	7.19	46.36	1	0.15	0.97	2	0.58	3.74	0	0.00	0.00	0	0.00	0.00	1	0.37	2.39
TUR046-SC	99	24.33	56	13.27	54.54	0	0.00	0.00	2	0.52	2.14	32	8.54	35.10	0	0.00	0.00	1	0.53	2.18	4	0.66	2.71	4	0.81	3.33	0	0.00	0.00
Other Boreholes																													
GEX001-SA	75	19.59	6	0.85	4.33	0	0.00	0.00	5	1.51	7.71	46	13.19	67.34	2	0.30	1.53	6	1.53	7.81	0	0.00	0.00	8	1.63	8.32	2	0.58	2.96
GEX003-SA	58	12.12	4	0.73	6.01	5	0.93	7.67	5	0.89	7.34	36	7.88	65.03	0	0.00	0.00	0	0.00	0.00	5	1.30	10.73	3	0.39	3.22	0	0.00	0.00
GEX003-SB	68	15.57	10	2.27	14.58	1	0.11	0.71	3	1.39	8.93	33	7.05	45.28	6	1.16	7.45	2	0.54	3.47	4	0.82	5.27	9	2.23	14.32	0	0.00	0.00
LOB001-SA	65	15.08	11	2.21	14.66	1	0.43	2.85	3	0.39	2.59	39	8.93	59.22	3	0.69	4.58	1	0.40	2.65	3	0.49	3.25	3	1.09	7.23	1	0.45	2.98
LOB001-SB	53	10.75	28	5.86	54.51	1	0.14	1.30	2	0.27	2.51	11	2.40	22.33	3	0.47	4.37	0	0.00	0.00	3	0.82	7.63	4	0.44	4.09	1	0.35	3.26
LOB001-SC	41	8.38	27	5.26	62.78	0	0.00	0.00	4	1.14	13.61	7	1.51	18.02	0	0.00	0.00	2	0.35	4.18	0	0.00	0.00	1	0.12	1.42	0	0.00	0.00
JSF001-SA	72	17.52	46	10.56	60.27	0	0.00	0.00	2	0.60	3.42	16	4.11	23.43	3	1.20	6.83	1	0.22	1.26	1	0.30	1.71	3	0.54	3.08	0	0.00	0.00
LOB003-SA	92	23.17	15	3.38	14.59	0	0.00	0.00	5	1.53	6.60	54	14.29	61.67	5	1.68	7.25	2	0.36	1.55	4	0.66	2.85	5	0.92	3.97	2	0.35	1.51
LOB003-SB	60	14.37	38	9.77	67.99	0	0.00	0.00	0	0.00	0.00	11	2.88	20.04	2	0.33	2.30	1	0.19	1.32	4	0.57	3.97	4	0.63	4.38	0	0.00	0.00
LOB002-SA	51	12.85	7	2.18	16.96	1	0.19	1.48	1	0.15	1.17	37	9.46	73.62	2	0.24	1.87	0	0.00	0.00	0	0.00	0.00	3	0.63	4.90	0	0.00	0.00
LOB002-SC	85	30.38	8	3.68	12.11	1	0.18	0.59	1	0.23	0.76	55	19.20	63.20	4	1.80	5.92	7	1.79	5.89	3	1.80	5.92	3	0.93	3.06	3	0.77	2.53

			Thelon Fm.			Pitz Fm.			Undiff. Sed.			Intrusives			Undiff. Volc.			Metased/Volc			Quartzite			Altered Clasts			Other		
Sample ID	**n tot.**	**wt. tot. (g)**	**n**	***wt.***	***wt. %***	***n***	***wt.***	***wt. %***	***n***	***wt.***	***wt. %***	***n***	***wt.***	***wt. %***	***n***	***wt.***	***wt. %***	***n***	***wt.***	***wt. %***	***n***	***wt.***	***wt. %***	***n***	***wt.***	***wt. %***	***n***	***wt.***	***wt. %***
MAM002-SA	25	6.17	8	2.35	38.08	0	0.00	0.00	0	0.00	0.00	10	2.41	39.05	2	0.26	4.24	1	0.34	5.51	2	0.49	7.94	1	0.17	2.75	1	0.15	2.43
MAM002-SB	114	28.08	28	6.51	23.19	2	0.04	0.14	1	0.92	3.28	67	16.99	60.51	4	0.93	3.31	5	0.78	2.78	2	0.30	1.07	2	0.36	1.28	3	1.25	4.44
MAM002-SC	40	7.47	28	4.77	63.86	0	0.00	0.00	0	0.00	0.00	10	2.09	27.98	0	0.00	0.00	1	0.14	1.87	0	0.00	0.00	1	0.47	6.29	0	0.00	0.00
MAM002-SE	26	5.31	21	4.32	81.36	0	0.00	0.00	1	0.14	2.64	2	0.62	11.68	1	0.11	2.07	0	0.00	0.00	0	0.00	0.00	0	0.00	0.00	1	0.12	2.26
MAM002-SF	24	5.94	22	5.21	87.71	0	0.00	0.00	1	0.09	1.52	0	0.00	0.00	0	0.00	0.00	1	0.64	10.77	0	0.00	0.00	0	0.00	0.00	0	0.00	0.00
MAM002-SG	32	10.92	30	10.48	95.97	0	0.00	0.00	1	0.18	1.65	1	0.26	2.38	0	0.00	0.00	0	0.00	0.00	0	0.00	0.00	0	0.00	0.00	0	0.00	0.00
HND001-SA	31	7.50	18	4.15	55.33	1	0.19	2.53	1	0.49	6.53	8	2.12	28.27	1	0.22	2.93	2	0.33	4.40	0	0.00	0.00	0	0.00	0.00	0	0.00	0.00
HND001-SB	77	16.99	23	4.58	26.96	4	0.52	3.06	7	2.05	12.07	24	5.39	31.72	3	0.63	3.71	3	0.80	4.71	5	1.70	10.01	5	1.05	6.18	3	0.27	1.59
HND001-SE	13	3.28	7	2.12	64.63	0	0.00	0.00	1	0.15	4.57	4	0.80	24.39	0	0.00	0.00	1	0.21	6.40	0	0.00	0.00	0	0.00	0.00	0	0.00	0.00
HND002-SA	32	6.70	13	2.85	42.54	0	0.00	0.00	0	0.00	0.00	14	3.18	47.46	1	0.12	1.79	0	0.00	0.00	2	0.32	4.78	1	0.11	1.64	1	0.12	1.79
Section Samples																													
12-TH-S073B	154	38.96	117	30.60	78.54	1	0.33	0.85	10	2.47	6.34	16	3.72	9.55	2	0.48	1.23	5	0.74	1.90	2	0.48	1.23	1	0.14	0.36	0	0.00	0.00
12-MR-S073D	182	40.85	112	24.33	59.56	2	0.45	1.10	8	2.10	5.14	47	11.52	28.20	5	1.16	2.84	1	0.17	0.42	6	1.02	2.50	1	0.10	0.24	0	0.00	0.00
12-TH-S073F	158	38.60	119	29.22	75.70	1	0.13	0.34	9	2.46	6.37	15	4.29	11.11	3	0.45	1.17	3	0.56	1.45	8	1.49	3.86	0	0.00	0.00	0	0.00	0.00
13-AB-265	149	34.84	112	25.55	73.34	0	0.00	0.00	0	0.00	0.00	22	5.51	15.82	0	0.00	0.00	12	2.91	8.35	3	0.87	2.50	0	0.00	0.00	0	0.00	0.00
13-AB-258A	132	35.06	86	23.33	66.54	3	1.00	2.85	5	1.22	3.48	25	5.91	16.86	1	0.25	0.71	6	1.23	3.51	6	2.12	6.05	0	0.00	0.00	0	0.00	0.00
13-AB-258B	168	40.99	105	25.92	63.23	1	0.22	0.54	2	0.87	2.12	39	8.50	20.74	2	0.36	0.88	10	2.04	4.98	6	2.30	5.61	0	0.00	0.00	3	0.78	1.90
13-AB-258C	121	30.65	84	20.63	67.31	3	1.77	5.77	5	0.73	2.38	14	3.51	11.45	0	0.00	0.00	12	2.78	9.07	3	1.23	4.01	0	0.00	0.00	0	0.00	0.00
13-AB-258D	166	39.64	126	29.73	75.00	1	0.25	0.63	0	0.00	0.00	17	4.12	10.39	2	0.47	1.19	14	3.98	10.04	6	1.09	2.75	0	0.00	0.00	0	0.00	0.00

8 mm + Section Clast Counts

			Thelon Fm.			Pitz			Undiff. Sed.			Felsic-Intermediate Intrusive			Mafic Intrusive			Undiff. Volcanics			Meta-sediments/volcanics			Quartzite			Altered Clasts			Other		
Sample ID	**n tot.**	**wt. tot. (g)**	**n**	***wt.***	***wt. %***	***n***	***wt.***	***wt. %***	***n***	***wt.***	***wt. %***	***n***	***wt.***	***wt. %***	***n***	***wt.***	***wt. %***	***n***	***wt.***	***wt. %***	***n***	***wt.***	***wt. %***	***n***	***wt.***	***wt. %***	***n***	***wt.***	***wt. %***	***n***	***wt.***	***wt. %***
13-AB-258A	82	443.11	61	379.42	85.63	0	0.00	0.00	0	0.00	0.00	16	51.17	11.55	0	0.00	0.00	0	0.00	0.00	4	10.40	2.35	1	2.12	0.48	0	0.00	0.00	0	0.00	0.00
13-AB-258B	115	287.53	77	218.37	75.95	0	0.00	0.00	0	0.00	0.00	27	46.32	16.11	0	0.00	0.00	2	6.05	2.10	4	9.50	3.30	1	2.12	0.74	0	0.00	0.00	4	5.17	1.80
13-AB-258C	146	473.24	119	417.70	88.26	0	0.00	0.00	1	1.19	0.25	18	46.30	9.78	0	0.00	0.00	2	2.35	0.50	5	4.90	1.04	0	0.00	0.00	0	0.00	0.00	1	0.80	0.17
13-AB-258D	93	527.99	78	484.17	91.70	0	0.00	0.00	0	0.00	0.00	4	5.66	1.07	0	0.00	0.00	1	4.15	0.79	5	10.21	1.93	3	21.99	4.16	0	0.00	0.00	2	1.81	0.34
13-AB-265	94	407.92	68	302.01	74.04	0	0.00	0.00	1	0.98	0.24	9	19.25	4.72	0	0.00	0.00	3	3.02	0.74	8	46.70	11.45	3	7.06	1.73	0	0.00	0.00	2	28.90	7.08

Comments

13-AB-258A Th: 2 Clasts heavily altered Thelon Fm. Clasts

13-AB-258B O: 3 Silica-rich clasts, 1 calcitic clast (vein-like in appearance)

13-AB-258C O: Silica rich clast

13-AB-258D O: Silica-rich clasts

13-AB-265 O: 2 Clasts have altered material on surfaces, unsure of lithology.

Appendix F – Drillcore logs

Drillhole	Top	Bottom	Recovery	Colour	Lithofacies 1	Lithofacies 2	Samples	Cameco_ID	Notes
ABR-009	0	5	6						P.C.N.M.
ABR-009	5	5.8	100	10R 6/3; Pale Red	Dmm				At 5.50m: till-till contact. Slightly gradational contact.
ABR-009	5.8	5.98	100	5YR 6/2; Pinkish Grey / 10R 6/3;	Fl				Partially washed out, poorly preserved but visible white and pale red laminations.
ABR-009	5.98	6.04	100	5YR 6/2; Pinkish Grey	Dmm				Diamictite rich in fine-grained material, poorly preserved
ABR-009	6.04	7.6	100		Wo				P.C.N.M.
ABR-011	0	4.5	0						Missing
ABR-011	4.5	5	100	10R 6/3; Pale Red	Dmm				At top of section: one cobble of 18cm
ABR-011	5	6.7	85	10R 6/3; Pale Red	Dmm				Gradational contact to different till
ABR-011	5.16	5.53					ABR011-SA	97599	SRC
ABR-011	5.53	5.65					ABR011-SA		UW
ABR-011	6.7	7.9	85	5YR 7/2; Pinkish Grey	Dmm				7.8-7.9m: Till is missing or washed away. Bedrock-Till contact at 7.9m.
ABR-011	6.97	7.07					ABR011-SB		UW
ABR-011	7.07	7.33					ABR011-SB	97600	SRC
ABR-012	0	3.1	0						P.C.N.M.
ABR-012	3.1	4.56	100						3.1-3.79m: P.C.N.M. 3.79-4.56m: two consecutive boulders, no matrix.
ABR-012	4.56	5	100	10R 4/4; Weak Red	Dmm				
ABR-012	5	8	42	10R 4/4; Weak Red	Dmm				Appears more pink, but probably the result of difference in moisture content.
ABR-012	8	9.2	100	10R 4/4; Weak Red	Dmm				
ABR-012	8.22	8.44					ABR012-SD	204633	SRC
ABR-012	8.44	8.65					ABR012-SD		UW
ABR-012	9.2	11	78	10R 4/4; Weak Red	Dmm				
ABR-012	11	12.8	98	10R 4/4; Weak Red	Dmm				
ABR-012	12.8	14	98	7.5 YR 6/3; Light Brown	Dmm				Unit of significantly different colour.
ABR-012	13.2	13.4					ABR012-SA		UW
ABR-012	13.65	14					ABR012-SA	97601	SRC
ABR-012	14	17	72	10R 8/2; Pinkish White	Dmm				Very clay and silt rich unit.
ABR-012	17	20	37	10R 8/2; Pinkish White	Dmm				Very clay and silt rich unit.
ABR-012	17.25	17.58					ABR012-SB	97602	SRC
ABR-012	17.58	17.83					ABR012-SB		UW; Sampled a further 12 cm of material for pebbles during 2013 field season
ABR-012	20	21.2	100	10R 8/2; Pinkish White	Dmm				Very clay and silt rich unit.
ABR-012	21.2	23	28	10R 8/2; Pinkish White	Dmm				Very clay and silt rich unit.
ABR-012	23	25.37	32	10R 8/2; Pinkish White	Dmm				Very clay and silt rich unit.
ABR-012	25.37	27.78	100	10R 8/2; Pinkish White	Dmm				Unit becomes more competent, less clay and silt content
ABR-012	27.78	28.08	100	10R 7/4 (clay), 10R 7/2 (laminae	Fl				Laminated clay layers, 3-4 mm laminations
ABR-012	28	28.05					ABR012-SC		UW
ABR-012	28.08	28.85	100						P.C.N.M.
ABR-012	27	27.4					ABR012-SE		UW
AYA-001	0	2	12						P.C.N.M.
AYA-001	2	5	13						P.C.N.M.
AYA-001	5	8	13						P.C.N.M.
AYA-001	8	11	25						P.C.N.M.
AYA-001	11	13.05	21						P.C.N.M. 12 cm of clay rich pale red diamicton near end.
AYA-001	13.05	15.7	100	10R 7/3; Pale Red	Dmm				Gradational contact to till of different colour
AYA-001	13.6	13.7					AYA001-SA		UW
AYA-001	13.7	14					AYA001-SA	97603	SRC
AYA-001	15.7	18.8	100	10R 6/3; Pale Red	Dmm				
AYA-001	17.97	18.07					AYA001-SB		UW
AYA-001	18.07	18.37					AYA001-SB	97604	SRC
AYA-001	18.8	20	46	10R 6/3; Pale Red	Dmm	Fl			Partially washed out, poor recovery. 27 cm washed out diamicton, 20 cm fine-grained unit with poorly preserved laminations (1-3 cm in thickness), last 10 cm partially washed out fine-grained unit with pebbles.
AYA-001	20	23	27						P.C.N.M.
AYA-001	23	26	56		Dmm				Washed out sandy diamicton, clast poor (matrix rich)
AYA-001	26	28	80		Dmm				Washed out sandy diamicton, clast poor (matrix rich). Last 23 cm cobbles, no matrix
AYA-002	0	2	18						Pebbles and cobbles, no matrix; largest 12 cm, granite
AYA-002	2	5	15						P.C.N.M.; Average size 4 cm
AYA-002	5	8	41						P.C.N.M.; largest 24 cm, granite

Drillhole	Top	Bottom	Recovery	Colour	Lithofacies 1	Lithofacies 2	Samples	Cameco_ID	Notes
AYA-002	8	11	100	10R 7/3; Pale Red	Dmm				Start of section 17 cm cobble
AYA-002	9.22	9.35					AYA002-SA		UW
AYA-002	9.35	9.66					AYA002-SA	97605	SRC
AYA-002	11	14	41	10R 7/3; Pale Red	Dmm				Core beyond 11.64 shows evidence of being washed out; most lost near 14 m
AYA-002	14	17	12						P.C.N.M.; average size 3-4 cm
AYA-002	17	20	31	5YR 8/2; Pinkish White	Dmm				Till heavily washed out from sitting outside, significant colour change evident though
AYA-002	20	21	100						P.C.N.M. A single clay-rich lense at 20.56 with slightly preserved laminations
AYA-003	0	2	15						P.C.N.M.; Up to 6 cm, various lithologies, granite most common.
AYA-003	2	5	19						P.C.N.M.; 8 cm of till with matrix at 1.92-2.00
AYA-003	5	8.4	98	10R 7/4; Pale Red	Dmm				Interval slightly washed out
AYA-003	7.75	8.1					AYA003-SA		UW; Collected more sample for pebble counts during 2013 field season
AYA-003	8.1	8.4					AYA003-SA	97606	SRC
AYA-003	8.4	8.6	88	10R 7/4; Pale Red	Dmm				
AYA-003	8.6	8.9	88	10R 7/4; Pale Red	Dml				
AYA-003	8.9	9.18	88	Clay - 7.5YR 8/1; White. Silt - 10R 7/2; Pale Red	F				White clay for the most part, laminations present at 8.98-9.14. Preservation is poor as the interval has been washed out.
AYA-003	9.18	10.45	88	10R 7/4; Pale Red	Dml				Laminations are white clay, fairly well preserved but interal slightly washed out.
AYA-003	10.45	11	88	10R 7/4; Pale Red	Dmm				
AYA-003	11	13.5	85	10R 7/4; Pale Red	Dmm				11.84 - fine-grained lamination of white clay and red silt, few cm in length. 13.2-13.5, sand content increases.
AYA-003	13.5	13.88	100	10R 7/4; Pale Red	Dml				First 10 cm washed out, similar to Dml seen earlier in core.
AYA-003	13.88	14	100	10R 7/4; Pale Red	Dmm				
AYA-003	14	14.95	100	10R 7/4; Pale Red	Dmm				
AYA-003	13.75	14.18					AYA003-SB		UW; Collected more sample for pebble counts during 2013 field season
AYA-003	14.18	14.51					AYA003-SB	97607	SRC
AYA-003	14.95	17	100	5YR 6/2; Pinkish Grey	Dmm				15.45-15.78 granitic boulder. 16.3-16.43 till partiall washed out.
AYA-003	17	17.8	100	5YR 6/2; Pinkish Grey	Dmm				17.2-17.64 granitic boulder
AYA-003	17.8	20	78	5YR 7/2; Pinkish Grey	Dmm				
AYA-003	18.47	18.77					AYA003-SC	97608	SRC
AYA-003	18.17	18.88					AYA003-SC		UW; Collected more sample for pebble counts during 2013 field season
AYA-003	20	23	79	5YR 7/2; Pinkish Grey					Partially washed out, some clay-rich intervals. 21.92-21.96 silt lense
AYA-003	23	24.5	28						Pebbles, no matrix.
AYA-003	24.5	26.6	23						Pebbles and cobbles, no matrix.
AYA-003	26.6	27.73	100	5YR 7/2; Pinkish Grey	Dmm				Last 23 cm (26.5-26.73) more fine grained rich and brittle.
AYA-003	27.03	27.31					AYA003-SD	97609	SRC
AYA-003	26.8	27.45					AYA003-SD		UW; Collected more sample for pebble counts during 2013 field season
AYA-003	27.73	29	100						P.C.N.M.; 60 cm boulder present. 28.95-29 clay rich interval rich in alteration material
AYA-003	29	29.6	20						P.C.N.M.; Bedrock contact at 29.6.
AYA-004	0	2	20						P.C.N.M.; Largest cobble 12 cm
AYA-004	2	5	49						P.C.N.M.; several cobbles 16-20 cm in length
AYA-004	5	8	34						P.C.N.M.; Two cobbles at 20 and 22 cm in length
AYA-004	8	9.3	100	10R 6/3; Pale Red	Dmm				
AYA-004	8.53	8.82					AYA004-SA	97610	SRC
AYA-004	8.82	8.97					AYA004-SA		UW
AYA-004	9.3	11	92	10R 6/3; Pale Red	Dmm				One 16 cm cobble
AYA-004	11	13	97	10R 6/3; Pale Red	Dmm				Gradational contact with underlying till
AYA-004	13	13.9	97	7.5YR 7/2; Pinkish Grey	Dmm				
AYA-004	13.31	13.48					AYA004-SB		UW
AYA-004	13.48	13.81					AYA004-SB	97611	SRC
AYA-004	13.9	14	100						Washed out diamicton
AYA-004	14	17	58	7.5YR 7/2; Pinkish Grey	Dmm				Some intervals washed out
AYA-004	17	20	13						P.C.N.M.; Some clay-rich diamicton present.
AYA-004	20	21.1		10R 8/1; White	Dmm				Rich in fine-grained material, no visible clasts larger than 2 cm. Till-Bedrock contact at 21.1.
AYA-004	20.23	20.44					AYA004-SC	97612	SRC
AYA-004	20.44	20.58					AYA004-SC		UW
AYA-005	0	2	40						P.C.N.M.

Drillhole	Top	Bottom	Recovery	Colour	Lithofacies 1	Lithofacies 2	Samples	Cameco_ID	Notes
AYA-005	2	5	31						P.C.N.M.; various lithologies
AYA-005	5	8	32						P.C.N.M.; One 38cm boulder, one 52cm boulder, several cobbles
AYA-005	8	12	41	5YR 7/2; Pinkish Grey	Dmm				Several intervals washed out in this section
AYA-005	11.16	11.48					AYA005-SA	97613	SRC
AYA-005	11.48	11.66					AYA005-SA		UW
AYA-005	12	12.4	100	5YR 7/2; Pinkish Grey	Dmm				This box was partially washed out.
AYA-005	12.4	15	70	5YR 7/2; Pinkish Grey	Dmm				This box was partially washed out
AYA-006	0	2	43						P.C.N.M.; boulders up to 32cm
AYA-006	2	5	19						P.C.N.M.
AYA-006	5	8	37						P.C.N.M.; granite boulder up to 40cm
AYA-006	8	11	93	7.5YR 7/2; Pinkish Grey	Dmm				At the top of the section, cobbles and pebbles; few pebbles
AYA-006	8.56	8.89					AYA006-SA	97614	SRC
AYA-006	8.89	9.02					AYA006-SA		UW
AYA-006	11	13.4	55	7.5YR 7/2; Pinkish Grey	Dmm				Base of till section rich in alteration clasts. Bedrock-Till contact at 13.4m.
AYA-006	12.52	12.66					AYA006-SB		UW
AYA-006	12.66	12.94					AYA006-SB	97615	SRC
AYA-009	0	3	14.3		Wo				All intrusives
AYA-009	3	6	23.3		Wo				All intrusives
AYA-009	6	9	38.0	10R 6/4; Pale Red	Wo	Dmm		`	First 15 cm P.C.N.M.; all intrusives; 35 cm Dmm, minor grey laminations present; 58 cm P.C.N.M. -Mostly intrusives, minor volcanic
AYA-009	9	11.5	88.0	10R 6/4; Pale Red	Dmm				
AYA-009	10.3	10.4					AYA009-SA		UW
AYA-009	10.4	10.65					AYA009-SA	204554	SRC
AYA-009	11.5	11.63	100.0	10R 6/4; Pale Red	Dmm				
AYA-009	11.63	12	100.0	5 YR 7/2; Pinkish Grey	Dmm				Box lithologies largely intrusives, some pitz clasts present
AYA-009	12	18	45.5	5 YR 7/2; Pinkish Grey	Dmm				
AYA-009	18	19.1	97.3	5 YR 7/2; Pinkish Grey	Dmm				
AYA-009	19.1	21	85.8	5 YR 7/2; Pinkish Grey	Dmm				Note: Some areas are wet, appear darker
AYA-009	21	23.8	100.0	5 YR 7/2; Pinkish Grey	Dmm				
AYA-009	22.89	22.97					AYA009-SB		UW
AYA-009	22.97	23.2					AYA009-SB	204555	SRC
AYA-009	23.8	24	100.0	5 YR 7/2; Pinkish Grey	Dmm				
AYA-009	24	26.4	100.0	5 YR 7/2; Pinkish Grey	Dmm				
AYA-009	26.4	28.1	100.0	2.5 7/2; Pinkish Grey	Dmm				Slight colour transition to a slightly more reddish till, contanct poorly defined and not definitive, mostly likely at large clast present
AYA-009	28.1	30	100.0	2.5 7/2; Pinkish Grey	Dmm				Same as previous unit at end of last box, slightly more redder
AYA-009	29.79	30					AYA009-SF	204618	SRC; DUPLICATE of AYA009-SC
AYA-009	30	30.14					AYA009-SC		UW
AYA-009	30	32.5	100.0	2.5 7/2; Pinkish Grey	Dmm				
AYA-009	30.14	30.41					AYA009-SC	204556	SRC
AYA-009	32.5	33	100.0	2.5 7/2; Pinkish Grey	Dmm				
AYA-009	33	34.3	100.0	2.5 7/2; Pinkish Grey	Dmm				
AYA-009	34.3	36.8	100.0	5YR 6/2; Pinkish Grey	Dmm				Slight colour transition greyer-brown colour
AYA-009	34.96	35.08					AYA009-SD		UW
AYA-009	35.08	35.32					AYA009-SD	204557	SRC
AYA-009	36.8	37.6	100.0	2.5 7/2; Pinkish Grey	Dmm				Gradationally to a more redder till, last 20 cm 10R 7/4 (pale red)
AYA-009	37.42	37.55					AYA009-SE	204558	SRC
AYA-009	37.55	37.6					AYA009-SE		UW
AYA-009	37.6	37.85	100.0	5YR 8/1; White	Fl	Fm			Sharp contact, slightly inclined at 40 (BH dips at 10 so 30) with overlying till;
AYA-010	0	3	11.0		Wo				Photos start at 2159; All intrusive clasts present
AYA-010	3	6	14.0		Wo				Clasts are mostly intrusives, some sedimentary (SS) and quartzite
AYA-010	6	9	70.0	10R 6/4; Pale Red	Dmm				Grey fine-grained laminations present at 6.45; several cm in thickness
AYA-010	9	10.3	96.2	10R 6/4; Pale Red	Dmm				
AYA-010	10.3	12	100.0	10R 6/4; Pale Red	Dmm				
AYA-010	10.53	10.77					AYA010-SA	204551	SRC
AYA-010	10.77	10.87					AYA010-SA		UW
AYA-010	12	15	73.3	10R 6/4; Pale Red	Dmm				

Drillhole	Top	Bottom	Recovery	Colour	Lithofacies 1	Lithofacies 2	Samples	Cameco_ID	Notes
AYA-010	15	15.5	100.0	5 YR 7/2; Pinkish Grey	Dmm				
AYA-010	15.5	18	90.0	5 YR 7/2; Pinkish Grey	Dmm				
AYA-010	17.28	17.43					AYA010-SB		UW
AYA-010	17.43	17.63					AYA010-SB	204552	SRC
AYA-010	18	20.1	100.0	5 YR 7/2; Pinkish Grey	Dmm				Clay lense at 20.87 (5YR 8/2; Pinkish White); 1 cm thick
AYA-010	20.1	21	100.0						
AYA-010	21	22.8	100.0						
AYA-010	21.86	22.05					AYA010-SC		UW
AYA-010	22.05	22.3					AYA010-SC	204553	SRC
GEX-001	0	4	17						P.C.N.M.
GEX-001	4	7	47						P.C.N.M.; Last 10cm: fine-grained diamicton, fairly washed out
GEX-001	7	10	69						P.C.N.M.; one large granitic boulder. 10cm interval of washed out, clay- and silt-rich diamicton.
GEX-001	10	21	41	10R 7/3; Pale Red	Dmm				
GEX-001	18.47	18.62					GEX001-SA		UW
GEX-001	18.62	18.97					GEX001-SA	97616	SRC
GEX-002	0	5	35						No depth blocks in first box (except 13 m block), pebbles-till contact estimated. Cobbles and pebbles, matrix washed out for the most part.
GEX-002	5	13	35	10R 7/3; Pale Red	Dmm				On original core photos, can see a more greyish unit at the top of the borehole!
GEX-002	12.49	12.6					GEX002-SA		UW (measured from 13 m block
GEX-002	12.6	13					GEX002-SA	97617	SRC
GEX-002	13	17		10R 7/3; Pale Red	Dmm				Box 2 was not properly labelled; 13-17 m interval completely missing but thought to exist in box 2 since there is more core in that box than listed.
GEX-002	17	20		10R 7/3; Pale Red	Dmm				
GEX-002	20	20.3		10R 7/3; Pale Red	Dmm				
GEX-002	20.3	20.94							Pebbles and cobbles, no matrix.
GEX-002	20.94	21.58		5YR 7/2; Pinkish Grey	Dmm				Gradual transition into differenct coloured diamicton, but can not distinguish contact exactly due to degree of till washout
GEX-002	21.57	21.72					GEX002-SB		UW
GEX-002	21.57	23.2		10R 7/2; Pale Red	Dmm				
GEX-002	21.72	22.03					GEX002-SB	97661	SRC
GEX-003	0	3	21		Wo				P.C.N.M; Last 10 cm Dmm (10R 7/2)
GEX-003	3	6	27	10R 8/2; Pinkish White	Dmm				Last 14 cm 5YR 8/1 (white) Dmm
GEX-003	6	9	41	5YR 8/1; White	Dmm				First 30 cm and last 27 cm cobbles, no matrix
GEX-003	9	11.1	33	5YR 8/1; White	Dmm				Till contact gradational, colour intermixed for ~5 cm
GEX-003	11.1	12	33	10R 7/3; Pale Red	Dmm				
GEX-003	11.42	11.57					GEX003-SA	97682	SRC (measured from 12 m block)
GEX-003	11.57	11.61					GEX003-SA		UW (measured from 12 m block)
GEX-003	12	15	94	10R 7/2; Pale Red	Dmm				Small clay lense at 13.08, mostly washed out white clay
GEX-003	15	18	100	10R 7/2; Pale Red	Dmm				Bedrock a hornblende syenite, unaltered
GEX-003	16.08	16.31					GEX003-SB	97683	SRC
GEX-003	16.31	16.41					GEX003-SB		UW
HND-001	0	2	25						P.C.N.M; Majority of clasts are a volcanic rock with a red matrix and larger black minerals, minor amounts of sandstones and granites
HND-001	2	7	27						P.C.N.M; Clasts are more granite rich, little to no sandstone clasts
HND-001	7	9	33	2.5 YR 7/3; Pink	Dmm				Pink Diamicton, matrix supported, massive. Poor recovery
HND-001	9	11	98	10 YR 7/3; Pale Red	Dmm				Clasts of red volcanic present. Great core recovery.
HND-001	10.25	10.5					HND001-SA		UW
HND-001	10.6	10.8					HND001-SA	97618	SRC
HND-001	11	13.5	7						Appears to be a coarser layer, but there is little to no core recovery. Potentially washed out diamicton.
HND-001	13.5	14	100	10 YR 7/3; Pale Red	Dmm				
HND-001	14	17	100	10 YR 7/3; Pale Red	Dmm				Dmm
HND-001	15.45	15.75					HND001-SB		UW
HND-001	15.75	15.98					HND001-SB	97619	SRC
HND-001	17	17.17	97	10 YR 7/3; Pale Red	Dmm				Sharp contact at 17.17

Drillhole	Top	Bottom	Recovery	Colour	Lithofacies 1	Lithofacies 2	Samples	Cameco_ID	Notes
HND-001	17.17	17.47	97	Silt - 2.5 YR 8/2; Pinkish White / Clay - 10 R 7/4; Pale Red	Fl				Clay w/ laminae 0.5 cm thick with silt partings (sub-mm thickness silt laminations)
HND-001	17.35	17.36					HND001-SC		UW; Fl grain size sample
HND-001	17.47	17.77	97		Dml	Fl/Fld			Clay rich diamicton with dropstones
HND-001	17.55	17.6					HND001-SD		UW; Dml sample taken below Fl unit
HND-001	17.77	18	97	10R 7/4; Pale Red	Dmm				Diamicton is coarser (gravelly) near 18.00 m
HND-001	18	18.84	91	10R 7/4; Pale Red	Dmm				Sandy diamicton, more diamictic at upper part and more sandy down-core
HND-001	18.84	19.26	91	10R 7/4; Pale Red	Dml				Diamicton with clay laminations
HND-001	19.26	20	91	10R 7/4; Pale Red	Dml				Similar to previous unit, but an increased pebble content
HND-001	19.72	19.82					HND001-SE		UW
HND-001	19.82	20					HND001-SE	97620	SRC
HND-001	20	20.15	100		Dmm				
HND-001	20.15	20.39	100	7.5 YR 7/2; Pinkish Grey	Sm	Fm			Fine grained sand and silt, massive
HND-001	20.28						HND001-SF		UW; Grain size sample of the sandy interval
HND-001	20.39	21.2	100	2.5 YR 8/2; Pinkish White	Fm				Silt with crude lamination but more massive. Some zones are laminated
HND-001	20.45						HND001-SG		UW; Grain size sample of silty material
HND-001	21.2	22.03	100		Fm				
HND-001	21.44	21.48					HND001-SH		UW
HND-001	22.03	22.15	100		Fl				Clay with laminations
HND-001	22.05	22.1					HND001-SI		UW
HND-001	22.15	22.8	100		Fm	Sm			Very fine sand and silt; massive
HND-001	22.65	22.74					HND001-SJ		UW
HND-001	22.8	23	100						P.C.N.M.; Four different lithologies visible
HND-001	23	26	83						P.C.N.M; boulders up to 45 cm present
HND-001	26	29	50						Pebbles and cobbles. Average 4 cm in a-axis length, subrounded and morphology suggests a suspected glacial-fluvial origin, fines gone. Clasts vary between sandstones, siltstones, mafics but not as many shield clasts
HND-001	29	35	0						No core recovery
HND-001	35	38	6						Pebbles. Average 7 cm in a-axis length, sub-rounded, glacial-fluvial. Can tell that the clasts used to be iron-shaped but edge have be rounded by fluvial processes
HND-001	38	41	0						No core recovery
HND-001	41	44	10						P.C.N.M; Avg. 4-5 cm in a-axis length, sub-rounded. Similar to 35-58 m of core
HND-001	44	46.7	55						P.C.N.M
HND-001	46.7	47	55						Sandy Gravel.
HND-001	47	50	5						Single cobble fragment of 15 cm length.
HND-001	50	53	32						P.C.N.M
HND-001	53	53.2	100						Pebbles. Average 4-6 cm in length, sub-rounded.
HND-001	53.2	53.6	57						Small pebbles.
HND-001	53.6	56	57						Pebbles and cobbles.
HND-001	56	56.82	70						Pebbles and cobbles.
HND-001	56.82	57.05	70		Dmm				Sandy diamicton
HND-001	57.05	59	70						Boulder(s).
HND-001	59	59.5	70						Boulders.
HND-002	0	12.95	1.5		Wo				
HND-002	12.95	15	100.0	10R 6/3: Pale Red	Dmm				Note: first marker is at 15, assumed core recovery was 100% from the the first marker back to the beginning of washed out material. Till is fairly competent in this interval.
HND-002	14.5	14.59							UW
HND-002	14.59	14.79					HND002-SA	204559	SRC
HND-002	15	17.24	65.5	10R 6/3: Pale Red	Dmm				15-15.55 material is 'slumped' in box
HND-002	17.24	18.1	65.5	10R 7/2; Pale Red	Dmm				Lighter coloured diamicton then further up in core.
HND-002	17.36	17.45							UW
HND-002	17.45	17.68					HND002-SB	204560	SRC
JSF-001	0	7.45	4						Single boulder
JSF-001	7.45	9	100	10R 7/3; Pale Red	Dmm				Assumed 100% recovery from 9 m block
JSF-001	9	12	60	10R 7/3; Pale Red	Dmm				
JSF-001	11.42	11.75					JSF001-SA		UW (measured from 12 m block); Further sampled 2013 field season (11.42-11.62)

Drillhole	Top	Bottom	Recovery	Colour	Lithofacies 1	Lithofacies 2	Samples	Cameco_ID	Notes
JSF-001	11.75	12					JSF001-SA	97621	SRC (measured from 12 m block)
JSF-001	12	15	0						A single pebble 4 cm in length
JSF-001	15	17.65	9						P.C.N.M
JSF-001	17.65	18	100	7.5YR 7/2; Pinkish Grey	Sm	Fm			Primarily sand with some fine grained material. Well-rounded cobble found at beginning of interval.
JSF-001	17.7	17.74					JSF001-SB		UW
JSF-001	18	21	21		Sm				Similar to previous unit, but with pebble/cobble intervals. 7 cm at bedrock contact (sharp)
LOB-001	0	5.5	0						No core recovered
LOB-001	5.5	6	100	10R 7/3; Pale Red	Dmm				
LOB-001	6	8.75	54	10R 7/3; Pale Red	Dmm				
LOB-001	6.55	6.84					LOB001-SA	97684	SRC (measured from 6 m block)
LOB-001	6.84	6.97					LOB001-SA		UW (measured from 6 m block)
LOB-001	8.75	9	54	10R 8/2; Pinkish White	Dmm				Till contact sharp with a cobble at the base
LOB-001	8.8	9.2					LOB001-SC		Unit not suitable for geochem, sample collected for grain size + pebble counts
LOB-001	9	12	23	10R 8/2; Pinkish White	Dmm				Poor recovery
LOB-001	12	14.3	100	2.5YR 7/2; Pale Red	Dmm				
LOB-001	14.3	15	100	2.5YR 7/2; Pale Red	Dmm				
LOB-001	15	15.25					LOB001-SB	97685	SRC (measured from 15 m block)
LOB-001	15	18	82	2.5YR 7/2; Pale Red	Dmm				Some areas where clay lense suspected to be, but have been washed out by drilling.
LOB-001	15.25	15.51					LOB001-SB		UW (measured from 15 m block)
LOB-001	18	18.4	82	2.5YR 7/2; Pale Red	Dmm				
LOB-002	0	3	12						Pebbles and cobbles, no matrix. Note: Freshly drilled hole, core is moist (may affect munsell colour codes).
LOB-002	3	5.48	21						41cm boulder at top, followed by 11cm of pebbles and cobbles
LOB-002	5.48	5.61	100	10R 5/3; Weak Red	Dmm				Sandy diamicton, not firm
LOB-002	5.61	5.7					LOB002-SC		UW; 5.36-5.5 sieved in the 2013 field season for more pebbles
LOB-002	5.61	5.87	100	5YR 7/1; Light Grey	Dmm				Firmer than previous lithofacies, slightly washed out.
LOB-002	5.87	6	100	10R 7/3; Pale Red	Dmm				Firmer than previous two lithofacies
LOB-002	6	9	77	10R 5/4; Weak Red	Dmm				White clay lens at 6.07 m
LOB-002	6.26	6.53					LOB002-SA	97686	SRC (measured from 6 m block)
LOB-002	6.53	6.62					LOB002-SA		UW(measured from 6 m block)
LOB-002	9	9.6	55	10R 6/4; Pale Red (laminations 5YR 8/1; White)	Dml				
LOB-002	9.6	12	55	10R 6/4; Pale Red	Dmm				
LOB-002	12	13.95	25	10R 6/4; Pale Red	Dmm				
LOB-002	13.95	15	100	10R 6/4; Pale Red (laminations 5YR 8/1; White)	Dml				Very clay rich diamicton, fine-grained sand only found in sandy laminations present. 14.43-15.00 m matrix sand content increases.
LOB-002	14.14	14.28					LOB002-SD		UW (alteration clast present within till)
LOB-002	14.28	14.38					LOB002-SB	97687	SRC (measured from 15 m block)
LOB-002	14.38	14.47					LOB002-SB		UW (measured from 15 m block)
LOB-002	15	18	26		Wo	Dml			Fairly washed out. 16 cm of same DML. 62 cm of P.C.N.M.
LOB-002	18	18.66	95		Wo				Boulders of same bedrock material
LOB-002	18.66	18.87					LOB002-SE		UW
LOB-002	18.66	18.87	95	10R 7/1; Light Grey (laminations 10R 6/4)	Fl				Lense of clay with smaller laminae, light grey 1 mm with sub mm 10R 4/6 laminae.
LOB-002	18.87	19.1	95		Wo				Boulders
LOB-003	0	3	11		Wo				All intrusives
LOB-003	3	6	10		Wo				All intrusive with exception of one sedimentary clast.
LOB-003	6	9	17		Wo				One SS clast, one Volc. clast, several syenite, several smaller clasts coated with light coloured matrix.
LOB-003	9	12	34		Sm				Very poorly sorted sand. 60cm. Pebly silty sand. Remainder washed out intrusive and sedimentary clasts.
LOB-003	12	15	70	10R 8/2; Pinkish White/5YR 8/1;	Fl		Fld		Potential lacustrine sediments with dropstones. Clay intervals are laminated localy
LOB-003	12.95	13.08					LOB003-SC		UW
LOB-003	15	15.3	100		Sm				
LOB-003	15.3	15.78	47	2.5YR 7/2; Pale Red	Dmm				

Drillhole	Top	Bottom	Recovery	Colour	Lithofacies 1	Lithofacies 2	Samples	Cameco_ID	Notes
LOB-003	15.3	18	47	10R 7/3; Pale Red	Dmm				
LOB-003	18	21	9	10R 5/3 Weak Red	Dmm				Different from above, diamicton. Near end of box so possibly moist.
LOB-003	21	24	89	10R 6/3; Pale Red	Dmm				Poorly consolidated for first 90 cm. Core slightly moist, some appears 10R 4/4
LOB-003	24	24.2	100	10R 6/3; Pale Red	Dmm				
LOB-003	24.2	27	46	10R 6/3; Pale Red	Dmm				
LOB-003	24.31	24.51					LOB003-SA		UW
LOB-003	24.51	24.71					LOB003-SA	204643	SRC
LOB-003	27	30	100	10R 6/3; Pale Red	Dmm				
LOB-003	30	32.4	100	10R 6/3; Pale Red	Dmm				Note: Box has a 'cave' interval within it. Assumed to be a repeat of earlier boxed core
LOB-003	31.89	32.08					LOB003-SB	204644	SRC
LOB-003	32.08	32.29					LOB003-SB		UW
LOB-003	32.4	32.8	100	10R 6/3; Pale Red	Dmm				
MAM-001	0	9	17						Note: Fresh core; P.C.N.M.Cobbles, some intervals of Dmm 10R 5/4
MAM-001	9	12	51	10R 5/3	Dmm				First 50 cm cobbles/boulders. 9.86-10.15 interval of more fine-grained rich till
MAM-001	12	15	26	10R 4/3	Dmm				First 30 cm P.C.N.M.; 40 cm of weak red till and washed out at 15 m block
MAM-001	15	18	90.00	10R 4/3	Dmm				
MAM-001	18	18.8	100	10R 4/4	Dmm				
MAM-001	18.8	21	27						P.C.N.M.
MAM-001	21	24	34.0	10R 4/4	Dmm				Appears washed out in middle of interval, core probably lost there
MAM-001	24	27	100.0	10R 4/4	Dmm				
MAM-001	27	30	93.0	10R 4/4	Dmm				Colour variations from water content, some intervals drier
MAM-001	30	33	90.0	10R 4/4	Dmm				
MAM-001	33	36	80.0	10R 5/4	Dmm				Interval fairly washed out, slighlty colour variation
MAM-001	36	39	42.0	10R 5/3	Dmm				Interval fairly washed out; sandstone subcropping
MAM-002	0	5.47	10.2		Wo				Intrusives + sed.
MAM-002	5.45	6	100.0	10R 7/2; Pale Red	Dmm				
MAM-002	5.45	5.67					MAM002-SA		UW
MAM-002	5.67	5.82					MAM002-SA	204645	SRC
MAM-002	6	9	92.3	10R 7/3; Pale Red	Dmm				Colour change to a more 'redder' till
MAM-002	9	9.5	100.0	10R 7/3; Pale Red	Dmm				
MAM-002	9.5	12	86.0	10R 7/3; Pale Red	Dmm				11.57-12 - Very clast rich diamicton
MAM-002	12	14.9	75.9	10R 7/3; Pale Red	Dmm				13.06-13.29 - clast poor dmm
MAM-002	14.9	15	100.0	10R 7/3; Pale Red	Dmm				
MAM-002	15	18	24.3	10R 7/3; Pale Red	Dmm				
MAM-002	17.33	17.57					MAM002-SB		UW;Measured from 18m block
MAM-002	17.57	17.77					MAM002-SB	204646	SRC; Measured from 18m block
MAM-002	18	21	100.0	10R 7/3; Pale Red	Dmm				
MAM-002	21	21.3	100.0	10R 7/3; Pale Red	Dmm				
MAM-002	21.3	24	93.7	10R 7/3; Pale Red	Dmm				
MAM-002	22.96	23.16					MAM002-SC		UW
MAM-002	23.16	23.36					MAM002-SC	204647	SRC
MAM-002	23.36	23.59					MAM002-SD	204648	SRC; Duplicate of SC
MAM-002	24	26	98.0	10R 7/3; Pale Red	Dmm				
MAM-002	26	27	100.0	10R 7/3; Pale Red	Dmm				
MAM-002	27	28.45	80.3	10R 7/3; Pale Red	Dmm				Gradational contact with underling till over ~40 cm
MAM-002	27.69	27.89					MAM002-SE		UW
MAM-002	27.89	28.09					MAM002-SE	204649	SRC
MAM-002	28.45	28.85	80.3	5YR 7/2; Pinkish Grey	Dmm				
MAM-002	28.85	30	80.3	10R 7/3; Pale Red	Dmm				
MAM-002	30	31	100.0	10R 7/3; Pale Red	Dmm				
MAM-002	31	33	34.0	10R 6/2 ; Pale Red	Dmm				
MAM-002	31	31.23					MAM002-SF		
MAM-002	31.23	31.46					MAM002-SF	204650	
MAM-002	33	35.85	30.0	2.5YR 7/2; Pale Red	Dmm				
MAM-002	33.05	33.25					MAM002-SG	215006	SRC
MAM-002	33.25	33.4					MAM002-SG		UW
MAM-002	35.85	36	50.0		Wo				Clasts dominantly (entirely?) sandstone coated in greenish matrix

Drillhole	Top	Bottom	Recovery	Colour	Lithofacies 1	Lithofacies 2	Samples	Cameco_ID	Notes
MAM-002	36	37.47	100.0	5Y 6/2; Light Olive Grey	Fm				Gradational contact over ~50 cm to more whitish fine-grained seds. Laminaed with organic horizons in some areas.
MAM-002	37.47	37.9	100.0	10YR 8.1; White	Fm				Sharp contact with underlying unit
MAM-002	37.9	38.5	100.0	10YR 8.1; White with 10YR 7/1;	Fl				Less compact/competent than both overlying fine-grained units
MAM-002	36	36.16					MAM002-SH		UW; Submitted for pollen/macrofossils
MAM-002	36.16	36.3					MAM002-SI		UW
MAM-002	36.3	36.42					MAM002-SJ		UW
MAM-002	36.42	36.51					MAM002-SK		UW; Submitted for pollen/macrofossils
MAM-002	36.51	36.56					MAM002-SL		UW; Piece of organic material (wood?) present within sample that is to be C14 dated. Also submitted as part of SK for pollen/macrofossils
MAM-002	36.56	36.74					MAM002-SM		UW
MAM-002	36.74	38.84					MAM002-SN		UW
MAM-002	36.96	37.08					MAM002-SO		UW
MAM-002	37.14	37.24					MAM002-SP		UW; Submitted for pollen/macrofossils
MAM-002	37.3	37.41					MAM002-SQ		UW
MAM-002	37.41	37.53					MAM002-SR		UW; Subsampled for paleomag
MAM-002	37.53	37.65					MAM002-SS		UW; Subsampled for paleomag
MAM-002	37.7	37.82					MAM002-ST		UW; Subsampled for paleomag
MAM-002	37.82	37.9					MAM002-SU		UW; Subsampled for paleomag
MAM-002	38.04	38.14					MAM002-SV		UW
MAM-002	38.23	38.3					MAM002-SW		UW
MAM-002	38.3	38.41					MAM002-SX		UW
SNB-001	0	3	5.3		Wo				All intrusives
SNB-001	3	6	27.0		Wo				first 50 cm are boulders - "basement lithology - biotite schist" boulder of 15 cm; syenite boulder of 34 cm. Rest pebbles and cobbles some sedimentary and intrusives.
SNB-001	6	9	20.0		Wo				Sedimentary + inrusives
SNB-001	9	12	9.3		Wo				Sedimentary + inrusives
SNB-001	12	13	62.0	10R 6/3; Pale Red	Dmm				Clay lense at 12.80 m, <1 cm thick
SNB-001	13	15	62.0	2.5YR 7/2; Pale Red	Dmm				Colour transition to a lighter coloured diamicton
SNB-001	15	15.6	100.0	2.5YR 7/2; Pale Red	Dmm				
SNB-001	15.6	18	42.5	2.5YR 7/2; Pale Red	Dmm				
SNB-001	18	21	25.7		Wo				18-33 - ALL sedimentary, mostly sandstone clasts. Most are at least sub-rounded to rounded interspersed with angular clasts.
SNB-001	21	24	11.7		Wo				
SNB-001	24	27	15.3		Wo				
SNB-001	27	30	42.0		Wo				
SNB-001	30	33	13.3		Wo				10 cm of massive sand near the 33 cm marker
TUR-018	0	2	50						One 45 cm boulder then 50 cm of till (10R 8/1; White). Partially washed out. White colour due to rain washing?
TUR-018	2	5	39	10R 8/1; White	Dmm				Washed out. Last 22 cm more pale red.
TUR-018	5	8	91	10R 7/3; Pale Red	Dmm				Washed out at 5-5.58, 6.92-7.07, 7.2-7.33
TUR-018	8	11	98	10R 7/3; Pale Red	Dmm				
TUR-018	11	11.5	100	10R 7/3; Pale Red	Dmm				Last 5 cm washed out
TUR-018	11.5	12.5		10R 7/3; Pale Red	Dmm				Very washed out
TUR-020	0	2	23	10R 8/1; White	Dmm				Fine-grained rich. Loose.
TUR-020	2	5	37						First 45 cm pebbles and cobbles, no matrix. Followed by pale red diamicton
TUR-020	5	8	95	10R 7/3; Pale Red	Dmm				
TUR-020	8	12.5	100	10R 7/3; Pale Red	Dmm				11.74-12 more clay-rich
TUR-020	12.5	12.69					TUR020-SA		UW
TUR-020	12.5	13.3	90	10R 7/2; Pale Red	Dmm				
TUR-020	12.69	12.97					TUR020-SA	97622	SRC
TUR-020									
TUR-021	0	2	10						Pebbles and cobbles, no matrix
TUR-021	2	4.05	25						Pebbles and cobbles, no matrix
TUR-021	4.05	8	100	10R 7/3; Pale Red	Dmm				
TUR-021	4.1	4.35					TUR021-SC		UW
TUR-021	4.35	4.6					TUR021-SC	204634	SRC

Drillhole	Top	Bottom	Recovery	Colour	Lithofacies 1	Lithofacies 2	Samples	Cameco_ID	Notes
TUR-021	5.56	5.86					TUR021-SA	97623	SRC
TUR-021	5.86	5.96					TUR021-SA		UW
TUR-021	8	11	95	10R 7/3; Pale Red	Dmm				
TUR-021	11	12.6	100	10R 7/3; Pale Red	Dmm				
TUR-021	11.61	11.94					TUR021-SB	97624	SRC
TUR-021	11.94	12.03					TUR021-SB		UW
TUR-022	0	2	0						
TUR-022	2	4.6	45		Wo				
TUR-022	4.6	8	96	10R 7/3; Pale Red	Dmm				
TUR-022	5.3	5.4					TUR022-SA		UW
TUR-022	5.4	5.7					TUR022-SA	97625	SRC
TUR-022	8	11	93	10R 7/3; Pale Red	Dmm				
TUR-022	8.84	9.5					TUR022-SB		UW; Collected more sample for pebble counts during 2013 field season
TUR-022	8.95	9.25					TUR022-SB	97626	SRC
TUR-022	10.53	10.74					TUR022-SE	204635	SRC
TUR-022	10.74	11					TUR022-SE		UW
TUR-022	11	12.4	100	10R 7/3; Pale Red	Dmm				
TUR-022	12.1	12.3					TUR022-SC	97628	SRC
TUR-022	11.9	12.4					TUR022-SC		UW; Collected more sample for pebble counts during 2013 field season
TUR-022	12.4	13.1	100	10R 7/3; Pale Red	Dmm				
TUR-022	13.12	13.71					TUR022-SF		UW
TUR-022	13.54	13.71					TUR022-SF	204636	SRC
TUR-022	13.1	15.91	100	10R 7/2; Pale Red	Dmm				Bedrock/till contact at 15.91m. NOTE: last box of core labeled incorrectly (12.4-14.5m when there is 3m of core in box)
TUR-022	15.55	15.76					TUR022-SD	97629	SRC
TUR-022	15.76	15.91					TUR022-SD		UW
TUR-023	0	10.61	6						Minimal core recovery. Pebbles and cobbles present, no matrix.
TUR-023	10.61	14	100	10R 7/3; Pale Red	Dmm				Bedrock/till contact at 14m. Alteration clasts within till up to 45cm from contact.
TUR-024	0	4							Missing
TUR-024	4	8	100	10R 7/3; Pale Red	Dmm				~First 20 cm appears white (suspected to be caused by rain action)
TUR-024	6.3	6.61					TUR024-SA	97630	SRC (measured from 8 m block)
TUR-024	6.61	6.73					TUR024-SA		UW (measured from 8 m block)
TUR-024	8	8.4	100	10R 7/3; Pale Red	Dmm				
TUR-024	8.4	11	84	10R 7/3; Pale Red	Dmm				Very washed out
TUR-024	11	12.9	100	10R 7/3; Pale Red	Dmm				Last 50 cm (12.4-12.9) enriched in altered bedrock material. Appears contact at 12.9, cameco's record - 13.2
TUR-025	0	2	3						Single clast recovered, no matrix
TUR-025	2	4.2	18						Poor recovery. Primarily pebbles averaging 4cm. Matrix content increases in last 10cm of this section.
TUR-025	4.2	5	100	10R 7/3; Pale Red	Dmm				
TUR-025	5	8.1	100	10R 7/3; Pale Red	Dmm				One large cobble from 5-5.24m.
TUR-025	7.2	7.3					TUR025-SA		UW
TUR-025	7.3	7.6					TUR025-SA	97631	SRC
TUR-025	8.1	11	97	10R 7/3; Pale Red	Dmm				Cobbles up to 15cm. One 15cm cobble appears to be altered sandstone.
TUR-025	11	12.4	100	10R 7/3; Pale Red	Dmm				Cobbles up to 14 cm (appears to be thelon formation)
TUR-025	12.4	13							Appears to be primarily altered bedrock material
TUR-025	13	13.3			Dmm				Clay-rich dimicton; contact at 13.3
TUR-028	0	2	10						3 cobbles. NOTE: all core boxes partially washed out.
TUR-028	2	5	33	5YR 7/3; Pink	Dmm				
TUR-028	5	17	100	10R 7/3; Pale Red	Dmm				Some intervals washed out
TUR-028	17	20	100	10R 7/3; Pale Red	Dmm				More washed out than other intervals
TUR-028	20	20.7	100	10R 7/3; Pale Red	Dmm				
TUR-029	0	4.1	28						Missing depth markers for 1st box. Depths are approximate (measured back from second box depth markers). Organic material for first 16 cm follow by pebbles and cobbles, no matrix
TUR-029	4.1	7.64	100		Dmm				
TUR-029	7.64	8	100	10R 7/3; Pale Red	Dmm				

Drillhole	Top	Bottom	Recovery	Colour	Lithofacies 1	Lithofacies 2	Samples	Cameco_ID	Notes
TUR-029	8	11	100	10R 7/3; Pale Red	Dmm				
TUR-029	9.77	9.87					TUR029-SA		UW
TUR-029	10.1	10.34					TUR029-SA	97632	SRC
TUR-029	11	14	100	10R 7/3; Pale Red	Dmm				First 22 cm of left side of box 3 washed out
TUR-029	14	16.9	100	10R 7/3; Pale Red	Dmm				
TUR-031	0	5	25						Pebbles and cobbles; largest cobble 14cm. Last 17cm: diamicton; massive, pale red
TUR-031	5	8	76	10R 6/3; Pale Red	Dmm				Largest cobble up to 18cm. Some sections of till more brown (2.5YR 4/4); probably a result of variations in moisture content
TUR-031	5.77	5.97					TUR031-SA	97633	SRC
TUR-031	6.07	6.17					TUR031-SA		UW
TUR-031	8	11.85	82	10R 6/3; Pale Red	Dmm				
TUR-031	11.85	14	89	10R 7/2; Pale Red	Dmm				
TUR-031	11.2	11.47					TUR031-SC	204629	SRC
TUR-031	11.47	11.66					TUR031-SC		UW
TUR-031	14	17	100	10R 7/2; Pale Red	Dmm				
TUR-031	14.2	14.44					TUR031-SD	204630	SRC
TUR-031	14.44	14.65					TUR031-SD		UW
TUR-031	14.65	14.88					TUR031-SE	204631	SRC; DUPLICATE OF TUR031-SD (CAM204630)
TUR-031	17	17.22					TUR031-SB	97634	SRC
TUR-031	17	18.4	100	10R 7/2; Pale Red	Dmm				
TUR-031	17.22	17.32					TUR031-SB		UW
TUR-031	18.4	20	100	10R 7/2; Pale Red	Dmm				
TUR-031	20	20.8	100	10R 7/2; Pale Red	Dmm				Bedrock/till contact at 20.8m. Altered bedrock at the contact (See photo 1361). Altered grains and clasts evident in till up to at least 1m from bedrock contact.
TUR-031	20	20.26					TUR031-SF	204632	SRC
TUR-031	20.36	20.58					TUR031-SF		UW
TUR-032	0	2	11						Pebbles and cobbles, no matrix
TUR-032	2	5	38	10R 7/3; Pale Red	Dmm				First 11 cm pobbles and cobbles, little matrix
TUR-032	4.26	4.51					TUR032-SC		UW
TUR-032	4.51	4.71					TUR032-SC	204642	SRC
TUR-032	5	8	79	10R 7/3; Pale Red	Dmm				
TUR-032	7.39	7.48					TUR032-SA		UW (measured from 8 m block)
TUR-032	7.48	7.81					TUR032-SA	97635	SRC (measured from 8 m block)
TUR-032	8	11	92	10R 7/3; Pale Red	Dmm				
TUR-032	11	13.2	100	10R 7/3; Pale Red	Dmm				
TUR-032	12.38	12.67					TUR032-SB	97636	SRC (Measured from contact - 13.2)
TUR-032	12.67	12.78					TUR032-SB		UW (Measured from contact - 13.2)
TUR-032									
TUR-034	0	2	10						Pebbles/Cobbles, little recovery
TUR-034	2	5	47	10R 7/3; Pale Red	Dmm				
TUR-034	3.02	3.3					TUR034-SA	97637	SRC
TUR-034	4.85	5					TUR034-SA		UW
TUR-034	5	8	36	10R 7/3; Pale Red	Dmm				
TUR-034	8	11	10						Boulders and cobbles; 2 cm of till prior to 11 m
TUR-034	11	14	38	10R 7/3; Pale Red	Dmm				
TUR-034	12.5	12.7					TUR034-SB	97638	SRC
TUR-034	13.5	13.6					TUR034-SB		UW
TUR-034	14	14.8	44		Dmm				Diamicton, but more matrix and less pebbles/cobbles than units above
TUR-034	14.8	14.95					TUR034-SC	97639	SRC
TUR-034	14.8	14.95	44		Dmm				Diamicton; Matrix-rich
TUR-034	14.95	15.25	44	10R 7/3; Pale Red	Dml	Fl			Laminated diamicton; silty-clay dominated with drop stones. Fl zones are defined within diamict. First 20 cm diamict, last 10 cm are not. Laminations are 2 mm thick.
TUR-034	15.2	15.23					TUR034-SC		UW
TUR-034	15.25	16.7			Dmm				Cobble near contact. Contact is at 16.7 m
TUR-034	16.5	16.55					TUR034-SD		UW
TUR-035	0	5	10						Pebbles and cobbles, no matrix. Last 5 cm pale red till
TUR-035	5	8	100	10R 7/3; Pale Red					

Drillhole	Top	Bottom	Recovery	Colour	Lithofacies 1	Lithofacies 2	Samples	Cameco_ID	Notes
TUR-035	6.06	6.14					TUR035-SA		UW
TUR-035	6.14	6.4					TUR035-SA	97640	SRC
TUR-035	8	12.5	100						
TUR-035	12.05	12.18					TUR035-SB		UW
TUR-035	12.18	12.41					TUR035-SB	97641	SRC
TUR-036	0	2	25						Pebbles/cobbles, little to no recovery
TUR-036	2	5	44	10R 7/4; Pale Red	Dmm				
TUR-036	4.55	4.75					TUR036-SA		UW
TUR-036	4.75	5					TUR036-SA	97642	SRC
TUR-036	5	8	61	10R 7/4; Pale Red	Dmm				
TUR-036	8	8.7	100	10R 7/4; Pale Red	Dmm				
TUR-036	8.7	14	44	10R 7/4; Pale Red	Dmm				
TUR-036	14	16.2	70	10R 7/4; Pale Red	Dmm				16-16.2; can start to visually see clasts of altered bedrock appearing in the core
TUR-036	16.2	16.74	80	10R 7/4; Pale Red	Dmm				
TUR-038	0	5	22						Pebbles and cobbles, no matrix. Last 27 cm pale red Dmm
TUR-038	5	8	89	10R 7/3; Pale Red	Dmm				
TUR-038	6.77	7.04					TUR038-SA	97643	SRC
TUR-038	7.04	7.19					TUR038-SA		UW
TUR-038	8	11	12	10R 7/3; Pale Red	Dmm				
TUR-038	11	14	80	10R 7/3; Pale Red	Dmm				
TUR-038	14	16.3	87	10R 7/3; Pale Red	Dmm				
TUR-038									
TUR-039	0	2	5						Little to no recovery
TUR-039	2	4	24						Pebbles/Small cobbles
TUR-039	4	5	24	10R 7/4; Pale Red	Dmm				
TUR-039	5	8	94	10R 7/4; Pale Red	Dmm				
TUR-039	7.4	7.62					TUR039-SC	204641	SRC
TUR-039	7.62	7.83					TUR039-SC		
TUR-039	8	8.7	100	10R 7/4; Pale Red	Dmm				
TUR-039	8.7	11	70	10R 7/4; Pale Red	Dmm				
TUR-039	11	14	95	10R 7/4; Pale Red	Dmm				
TUR-039	14	16.16	96	10R 7/4; Pale Red	Dmm				Diamicton; massive. 15.5-16.16, the till is rich in clasts of bedrock alteration
TUR-039	14.82	15.1					TUR039-SB	97645	SRC
TUR-039	15.1	15.2					TUR039-SB		UW
TUR-039	15.7	16					TUR039-SA	97644	SRC; Base of till layer is rich in alteration clasts. Sample A should reflect this and sample B used for comparison of till higher in the core
TUR-039	16	16.1					TUR039-SA		UW
TUR-040	0	2	31						Cobbles and boulders, no matrix
TUR-040	2	5	37	10R 7/3; Pale Red	Dmm				Slightly washed out; first 13 cm cobbles and pebbles
TUR-040	5	8	95	10R 7/3; Pale Red	Dmm				Some intervals washed out (most notably at 6.1-6.24, 7.7-8)
TUR-040	5.47	5.74					TUR040-SA	97646	SRC
TUR-040	5.74	5.85					TUR040-SA		UW
TUR-040	8	11	88	10R 7/3; Pale Red	Dmm				Note: Box 2 fairly washed out
TUR-040	11	12.2	100	10R 7/3; Pale Red	Dmm				
TUR-040	12.2	15.7	62		Dmm				Dmm has been 'reworked' and silt and clay deposited elsewhere in the corebox
TUR-040									
TUR-041	0	2	8						P.C.N.M.
TUR-041	2	5	27	10R 7/4; Pale Red	Dmm				
TUR-041	5	6.12	42	10R 7/4; Pale Red	Dmm				
TUR-041	6.12	9.2	100	10R 7/4; Pale Red	Dmm				
TUR-041	8.82	8.97					TUR041-SA		UW
TUR-041	8.97	9.2					TUR041-SA	97647	SRC
TUR-041	9.2	11	98	10R 7/4; Pale Red	Dmm				
TUR-041	11	13.9	94	10R 7/4; Pale Red	Dmm				53 cm boulder at 13.0 m
TUR-041	13.9	15	100	10R 7/4; Pale Red	Dmm				
TUR-041	14.43	14.65					TUR041-SB		UW
TUR-041	14.65	14.9					TUR041-SB	97648	SRC

Drillhole	Top	Bottom	Recovery	Colour	Lithofacies 1	Lithofacies 2	Samples	Cameco_ID	Notes
TUR-042	0	5	13						P.C.N.M.; little bit of till near 5.0 m
TUR-042	5	8	53	10R 7/4; Pale Red	Dmm				
TUR-042	7.55	7.7					TUR042-SA		UW
TUR-042	7.7	7.9					TUR042-SA	97649	SRC
TUR-042	8	11	100	10R 7/4; Pale Red	Dmm				
TUR-042	11	14.2	100	10R 7/4; Pale Red	Dmm				
TUR-042	14.2	18.7	100	10R 7/4; Pale Red	Dmm				
TUR-042	14.4	14.6					TUR042-SB	97650	SRC
TUR-042	14.6	14.7					TUR042-SB		UW
TUR-042	18.7	23.1	100	10R 7/4; Pale Red	Dmm				
TUR-042	20.75	21.01					TUR042-SD	204637	SRC
TUR-042	21.01	21.28					TUR042-SD		
TUR-042	23.1	26	85	10R 7/4; Pale Red	Dmm				Contact at 25.8m, fairly homogeneous core overall
TUR-042	25.16	25.5					TUR042-SC	97651	SRC
TUR-042	25.5	25.8					TUR042-SC		UW
TUR-043	0	5	8						Cobbles and pebbles, no matrix
TUR-043	5	8	74	10R 7/3; Pale Red	Dmm				
TUR-043	7.48	7.6					TUR043-SA		UW (measured from 8 m block)
TUR-043	7.6	7.89					TUR043-SA	97652	SRC (measured from 8 m block)
TUR-043	8	10.7	69	10R 7/3; Pale Red	Dmm				
TUR-043	10.7	11	100	10R 7/3; Pale Red	Dmm				Washed out
TUR-043	11	14.9	100	10R 7/3; Pale Red	Dmm				Washed out from 11-14.9
TUR-043	14.9	17	92	10R 7/3; Pale Red	Dmm				Note: 14.9-19.6 m box washed out
TUR-043	17	19.6	100	10R 7/3; Pale Red	Dmm				
TUR-043	19.6	20	100	10R 7/3; Pale Red	Dmm				Partially washed out
TUR-043	20	21.4	100	10R 7/3; Pale Red	Dmm				Partially washed out
TUR-043	21.4	23	100	10R 7/2; Pale Red	Dmm				Partially washed out
TUR-043	22	22.1					TUR043-SB		UW
TUR-043	22.1	22.4					TUR043-SB	97653	SRC
TUR-044	0	2	75						Pebbles
TUR-044	2	5	32						Pebbles, boulders, cobbles, no matrix. Some till matrix present around boulders.
TUR-044	5	8	46	10R 8/1; White	Dmm				Washed out till, white in colour. Breaks easily.
TUR-044	8	10.5	75	10R 7/3; Pale Red	Dmm				Some intervals washed out
TUR-044	10.5	11	100	10R 7/3; Pale Red	Dmm				
TUR-044	11	14	77						Last 35 cm washed out
TUR-044	12.18	12.46					TUR044-SA	97654	SRC (measured from 11 m block)
TUR-044	12.46	12.6					TUR044-SA		UW (measured from 11 m block)
TUR-044	14	15.5	100	10R 7/3; Pale Red	Dmm				
TUR-044	15.5	17	100	10R 7/3; Pale Red	Dmm				
TUR-044	17	18.1	100	10R 7/3; Pale Red	Dmm				
TUR-044	17.4	17.58					TUR044-SB		UW
TUR-044	17.58	17.92					TUR044-SB	97655	SRC
TUR-044	18	18.1	100	10R 7/3; Pale Red	Dmm				
TUR-045B	0	2	0						
TUR-045B	2	5	25						P.C.N.M.; boulders up to 30cm
TUR-045B	5	8	29	10R 6/3; Pale Red	Dmm				
TUR-045B	8	10.5	100	10R 6/3; Pale Red	Dmm				
TUR-045B	10.5	11	90	10R 6/3; Pale Red	Dmm				
TUR-045B	11	14	71	10R 6/3; Pale Red	Dmm				
TUR-045B	14	16.5	70	10R 6/3; Pale Red	Dmm				
TUR-045B	16.5	17	100	10R 6/3; Pale Red	Dmm				One 37cm boulder
TUR-045B	17	20	95	10R 6/3; Pale Red	Dmm				
TUR-045B	17.99	18.31					TUR045B-SA	97656	SRC
TUR-045B	18.31	18.46					TUR045B-SA		UW
TUR-045B	20	20.9	100	10R 6/3; Pale Red	Dmm				
TUR-045B	20.9	23	91	10R 6/3; Pale Red	Dmm				
TUR-045B	23	25.8	94	10R 6/3; Pale Red	Dmm				

Drillhole	Top	Bottom	Recovery	Colour	Lithofacies 1	Lithofacies 2	Samples	Cameco_ID	Notes
TUR-045B	23.37	23.58					TUR045B-SC	204638	SRC
TUR-045B	23.58	23.76					TUR045B-SC		UW
TUR-045B	25.8	26	100	10R 6/3; Pale Red	Dmm				
TUR-045B	26	29	37	10R 6/3; Pale Red	Dmm				
TUR-045B	26.13	26.45					TUR045B-SB	97657	SRC
TUR-045B	26.45	26.56					TUR045B-SB		UW
TUR-045B	29	32	26	10R 6/3; Pale Red	Dmm				Last 30cm P.C.N.M.
TUR-045B	32	33.77	12	10R 6/3; Pale Red	Dmm				Bedrock-Till contact at 33.77m
TUR-045B									NOTE: Boxes 1, 2 & 3 have washed out intervals
TUR-046	0	3.57	7						Cobbles, no matrix
TUR-046	3.57	5	100	10R 7/3; Pale Red	Dmm				
TUR-046	3.84	4.09					TUR046-SB	204639	SRC
TUR-046	4.09	4.3					TUR046-SB		UW
TUR-046	5	8	48	10R 7/3; Pale Red	Dmm				
TUR-046	7.1	7.22					TUR046-SA		UW (measured from 8 m block)
TUR-046	7.22	7.51					TUR046-SA	97658	SRC (measured from 8 m block)
TUR-046	8	11	98	10R 7/3; Pale Red	Dmm				Note: Till washed out near left end of core (from rain)
TUR-046	11	12.8	100	10R 7/3; Pale Red	Dmm				
TUR-046	12.28	12.5					TUR046-SC		UW
TUR-046	12.56	12.8					TUR046-SC	204640	SRC
TUR-046	12.8	13.6	100	10R 7/3; Pale Red	Dmm				23 cm cobble with similar lithology to bedrock at 10 cm from contact
TUR-047	0	4.1	12						Pebbles and cobbles, till matrix mostly washed out
TUR-047	4.1	5	100	10R 7/3; Pale Red	Dmm				
TUR-047	4.34	4.45					TUR047-SA		UW
TUR-047	4.45	4.74					TUR047-SA	97659	SRC
TUR-047	5	8	100	10R 7/3; Pale Red	Dmm				At 7.25 clay lense (white, several mm in thickness)
TUR-047	8	11.84	100	10R 7/3; Pale Red	Dmm				
TUR-047	10.3	10.4					TUR047-SB		UW
TUR-047	10.4	10.7					TUR047-SB	97660	SRC
TUR-047									
TUR-048	0	6.95	12						P.C.N.M.; various lithologies, one boulder (27cm). Very poor core recovery.
TUR-048	6.95	9	100	10R 7/3; Pale red	Dmm				
TUR-048	9	9.28					TUR048-SA	97662	SRC
TUR-048	9	10.5	100	10R 7/3; Pale red	Dmm				
TUR-048	9.28	9.43					TUR048-SA		UW
TUR-048	10.5	12	100	10R 7/3; Pale red	Dmm				
TUR-048	12	15	100	10R 7/3; Pale red	Dmm				
TUR-048	14.93	15.05					TUR048-SB		UW
TUR-048	15	18	52	10R 7/3; Pale red	Dmm				
TUR-048	15.05	15.31					TUR048-SB	97663	SRC
TUR-048	17.9	18					TUR048-SC		UW
TUR-048	18	18.31					TUR048-SC	97664	SRC
TUR-048	18	18.31	100	10R 7/3; Pale red	Dmm				Bedrock/till contact at 18.31m. In the last 40cm before contact, alteration minerals are present in the till.
TUR-049	NOTE: Core depth								
TUR-049	0	4.19	37						P.C.N.M.; Last 32cm of pebbles and cobbles coated in till matrix.
TUR-049	4.19	4.42	100	10R 8/1; White	Dmm				Clast-poor, matrix rich in silt and clay
TUR-049	4.42	7.12	100	10R 7/3; Pale Red	Dmm				At 4.92m and 5.08m, clay lamination present (10R 8/1; White)
TUR-049	4.51	4.92					TUR049-SC		UW; Brackets the geochemical sample
TUR-049	4.59	4.83					TUR049-SC	204616	SRC
TUR-049	7.12	11.77	100	10R 7/3; Pale Red	Dmm				Right side of core box slightly darker due to higher moisture content; matrix slightly washed out in some areas.
TUR-049	8.76	9					TUR049-SA	97665	SRC
TUR-049	9	9.1					TUR049-SA		UW
TUR-049	11.77	13.19	100	10R 7/3; Pale Red	Dmm				At 12.7m and 13.0m, clay lenses present, each approx. 1cm thick.

Drillhole	Top	Bottom	Recovery	Colour	Lithofacies 1	Lithofacies 2	Samples	Cameco_ID	Notes
TUR-049	13.19	13.44	100	10R 7/3; Pale Red; Sub-mm lami	Fl				Fine-grained unit. Very thin sub-mm clay lamination present. Sand-rich layers present within unit.
TUR-049	13.44	14.31	100	10R 7/3; Pale Red	Dmm				At 13.89m, clay lens 5mm in thickness. Bedrock-Till contact at 14.31m
TUR-049	13.87	14.16					TUR049-SB	97666	SRC
TUR-049	14.16	14.21					TUR049-SB		UW
TUR-050	0	9	19						First 44cm: Pebbles and cobbles, one large boulder. Followed by 78cm of intact till. Remaining 49cm is partially washed out till.
TUR-050	0	7.64	18						P.C.N.M.; Three lithologies identified
TUR-050	7.64	9	18	10R 7/3; Pale Red	Dmm				Slight colour change seen at 8.13 m
TUR-050	7.64	7.84					TUR050-SC	204613	SRC; Not great positional certainty on sample as 0-9 interval fairly washed out, but appears texturally distinct from underling tills
TUR-050	7.84	8.03					TUR050-SC		UW; Note slight colour change in sampled interval, sampled above
TUR-050	9	10.65	63	10R 7/3; Pale Red	Dmm				Dominantly granite clasts. Appears most diamicton was lost in this region.
TUR-050	9	10.65	34	10R 7/3; Pale Red	Dmm				P.C.N.M.; Remaining till is partially washed out.
TUR-050	10.65	12	63	10R 7/3; Pale Red	Dmm				Less cobble-rich, more pebbles
TUR-050	10.65	12	100	10R 7/3; Pale Red	Dmm				Some till sections partially coated in gray film (1mm thickness). Less cobble-rich, more pebbles
TUR-050	11.63	11.72					TUR050-SA		UW
TUR-050	11.72	12					TUR050-SA	97667	SRC
TUR-050	12	12.8	100	10R 7/3; Pale Red	Dmm				
TUR-050	12	15		10R 7/3; Pale Red					
TUR-050	12.8	15	50	10R 7/3; Pale Red	Dmm				Boulder/cobbles present near end of section (~14m).
TUR-050	15	15.4	64	10R 7/2; Pale Red	Dmm				Base of interval: 2 boulders, one of 23cm and one of 32cm in length.
TUR-050	15	16.53	93	10R 7/3; Pale Red	Dmm				Same red diamicton. Bedrock/till contact at 16.53m.
TUR-050	15	15.4		10R 7/2					
TUR-050	15.4	16.51	91	10R 5/4	Dmm				Bedrock-Till contact at 16.51m.
TUR-050	15.4	16.51		10R 5/4					
TUR-050	15.52	15.82					TUR050-SB	97668	SRC
TUR-050	15.82	15.95					TUR050-SB		UW
TUR-051	0	3	17						Pebbles and cobbles, no matrix
TUR-051	3	6	35						Pebbles and cobbles. Last 15cm: pebbles coated with matrix material.
TUR-051	6	7.39	41	10R 7/3; Pale Red	Dmm				
TUR-051	7.39	7.7	100	10R 7/3; Pale Red	Dmm				
TUR-051	7.7	7.8	100	5YR 8/2; Pinkish White	Dmm				Clay and silt rich, no clasts greater than 2cm size. Material much less compact
TUR-051	7.8	9	100	10R 7/3; Pale Red	Dmm				7.97-8.06; Lenses 4-5mm in thickness (in-tact laminations)
TUR-051	8.57	8.67					TUR051-SA		UW
TUR-051	8.67	9					TUR051-SA	97669	SRC
TUR-051	9	12	100	10R 7/3; Pale Red	Dmm				
TUR-051	12	14.3	90						Last 40cm are more red (10R 5/4; Weak Red). Bedrock-Till contact at 14.3m.
TUR-051	12.83	12.9					TUR051-SB		UW
TUR-051	12.9	13.2					TUR051-SB	97670	SRC
TUR-052	0	4	20						P.C.N.M.; About 4 lithologies: volcanic with black minerals, white rock (possibly pegmatite), mafic and granite.
TUR-052	4	6	50						Dominantly cobbles (<16cm), similar lithologies as above
TUR-052	6	9	90	10R 7/2; Pale red	Dmm				20cm of cobbles at the top of this section, containing no matrix.
TUR-052	7.27	7.55					TUR052-SA	97671	SRC
TUR-052	7.55	7.67					TUR052-SA		UW
TUR-052	9	9.6	100	10R 7/2; Pale red	Dmm				
TUR-052	9.6	12	83	10R 7/2; Pale red	Dmm				
TUR-052	12	14.4	89	10R 7/2; Pale red	Dmm				Slight increase in cobble content.
TUR-052	13.94	14.08					TUR052-SB		UW
TUR-052	14.08	14.4					TUR052-SB	97672	SRC
TUR-052	14.4	14.63	89	10R 7/2; Pale red	Dmm				Bedrock/till contact at 16.63m, fairly sharp contact.
TUR-053	0	3	16						Pebbles and cobbles, no matrix
TUR-053	3	6	28						Pebbles and cobbles, no matrix
TUR-053	6	8.35	35						6.09-6.77m; boulder. Followed by 10cm interval of cobbles.
TUR-053	8.35	9	100	10R 7/3; Pale Red	Dmm				

Drillhole	Top	Bottom	Recovery	Colour	Lithofacies 1	Lithofacies 2	Samples	Cameco_ID	Notes
TUR-053	8.45	8.86					TUR053-SA	97673	SRC
TUR-053	8.86	9					TUR053-SA		UW
TUR-053	9	12	89	10R 7/3; Pale Red	Dmm				
TUR-053	11.65	11.8					TUR053-SB		UW
TUR-053	11.8	12					TUR053-SB	97674	SRC
TUR-053	12	14.12	92	10R 7/3; Pale Red	Dmm				Bedrock-Till contact at 14.12
TUR-053	13.83	13.96					TUR053-SC		UW
TUR-053	13.96	14.12					TUR053-SC	97675	SRC
TUR-054	0	3	13						Pebbles and cobbles; no matrix
TUR-054	3	6	19						Pebbles and cobbles; no matrix
TUR-054	6	9	47	10R 7/3; Pale Red	Dmm				Some intervals partially washed out
TUR-054	9	12	73	10R 7/3; Pale Red	Dmm				Slight change in matrix colour as a result of increase in moisture content. Some intervals partially washed out.
TUR-054	11.03	11.14					TUR054-SA		UW
TUR-054	11.14	11.46					TUR054-SA	97676	SRC
TUR-054	12	13.5	75	10R 7/3; Pale Red	Dmm				
TUR-054	13	13.15					TUR054-SC		UW; Clast count only
TUR-054	13.5	15	75	10R 7/2; Pale Red					Colour change visible to more 'purple' core
TUR-054	14.5	14.62					TUR054-SD		UW; Clast count only
TUR-054	15	17.5	79	10R 7/2; Pale Red	Dmm				
TUR-054	17.1	17.2					TUR054-SB		UW
TUR-054	17.2	17.5					TUR054-SB	97678	SRC
TUR-054	17.5	18	96	10R 7/3; Pale Red	Dmm				
TUR-054	18	19.9	66	10R 7/3; Pale Red	Dmm				Intervals in unit appear to be partially washed out. Bedrock-Till contact at 19.9m.
TUR-054	18.18	18.38					TUR054-SE		
TUR-054	18.38	18.58					TUR054-SE	204615	SRC
TUR-055	0	9	8	10R 6/3; Pale red					Very poor recovery. 17cm cobble at the top, followed by 6cm of red diamicton, followed by a 21cm cobble and more red diamicton.
TUR-055	9	12	35	10R 6/3; Pale red	Dmm				20cm cobble at the top of this section.
TUR-055	12	14.17	64	10R 6/3; Pale red	Dmm				Bedrock/till contact at 14.17m, fairly sharp contact. The base of the till (last 20cm) in this section becomes slightly more purple (10R 6/2), and more alteration clasts are visible in the till
TUR-055	12.64	12.93					TUR055-SA	97679	SRC
TUR-055	12.93	13.03					TUR055-SA		UW
TUR-056	0	3	17						Dominantly pebbles with one large granitic cobble (18cm).
TUR-056	3	6	32	10R 6/3; Pale red	Dmm				First 38cm: extremely outwashed, one granitic boulder (28cm). Remaining section appears to also be washed out
TUR-056	6	9	100	10R 7/3; Pale red	Dmm				From 6.17-6.32: one cobble of 15cm. Composed of clasts of several lithologies.
TUR-056	6.4	6.66					TUR056-SA	97680	SRC
TUR-056	6.66	6.82					TUR056-SA		UW
TUR-056	9	12	100	10R 7/3; Pale red	Dmm				
TUR-056	12	13.3	100	10R 7/3; Pale red	Dmm				
TUR-056	12.81	12.94					TUR056-SB		UW
TUR-056	12.94	13.3					TUR056-SB	97681	SRC
TUR-056	13.3	15.36	96	10R 7/3; Pale red	Dmm				Bedrock/till contact at 15.36m.
TUR-057	0	3	10		Wo				
TUR-057	3	5.27	13		Wo				
TUR-057	5.27	6	100	10R 7/3; Pale Red	Dmm				
TUR-057	5.37	5.6					TUR057-SA		UW; Further pebbles collected via wet sieving during 2013 field season
TUR-057	5.6	6					TUR057-SA	97688	SRC
TUR-057	6	9	85	10R 7/3; Pale Red	Dmm				
TUR-057	7.02	7.22					TUR057-SF		UW
TUR-057	7.22	7.47					TUR057-SF	204561	SRC
TUR-057	9	12	97	10R 7/3; Pale Red	Dmm				
TUR-057	9.1	9.3					TUR057-SG		UW
TUR-057	9.3	9.6					TUR057-SG	204562	SRC; Dup (Sampled directly above TUR057-SB) to tie in with 2012 samples
TUR-057	9.6	10					TUR057-SB	97689	SRC
TUR-057	9.87	10.08					TUR057-SB		UW; Further pebbles collected via wet sieving during 2013 field season

Drillhole	Top	Bottom	Recovery	Colour	Lithofacies 1	Lithofacies 2	Samples	Cameco_ID	Notes
TUR-057	11.57	11.75					TUR057-SH		UW
TUR-057	11.75	12					TUR057-SH	204563	SRC
TUR-057	12	13.39	0.1	10R 7/3; Pale Red	Dmm				
TUR-057	12.67	12.86					TUR057-SI		UW
TUR-057	12.86	13.1					TUR057-SI	204564	SRC
TUR-057	13.39	14.1		10R 7/2; Pale Red					Unit changes colour to a more 'purpley colour'
TUR-057	13.52	13.71					TUR057-SC		UW; Further pebbles collected via wet sieving during 2013 field season
TUR-057	13.71	14.1					TUR057-SC	97690	SRC
TUR-057	14.1	15	96	10R 7/2; Pale Red	Dmm				
TUR-057	14.49	14.72					TUR057-SJ		UW
TUR-057	14.72	15					TUR057-SJ	204565	SRC
TUR-057	15	16.01	100	10R 7/2; Pale Red	Dmm				
TUR-057	15.58	15.77					TUR057-SK		UW
TUR-057	15.77	15.97					TUR057-SK	204566	SRC
TUR-057	16.01	16.1	100	10R 6/3; Pale Red; Sub-mm lami	Fld				White laminations are sub-millimeter, drop stones are evident at top of unit and within unit. Some snady intervals also interbedded
TUR-057	16.04	16.05					TUR057-SD		UW
TUR-057	16.1	16.17	100	10R 6/3; Pale Red	Dml				
TUR-057	16.17	16.86	100	10R 5/4; Weak Red	Dmm			Bedrock-Till contact at 16.86m	
TUR-057	16.26	16.66					TUR057-SE	97691	SRC
TUR-057	16.66	16.77					TUR057-SE		UW
TUR-058	0	12	21	10R 7/3; Pale Red	Dmm				Unable to distinguish where majority of core was lost; suspected to near the top
TUR-058	11.33	11.59					TUR058-SC	204614	SRC: Not great positional certainty in 0-12 interval; measured form 12 m block
TUR-058	11.59	11.8					TUR058-SC		UW; measured from 12 m block
TUR-058	12	13.22	93	10R 7/3; Pale Red	Dmm				NOTE: Same subtle colour change observed to that in TUR-057. Initial -SA sample is potentially at the 'contact'
TUR-058	12.3	12.58					TUR058-SA	97692	SRC
TUR-058	12.58	12.67					TUR058-SA		UW
TUR-058	13.22	13.51					TUR058-SB		UW
TUR-058	13.22	13.38	93	10R 7/2; Pale Red	Dml				Fine-grained rich diamicton with clay laminations, clast poor
TUR-058	13.38	13.51	93	10R 7/2; Pale Red	Fld	S			Laminated fine-grained sediments with dropstones present. Sand particles are also plentiful in. Sample taken for further lab analysis
TUR-058	13.51	14.7	100	10R 7/2; Pale Red	Dmm				Bedrock-Till contact at 14.7m. Last 28cm: diamicton very rich in alteration
TUR-058	14.28	14.47					TUR058-SD		UW; For pebs and grain size
TUR-059	0	2.6	8						Pebbles for the top 7cm of various lithologies: gneissic, Thelon Formation. Largest cobble is granitic.
TUR-059	2.6	2.85					TUR059-SB	UW	2.7-2.85 sieved in the field for pebbles
TUR-059	2.6	3	100	2.5YR 7/2	Dmm				
TUR-059	2.85	3					TUR059-SB	204567	SRC
TUR-059	3	6	15						One large gneissic boulder with large white bands.
TUR-059	6	9	93	10R 7/3: Pale Red	Dmm				
TUR-059	9	9.5	100	10R 7/3: Pale Red	Dmm				
TUR-059	9.5	12.1	89	10R 7/3: Pale Red	Dmm				Start of a colour gradation towards brown.
TUR-059	12	14.2	98	10R 7/2; Pale Red	Dmm	Dml			At 12.95m-13.15m: clay lens. Below 13.15m, diamicton; massive with clay lenses present at 13.55-13.58m and at 13.91-13.97m. Sample taken at 12.4-12.6m (SRC), 12.25-12.4M (UW); [TUR059-SA]
TUR-059	12.25	12.4					TUR059-SA		UW
TUR-059	12.4	12.6					TUR059-SA	97693	SRC
TUR-059	14.2	14.65	100	10R 7/2; Pale Red	Dmm				Increase in cobble content from 14.55-15m, including sandstone and granite. Cobble size up to 13cm.
TUR-059	14.65	15.46	100	Weak Red	Dmm				Bedrock/till contact at 15.46m. From 15.19-15.24m, piece of purple bedrock separates diamicton layers.
TUR-060	0	3	17						Pebbles and cobbles, no matrix.
TUR-060	3	6	49	10R 7/3; Pale Red	Dmm				Interval is fairly washed out
TUR-060	5.56	5.82					TUR060-SA	97694	SRC (measured from 6m block)
TUR-060	5.82	6					TUR060-SA		UW; More pebbles collected via wet sieving during 2013 field season (5.93-6)
TUR-060	6	9	100	10R 7/3; Pale Red	Dmm				

Drillhole	Top	Bottom	Recovery	Colour	Lithofacies 1	Lithofacies 2	Samples	Cameco_ID	Notes
TUR-060	8.2	8.4					TUR060-SG	204617	SRC: DUPLICATE of TUR060-F
TUR-060	8.4	8.6					TUR060-SF		UW
TUR-060	8.6	8.83					TUR060-SF	204569	SRC
TUR-060	9	12	100	10R 7/3; Pale Red	Dmm				Some clay-rich lenses (10.2m, 10.5m)
TUR-060	11.22	11.52					TUR060-SB	97695	SRC
TUR-060	11.52	11.72					TUR060-SB		UW; More pebbles collected via wet sieving during 2013 field season (11.62-11.72)
TUR-060	12	15	88	10R 7/3; Pale Red	Dmm				Clay lens (12.4m)
TUR-060	15	15.47	97	10R 7/3; Pale Red	Dmm				
TUR-060	15	15.3					TUR060-SE	204568	SRC
TUR-060	15.3	15.42					TUR060-SE		UW
TUR-060	15.47	15.49			S				15.47-15.49m: fine-grained sand with sub-mm silt and clay laminations.
TUR-060	15.49	15.6		10R 7/3; Pale Red	Dmm				15.49-15.6m: Dmm, 10R 7/3. 15.6-15.63m: sandy diamict bounded by clay lenses.
TUR-060	15.6	15.75			Suc	Fl			15.63-15.635m: laminated silty clay. 15.635-15.75m: silty-clay at base (15.75m), coarsening upwards to medium to coarse-grained sand lenses. Sample of whole interval sent to UW.
TUR-060	15.63	15.75					TUR060-SC		UW
TUR-060	15.75	18		10R 7/3; Pale Red	Dmm				
TUR-060	16.94	17.14					TUR060-SD		UW; More pebbles collected via wet sieving during 2013 field season (16.94-17.04)
TUR-060	17.14	17.4					TUR060-SD	97696	SRC
TUR-060	18	18.2	100	10R 7/3; Pale Red	Dmm				Bedrock-Till contact at 18.2m. 17.9-18.2m: diamicton rich in altered bedrock material
TUR-061	0	10	24	10R 7/3; Pale Red	Dmm				First 46 cm P.C.N.M.; some matrix in last 15 cm. Last 9 cm pebbles and cobbles, no matrix. Rest of section in-tact. White clay lense at 90 cm from 10 m block
TUR-061	10	12	88	10R 7/3; Pale Red	Dmm				
TUR-061	11.52	11.6					TUR061-SA		UW
TUR-061	11.6	11.87					TUR061-SA	97697	SRC
TUR-061	12	15	80	10R 7/3; Pale Red	Dmm				
TUR-061	15	17	93	10R 7/3; Pale Red	Dmm				Sharp contact, not much bedrock incorporated at base of till (more competent bedrock). 16.23-16.24 clay with fine-grained sand intervals.
TUR-061	15.77	15.9					TUR061-SB		UW
TUR-061	15.9	16.16					TUR061-SB	97698	SRC
SNB-002	0	6	9.50		Wo				
SNB-002	6	9	20.00		Wo				
SNB-002	9	12	36.67		Wo				
SNB-002	11.32	12	100.00	10R 8/2; Pinkish White	Dmm				
SNB-002	11.7	11.92					SNB002-SA		UW
SNB-002	12	15	34.67	5YR 8/2; Pinkish White	Dmm				Sandier diamict than above
SNB-002	15	15.1	100.00	5YR 8/2; Pinkish White	Dmm				
SNB-002	15.1	15.3	100.00	laminations white with pinkish w	Fl				Sandy laminae present within unit as well
SNB-002	15.3	18	15.00	10R 7/2; Pale Red	Dmm				Sandy diamict with fines washed out and deposited at end of box
SNB-002	18	21	17.67		Wo				Washed out material in rest of box mostly Thelon clasts
SNB-002	21	24	10.00		Wo				
SNB-002	24	27	10.33		Wo				
SNB-002	27	30	10.00		Wo				
SNB-002	30	33	8.33		Wo				
SNB-002	33	36	8.00		Wo				
SNB-002	36	39	35.00		Wo				
SNB-002	39	42	26.67		Wo				
SNB-002	42	45	10.33		Wo				
SNB-002	45	48	13.33		Wo				
SNB-002	48	51	16.67		Wo				
SNB-002	51	54	24.00		Wo				
SNB-002	54	57	61.33		Wo				
SNB-002	57	60	34.67		Wo				
SNB-002	60	63	6.67		Wo				
SNB-002	63	66	21.00		Wo				
SNB-002	66	69	6.67		Wo				
SNB-002	69	71.7	12.96		Wo				

Drillhole	Top	Bottom	Recovery	Colour	Lithofacies 1	Lithofacies 2	Samples	Cameco_ID	Notes
Legend									

lithocodes

Dmm = Diamicton, matrix supported, massive

Dml = Diamicton, matrix supported, laminated

Wo = Washed out. Pebbles and cobbles present, no matrix

Fm = Fine-grained (silt + clay), massive

Fl = Fine-grained, laminated

Fld = Fine-grained, laminated, dropstones present

Sm = Sand, massive

S = Sand

Suc = Sand, upward coarsening

P.C.N.M. = Pebbles, cobbles, no matrix present

UW = University of Waterloo Sample

SRC = Saskatchewan Research Council Sample

Appendix G – Additional Figures

Select Drillcore Photos

Photo 1: Drillcore TUR-057

Photo 2: Drillcore TUR-049

Photo 3: Drillcore TUR-033

Photo 4: Drillcore TUR-022

Photo 5: Drillcore MAM-002

Select Field Photos

Photo 6: Kames observed west of the Ayra drilling target.

Photo 7: Station 13-AB-219. Boulder lagged drumlin sampled near the Ayra grid.

Photo 8: Example of a boulder lagged drumlin sampled near the Ayra drilling target.

Photo 9: Example of a mudboil sampled near the Tatiggaq drilling target.

Photo 10: Section 12-MR-073 clast fabric locations. 13-AB-265 (Top). 13-AB-242 and 13-AB-241 (Bottom).

Photo 11: Photo exhibiting the bedrock topography (dotted yellow line) in relation to Till Fabric 13-AB-241 (red X). Paleo-ice flow inferred from bedrock striae is from right to left.

Photo 12: Station 13-TH-257. Three generations of striae exhibited on a mafic dyke indicating a shift in ice flow from 310°-284°- 270°.

Photo 13: Station 13-TH-257. Striae widening down-ice similar to 'nail-head' striae, indicating ice flow toward the south (180°).

Photo 14: Station 13-TH-257. Striae indicating an old 255° likely protected by the more resistant felsic rock and is cross-cut by later 280° ice flow.

Photo 15: Station 13-TH-257. Striae widening in the down-ice direction cross-cutting previous striae and a crescentic gouge indicating ice flow in the 270° direction, the last ice flow this outcrop experienced.

Photo 16: Very well polished outcrops in the west portion of the field study area, with meter + striae in some instances.

Photo 17: Paleo-shoreline with large boulders, likely indicative of a lake/marine ice encroached shoreline.

Photo 18: Perched boulder near the Qamanaarjuk Lake camp

Photo 19: Lodged boulder within Unit 1 of the Qamanaarjuks section. Striae on top indicating ice flow in the 330° direction.

Photo 20: Two unit stratigraphy observed from the helicopter. The top unit is a sandy surficial material with developed frost polygons. Note this section was not thoroughly investigated in the field.

Photo 21: Muskox roaming a delta.

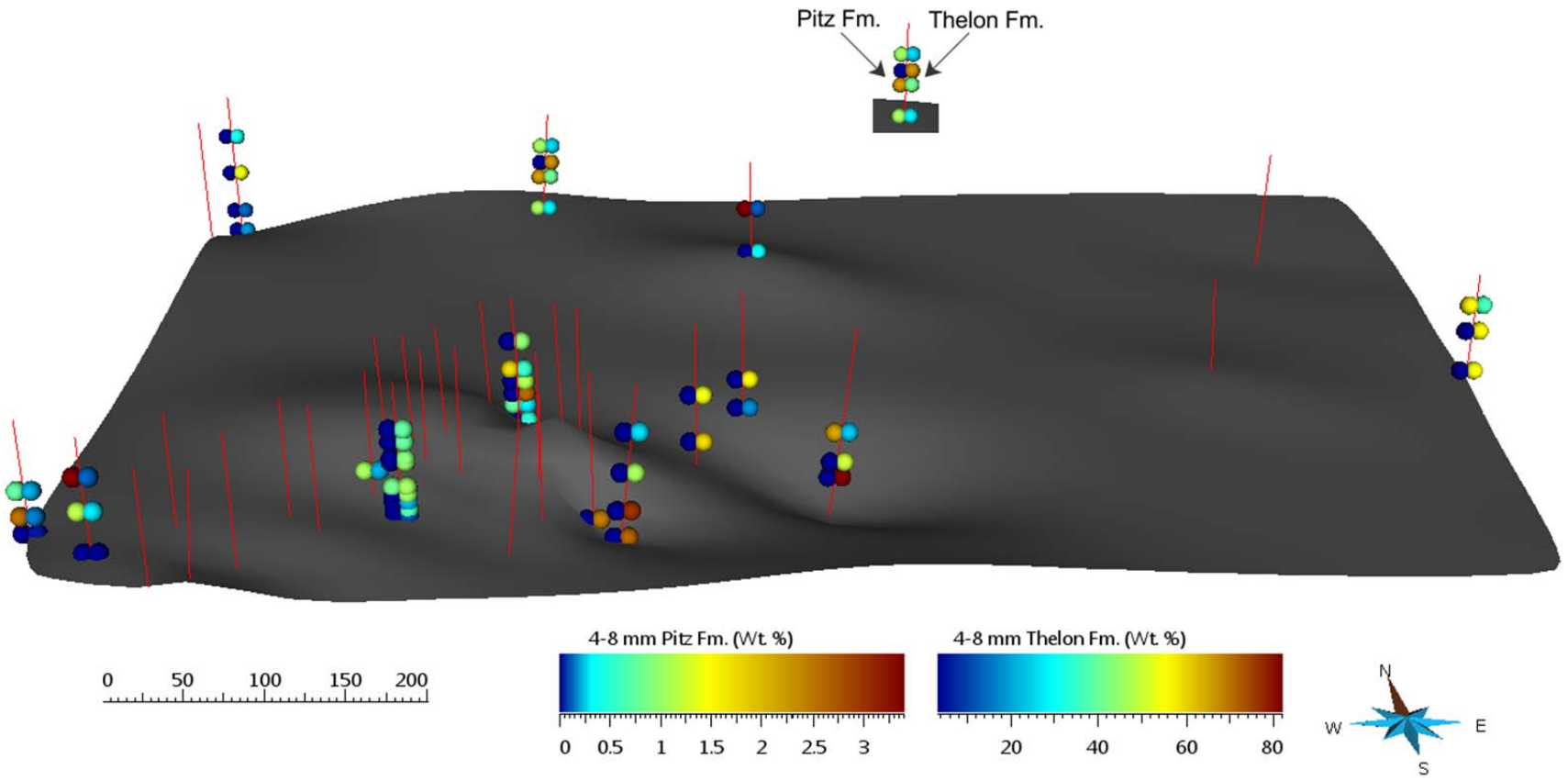

Figure 1: Oblique north view of the Tatiggaq grid. 4-8 mm clast counts are presented with Pitz Fm. presented on the left side of the drillcore paths and Thelon Fm. on the right side. Vertical Exaggeration = 5.

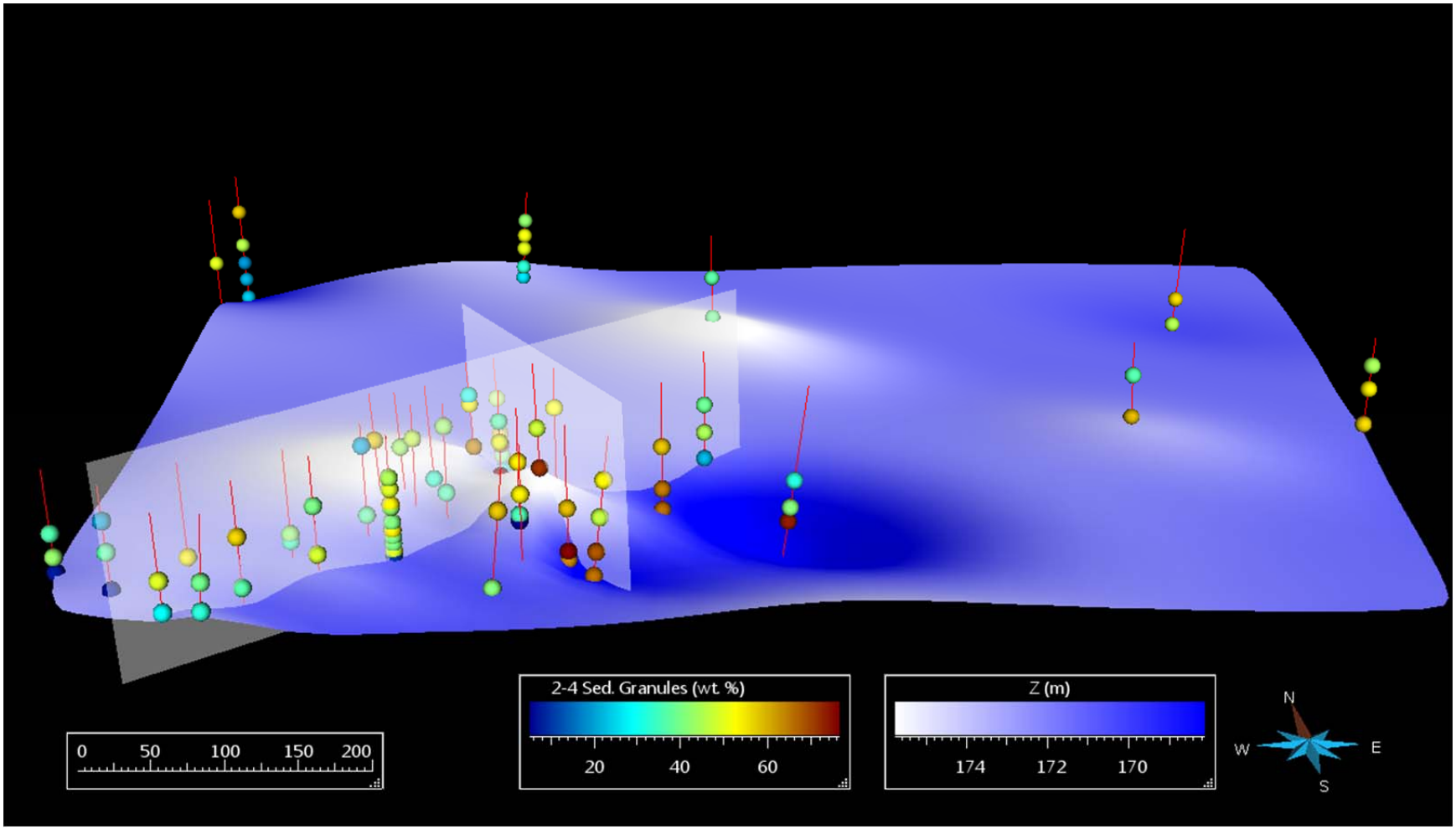

Figure 2: Oblique 3D view of the Tatiggaq grid from the south. The bedrock topography is interpolated from drillholes and dark blue colours represent lower elevations. 2-4 mm sedimentary granule counts are displayed along drillcore paths. The location of the cross-sections displayed in Chapter 3 are shown by the white semi-transparent vertical planes. Vertical Exaggeration = 5x

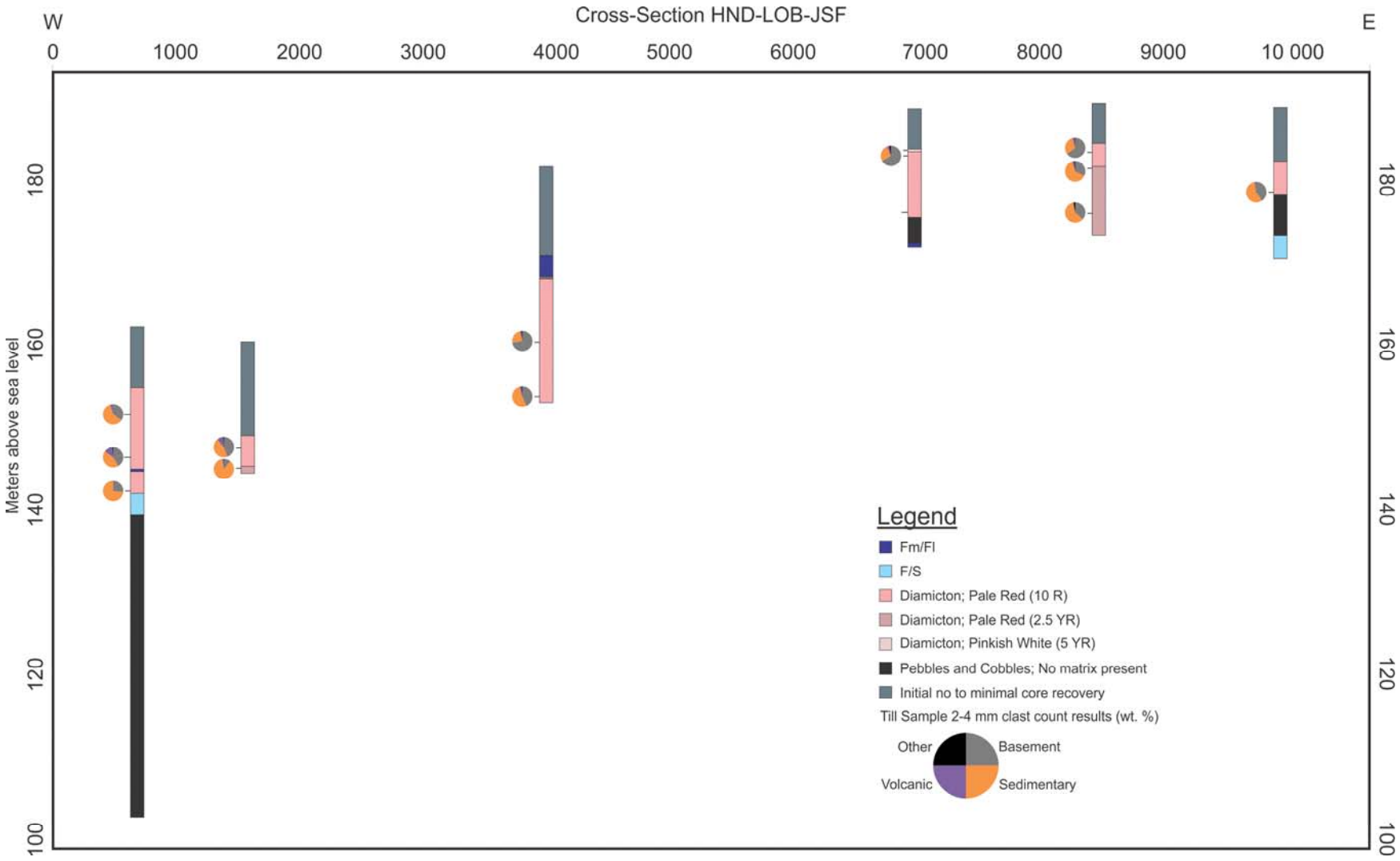

Figure 3: Cross-section HND-LOB-JSF displaying stratigraphic logs compiled from drillcores logging. This logging revealed the dominant subsurface Quaternary sediment is diamicton, which is typical various shades of Pale Red (munsell 10R and 2.5YR). Note the clast counts reveal the diamicton samples from lower in the drillcores are relatively enriched in sedimentary clasts.

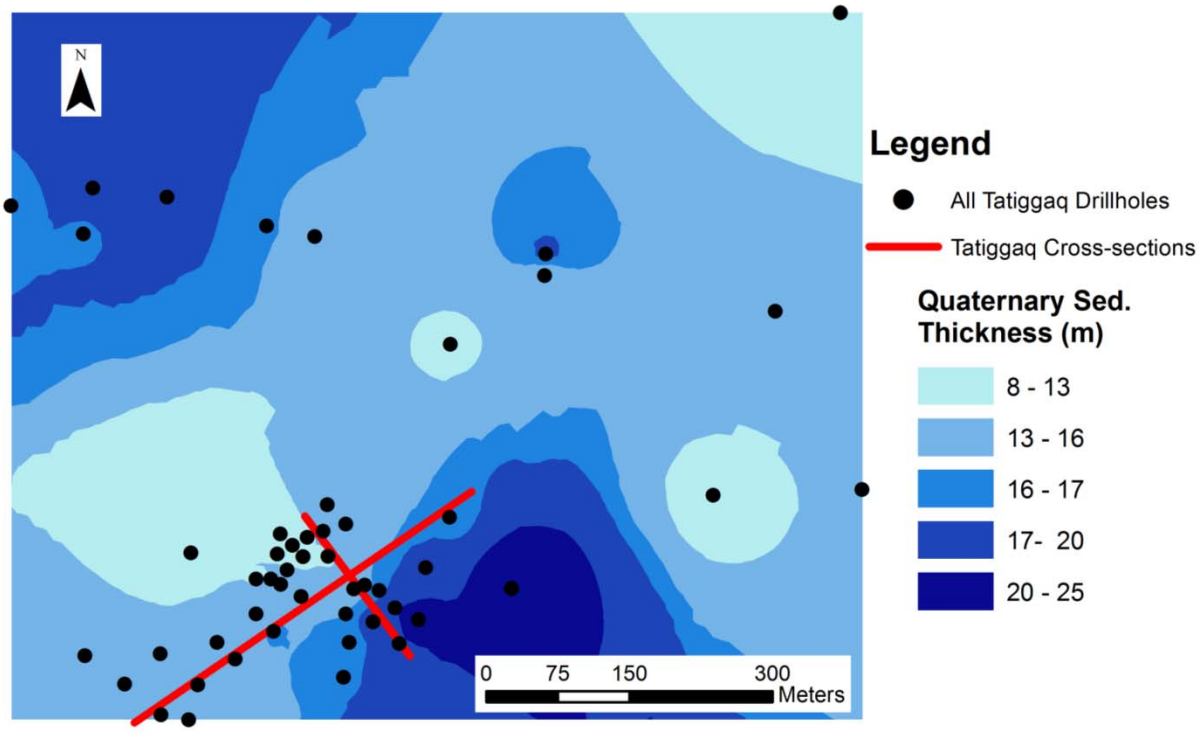

Figure 4: Inverse distance weighted interpolation of Quaternary sediment thickness at the Tatiggaq grid from drillhole data.

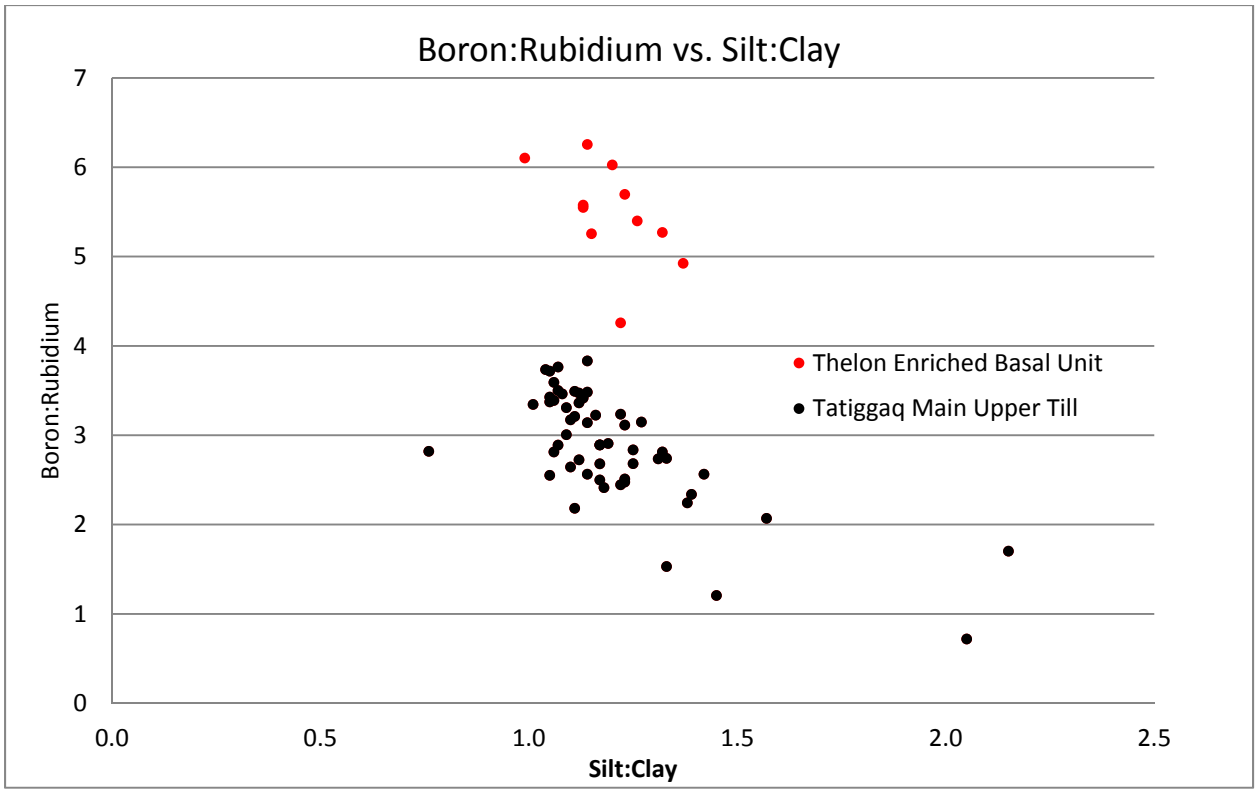

Figure 5: B:Rb ratio plotted against the silt:Clay ratio of the sample. It is apparent from the results that the proportion of clay has an influence on the magnitude of the B;Rb signal. It is not the only controlling factor on the B:Rb signal as samples enrich in Thelon Fm., have a high B:Rb signal, with a similar silt:clay ratio.

Appendix H – Till Fabric Measurements

A-Axis Dip Direction (°)	A-Axis Dip (°)	A-Axis (cm)	B-Axis (cm)	C-Axis (cm)	A:B	B:C
13-AB-241						
324	**32**	2.2	1.1	1	2.00	1.10
255	**4**	1.5	0.8	0.4	1.88	2.00
316	**47**	2.3	1.1	0.8	2.09	1.38
249	**46**	2.6	1.4	1.3	1.86	1.08
320	**25**	2.2	1.4	1	1.57	1.40
285	**0**	2.5	1.1	1.1	2.27	1.00
27	**24**	3.3	1.8	1.6	1.83	1.13
305	**0**	2.3	1.5	0.6	1.53	2.50
154	**18**	1.2	0.7	0.4	1.71	1.75
125	**37**	4.1	2.6	1.7	1.58	1.53
208	**25**	2.6	1.6	1.2	1.63	1.33
330	**14**	2.2	0.8	0.8	2.75	1.00
310	**11**	1.7	0.8	0.5	2.13	1.60
160	**14**	3	1.8	1.3	1.67	1.38
320	**41**	2.7	1.8	0.8	1.50	2.25
3	**15**	2.5	1.5	0.6	1.67	2.50
112	**64**	1.5	0.9	0.5	1.67	1.80
17	**70**	2.5	1.5	1.4	1.67	1.07
250	**5**	2.2	1.2	0.9	1.83	1.33
320	**3**	1.2	0.6	0.5	2.00	1.20
296	**52**	2.9	1.9	1.2	1.53	1.58
10	**6**	1.7	0.7	0.7	2.43	1.00
10	**35**	2.4	1.5	1	1.60	1.50
324	**11**	2	1	0.9	2.00	1.11
9	**9**	1.8	1	0.8	1.80	1.25
295	**24**	2.4	1.5	1.3	1.60	1.15
318	**32**	3	1.6	1.2	1.88	1.33
112	**13**	1.9	1	0.9	1.90	1.11
24	**4**	3	2	0.8	1.50	2.50
4	**27**	2.5	1.3	1.2	1.92	1.08
13-AB-242						
154	**15**	1.8	1.1	0.9	1.64	1.22
346	**37**	2.5	1.3	1	1.92	1.30
14	**12**	2.1	1.2	0.8	1.75	1.50
135	**25**	4.8	2.8	1.9	1.71	1.47
102	**30**	1.5	0.9	0.8	1.67	1.13
233	**38**	2.2	1.3	1	1.69	1.30
146	**40**	3.6	2	1.8	1.80	1.11
220	**26**	1.4	0.9	0.4	1.56	2.25
191	**33**	1.6	1	0.5	1.60	2.00
152	**18**	2	1.1	0.8	1.82	1.38
354	**12**	3.7	1.7	1.7	2.18	1.00
151	**12**	4.4	2.1	1	2.10	2.10
172	**38**	2.2	1	0.7	2.20	1.43
205	**3**	1.5	0.7	0.5	2.14	1.40
150	**26**	2.1	1.3	1	1.62	1.30
183	**24**	1.7	1	0.6	1.70	1.67
170	**26**	1.6	0.9	0.7	1.78	1.29
175	**28**	1	0.6	0.3	1.67	2.00

145	**25**	1.7	0.7	0.5	2.43	1.40
131	**65**	1.8	1.2	1.1	1.50	1.09
351	**1**	1.9	0.9	0.7	2.11	1.29
260	**44**	1.1	0.6	0.4	1.83	1.50
160	**15**	1.1	0.9	0.4	1.22	2.25
1	**11**	2.5	1.5	1.2	1.67	1.25
184	**13**	2.2	1.2	0.6	1.83	2.00
158	**5**	0.9	0.5	0.4	1.80	1.25
220	**34**	1.2	0.7	0.5	1.71	1.40
98	**16**	3	1.8	1	1.67	1.80
146	**30**	1.5	1	0.6	1.50	1.67
154	**25**	1.8	0.8	0.8	2.25	1.00
13-AB-243						
70	**16**	2.4	1.3	1.1	1.85	1.18
150	**12**	1.3	0.8	0.6	1.63	1.33
216	**8**	2.7	1.4	1	1.93	1.40
58	**5**	2.1	1.3	0.9	1.62	1.44
320	**35**	2.3	1.3	0.5	1.77	2.60
243	**34**	2.2	1.1	0.8	2.00	1.38
325	**64**	2.4	1.6	0.6	1.50	2.67
261	**18**	1.7	0.9	0.6	1.89	1.50
228	**12**	3	2	0.9	1.50	2.22
87	**42**	2.3	1.5	1	1.53	1.50
234	**21**	2.3	1.4	0.9	1.64	1.56
180	**34**	2.2	1.2	1.1	1.83	1.09
239	**10**	1.6	1	0.6	1.60	1.67
85	**23**	3.4	1.6	1.1	2.13	1.45
254	**24**	1.5	0.9	0.6	1.67	1.50
156	**35**	1.1	0.6	0.3	1.83	2.00
256	**13**	2	1.2	0.8	1.67	1.50
140	**1**	3	1.9	1.6	1.58	1.19
114	**24**	1.9	0.8	0.4	2.38	2.00
96	**21**	2.1	1.3	1	1.62	1.30
230	**9**	2.2	1.4	1	1.57	1.40
135	**10**	2.1	1.2	1.2	1.75	1.00
245	**25**	2.1	1.3	1	1.62	1.30
170	**34**	2.3	1.3	0.9	1.77	1.44
256	**19**	2.2	1.2	1	1.83	1.20
283	**4**	2.5	1.5	0.9	1.67	1.67
262	**16**	3	1.6	0.8	1.88	2.00
316	**15**	2.5	1.4	1.1	1.79	1.27
265	**24**	2.7	1.7	1.2	1.59	1.42
13-AB-258						
300	**18**	2.4	1.3	1.2	1.85	1.08
340	**20**	2.5	1.5	0.5	1.67	3.00
13	**9**	3.1	1.6	1.1	1.94	1.45
40	**35**	2.3	1.4	1.2	1.64	1.17
145	**16**	2.8	1.6	1	1.75	1.60
290	**44**	1.5	1	0.7	1.50	1.43
34	**16**	2.2	1.3	0.7	1.69	1.86
20	**26**	2.3	1.5	0.8	1.53	1.88

294	**40**	4	2.4	2	1.67	1.20
54	**22**	2.3	1.3	1	1.77	1.30
138	**16**	6.4	2.6	2.5	2.46	1.04
29	**8**	1.6	0.8	0.5	2.00	1.60
225	**26**	3.5	1.2	0.6	2.92	2.00
61	**60**	1.7	1	0.9	1.70	1.11
215	**44**	2	0.9	0.7	2.22	1.29
165	**15**	1.8	0.8	0.7	2.25	1.14
325	**10**	2.4	1.3	0.7	1.85	1.86
14	**6**	1.5	0.9	0.6	1.67	1.50
340	**34**	4.1	2.2	1.6	1.86	1.38
18	**28**	2.5	1.7	1	1.47	1.70
305	**18**	2.2	1.4	0.9	1.57	1.56
24	**9**	2.7	1.5	1.1	1.80	1.36
28	**40**	3.4	1.7	1.4	2.00	1.21
75	**41**	3	1.9	1.4	1.58	1.36
140	**20**	2	1.1	0.4	1.82	2.75
30	**15**	1.7	1	0.6	1.70	1.67
11	**8**	1.8	1.2	0.8	1.50	1.50
32	**23**	2.3	1.5	1	1.53	1.50
130	**24**	7.2	3.8	3.1	1.89	1.23
322	**25**	2.8	1.7	0.9	1.65	1.89

A-Axis Dip Direction (°)	A-Axis Dip (°)	B-Axis Dip Direction (°)	B-Axis Dip (°)	A-Axis (cm)	B-Axis (cm)	C-Axis (cm)	A:B*	B:C
13-AB-265								
53	**26**	**141**	**25**	2.3	0.9	0.8	2.56	1.13
240	**21**	**146**	**14**	1.9	0.9	0.6	2.11	1.50
26	**10**	**120**	**9**	1.4	0.7	0.3	2.00	2.33
75	**10**	**335**	**5**	1.6	0.8	0.6	2.00	1.33
270	**60**	**180**	**20**	2.1	1.1	0.8	1.91	1.38
64	**28**	**142**	**7**	2.8	1.5	1.3	1.87	1.15
54	**32**	**312**	**34**	1.3	0.7	0.5	1.86	1.40
79	**9**	**169**	**19**	3.9	2.1	1.7	1.86	1.24
219	**25**	**129**	**68**	2.4	1.3	1.1	1.85	1.18
59	**18**	**144**	**25**	2.2	1.2	0.7	1.83	1.71
26	**36**	**290**	**36**	3.3	1.8	1.1	1.83	1.64
230	**9**	**145**	**35**	1.8	1	0.6	1.80	1.67
315	**11**	**234**	**30**	2.7	1.5	1.2	1.80	1.25
80	**38**	**325**	**46**	1.6	0.9	0.5	1.78	1.80
266	**28**	**65**	**76**	2.6	1.5	1.2	1.73	1.25
265	**4**	**350**	**76**	1.7	1	0.9	1.70	1.11
282	**16**	**3**	**57**	2.2	1.3	0.5	1.69	2.60
30	**15**	**125**	**38**	2.2	1.3	0.9	1.69	1.44
288	**40**	**200**	**28**	2	1.2	0.7	1.67	1.71
78	**22**	**348**	**25**	1.5	0.9	0.6	1.67	1.50
55	**18**	**149**	**10**	2.3	1.4	1	1.64	1.40
295	**4**	**210**	**5**	1.8	1.1	0.7	1.64	1.57
330	**12**	**225**	**38**	1.3	0.8	0.3	1.63	2.67
14	**2**	**106**	**24**	2.1	1.3	1.1	1.62	1.18
96	**9**	**24**	**46**	2.1	1.3	0.4	1.62	3.25
33	**5**	**107**	**10**	1.1	0.7	0.4	1.57	1.75
142	**16**	**69**	**42**	2.2	1.4	1	1.57	1.40
358	**16**	**85**	**47**	3.1	2	1	1.55	2.00
300	**21**	**49**	**46**	1.7	1.1	0.5	1.55	2.20
242	**5**	**132**	**21**	2	1.3	1	1.54	1.30
78	**8**	**164**	**43**	2	1.3	0.8	1.54	1.63
41	**9**	**307**	**4**	1.8	1.2	0.8	1.50	1.50
45	**12**	**123**	**3**	0.9	0.6	0.3	1.50	2.00
215	**64**	**112**	**26**	2.2	1.5	0.6	1.47	2.50
338	**27**	**73**	**18**	2.2	1.5	0.9	1.47	1.67
356	**6**	**94**	**10**	1.6	1.1	1	1.45	1.10
348	**22**	**245**	**18**	1.6	1.1	0.5	1.45	2.20
304	**20**	**212**	**45**	3.3	2.3	1.6	1.43	1.44
80	**22**	**127**	**7**	1	0.7	0.5	1.43	1.40
3	**9**	**88**	**6**	2.1	1.5	0.9	1.40	1.67
88	**14**	**356**	**17**	2.8	2	1.1	1.40	1.82
230	**15**	**150**	**16**	1.8	1.3	0.9	1.38	1.44
100	**37**	**350**	**62**	2.3	1.7	1.2	1.35	1.42
52	**0**	**320**	**12**	1.2	0.9	0.2	1.33	4.50

202	**16**	**5**	**6**	4.3	3.3	2.5	1.30	1.32
305	**5**	**218**	**56**	1.3	1	0.6	1.30	1.67
135	**8**	**45**	**20**	2.4	1.9	1	1.26	1.90
212	**12**	**103**	**53**	3.7	3	2.1	1.23	1.43
308	**30**	**225**	**12**	1.8	1.5	1	1.20	1.50
260	**30**	**153**	**10**	5.9	5	3.4	1.18	1.47
160	**32**	**248**	**10**	2.7	2.3	1.8	1.17	1.28

Note:

***Only those measurements whos A:B ratio was greater than 1.50 was used within the analysis**

Appendix I – Beta Analytic Radiocarbon Dating Results

Beta Analytic Inc.
4985 SW 74 Court
Miami, Florida 33155 USA
Tel: 305 667 5167
Fax: 305 663 0964
Beta@radiocarbon.com
www.radiocarbon.com

Consistent Accuracy . . .
. . . Delivered On-time

February 12, 2014

Mr. Martin Ross
University of Waterloo
200 University Avenue West
Waterloo, ON N2L 3G1
Canada

RE: Radiocarbon Dating Result For Sample MAM002-SL

Dear Mr. Ross:

Enclosed is the radiocarbon dating result for one sample recently sent to us. The sample provided plenty of carbon for accurate measurement and the analysis proceeded normally. As usual, the method of analysis is listed on the report with the results and calibration data is provided where applicable.

The web directory containing the table of all your results and PDF download also contains pictures including, most importantly the portion actually analyzed. These can be saved by opening them and right clicking. Also a cvs spreadsheet download option is available and a quality assurance report is posted for each set of results. This report contains expected versus measured values for 3-5 working standards analyzed simultaneously with your sample.

The reported result is accredited to ISO-17025 standards and the analysis was performed entirely here in our laboratories. Since Beta is not a teaching laboratory, only graduates trained in accordance with the strict protocols of the ISO-17025 program participated in the analyses. When interpreting the result, please consider any communications you may have had with us regarding the sample.

If you have specific questions about the analyses, please contact us. Your inquiries are always welcome.

Our invoice will be emailed separately. Please, forward it to the appropriate officer or send VISA charge authorization. Thank you. As always, if you have any questions or would like to discuss the results, don't hesitate to contact me.

Sincerely,

Digital signature on file

BETA ANALYTIC INC.
DR. M.A. TAMERS and MR. D.G. HOOD
4985 S.W. 74 COURT
MIAMI, FLORIDA, USA 33155
PH: 305-667-5167 FAX:305-663-0964
beta@radiocarbon.com

REPORT OF RADIOCARBON DATING ANALYSES

Mr. Martin Ross

Report Date: 2/12/2014

University of Waterloo

Material Received: 1/28/2014

Sample Data	Measured Radiocarbon Age	13C/12C Ratio	Conventional Radiocarbon Age(*)
Beta - 371428	NA	-30.5 o/oo	> 43500 BP

SAMPLE : MAM002-SL
ANALYSIS : AMS-Standard delivery
MATERIAL/PRETREATMENT : (wood): acid/alkali/acid
COMMENT:

(1) The 14C activity was extremely low and almost identical to the background signal. In such cases, indeterminate errors associated with the background add non-measurable uncertainty to the result. Always, the result should be considered along with other lines of evidence. The most conservative interpretation of age is infinite (i.e. greater than).

(2) A Measured Radiocarbon Age is not reported for infinite dates since corrections may imply a greater level of confidence than is appropriate.

Dates are reported as RCYBP (radiocarbon years before present, "present" = AD 1950). By international convention, the modern reference standard was 95% the 14C activity of the National Institute of Standards and Technology (NIST) Oxalic Acid (SRM 4990C) and calculated using the Libby 14C half-life (5568 years). Quoted errors represent 1 relative standard deviation statistics (68% probability) counting errors based on the combined measurements of the sample, background, and modern reference standards. Measured 13C/12C ratios (delta 13C) were calculated relative to the PDB-1 standard.

The Conventional Radiocarbon Age represents the Measured Radiocarbon Age corrected for isotopic fractionation, calculated using the delta 13C. On rare occasion where the Conventional Radiocarbon Age was calculated using an assumed delta 13C, the ratio and the Conventional Radiocarbon Age will be followed by "*". The Conventional Radiocarbon Age is not calendar calibrated. When available, the Calendar Calibrated result is calculated from the Conventional Radiocarbon Age and is listed as the "Two Sigma Calibrated Result" for each sample.

Appendix J – Pollen and Macrofossil Analysis Results

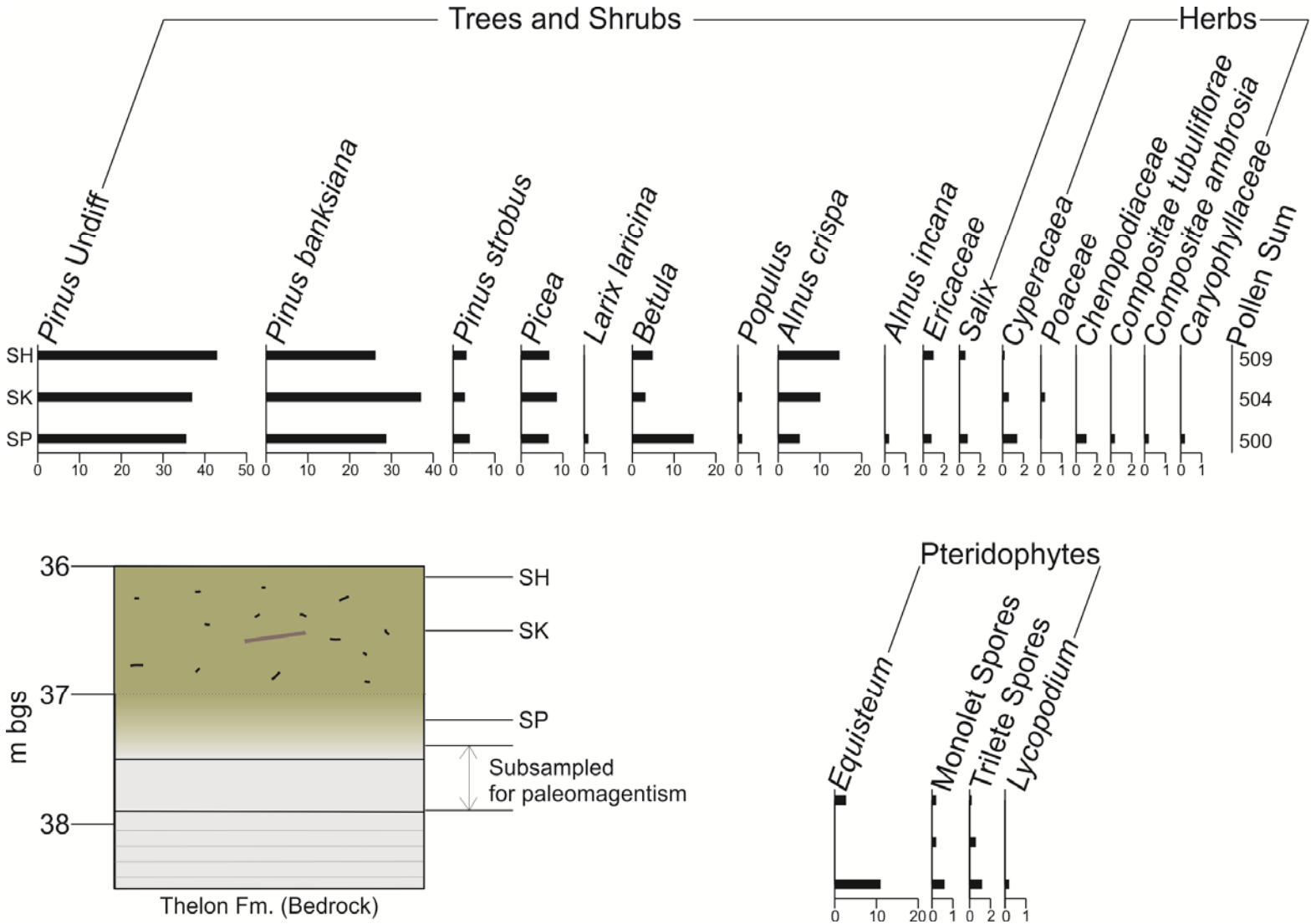

Figure 1: Results of the pollen analysis conducted on the non-glacial sediments at the base of drillcore MAM-002. The region subsampled for paleomagnetism (Appendix K) is also exhibited.

UNIVERSITÉ LAVAL
Faculté de foresterie, de géographie et de géomatique
Département de géographie

Québec, le 28 novembre 2013

M. Martin Ross
Department of Earth and Environmental Sciences
University of Waterloo
200 University Avenue West
Waterloo, Ontario, Canada

Objet : Analyses macrofossile et sporopollinique des échantillons MAMM002-SH, MAMM002-SK et MAMM002-SP

Monsieur,

Vous trouverez ci-après le rapport des analyses macrofossile et sporopollinique effectuées sur les échantillons MAMM002-SH, MAMM002-SK et MAMM002-SP provenant d'un forage. Les analyses ainsi que la rédaction du rapport ont été effectuées par Mme Élisabeth Robert, professionnelle de recherche spécialisée en analyse macrofossile et sporopollinique au Laboratoire de paléoécologie terrestre du Centre d'études nordiques de l'Université Laval. En espérant le tout à votre satisfaction, n'hésitez pas à nous contacter si vous avez besoin d'informations supplémentaires.

Martin Lavoie
Professeur titulaire
Département de géographie
et Centre d'études nordiques
Université Laval
Pavillon Abitibi-Price
2405, rue de la Terrasse
Québec (Québec)
G1V 0A6

Téléphone : 418-656-2131, poste 2230
Courriel : martin.lavoie@cen.ulaval.ca

Analyse macrofossile des échantillons MAM002-SH, MAM002-SK et MAM002-SP provenant d'un forage

Les analyses macrofossiles des échantillons MAM02-SH, MAM02-SK et MAM02-SP ont effectuées au Laboratoire de paléoécologie terrestre du Centre d'études nordiques de l'Université Laval par Mme Élisabeth Robert. Les échantillons ont trempé pendant plusieurs jours dans 500 ml d'une solution de métahexaphosphate de sodium 5 %, renouvelée trois fois pour les échantillons MAM02-SH et MAM02–SK afin de bien nettoyer et séparer le matériel présent dans la matrice argileuse séchée. Le matériel a ensuite été rincé sous jet d'eau délicat dans des tamis superposés de maille 850, 450 et 180 micromètres.

L'analyse macrofossile des trois échantillons a été faite sur un volume de 50 cm^3 de matériel en deux étapes d'analyse de 25 cm^3. Cette approche, dite des rendements décroissants, a été adoptée afin de déterminer le minimum de matériel à analyser pour obtenir un maximum de diversité des macrorestes végétaux ou autres. Pour les trois échantillons, l'analyse du deuxième 25 cm^3 n'a pas permis de trouver de pièces absentes dans le premier 25 cm^3. Les pièces ont été identifiées à l'aide des collections de référence de pièces actuelles et de pièces fossiles du Laboratoire de paléoécologie terrestre ainsi qu'à l'aide d'ouvrages de référence (Lévesque et al., 1988 ; Montgomery, 1977). Les résultats sont présentés dans le Tableau 1.

Les trois échantillons contiennent très peu de pièces fossiles, l'échantillon **MAM00–SP** étant celui qui en contient le plus. Toutes les pièces végétales présentes sont très petites, considérablement sous la taille requise pour en faire une identification autre que générique (charbons, fragments ligneux ou végétaux). À l'exception de quelques fragments de feuilles de plantes vasculaires dicotylédones et une graine de *Drosera* (MAM02-SP), seules des feuilles de sphaignes (MAM02-SP) et de mousses brunes (MAM02-SH et MAM02-SP) ont été trouvées. Le *Cristatella mucedo* et les *Plumatella* sont des bryozoaires habitant des eaux douces stagnantes ou courantes (Pennack, 1978). Les *Daphnia* sont de petits crustacés d'eaux douces dont la majorité des espèces se rencontrent dans les eaux stagnantes d'étangs, de lacs ou de mares ; quelques espèces peuvent aussi coloniser les eaux saumâtres.

Analyse sporopollinique des échantillons MAM002-SH, MAM002-SK et MAM002-SP provenant d'un forage

Pour chaque échantillon, trois centimètres cubes de matériel ont été prélevés et traités selon la méthode de Faegri et Iversen (1989) adaptée pour les échantillons argileux en remplaçant l'hydroxyde de potassium (KOH) par du métahexaphosphate de sodium ($(NaPO_3)_6$) afin de briser la structure de l'argile. Au début du traitement chimique, un volume connu d'une suspension de pollen exotique d'*Eucalyptus globulus*, dont la concentration fut préalablement déterminée, a été ajouté à chacun des échantillons afin de calculer la concentration pollinique (nombre de grains par centimètre cube de sédiments) des échantillons. La suite des traitements consiste en une série d'attaques chimiques (HCl 10 %, acide fluorhydrique, acide acétique, anhydride acétique et acide sulfurique) permettant d'extraire les grains de pollen et les spores des sédiments. Les grains de pollen et les spores ont été identifiés et dénombrés au microscope à un grossissement de 400×. Seuls les grains des plantes vasculaires terricoles (arbres, arbustes, herbes) sont inclus dans la somme pollinique de base. Les spores des ptéridophytes ne sont pas incluses dans la somme pollinique mais leurs pourcentages sont quand même calculés en utilisant la somme pollinique de base. Les résultats des analyses sporopolliniques sont présentés en pourcentages dans le Tableau 2 avec les informations suivantes : somme pollinique, nombre de grains d'*Eucalyptus globulus* dénombrés et concentration pollinique de l'échantillon.

L'échantillon MAM002-SP présente le plus grand nombre de taxons (Tableau 2), le cortège des plantes herbacées y est nettement plus riche que celui des deux autres échantillons. Malgré cette plus grande diversité, la concentration pollinique de cet échantillon est peu élevée en comparaison des deux autres échantillons. L'échantillon MAM002-SK est celui qui présente la plus forte concentration pollinique.

Dans les trois échantillons, les grains de pollens de plantes arborées dominent largement. Les conifères sont beaucoup plus abondants que les feuillus. Parmi les conifères, le taxon le mieux représenté est le *Pinus* sp. (pin) avec un pourcentage total de plus de 68 % dans chaque échantillon. Un grand nombre de grains de pollen de *Pinus* entiers ayant pu être identifiés à l'espèce, il apparait que le *Pinus banksiana* est nettement plus abondant que le *Pinus strobus*. Le nombre élevé de *Pinus* sp. s'explique par le fait que ces grains de pollen sont constitués d'un corps et de deux

ballonnets qui se brisent facilement, empêchant ainsi l'identification à l'espèce. Le *Picea* sp. (épinette), un taxon difficilement identifiable à l'espèce sur la base des seuls critères anatomiques, est plus abondant que le *Pinus strobus*. Un seul grain de pollen de *Larix laricina* (mélèze laricin) a été trouvé dans l'échantillon MAM002-SP. Le principal taxon feuillu est le *Betula* (bouleau) qui ne peut pas non plus être identifié à l'espèce. Son pourcentage est au moins quatre fois plus élevé dans l'échantillon MAM002-SP que dans les deux autres échantillons.

Dans les trois échantillons les arbustes sont dominés par l'*Alnus* type *crispa* (aulne crispé), un seul grain de pollen d'*Alnus* type *rugosa* (aulne rugueux) ayant été trouvé dans l'échantillon MAM002-SP. À l'exception de l'échantillon MAM002-SK, les grains de pollen de la famille des éricacées et du genre *Salix* sont aussi présents mais en faible quantité.

Les plantes herbacées sont représentées par les cypéracées dans les trois échantillons. Un grain de pollen de graminées a été rencontré dans l'échantillon MAM002-SK. L'échantillon le plus diversifié, le MAM00-SP, contient cinq taxons herbacés. Enfin, les spores des ptéridophytes sont aussi plus abondantes dans l'échantillon MAM002-SP que dans les deux autres échantillons. Les spores d'*Equisetum* (prêle) sont particulièrement nombreux.

RÉFÉRENCES

Faegri, K. et Iversen, J. (1989), Textbook of Pollen Analysis, 4ième éd., révisée par K. Faegri, P.E. Kaland et K. Krzywinski, Wiley, Chichester.

Lévesque, P.E.M., Dinel, H. et Larouche, A., 1988, Guide illustré des macrofossiles végétaux des tourbières du Canada, Agriculture Canada, Publication No. 1817.

Montgomery, F.H., 1977, Seeds and Fruits of Plant of Eastern Canada and Northeastern United States. Buffalo, University of Toronto Press, Toronto.

Pennack, R.W., 1978, Fresh-water Invertebrates of the United States, John Wiley & Sons.

Élisabeth Robert
Professionnelle de recherche
Centre d'études nordiques
Université Laval
Québec

28 novembre 2013

Tableau 1. Pièces macrofossiles présentes dans les échantillons MAMM002-SH, -SK et –SP.

	MAMM002-SH	MAMM002-SK	MAMM002-SP
VÉGÉTAUX			
Charbons	392	29	150-175
Fragments végétaux (ligneux et autres)	30-40	15-25	40-50
Fragments de feuilles de dicotylédones	1	0	1
Drosera sp., graines (drosera)	0	0	1
Mousses brunes, feuilles	2	0	15-20
Sphagnum sp., feuilles	0	0	10-15
Fragments de feuilles de dicotylédones	1	0	1
Macrofossile hyalin non identifié	27	0	39
ANIMAUX			
Cristatella mucedo, statoblastes (cristatelle moisissure)	12	4	88
Plumatella sp., statoblastes (plumatelle)	1	1	79
Daphnia sp., ephippies (daphnies)	0	0	30
INSECTES			
Acari, corps entiers	0	0	2
Chironomides, capsules céphaliques	0	0	30
Autres fragments d'insectes	23	2	4

Tableau 2. Pourcentages des grains de pollen et des spores des échantillons MAM002-SH, MAM002-SK et MAM002-SP.

ÉCHANTILLON	MAM002-SH	MAM002-SK	MAM002-SP
ARBRES			
CONIFÈRES			
Pinus sp. (Pin)	43	36,9	35,8
Pinus banksiana (Pin gris)	26,1	37,1	28,8
Pinus strobus (Pin blanc)	3,3	3	4
Pinus (Pin), pourcentage total	72,4	77	68,6
Picea sp. (Épinette)	6,9	8,7	6,9
Larix laricina (Mélèze laricin)	0	0	0,2
FEUILLUS			
Betula sp. (Bouleau)	4,9	3,17	14,4
Populus sp. (Peuplier)	0	0,2	0,2
ARBUSTES			
Alnus type *crispa* (Aulne crispé)	14,7	10,1	5,2
Alnus type *incana* (Aulne rugueux)	0	0	0,2
Ericaceae (famille des éricacées)	1	0	0,8
Salix sp. (Saule)	0,6	0	0,8
HERBES			
Cyperaceae (famille des cypéracées)	0,2	0,6	1,4
Poaceae (Graminées)	0	0,2	0
Chenopodiaceae (famille des chénopodiacées)	0	0	1
Tubuliflorae (famille des composées)	0	0	0,4
Type Ambrosia (famille des composées)	0	0	0,2
Caryophyllaceae (famille des caryophyllacées)	0	0	0,2
Nombre de taxons polliniques	8	9	15
Pourcentages des groupes de plantes vasculaires			
Arbres	83,5	89,1	90
Arbustes	16,3	10,1	7
Herbes	0,2	0,8	3,2
Somme pollinique	509	504	500
Nombre de grains d'*Eucalyptus globulus*	22	9	133
Concentration pollinique (grains/cm^3)	857,461	2,075,425	139,328
PTÉRIDOPHYTES			
Equisteum sp. (Prêle)	1,4	0	11
Spores monolètes	0,2	0,2	0,6
Spores trilètes	0,2	0,6	1,2
Lycopodium sp. (Lycopode)	0	0	0,2

Appendix K – Paleomagentic Analysis Results

Lethbridge_Sample_ID	Core_Sample (MAM002-__)	Summary of Results
RTH_011	SR	RTH011-normal, magnetite, some hematite
RTH_013	ST	RTH013-normal with a reversed overprint, magnetite with some hematite
RTH-014	ST	RTH014-normal, mostly fine-grained hematite
RTH_015	SR	RTH015-normal, magnetite and hematite mix
RTH_016	SR	RTH-016-normal, magnetite
RTH_017	ST	RTH-017-normal, very shallow inclination (possibly mis-oriented sample) hematite-rich
RTH_018	SU	RTH018-normal, shallow inclination, magnetite, minor hematite
RTH_019*	SS	RTH019-reversed, magnetite
RTH_020*	SS	RTH020-reversed, magnetite

*Note the reversed results are from the same field sample. It is interpreted that this result is an artifact of the field sampling and that the top and bottom of the sample was improperly logged.

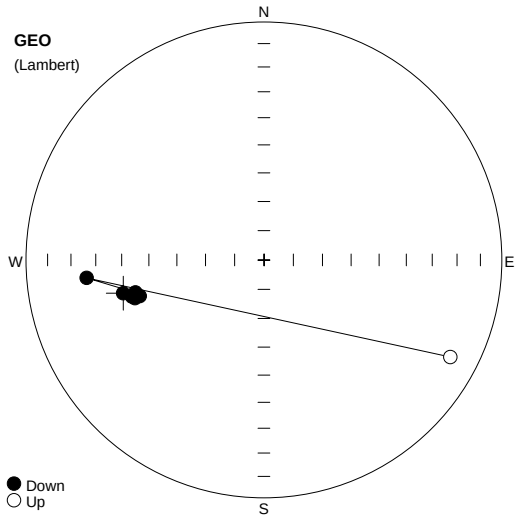

RTH011

AF demag

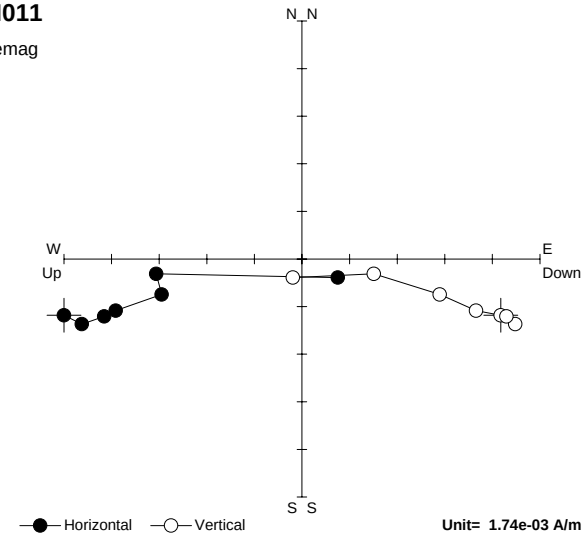

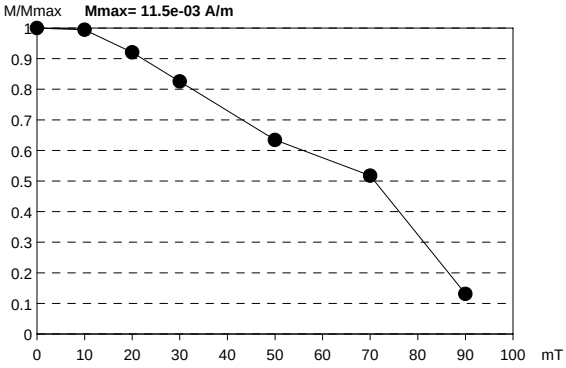

Name	Site	Latitude	Longitude	Height	Rock	Age	Fm	SDec	SInc	BDec	BInc	FDec	FInc	P1	P2	P3	P4	Note
RTH011								0	90					6	0	12	90	

#	State	M[A/m]	Dsp	Isp	Dge	Ige	Dtc	Itc	Dfc	Ifc	Prec	Limit1	Limit2	Note	K[e-06 SI]
1	NRM	11.5e-03	50.1	-10.3	256.7	39.1					1.0				
2	10mT	11.5e-03	45.9	-12.0	253.5	42.9					1.0				
3	20mT	10.6e-03	44.0	-11.5	253.8	44.8					1.0				
4	30mT	9.53e-03	46.9	-11.4	254.5	42.0					1.0				
5	50mT	7.32e-03	45.5	-10.2	255.8	43.6					1.0				
6	70mT	5.98e-03	63.8	-5.2	264.2	26.1					1.0				
7	90mT	1.51e-03	255.7	-26.8	117.5	-12.7					1.0				

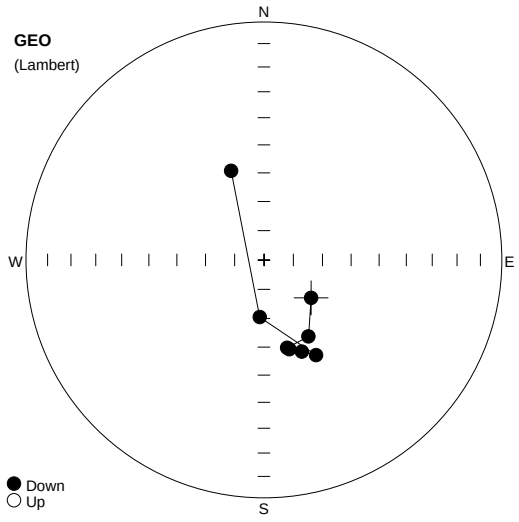

RTH013

AF demag

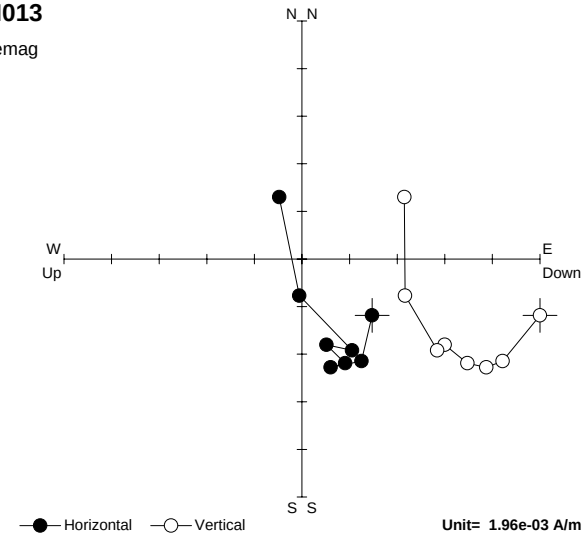

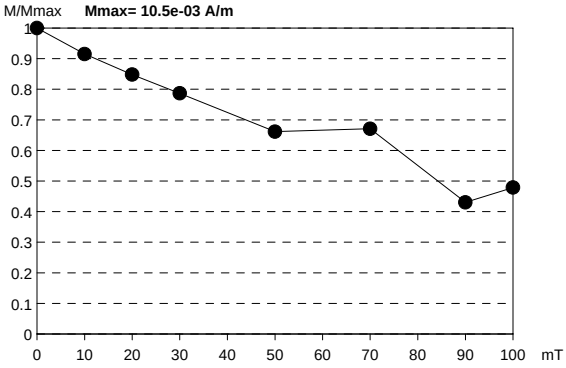

Name	Site	Latitude	Longitude	Height	Rock	Age	Fm	SDec	SInc	BDec	BInc	FDec	FInc	P1	P2	P3	P4	Note
RTH013								0	90					6	0	12	90	

#	State	M[A/m]	Dsp	Isp	Dge	Ige	Dtc	Itc	Dfc	Ifc	Prec	Limit1	Limit2	Note	K[e-06 SI]
1	NRM	10.5e-03	343.6	-12.8	128.8	69.3					0.0				
2	10mT	9.60e-03	343.5	-26.0	149.8	59.5					0.0				
3	20mT	8.89e-03	351.2	-30.1	165.2	58.7					0.0				
4	30mT	8.25e-03	345.4	-31.3	157.5	55.7					0.0				
5	50mT	6.94e-03	350.3	-30.7	164.1	58.0					0.0				
6	70mT	7.03e-03	339.7	-32.4	151.3	52.4					0.0				
7	90mT	4.51e-03	1.5	-19.6	184.2	70.4					0.0				
8	100mT	5.02e-03	12.6	30.5	339.8	57.2					0.0				

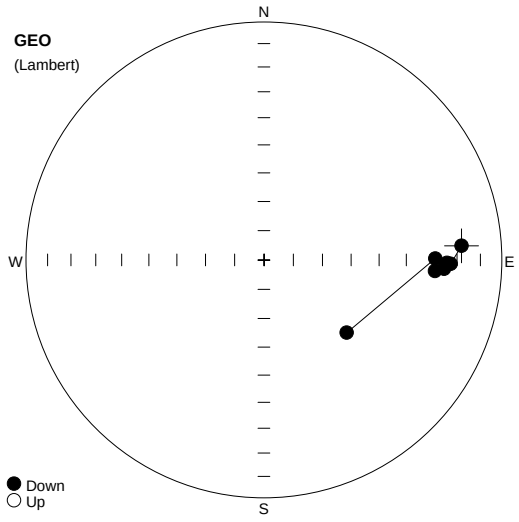

RTH014

AF demag

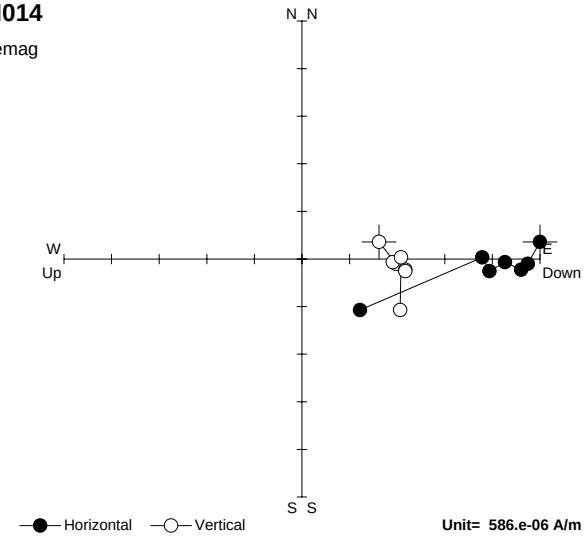

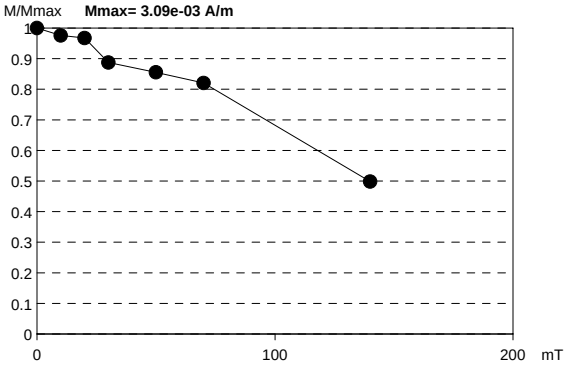

Name	Site	Latitude	Longitude	Height	Rock	Age	Fm	SDec	SInc	BDec	BInc	FDec	FInc	P1	P2	P3	P4	Note
RTH014								0	90					6	0	12	90	

#	State	M[A/m]	Dsp	Isp	Dge	Ige	Dtc	Itc	Dfc	Ifc	Prec	Limit1	Limit2	Note	K[e-06 SI]
1	NRM	3.09e-03	288.0	3.9	85.9	17.9					1.0				
2	10mT	3.01e-03	292.6	-1.1	91.2	22.6					1.0				
3	20mT	2.99e-03	295.2	-2.5	92.8	25.2					1.0				
4	30mT	2.74e-03	294.1	-0.8	90.9	24.1					1.0				
5	50mT	2.64e-03	298.8	-3.3	93.7	28.8					1.0				
6	70mT	2.53e-03	298.8	0.5	89.5	28.8					2.0				
7	140mT	1.54e-03	329.4	-24.1	131.3	51.8					1.0				

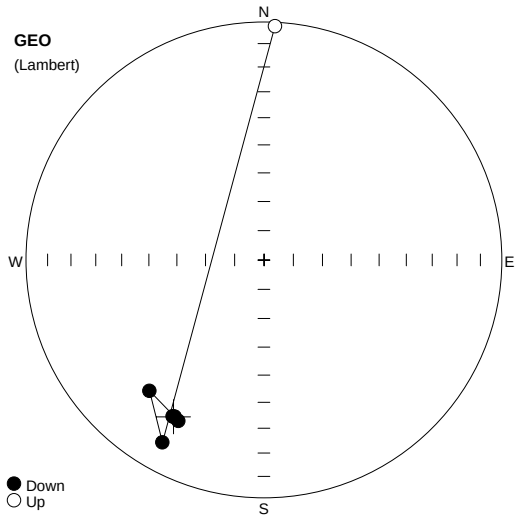

RTH015

AF demag

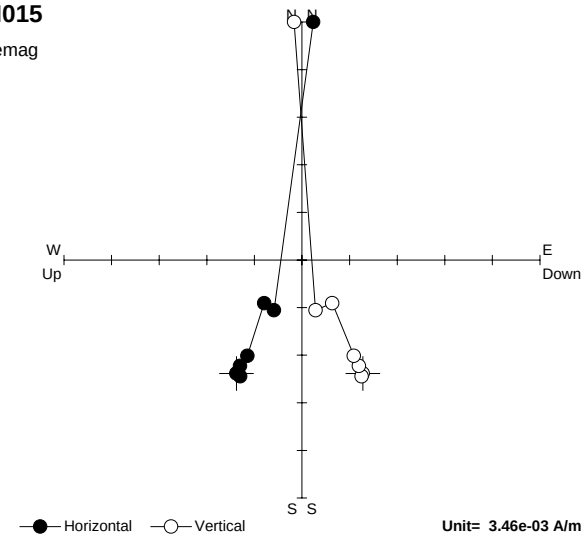

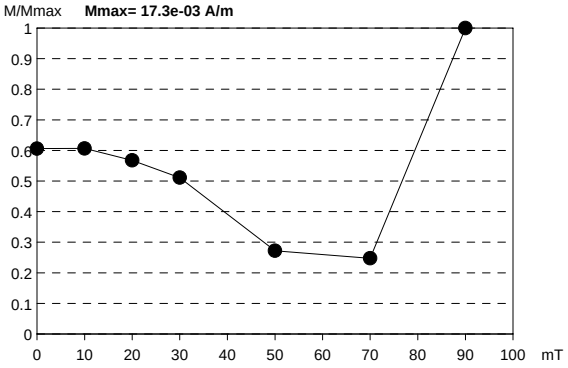

Name	Site	Latitude	Longitude	Height	Rock	Age	Fm	SDec	SInc	BDec	BInc	FDec	FInc	P1	P2	P3	P4	Note
RTH015								0	90					6	0	12	90	

#	State	M[A/m]	Dsp	Isp	Dge	Ige	Dtc	Itc	Dfc	Ifc	Prec	Limit1	Limit2	Note	K[e-06 SI]
1	NRM	10.5e-03	47.1	-51.7	210.0	24.9					1.0				
2	10mT	10.5e-03	45.9	-53.5	208.0	24.4					1.0				
3	20mT	9.84e-03	47.4	-51.6	210.3	24.9					1.0				
4	30mT	8.86e-03	46.5	-51.9	209.7	25.2					1.0				
5	50mT	4.72e-03	51.3	-41.7	221.2	27.8					1.0				
6	70mT	4.29e-03	64.0	-58.3	209.1	13.3					0.0				
7	90mT	17.3e-03	235.5	86.7	2.7	-1.9					1.0				

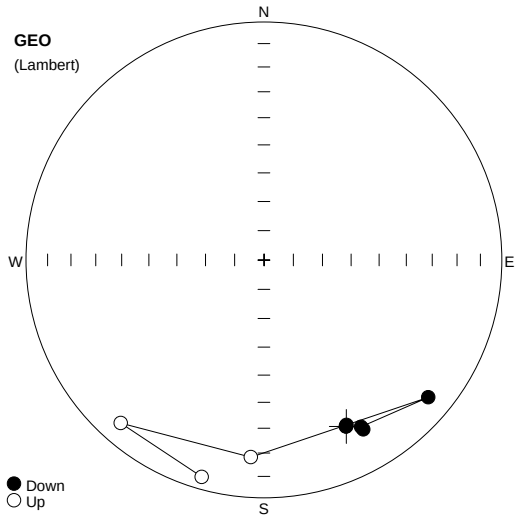

RTH016

AF demag

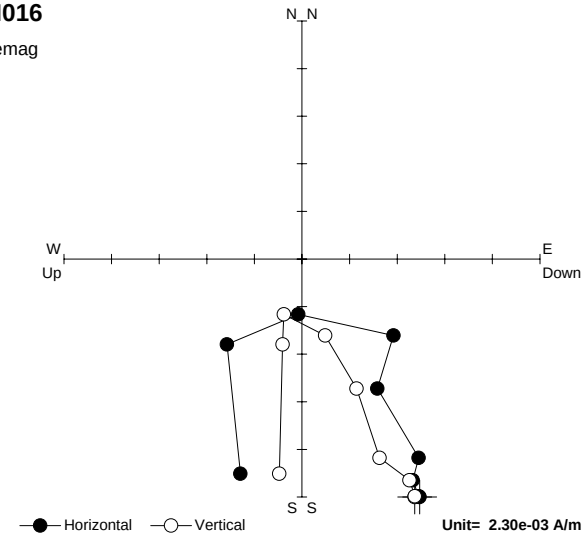

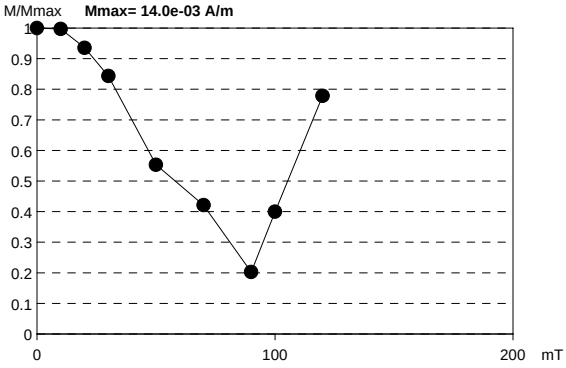

Name	Site	Latitude	Longitude	Height	Rock	Age	Fm	SDec	SInc	BDec	BInc	FDec	FInc	P1	P2	P3	P4	Note
RTH016								0	90					6	0	12	90	

#	State	M[A/m]	Dsp	Isp	Dge	Ige	Dtc	Itc	Dfc	Ifc	Prec	Limit1	Limit2	Note	K[e-06 SI]
1	NRM	14.0e-03	313.8	-55.6	153.7	23.0					0.0				
2	10mT	13.9e-03	314.1	-55.6	153.8	23.1					0.0				
3	20mT	13.1e-03	314.1	-55.1	153.4	23.5					0.0				
4	30mT	11.8e-03	303.6	-54.8	149.6	18.6					1.0				
5	50mT	7.72e-03	305.9	-54.3	149.8	20.0					1.0				
6	70mT	5.88e-03	284.2	-39.0	129.9	11.0					1.0				
7	90mT	2.83e-03	168.4	-71.5	183.8	-18.1					0.0				
8	100mT	5.58e-03	104.5	-47.8	221.3	-9.7					1.0				
9	120mT	10.9e-03	110.3	-73.0	196.0	-5.8					1.0				

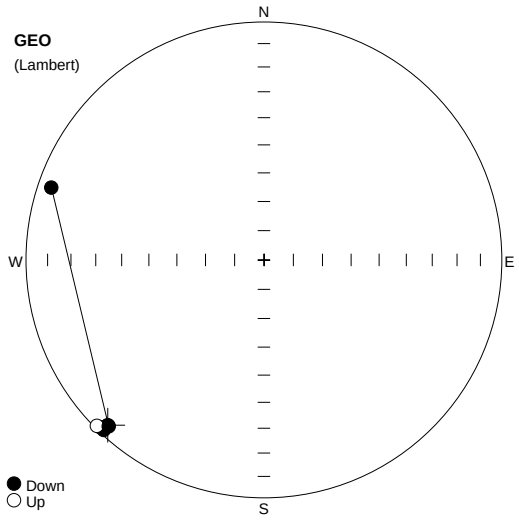

RTH017

AF demag

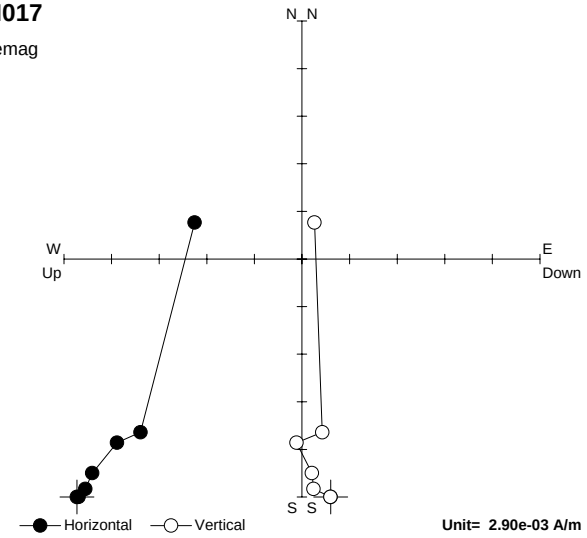

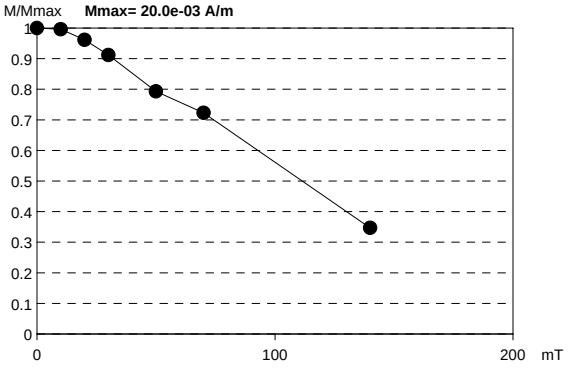

Name	Site	Latitude	Longitude	Height	Rock	Age	Fm	SDec	SInc	BDec	BInc	FDec	FInc	P1	P2	P3	P4	Note
RTH017								0	90					6	0	12	90	

#	State	M[A/m]	Dsp	Isp	Dge	Ige	Dtc	Itc	Dfc	Ifc	Prec	Limit1	Limit2	Note	K[e-06 SI]
1	NRM	20.0e-03	82.7	-46.3	223.4	5.0					1.0				
2	10mT	20.0e-03	82.8	-46.6	223.2	5.0					0.0				
3	20mT	19.3e-03	87.0	-46.7	223.3	2.1					0.0				
4	30mT	18.3e-03	87.4	-45.6	224.4	1.9					0.0				
5	50mT	15.9e-03	91.6	-44.8	225.2	-1.2					1.0				
6	70mT	14.5e-03	82.8	-46.7	223.0	4.9					1.0				
7	140mT	6.95e-03	83.4	18.7	288.8	6.3					1.0				

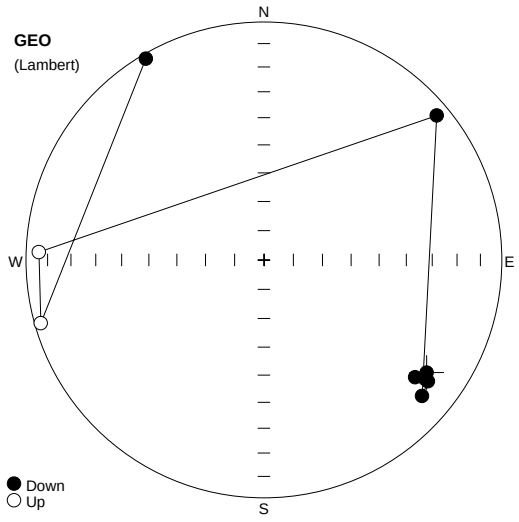

RTH018

AF demag

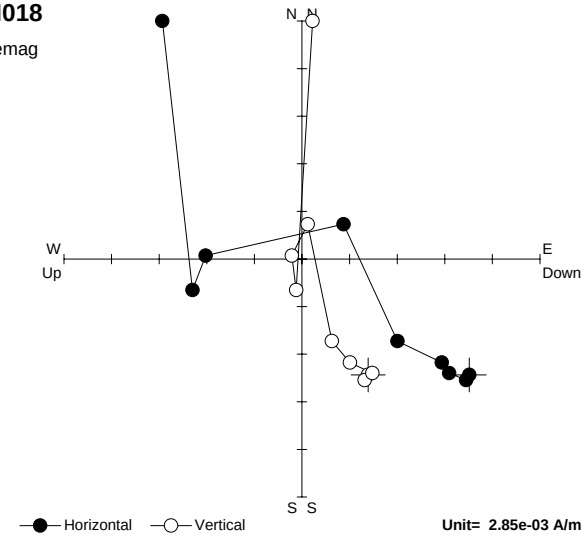

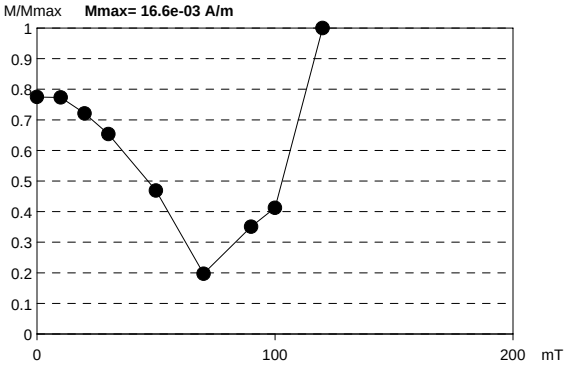

Name	Site	Latitude	Longitude	Height	Rock	Age	Fm	SDec	SInc	BDec	BInc	FDec	FInc	P1	P2	P3	P4	Note
RTH018								0	90					6	0	12	90	

#	State	M[A/m]	Dsp	Isp	Dge	Ige	Dtc	Itc	Dfc	Ifc	Prec	Limit1	Limit2	Note	K[e-06 SI]
1	NRM	12.8e-03	291.5	-32.8	124.7	18.0					1.0				
2	10mT	12.8e-03	290.9	-34.5	126.4	17.1					1.0				
3	20mT	11.9e-03	295.6	-35.0	127.8	20.7					1.0				
4	30mT	10.8e-03	288.9	-35.0	126.5	15.4					1.0				
5	50mT	7.76e-03	287.5	-39.4	130.7	13.4					1.0				
6	70mT	3.26e-03	277.8	39.6	50.1	6.0					1.0				
7	90mT	5.81e-03	96.0	2.0	272.0	-6.0					1.0				
8	100mT	6.83e-03	93.0	-15.8	254.2	-2.9					1.0				
9	120mT	16.6e-03	85.7	59.6	329.6	2.2					0.0				

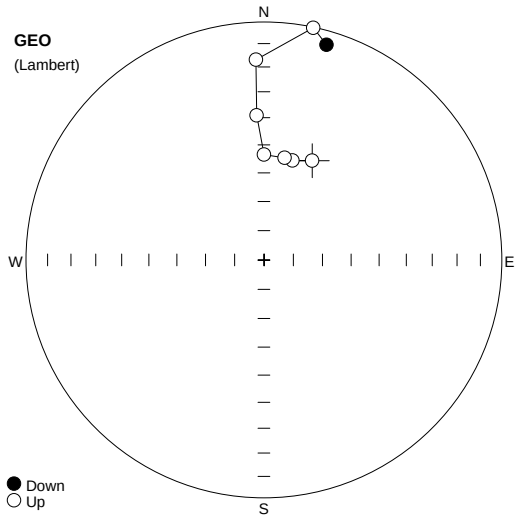

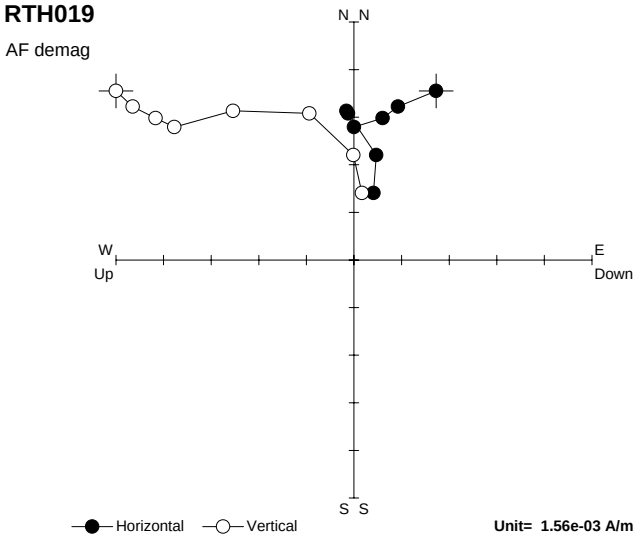

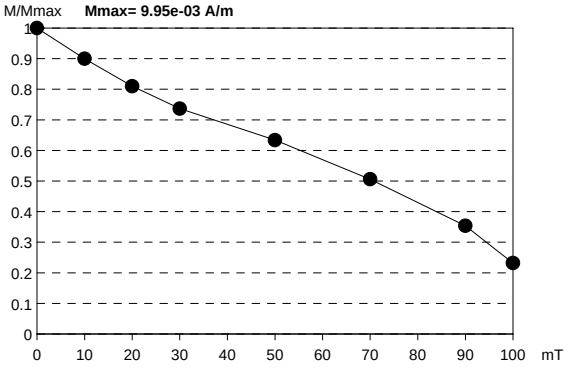

Name	Site	Latitude	Longitude	Height	Rock	Age	Fm	SDec	SInc	BDec	BInc	FDec	FInc	P1	P2	P3	P4	Note
RTH019								0	90					6	0	12	90	

#	State	M[A/m]	Dsp	Isp	Dge	Ige	Dtc	Itc	Dfc	Ifc	Prec	Limit1	Limit2	Note	K[e-06 SI]
1	NRM	9.95e-03	199.0	33.8	25.9	-51.7					1.0				
2	10mT	8.95e-03	191.2	34.2	16.0	-54.2					0.0				
3	20mT	8.06e-03	188.2	35.3	11.4	-53.9					1.0				
4	30mT	7.33e-03	180.0	36.5	360.0	-53.5					0.0				
5	50mT	6.30e-03	176.4	50.9	357.1	-39.0					1.0				
6	70mT	5.03e-03	172.6	73.0	357.7	-16.9					1.0				
7	90mT	3.52e-03	268.4	78.0	12.0	-0.3					1.0				
8	100mT	2.31e-03	292.1	72.6	16.2	6.5					1.0				

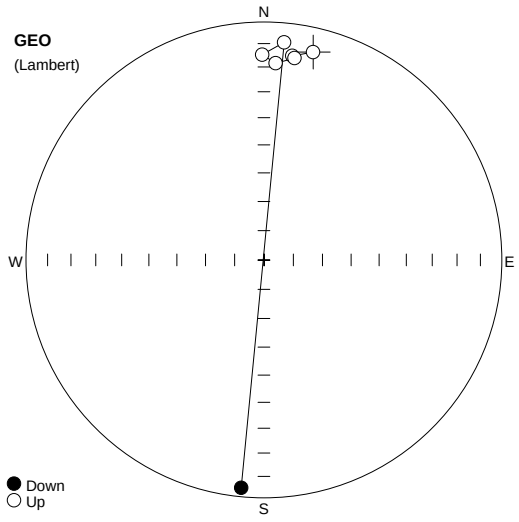

RTH020

AF demag

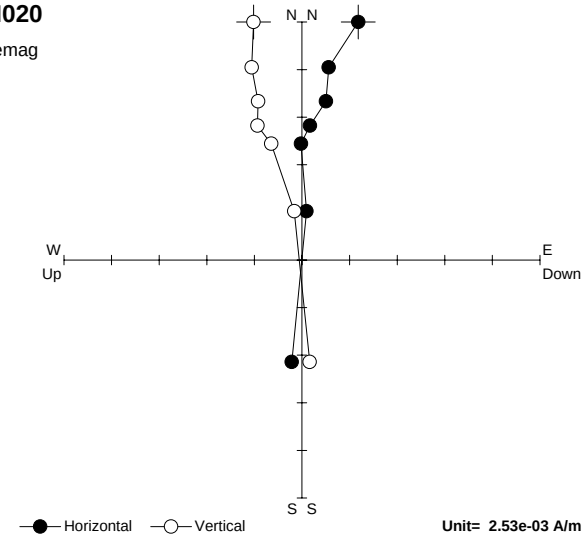

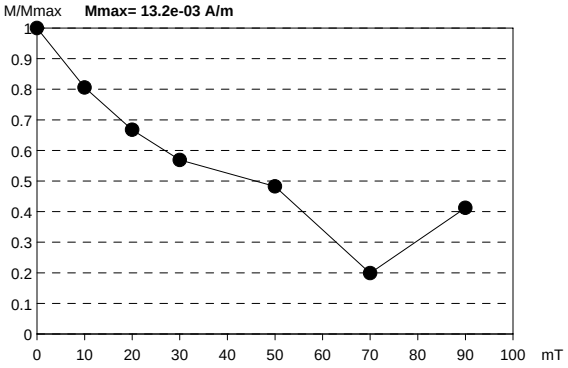

Name	Site	Latitude	Longitude	Height	Rock	Age	Fm	SDec	SInc	BDec	BInc	FDec	FInc	P1	P2	P3	P4	Note
RTH020								0	90					6	0	12	90	

#	State	M[A/m]	Dsp	Isp	Dge	Ige	Dtc	Itc	Dfc	Ifc	Prec	Limit1	Limit2	Note	K[e-06 SI]
1	NRM	13.2e-03	229.2	72.7	13.3	-11.2					0.0				
2	10mT	10.7e-03	208.0	73.5	7.9	-14.5					1.0				
3	20mT	8.84e-03	208.7	72.4	8.6	-15.3					0.0				
4	30mT	7.54e-03	190.3	71.4	3.4	-18.3					0.0				
5	50mT	6.39e-03	178.2	75.2	359.5	-14.8					0.0				
6	70mT	2.63e-03	210.3	79.6	5.3	-9.0					1.0				
7	90mT	5.46e-03	52.8	-82.9	185.7	4.3					0.0				

Appendix L – Micromorphology Observations and Select Photos

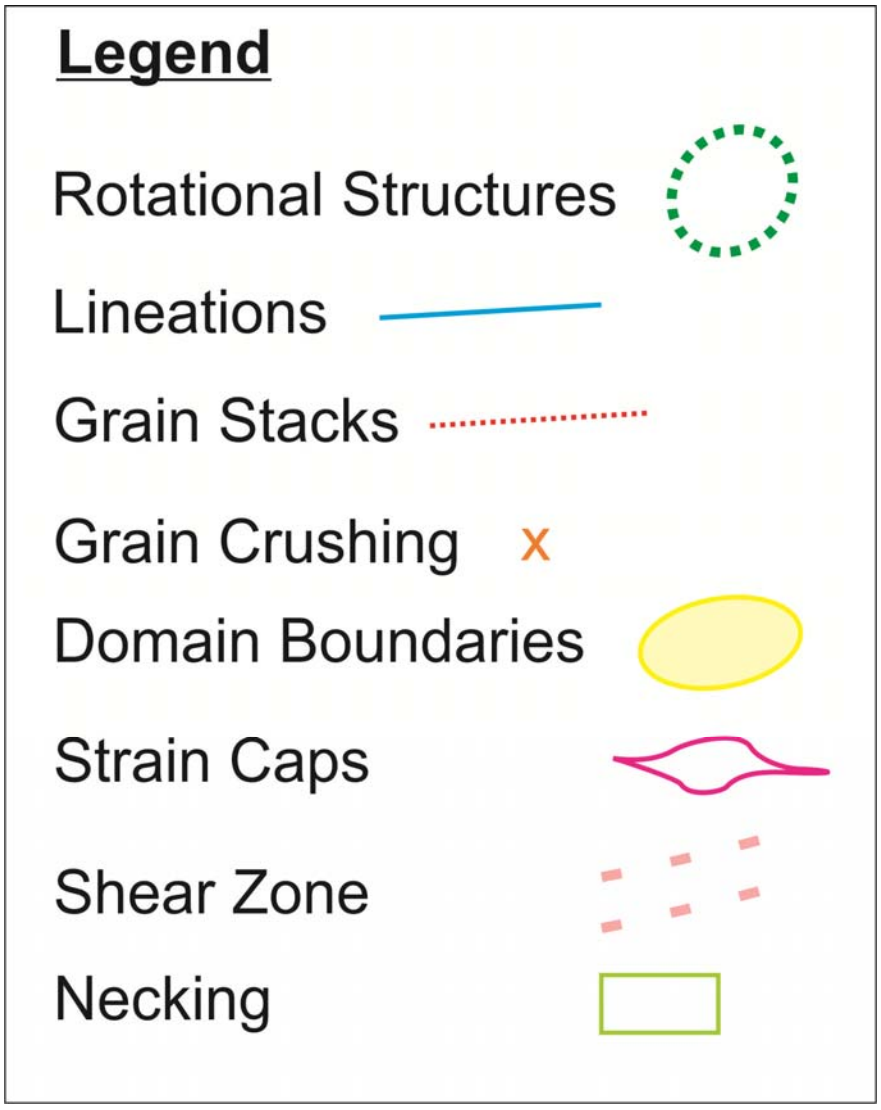
Legend
Rotational Structures
Lineations
Grain Stacks
Grain Crushing
x
Domain Boundaries
Strain Caps
Shear Zone
Necking

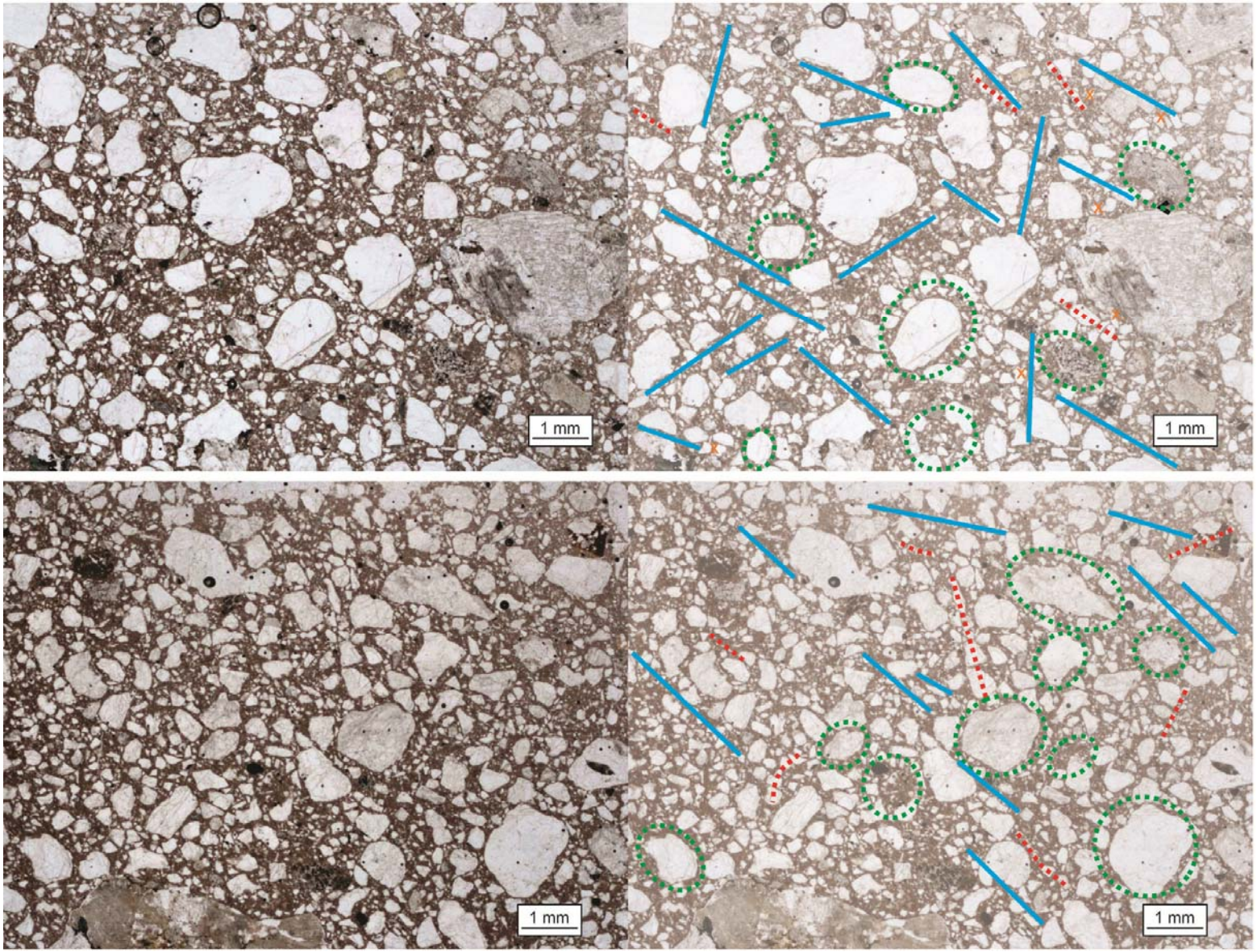

Figure 1: Drillcore MAM-002 sample B (Upper) and C (Lower).

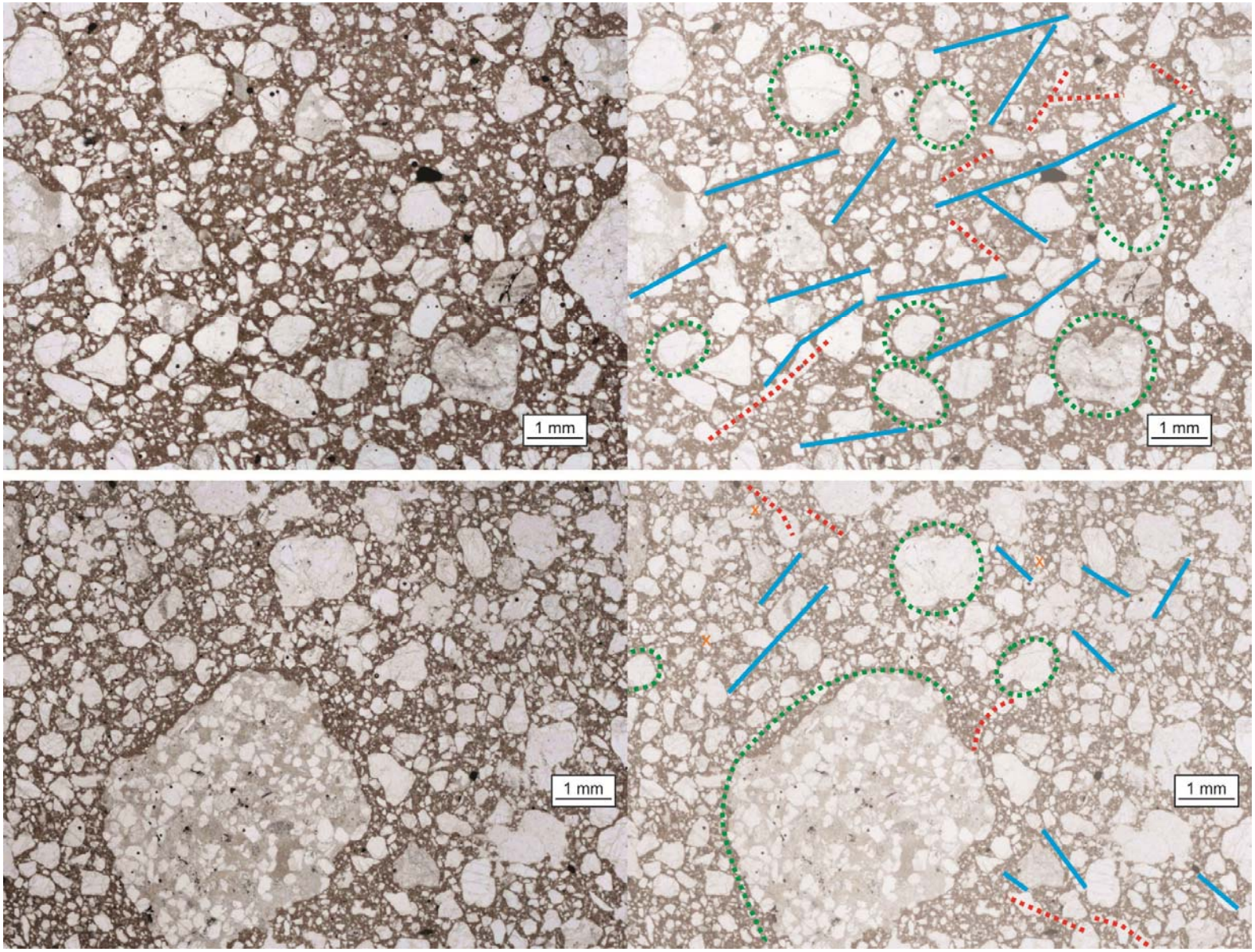

Figure 2: Drillcore MAM-002 sample E (upper) and F (lower).

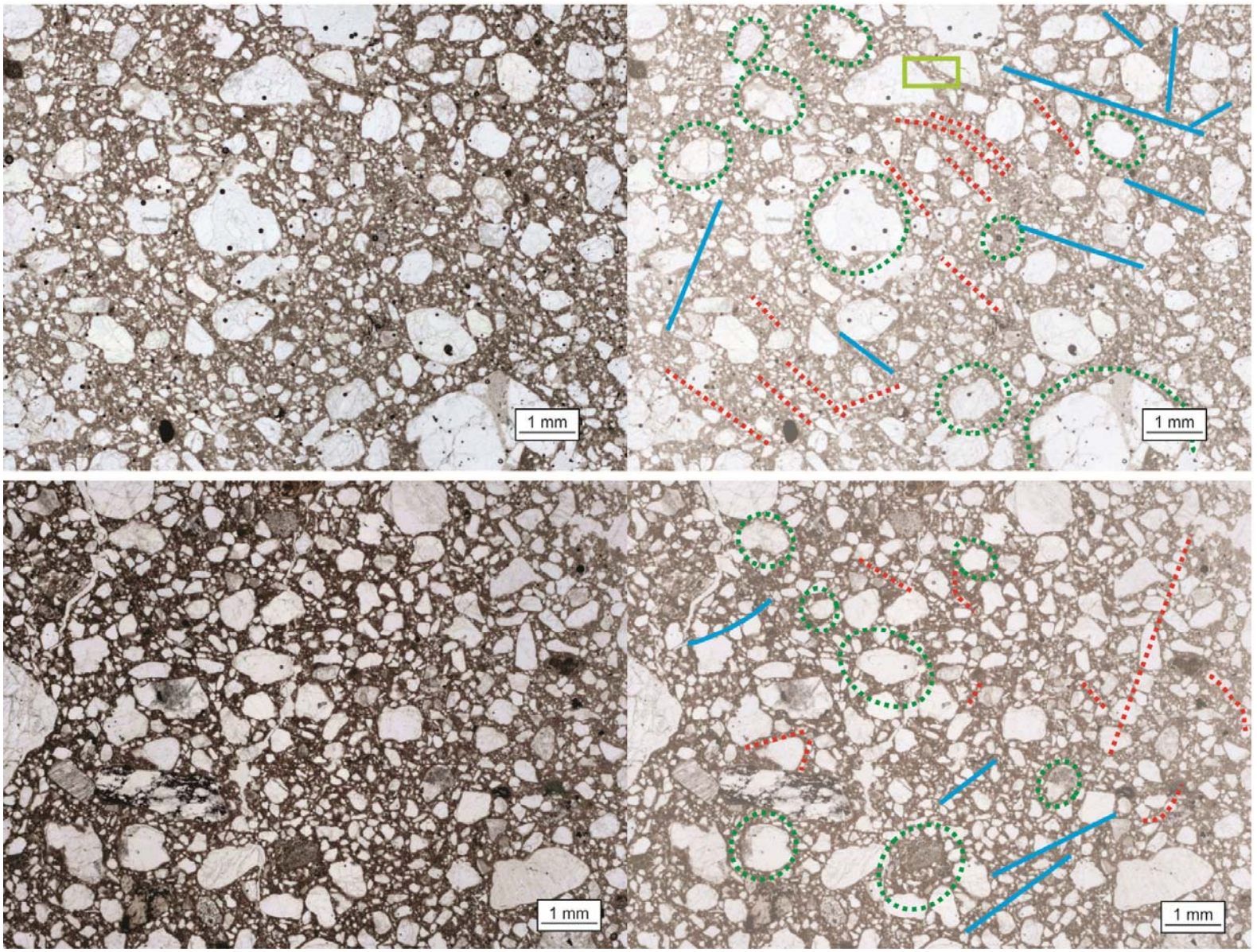

Figure 3: Drillcore MAM-002 sample G (upper). Drillcore TUR-057 sample J (lower).

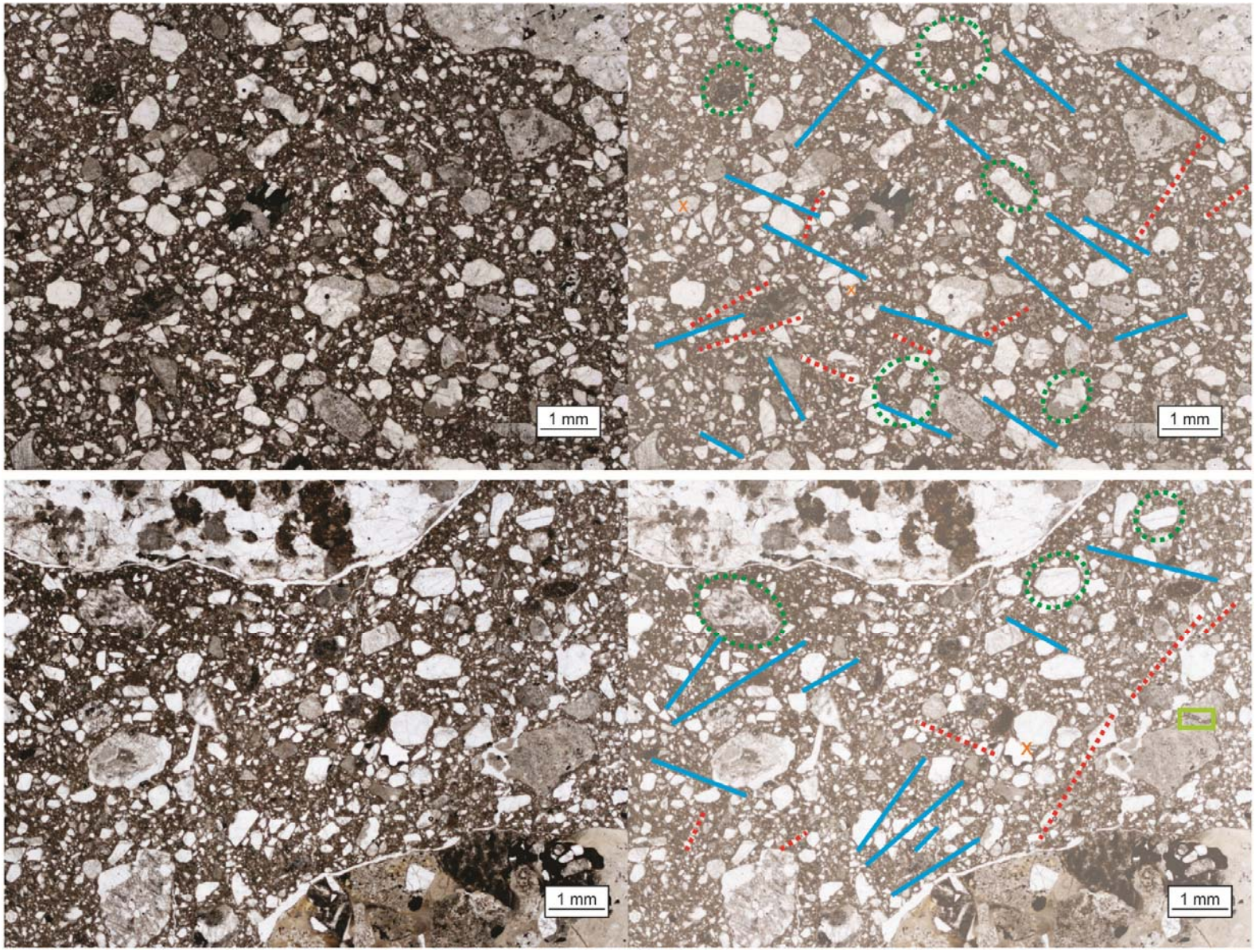

Figure 4: Drillcore AYA-010 sample B (upper) and C (lower).

COMPARING BROWN TILL AYRA LITHOFACIES (BOTTOM) TO PALE RED DMM 3 TATIGGAQ LITHOFACES (TOP)